GLIAL DEVELOPMENT, SYNAPTIC PLASTICITY AND NEUROTRANSMITTER RECYCLING IN THE VISUAL SYSTEM OF THE FRUIT FLY *DROSOPHILA MELANOGASTER*

by

Tara N. Edwards

Submitted in partial fulfillment of the requirements
for the degree of Doctor of Philosophy

at

Dalhousie University
Halifax, Nova Scotia
December 2010

© Copyright by Tara N. Edwards, 2010

DALHOUSIE UNIVERSITY

DEPARTMENT OF BIOLOGY

The undersigned hereby certify that they have read and recommend to the Faculty of Graduate Studies for acceptance a thesis entitled "GLIAL DEVELOPMENT, SYNAPTIC PLASTICITY AND NEUROTRANSMITTER RECYCLING IN THE VISUAL SYSTEM OF THE FRUIT FLY *DROSOPHILA MELANOGASTER*" by Tara N. Edwards in partial fulfillment of the requirements for the degree of Doctor of Philosophy.

Dated: December 6, 2010

External Examiner: _____

Research Supervisor: _____

Examining Committee: _____

_____

Departmental Representative: _____

DALHOUSIE UNIVERSITY

DATE: December 6, 2010

AUTHOR: Tara N. Edwards

TITLE: GLIAL DEVELOPMENT, SYNAPTIC PLASTICITY AND NEUROTRANSMITTER RECYCLING IN THE VISUAL SYSTEM OF THE FRUIT FLY *DROSOPHILA MELANOGASTER*

DEPARTMENT OR SCHOOL: Department of Biology

DEGREE: PhD CONVOCATION: May YEAR: 2011

Permission is herewith granted to Dalhousie University to circulate and to have copied for non-commercial purposes, at its discretion, the above title upon the request of individuals or institutions. I understand that my thesis will be electronically available to the public.

The author reserves other publication rights, and neither the thesis nor extensive extracts from it may be printed or otherwise reproduced without the author's written permission.

The author attests that permission has been obtained for the use of any copyrighted material appearing in the thesis (other than the brief excerpts requiring only proper acknowledgement in scholarly writing), and that all such use is clearly acknowledged.

_____

Signature of Author

DEDICATION

for my mother and my sisters

TABLE OF CONTENTS

LIST OF TABLES

LIST OF FIGURES

ABSTRACT

The visual system of the fruit fly is ideal for studying the association between neurons and glia. These interact during the morphogenesis of brain neuropiles and, in the adult, work together to maintain an ideal environment for neuronal function. In this thesis I characterise the pupal metamorphosis and adult structure of glia in the optic lobe's lamina and medulla neuropiles. Photoreceptor axons from the fly's compound eyes terminate at locations within these neuropiles that allow them intimate contact with glia. Some neuropile glia take up and inactivate the neurotransmitter histamine after its release at photoreceptor synapses. A shuttle pathway between the glia and photoreceptors then transports inactivated histamine back to photoreceptors for reuse. The gene *CG12120* encodes the protein Tan, which liberates recycled histamine within the photoreceptor cytoplasm, it is then pumped into vesicles for re-release. Histamine, however, is not exclusive to the visual system. A system of glial barriers in the lamina, and around the brain, controls the movement of histamine between neuropiles as well as between the body and the brain. How histamine is reciprocally transported between photoreceptors and glia remains unknown despite attempts to uncover candidate transporters. Photoreceptor-specific capitate projections form as invaginations from neuropile glia into photoreceptor terminals. The transmitter needs of the photoreceptor appear to dictate the dynamic structure of capitate projections, which change in shape and number after perturbations that affect terminal location, synapse number or histamine release at the photoreceptor. This dynamism suggests that capitate projections play an important role, not only in recycling synaptic vesicles, but also in recycling histamine.

LIST OF ABBREVIATIONS USED

5-HT	5-hydroxytryptamine/serotonin
ABC	ATP-binding cassette transporter
BBB	Blood brain barrier
β-gal	β-galactosidase
BL#	Bloomington stock center order number
BOSS	Bride of sevenless
BrdU	Bromodeoxyuridine
CED	*C. elegans* cell death gene
CNS	Central nervous system
DAB	3,3'-diaminobenzidine
DEPC	Diethylpyrocarbonate
Df	Deficiency
DIG	Digoxygenin
Disco	Disconnected
DNT	*Drosophila* neurotrophin
Drpr	Draper
EAAT	Excitatory amino acid transporter
EGFR	Epidermal growth factor receptor
EGUF-hid	Eyeless, GAL4, UAS, FLPase – head involution defective
EM	Electron microscope
ERG	Electroretinogram
FasII	FasciclinII
FGF	Fibroblast growth factor
FLP	Flipase recombinase
FRT	Flipase recombinase target
GABA	γ-Aminobutyric acid
GAL4	Galactosidase 4
GCM	Glial cells missing
GFP	Green fluorescent protein
Gli	Gliotactin
GMR	Glass multimer reporter
GPZ	Glial precursor zone
GSK-3β	Glycogen synthase kinase-3β
hdc	Histidine decarboxylase
HisCl	Histamine gated-chloride channel receptor
HPLC	High performance liquid chromatography
HRP	Horse radish peroxidise
Ine	Inebriated
Inx	Innexin
IR	Ionotropic glutamate receptor gene family olfactory receptor
L (1-5)	Lamina monopolar neuron 1 through 5
Lz	Lozenge
M (1-10)	Medulla strata
MARCM	Mosaic analysis with a repressible cell marker
MCS	Multiple cloning site
NAD	Nicotinamide adenine dinucleotide
NGS	Normal goat serum
NMJ	Neuromuscular junction

Nmnat	Nicotinamide mononucleotide adenyltransferase
NonC	No ‘on’ or ‘off’ transient C
NTE	Neuropathy target tsterase
Nrv2	Nervana2
Ogre	Optic ganglion reduced
OR	G-protein coupled receptor gene family olfactory receptor
Orct	Organic cation transporter
ORN	Olfactory receptor neuron
Ort	Outer rhabdomeres transientless
Otd	Orthodenticle
PB	Phosphate buffer
PBS	Phosphate buffered saline
PCD	Programmed cell death
PDF	Pigment dispersing factor
PFA	Paraformaldehyde
PKA-C3	cAMP activated protein kinase
PNS	Peripheral nervous system
PtdCho	Phosphatidylcholine
R (1-8)	Photoreceptor 1 through 8
RBG	Retinal basal glia
Rdg	Retinal degeneration
Repo	Reversed polarity
Rh (1-6)	Rhodopsin 1 through 6
RNAi	RNA interference
Sev	Sevenless
SIMU	Six microns under
Sina	Seven in absentia
SLC	Solute-linked carrier transporter
Src42A	Src family kinase 42A
SSC	Saline sodium citrate
Sws	Swiss cheese
VMAT	Vesicular monoamine transporter
TeTxLC	Tetanus toxin light chain
Tx	Triton X
UAS	Upstream activating sequence
UV	Ultraviolet
Wld^s	Wallerian degeneration slow
ZT	Zeitgeber time

ACKNOWLEDGEMENTS

First and formost I would like to thank my supervisor Ian A. Meinertzhagen for his support and encouragement over the years. He taught me how to write a wordy manuscript (enjoy), and to do so with Oxford English Dictionary-approved words and not my usual colourful and often made-up language. I would also like to thank Zhiyuan Lu for making me look like a good scientist. If it were not for Zhiyuan I would never have finished this thesis, as I would still be sitting in the histology lab chasing a sliver of plastic around a drop of water with an eyelash. I don't have a God, but if I did - it would be Zhiyuan Lu. I am also indebted to my committee members, Vett Lloyd for teaching me how to cross flies and Steve R. Shaw for confusing me with circuit diagrams. Evidence of their handywork is hidden somewhere in this thesis.

My mental health and sanity have been placed in the hands of those who work around me and so for that I would like to thank everyone who has ever worked inside the Meinertzhagen lab over these many years. This includes my beautiful girls: Nancy Butcher, Andrea Nuschke, Claudia Groh, Jane Anne Horne, Kerrianne Ryan, Birgit Greiner, Janice Imai, Nicole Delaney, Claire Hamilton, Monika Balys, Agnieska Kwasniowska, and Jola Górska-Andrzejak. Thanks for keeping me company inside and outside of the lab. I would also like to thank the lab "family": Jola and Janusz Borycz, Dorota Tarnogorska, Harjit Seyan, P. Robin Hiesinger, Rita Kostyleva, Yoshitaka Hamanaka, Shin-ya and SatokoTakemura, Jacek Panek, Valentina Oulyanova, Ruth Fabian-Fine, Xuetao Sun, Anya Kubów and Qurat-ul-ain Haider.

The Lloyd lab provided not only molecular techniques and reagents but also drinking buddies and a place to escape. Thus, I would like to thank the Lloyd lab crew which includes, but is not limited to, actual Lloyd lab members: Andrew Haigh, Lori McEachern and Greg Handrigan. Special thanks to William MacDonald, who is my format editor, *in situ* hybridization coach, personal chef, masseur, pet wrangler, teammate and therapist. He tolerates me, in all my foolishness and insecurity. It is for this, and many other reasons, that I love him.

CHAPTER 1

INTRODUCTION

1.1 VISION, A PRINCIPAL SENSORY SYSTEM

The ability of any animal to sense and react appropriately to changes in its environment is a powerfully adaptive key to its survival. In more derived species, distinct sensory systems provide animals with information about their environment and a brain with the requisite neural apparatus to process this sensory information in order to generate a plan of action and implement it. Even small species, such as the fruit fly *Drosophila melanogaster,* have an intricate brain with specified ganglia for processing vision (Heisenberg and Wolf, 1984), smell and taste (Vosshall and Stocker, 2007), and mechanoreception and sound (Boekhoff-Falk, 2005; Nadrowski *et al.*, 2010). I have used the visual system of the fruit fly to understand the development and plasticity of photoreceptor axon targeting and synaptic connection, which is the first step in conveying and processing visual information. The function of the visual system depends on its anatomical substrate: the proper synaptic connections between groups of neurons which convey visual information, and the proper association between those neurons and their surrounding glia. Glia are important not only for the axonal targeting during development, but also for axonal pruning and phagocytosis of apoptotic neurons in the adult visual system. In the adult, glia also serve a role in recycling neurotransmitters, regulating neurotransmitter levels in the synaptic cleft, and regulating the internal environment of the brain by forming the blood brain barrier.

In this thesis I examine genetically induced errors in photoreceptor axon targetinging and synapse formation. I also set out to comprehensively characterise the development and anatomy of *Drosophila* visual system glia, which are not only involved in the correct targeting of photoreceptor axons but also regulate the recycling of the photoreceptor neurotransmitter, histamine (Hardie, 1987).

1.2 THE ORGANISATION OF THE COMPOUND EYE AND OPTIC NEUROPILES OF *DROSOPHILA*

Each compound eye of the fruit fly *Drosophila melanogaster* is composed of a regularly repeating hexagonal array of approximately 750 ommatidial units (Ready *et al.*, 1976). Each ommatidium contains 26 cells including 8 photoreceptor cells (or R cells), 4 cone cells, 2 primary pigment cells as well as the secondary and tertiary pigment cells that it shares with neighbouring ommatidia (Ready *et al.*, 1976; Cagan and Ready, 1989a). The photoreceptor cells within each ommatidium are arranged so that in cross-section

their light-absorbing rhabdomeres form an asymmetric trapezoidal pattern. The orientation of this trapezoid differs depending upon the location of its ommatidium within the eye (Dietrich, 1909). A horizontal line of pattern symmetry, the equator, divides the dorsal from the ventral half of each eye. Not only does photoreceptor cell pattern in the dorsal half of the eye mirror that in the ventral half, the arrangements of photoreceptor cells in the right eye also mirror those in the left so that the pattern of a dorsal right ommatidium, with reference to absolute external landmarks, is exactly the same as that of a ventral left ommatidium. This planar polarity, which is established in the early stages of pupal development (Usui *et al.*, 1999; Chou and Chien, 2002; Yang *et al.*, 2002; Brown and Freeman, 2003; Domingos *et al.*, 2004a), ensures that in the adult four of the outer photoreceptors, R2-R5, are always orientated towards the equator while R1 and R6 are orientated towards the dorsal or ventral poles (Braitenberg, 1967; Ready *et al.*, 1976).

Photoreceptor cells in many Brachycera including *Drosophila* can be divided into three classes based upon their location in the retina, the size of their rhabdomere, and where their axons terminate in the brain (Strausfeld, 1970; Shaw and Moore, 1989; Meinertzhagen and Hanson, 1993). In *Drosophila* these three classes also express different photo-pigments, thus conferring a unique spectral sensitivity to each class (Pichaud *et al.*, 1999; Yamaguchi *et al.*, 2010). R1-R6 lie around the outside of the ommatidial cluster and express a single blue-green sensitive opsin, Rhodopsin1 (Rh1), in their large rhabdomeres (O'Tousa *et al.*, 1985; Cowman *et al.*, 1986; Yamaguchi *et al.*, 2010). These outer photoreceptors extend their axons into the first optic neuropile, the lamina ganglionaris, where they synapse upon monopolar interneurons (Figure 1.1A; Meinertzhagen and O'Neil, 1991). R7 and R8 provide spectral discrimination pathways and have small, axially located rhabdomeres that lie in tandom, R7's over R8's, and that express one of two opsins, Rh3 or Rh4 (in R7), and Rh5 or Rh6 (in R8). These photoreceptors have long axons that project to distinct layers within the second optic neuropile, the medulla (Montell *et al.*, 1987; Fischbach and Dittrich, 1989; Meinertzhagen and Hanson, 1993; Chou *et al.*, 1996; Huber *et al.*, 1997; Papatsenko *et al.*, 1997; Pichaud *et al.*, 1999; Yamaguchi *et al.*, 2010), although in one basal Bracyceran examined, both R7 and R8 also make synapses in the lamina (Shaw and Moore, 1989)

The lamina is characterised by its regularly repeating array of visual interneurons in columns called cartridges. Each cartridge contains five monopolar (L1-5) neurons and their associated R1-R6 axon terminals all surrounded by a sheath of epithelial glia (Figure 1.1C; Meinertzhagen and O'Neil, 1991), similar to the organisation first described in *Musca* (Boschek, 1971).

Axons projecting from the retina to the lamina do so in precise retinotopic order as an array of ommatidial axon bundles so that the number of cartridges in the lamina exactly matches the number of ommatidia in the retina (Braitenberg, 1967). The six outer photoreceptors in each ommatidium have their rhabdomeres oriented so as to view a different visual axis. Neighbouring ommatidia diverge at an angle corresponding to the curvature of the eye, and this angle is almost exactly the same as that between the axis of neighbouring photoreceptors in a single ommatidium. As a result, each R1-R6 cell has a visual axis aligned with that of five others in neighbouring ommatidia (Kirschfeld, 1967). The lamina cartridge that underlies a single retinal ommatidium receives no direct projection from the R1-R6 cells that overly it (Figure 1.1B). Instead each cartridge receives retinal input from six R1-R6 cells, one each, belonging to six of the directly adjacent and sub-adjacent ommatidial neighbours (Braitenberg, 1967; Trujillo-Cenóz and Melamed, 1973) in a pattern of neural superposition reasoned to increase the light sensitivity of the eye by capturing light through a wider effective aperture (Braitenberg, 1967; Kirschfeld, 1967). Because the eye is curved, and because the divergence angle between adjacent ommatidia exactly equals the divergence angle between adjacent R1-R6 photoreceptors (Kirschfeld, 1967), it follows that photoreceptor cells in neighbouring ommatidia view the same point in visual space, and it is exactly these photoreceptor cells that project to a single lamina cartridge. This has been claimed to increase the input signals from any individual point in visual space, allowing increased acuity for vision at low light levels and at low pattern contrast (Kirschfeld, 1967; Heisenberg and Wolf, 1984). The projection of R1-R6 axons, initially retinotopic, thus becomes visuotopic.

How this seemingly amazing pattern of neural connectivity arises during the development of the adult eye provides a major morphogenetic challenge. The axons from photoreceptor cells within a single ommatidium must project to the lamina and there sort individually into different target cartridges, each seemingly identical. The solution to this sorting problem has to be sought through studies on development.

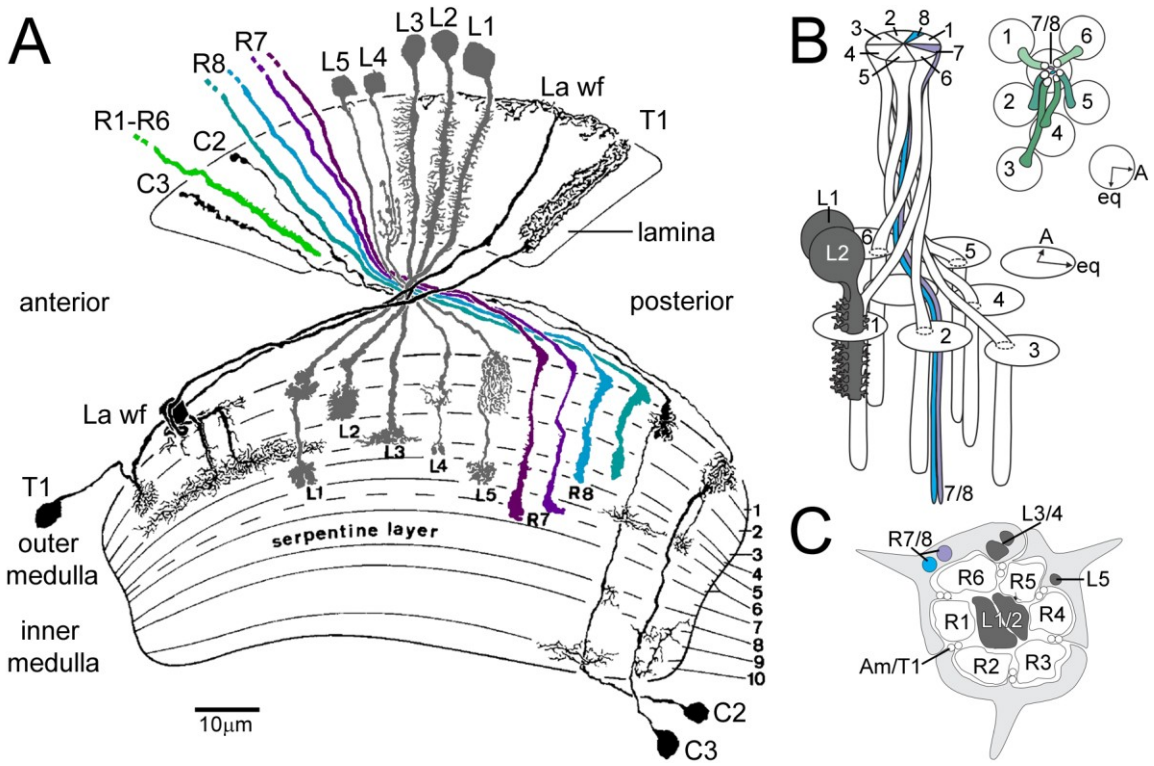

FIGURE 1.1 - THE BASIC STRUCTURE OF THE VISUAL SYSTEM OF *DROSOPHILA.*

A: Modified representation of compiled camera lucida tracings from individual Golgi-impregnated neurons, as viewed in a horizontal section through the *Drosophila* lamina and medulla neuropiles (Fischbach and Dittrich, 1989). The axons of photoreceptors R1-R6 terminate in the lamina, and are illustrated here in green, reflecting their broad blue-green range peak spectral sensitivity. The photoreceptors R7 (shades of violet), with peak sensitivities in the ultraviolet, and R8, with peak sensitivities in the blue/green (shades of blue), have axons which project to distinct layers of the distal medulla. Nine types of interneurons are depicted: five lamina monopolar neurons (L1-L5, grey) have cell bodies in the cortex distal to the lamina neuropile, L1-L4 with dendrites in the lamina and all of L1-L5 with terminal expansions in distinct layers of the distal medulla, partially defining strata M1-M6. Other neurons depicted include lamina wide-field neurons (La wf), the tangential basket cell (T1), and medulla centrifugal neurons (C2-C3). The serpentine layer (M7) separates the strata M1-M6 of the distal medulla from the proximal medulla. **B**: Muscid flies, such as *Drosophila*, have a “neural superposition eye” with a diverging pattern of photoreceptor axon projection from each ommatidium. R1-R6 photoreceptors from a single ommatidium have axons which twist 180° about their axis in the lamina cortex and branch to terminate in six neighbouring cartridges of the lamina neuropile. Photoreceptors terminate in a predictable circumferential position within their cartridge, which they share with an associated group of monopolar neurons (L1-L5). R1-R6 photoreceptors form synapses along their entire length with dendrites from the paired L1 and L2 neurons (grey, shown here in association with the cartridge of terminal 1). R7 (magenta) and R8 (blue) photoreceptors have axons which project straight to the medulla, but which in the lamina run *en passant* alongside the cartridge that underlies their ommatidium of origin. This projection pattern is depicted in an *en face* view from

(FIGURE 1.1 – CONTINUED, 2 OF 2)

the retina looking down into the lamina. **C**: The lamina cartridge is a fixed constituency of neurons that comes together to process light information derived from a single point in visual space. Photoreceptors from different ommatidia, with rhabdomeres orientated so as to view the same point in visual space, terminate in a single lamina cartridge. The terminals of R1-R6 expand in the lamina and form a ring that surrounds the branching neurites of axially located L1 and L2 axons (dark grey). The unexpanded *en passant* axons of R7/R8 lie near the terminal of R6 while monopolar neurons L3-L4 lie near the terminal of R5. The axon of L5 bypasses the lamina. Dendrites from amacrine (Am) and T1 neurons lie between each photoreceptor terminal. The entire cartridge is surrounded by a sheath composed of extensions from three epithelial glia (G, light grey). Panel A redrawn from Fischbach and Dittrich, 1989; B Redrawn from Meinertzhagen (1975).

1.3 EYE DEVELOPMENT

The compound eye develops from the eye imaginal disc, a simple epithelium of hypodermal origin (Green *et al.*, 1993) which is attached by the optic stalk to the supraoesophageal hemisphere of the larval brain (Trujillo-Cenóz and Melamed, 1973; Ready *et al.*, 1976). The supraoesophageal hemisphere contains the primordia of the optic lobe, the optic anlagen (Meinertzhagen and Hanson, 1993). In the early third-instar larva a wave of mitotic division progresses across the eye disc in an anterior direction. It is followed by the progression of the morphogenetic furrow, wherein postmitotic cells condense to allow intimate cell-cell contact and the onset of cellular differentiation (Ready *et al.*, 1976; Kumar and Moses, 2001). The first wave of mitotic activity gives rise to cells destined to become the R8 and R2-R5 photoreceptors of each ommatidium, while a second wave of mitotic activity later gives rise to cells that become R1, R6, R7 and the support cells of the ommatidium (Ready *et al.*, 1976; Tomlinson and Ready, 1987a; Tomlinson and Ready, 1987b; Wolff and Ready, 1991). Photoreceptors within an ommatidium differentiate either as individual cells or as cell pairs. First to differentiate is the centrally located R8, followed in a precisely timed stepwise fashion by three pairs, R2/R5, R3/R4, R1/R6, and then finally by R7 (Tomlinson and Ready, 1987a; Tomlinson and Ready, 1987b). Cells of a single ommatidium adopt their final fate as the result of inductive interactions with neighbouring cells (Ready *et al.*, 1976; Campos-Ortega and Hofbauer, 1977; Tomlinson and Ready, 1987a; Freeman, 1997). Cells within an ommatidium express a number of different transcription factors that drive the expression of ligands, receptors, or intracellular messenger systems and this ultimately results in the differentiation of neighbouring photoreceptors by a “combinatorial code” of inductive interactions (Tomlinson, 1988; Kumar and Moses, 1997). Other transcription factors later determine the adult phenotypes of the photoreceptor cells that express them (Morante *et al.*, 2007).

1.4 AXONAL PATHFINDING AND LAMINA INDUCTION

Neurons find their targets by means of the growth cone, an elaborate, motile chemosensory structure at the tip of the growing axon. The nature of growth cone movement is fairly well understood and is discussed in a number of comprehensive reviews (Goodman, 1996; Tessier-Lavigne and Goodman, 1996; Korey and Van Vactor, 2000; Lowery and Van Vactor, 2009). Shortly after R8 differentiates, branched filopodia

of the R8 growth cone extend basally and the axon travels in a posterior direction along the basement membrane and toward the optic stalk (Tomlinson & Ready, 1987a). The blunt-tipped growth cones of photoreceptors added subsequently from the same ommatidium follow the path pioneered by R8 to form a bundle, or fascicle (Trujillo-Cenóz and Melamed, 1973). Photoreceptor axon fascicles appear to follow the path of the larval photoreceptor organ, called Bolwig's organ, through the optic stalk and into the optic lobe anlage (Meinertzhagen and Hanson, 1993). Subsequent axon fascicles from progressively anterior ommatidia extend retinotopically toward the anlage through the optic stalk (Meinertzhagen, 1977). Each individual axon fascicle has the means to find the optic anlage correctly, without input from neighbouring fascicles or from a pre-existing larval path (Kunes and Steller, 1993).

Development of the fly's optic lobe commences as the posterior field of differentiating ommatidia innervate lamina precursor cells generated within the outer optic anlage (Meinertzhagen and Hanson, 1993). As photoreceptor axons pass through the lamina they encounter putative monopolar cells (L1-4) arrested in the G1 phase of mitosis (Selleck and Steller, 1991; Selleck *et al.*, 1992). Pattern abnormalities in the retina are impressed on the underlying lamina (Meyerowitz and Kankel, 1978), so that reducing the number of incoming photoreceptor cells reduces the lamina correspondingly (Selleck and Steller, 1991), suggesting that retinal input is required for the development of target neurons within the lamina. Photoreceptor cell axons express *hedgehog* and *spitz* when they approach the lamina anlage (Salecker *et al.*, 1998). Hedgehog, secreted from the photoreceptor growth cone, induces lamina precursor cells to transition from the G1- to the S-phase of their final mitosis (Selleck *et al.*, 1992; Huang and Kunes, 1998). Then the Epidermal growth factor receptor (EGFR) ligand Spitz promotes differentiation and migration of lamina precursor cells (Huang *et al.*, 1998) that have been primed for differentiation by Daschund-mediated regulation of EGFR levels in these putative neurons (Chotard *et al.*, 2005). The fifth monopolar cell, L5, differs from the first four not only in the timing, but also in the means of its origin, and so may have a unique means of differentiation (Meinertzhagen and Hanson, 1993; Huang *et al.*, 1998) compatible with its being a later evolutionary step in lamina development.

Upon contacting the underlying lamina precursor cells, developing photoreceptor axons begin to twist, rotating about their central axis in a direction corresponding to the inverse sequence of their photoreceptor cell number. Thus, photoreceptor terminals attain a

position in the lamina that is rotated counterclockwise for a left dorsal ommatidium (Braitenberg, 1967). In addition a twist is generated in the retina itself. Maturing pupal ommatidia rotate 90˚ in a direction opposite that of their photoreceptor sequence (Tomlinson & Ready, 1987b). The combined effect of opposing ommatidial and axonal twists is a 180˚ rotational difference between photoreceptors in the retina and their terminals in the lamina, as seen in the adult (Braitenberg, 1967). This rotation is required to align the terminals of R1-R6 into their correct visuotopic position so as to offset the rotation of each ommatidial image suffered at the corneal lenslet.

As R1-R6 axons penetrate the lamina anlage in the wake of R8, they encounter a glial monolayer at the base of the lamina (Winberg *et al.*, 1992). These 'marginal glia' are, in a strict sense, the immediate lamina targets of R1-R6 and they prevent the passage of these axons into the medulla. When the marginal glia fail to migrate to their correct target within the lamina, as in the *non-stop* mutant and the *JAB1/CSN5* COP9 signalosome subunit mutant, the axons of R1-R6 bypass the lamina and follow R8 into the medulla neuropile (Poeck *et al.*, 2001; Suh *et al.*, 2002). During normal development, the growth cones of R1-R6 come to rest between the epithelial and marginal glia, and there they form the lamina plexus. It is in the lamina plexus that growth cones expand and the process of axon sorting begins. Positional information in the form of membrane-borne ligands is interpreted by the intracellular domain of receptors on the responding growth cone surface and translated into movement by the cytoskeleton within the growth cone (Bashaw and Goodman, 1999). The growth cone is a motile organelle with a dynamic organisation. Not only can it change its shape throughout development but it can change its intracellular properties and the combination of receptors on its membrane surface. Information received by the growth cone is transmitted to the nucleus, where the neuron responds by modifying nuclear transcription and ultimately altering the proteins expressed in the growth cone (Yu and Bargmann, 2001). In this way, ligands expressed over the surfaces of a growth substrate, for example another neuron, can cause intracellular signalling in the growth cone that, via altered transcription in the nucleus, causes newly transcribed adhesion molecules to insert into the growth cone membrane and alter the axon's growth trajectory. At the nuclear level, both Breakless and Runt have been shown to control the downstream effectors that allow extending photoreceptor axons to stop in either the lamina plexus or in the medulla (Senti *et al.*, 2000; Kaminker *et al.*, 2002). Sorting of photoreceptor terminals into their correct lamina cartridges involves interactions between

neighbouring photoreceptors (Clandinin and Zipursky, 2000; Prakash *et al.*, 2009) and utilizes the receptor tyrosine phosphatase Lar (Clandinin *et al.*, 2001), the scaffolding protein Liprin-α (Choe *et al.*, 2006), the cell adhesion molecule N-cadherin (Prakash *et al.*, 2005; Nern *et al.*, 2008), and the cadherin-like cell surface protein Flamingo (Lee *et al.*, 2003).

Concurrent with the process of photoreceptor terminal targeting, the lamina monopolar cells that they originally induced to differentiate migrate to their adult positions and extend deep into the lamina to form the lamina columns (reviewed in Meinertzhagen and Hanson 1993). Photoreceptors also navigate by interacting with their target neurons in the lamina. During the early stages of axonal pathfinding photoreceptors express the ligand Jelly belly on their growth cones, while target monopolar neurons express the receptor tyrosine kinase Anaplastic lymphoma kinase. Jelly belly-activates Anaplastic lymphoma kinase in monopolar neurons, which then modulates expression of cell adhesion molecules that are required for targeting (Bazigou *et al.*, 2007). The first half of pupal development concludes with the assembly of complete cartridges (Meinertzhagen and Hanson, 1993). Subsequently, R1-R6 elongate to form synaptic terminals along the length of the two axial monopolar neurons (L1, L2), commencing synaptogenesis in the second half of pupal life, around P+60% (Fröhlich and Meinertzhagen, 1983; Meinertzhagen and Hanson, 1993; Meinertzhagen, 2000).

The R7 and R8 photoreceptors provide input to pathways for spectral sensitivity in the adult. During development, their axons project as a single fascicle from each ommatidium and bypass the underlying lamina cartridge to terminate in distinct layers of the medulla. The synapses formed by their terminals there, together with those of a number of lamina monopolar neurons, transmedulla neurons, centrifugal neurons, intrinsic neurons, amacrine-like neurons and even glial-like cells, all provide input to the pathways for spectral preference (Gao *et al.*, 2008; Takemura *et al.*, 2008). The correct targeting of R7 and R8 is dependent upon interactions between photoreceptors and their target cells, similar to those in the lamina. Photoreceptors must not only find their correct layer in the medulla but must also make and maintain connections therein with the correct medulla target neurons. N-cadherin mediates homophilic interactions between R7 cells and medulla neurons, helping axons to extend and then target within this neuropile (Nern *et al.*, 2005; Ting *et al.*, 2005; Yonekura *et al.*, 2007). Lar and Liprin-α are required in R7 for its axon terminal to maintain its position in the M6 layer of

the medulla. In these mutants, R7 photoreceptor terminals retract so that, in the adult, they terminate alongside R8 in M3 instead of in the deeper M6 layer (Clandinin *et al.*, 2001; Choe *et al.*, 2006; Hofmeyer *et al.*, 2006). Mutations of *protein tyrosine phosphatise 69D* have a similar R7 mistargeting phenotype as those of *lar* and *liprin-α*, but it is not known how this protein functions in R7 targeting (Newsome *et al.*, 2000). Flamingo is required cell-autonomously in R8, where it facilitates competitive interactions between neighbouring R8 axons to establish correct spacing of terminals in their respective medulla columns. Flamingo also promotes the association and connection of R8 axon terminals and their target cells in the medulla (Senti *et al.*, 2003). Irregular expression of Jelly Belly/Anaplastic lymphoma kinase also affects layer-specific expression of the cell adhesion molecules Dumbfounded/Kirre, Roughest/Irregular chiasms and Flamingo, which ultimately results in the over-fasciculation and targeting defects of R8 axons in the medullas of these mutants (Bazigou *et al.*, 2007). The transmembrane cell adhesion molecule Capricious is expressed in both R8 and in its neuronal targets in M3, where it promotes both the layer specific and column specific targeting of R8 neurons (Shinza-Kameda *et al.*, 2006).

The molecular mechanisms that control photoreceptor targeting in both the lamina and medulla have been reviewed (Mast *et al.*, 2006; Ting and Lee, 2007). Using over-expression of the transcription factor Runt, we demonstrate an association between Runt and the determination of R7 or R8 cell fate characteristics that range from rhabdomere size, to opsin expression and photoreceptor axon terminal location (Edwards *et al.*, 2009). As detailed in Chapter 6 and its addendum, I examined not only Runt-induced alterations in photoreceptor cell fate but also the ultrastructure of mistargeted R1-R6 axon terminals. Mistargeted photoreceptors form ectopic synapses with novel partners in the medulla and have large capitate projections that are similar in appearance to the capitate projections found in R1-R6 in the lamina. Capitate projections are specialised invaginations from epithelial glia into photoreceptors that play a role in clathrin-mediated vesicle recovery in the lamina (Fabian-Fine *et al.*, 2003). However, epithelial glia are lacking in the medulla. Instead, the terminals of R7 and R8 photoreceptors normally contain small capitate-like projections, probably arising from their neighbouring medulla neuropile glia. The uniformity of both the tetrad synapse and the capitate projection, irrespective of R1-R6 photoreceptor axon terminal location, suggests that synaptic organelles are a cell-autonomous feature determined by the

presynaptic photoreceptor terminal. The effects of Runt over-expression in the retina have been published in the January 2009 issue of *The Journal of Neuroscience*.

1.5 SYNAPTIC STRUCTURE AND NEURONAL NETWORKS

Once photoreceptors have found their correct targets in the lamina and medulla they begin to form synapses. On their presynaptic side, each synapse contains specialised machinery for the release of neurotransmitter, while their postsynaptic partners contain corresponding specialised machinery for neurotransmitter reception. The photoreceptor synapse itself is composed of a presynaptic T-bar ribbon which corrals vesicles for release and lies adjacent to a number of postsynaptic elements. In the lamina of advanced Brachycera, photoreceptor synapses from R1-R6 are invariably tetrads, with four postsynaptic elements consisting of paired dendrites from L1 and L2 and, as the remaining two elements, some combination of contributions from L3, amacrine neurons or epithelial glia (Meinertzhagen and O'Neil, 1991; Meinertzhagen and Sorra, 2001). In *Drosophila,* each of the photoreceptor terminals in the lamina contains about 50 evenly spaced tetrad synapses (Meinertzhagen and Sorra, 2001) all of which utilize histamine as a neurotransmitter (Hardie, 1987; Nässel *et al.*, 1988; Gengs *et al.*, 2002). This redundancy of synaptic input is reported to amplify the signal from the retina and increase the signal to noise ratio of light-evoked signals on lamina interneurons in dragonflies (Laughlin, 1973), but with respect to an unknown reference point. That input in flies is balanced between the post synaptic monopolar neurons L1 and L2 (Meinertzhagen and Sorra, 2001).

Photoreceptor terminals form either triad or tetrad synapses in the medulla. R7 neurons form most of their synapses in layer M5 but have vesicles throughout M5 and M6 and a few synapses in M1. R8 terminals have synapses distributed throughout the distal medulla in M1, M2 and M3 (Takemura *et al.*, 2008). The locations of these synapse determines the layer-specific partnering of photoreceptors and targets (Bausenwein *et al.*, 1992; Morante and Desplan, 2008).

The postsynaptic partners of histamine-releasing photoreceptors contain one of two varieties of histamine gated-chloride channel receptor, HisCl1 or HisCl2 (also known as Outer rhabdomeres transientless, Ort), on their surface which allows them to receive chemical signals from photoreceptors (Gengs *et al.*, 2002; Gisselmann *et al.*, 2002; Witte

et al., 2002; Zheng *et al.*, 2002; Zheng *et al.*, 2006; Gao *et al.*, 2008; Pantazis *et al.*, 2008). Mutants of *ort* have defects not only in their electroretinogram (ERG), but also in motion detection based behaviours (Gengs *et al.*, 2002). Light, and hence motion-based information, is conveyed from the R1-R6 photoreceptors and through the lamina to result in stereotypical optomotor responses (Zhu *et al.*, 2009). In the lamina HisCl2/Ort expression is detected in L1, L2, L3 and amacrine neurons (Witte *et al.*, 2002; Pantazis *et al.*, 2008), all of which are postsynaptic partners at the tetrad synapse (Meinertzhagen and O'Neil, 1991). Histamine activation of histamine ligand-gated chloride channels encoded by the *ort* gene causes the postsynaptic cells to hyperpolarize (Hardie, 1989), and thus to signal light as a hyperpolarization (Laughlin and Hardie, 1978). The expression of Ort in lamina monopolar neurons L1 and L2 is both necessary and sufficient to induce a directional response in the lamina to motion-based visual stimulation in the environment (Rister *et al.*, 2007). Lights 'off' (brightness decrements), but not lights 'on' (brightness increments), cause a strong increase in intracellular Ca^{+2} in L2 axon terminals, thus L2 functions by conveying information about brightness decrements to downstream circuits which then determine the direction of an object's motion (Reiff *et al.*, 2010). HisCl1 is expressed only in the epithelial glia of the lamina but mutations of this gene have no loss of the 'on' or 'off' transients of the ERG (Pantazis *et al.*, 2008), which have been proposed to be primarily derived from the response of the lamina monopolar neurons to light (Heisenberg, 1971; Coombe, 1986). Instead HisCl1 in epithelial glia acts to modify the size of the 'on' transient of the ERG and the intracellular rise time of monopolar neurons in response to both a light flash and changes in histamine release from the R1-R6 photoreceptor neurons (Pantazis *et al.*, 2008).

Within the medulla, HisCl2/Ort is expressed in the target neurons that synapse with R7 and R8 photoreceptor terminals (Gao *et al.*, 2008). Small-field transmedullary projection neurons Tm3 and Tm9 receive direct input from wavelength-sensitive R7 and R8 photoreceptors, while wild-field Dm8 amacrine neurons receive input only from ultraviolet (UV) sensitive Rh3 and Rh4 expressing R7 neurons. It is the activity of these Ort-expressing Dm8 neurons that modifies responses in downstream neurons and causes flies to generate a selective phototactic response to UV light (Gao *et al.*, 2008).

1.6 HISTAMINE RELEASED AT PHOTORECEPTOR SYNAPSES IS DEACTIVATED AND RECYCLED THROUGH GLIA

Once released from the photoreceptor terminal into the synaptic cleft, histamine binds with its targets on postsynaptic neurons. In order to sustain the high temporal frequency and resolution of the signal it must then be immediately inactivated or cleared from the synaptic cleft. While the possibility exists that some histamine is recovered by direct re-uptake into the photoreceptors, as has been observed in the photoreceptors of the barnacle (Stuart *et al.*, 1996; Stuart *et al.*, 2002), within the lamina, most histamine is removed from the photoreceptor synaptic cleft by uptake at the epithelial glia (Borycz *et al.*, 2002; Richardt *et al.*, 2002). Within these glia, a β-alanyl-biogenic amine synthetase, Ebony, conjugates β-alanine to histamine thereby producing a β-alanyl conjugate called carcinine. The importance of Ebony in the visual system is demonstrated by the loss of 'on' and 'off' transients in *ebony* mutants (Hotta and Benzer, 1969). The *de novo* synthesis of histamine from the amino acid L-histidine by Histidine decarboxylase (Burg *et al.*, 1993) in the photoreceptors is almost certainly not sufficient to produce enough histamine to support tonic synaptic release at the ~37,500 photoreceptor synapses in the lamina (Melzig *et al.*, 1996; Melzig *et al.*, 1998; Morgan *et al.*, 1999; Borycz *et al.*, 2005; Stuart *et al.*, 2007). Indeed *ebony* mutants that have only *hdc* action to support histamine supply have reduced phototaxis and optomotor responses, suggesting that they are essentially blind (Heisenberg, 1972). Histamine must, therefore, be recycled. This is accomplished in the photoreceptor terminal by the action of Tan, a hydrolase which dissociates β-alanine from histamine in the cytoplasm of photoreceptors, where Tan is expressed, from there allowing the neurotransmitter to be re-packaged into vesicles for its inevitable re-release (True *et al.*, 2005; Wagner *et al.*, 2007). In Chapter 6, I characterise the effects of different *tan* mutant alleles on the contents of histamine in the heads of *Drosophila*. Using *in situ* hybridization I was able to localise *tan* transcripts to the photoreceptors, and with a Tan::eGFP fusion protein Tan was specifically localised to the cytoplasm in cell culture. I also explore the possible effects of cuticular and corporeal Tan expression on measurements of whole-head histamine contents. Part of this work was published in collaboration with the True (NYU Stony Brook, Stony Brook, NY, USA), Hovemann (Ruhr-Universität Bochum, Bochum, De) and Li (University of Illinois, Urbana Il., USA) labs, and is referenced above and throughout the text as True *et al*. (2005).

1.7 *DROSOPHILA* AS A MODEL SYSTEM FOR UNDERSTANDING GLIAL STRUCTURE AND FUNCTION, NEUROTRANSMITTER RECYCLING, NEURONAL AXON TARGETING AND CELL FATE-SPECIFICATION

I begin my thesis with a thorough introduction to the glia of insects in Chapter 2. This review has been published in the April 2010 issue of *Progress in Neurobiology*. "*The functional organisation of glia in the adult brain of Drosophila and other insects*" attempts to clarify the distinctions between glial subtypes by compiling evidence and nomenclature from anatomical studies in a variety of insect species. Formerly this topic for the fly's lamina has been poorly represented in the *Drosophila* literature, despite excellent accounts from large fly species (Saint Marie and Carlson, 1983a, b). The intricate details of glial anatomy are explored for known glial subtypes in various neuropiles including the lamina, the antennal lobes, and for some species, the mushroom bodies. Glia are subdivided into four major categories: surface glia, cortex glia, neuropile glia and tract glia, and the roles that each of these glial subtypes plays in the proper function of the adult neurons in their respective neuropiles is examined.

In Chapter 3, I describe the anatomy of the lamina and medulla glia based on the glia-specific expression of GFP in a number of newly characterised transgenic lines that were generated to screen for the expression patterns of known gene promoters (Pfeiffer *et al.*, 2008). At least six unique glial subtypes have been previously described for the lamina (Eule *et al.*, 1995; Tix *et al.*, 1997). Using subtype-specific glial driver lines, I have traced the metamorphic development for at least three of these glial subtypes. My detailed studies have revealed unique anatomical peculiarities for some of the described subtypes which had not been previously illustrated, and these details help to identify the failure of current studies in *Drosophila* neurobiology to correctly and consistently identify cell types in the developing optic lobes.

We know that histamine must be transported into glia wherein it can be inactivated by conjugation to β-alanine to form carcinine (Hovemann *et al.*, 1998; Borycz *et al.*, 2002; Richardt *et al.*, 2002; Richardt *et al.*, 2003). This carcinine must then exit the glia and be transported back into photoreceptors where Tan liberates the histamine for re-release by the photoreceptor terminal, as described in Chapter 4. Yet, how histamine, carcinine or β-alanine travel back and forth between these cell types, and whether their movement involves membrane transporters, remains unknown. A number of candidate transporters have been examined over the years, but few have been localised to the appropriate tissues and, those that have (e.g. Inebriated/White), have not been definitively shown to

transport histamine/carcinine or β-alanine (Gavin *et al.*, 2007; Borycz *et al.*, 2008). In Chapter 5, I examine a number of genes: *organic cation transporters*, gap junction *innexins* and the uncharacterised gene *no on nor off transient C* (*nonC*), for their potential, albeit unconventional, role as transporters in the visual system of *Drosophila*. Based on their expression patterns neither of the *organic cation transporter* genes, nor the Innexin1/ Innexin2 proteins is expressed in a manner consistent with a role in photoreceptor neurotransmitter related transport. The gene for *nonC* is not mapped to the *Drosophila* genome but mutations of *nonC* display a number of photoreceptor phenotypes, such as alterations in the ERG (Heisenberg and Götz, 1975; Pak, 1975), an increase in the concentration of head histamine (Meinertzhagen *et al.*, 2000), and a change in vesicle number and histamine distribution as well as alterations in the distribution of capitate projections (Meinertzhagen lab, unpublished data). Using the ERG phenotype I attempted to map the *nonC* gene to the X-chromosome. While I was unable to localise *nonC*, I was able to restrict its location to a few small cytological regions on the X-chromosome.

1.8 TRANSITION TO CHAPTER TWO

Three recognised lines of biological enquiry address what biological organisation is, how it functions and how it got there. In this thesis, I address these ‘‘what,’’ ‘‘how,’’ and ‘‘why’’ questions (Mayr, 1997) to the first optic neuropile of the fly’s visual system, in particular to its photoreceptor neurons and associated glial cells. The following chapter is a comprehensive review of the glial subtypes in the CNS of insects. This review was published in the April 2010 edition of *Progress in Neurobiology*. In it I define the subtypes of glia in the CNS of the adult, with a concentration on those in the visual and olfactory systems. Structure then gives way to function as the remainder of the chapter explores how different subtypes of glia are specially designed for their duties based on their structure, location and gene expression. The functions of glia include, but are not limited to, barrier formation, neurotransmitter uptake and cellular maintenance.

CHAPTER 2

THE FUNCTIONAL ORGANISATION OF GLIA IN THE ADULT BRAIN OF *DROSOPHILA* AND OTHER INSECTS

Tara N. Edwards and Ian A. Meinertzhagen

Manuscript submitted September 10, 2009, revised January 14, 2010 and accepted January 14, 2010. Available online January 29, 2010.

Published in *Progress in Neurobiology* 90(4): 471-497.

2.1 ABSTRACT

This review annotates and categorises the glia of adult *Drosophila* and other model insects and analyses the developmental origins of these in the *Drosophila* optic lobe. The functions of glia in the adult vary depending upon their sub-type and location in the brain. The task of annotating glia is essentially complete only for the glia of the fly's lamina, which comprise: two types of surface glia - the pseudocartridge and fenestrated glia; two types of cortex glia - the distal and proximal satellite glia; and two types of neuropile glia - the epithelial and marginal glia. We advocate that the term subretinal glia, as used to refer to both pseudocartridge and fenestrated glia, be abandoned. Other neuropiles contain similar glial subtypes, but other than the antennal lobes these have not been described in detail. Surface glia form the blood brain barrier, regulating the flow of substances into and out of the nervous system, both for the brain as a whole and the optic neuropiles in particular. Cortex glia provide a second level of barrier, wrapping axon fascicles and isolating neuronal cell bodies both from neighbouring brain regions and from their underlying neuropiles. Neuropile glia can be generated in the adult and a subtype, ensheathing glia, are responsible for cleaning up cellular debris during Wallerian degeneration. Both the neuropile ensheathing and astrocyte-like glia may be involved in clearing neurotransmitters from the extracellular space, thus modifying the levels of histamine, glutamate and possibly dopamine at the synapse to ultimately affect behaviour.

2.2 INTRODUCTION

Glia are important but relatively neglected players in nervous system function. They aid neuronal development by providing trophic support, landmarks for axonal pathfinding, cellular maintenance and neuronal insulation; they also function to regulate the extracellular space around mature neurons by acting in neurotransmitter clearance and recycling as well as in ionic regulation. Changes in glial function can manifest themselves in behaviours as varied as locomotion, sleep cycles, and mate choice. Unlike mammals, in which glia can account for up to 90% of brain cells (Blinkov and Glezer, 1968), insect nervous systems have far fewer glial cells, perhaps only 10% of the 90,000 cells estimated to occur in the adult Central Nervous System (CNS) of the fruit fly *Drosophila melanogaster* (Ito, pers. comm.).

Various genetic markers, for example expression of the genes *reversed polarity* (*repo*) or *glial cells missing* (*gcm*), exist for glia of the adult *Drosophila* nervous system, and as a result glial cells are now easily distinguished from neurons in this species. Amongst glia themselves though, even those with structural similarities, such as the glia of the larval peripheral nervous system (PNS), can have distinct origins and genetic identities (von Hilchen *et al.*, 2008). Just knowing the level of glial diversity within the larval CNS and PNS highlights our general ignorance of the diversity of subtypes in the adult CNS, in which different subpopulations of glial cells are poorly distinguished. While glial subtypes are diverse they can be categorized into five major subclasses, each further distinguished according to the particular neuropile with which the glia is associated. The use of alternative terminologies among members of these five subtypes has been a source of confusion in the field. Apart from the glia of the fly's visual and olfactory system, moreover, glial cell types have not been adequately identified for different regions of the brain. Studies from other systems and insect species, such as the tobacco hornworm moth *Manduca sexta* or the honeybee *Apis mellifera*, provide valuable anatomical information, yet the availability of genetic tools and approaches in *Drosophila* makes this clearly the most propitious insect in which to analyse the functional roles of glia in the adult insect nervous system. These roles include not only their molecular functions but also the effects of glia on nervous system survival, function and ultimately, behaviour.

2.2.1 Types of Glia

Glia can be classified by their location, their ultrastructure (Hoyle, 1986), function or patterns of gene expression (Table 2.1). In flies such as *Drosophila* or the housefly *Musca domestica*, glial types are divisible into four (Freeman and Doherty, 2006) or five (Awasaki *et al.*, 2008) groups, which can then be further subdivided into unique classes for each region of the brain (Freeman and Doherty, 2006). The insect brain is a complex of three fused bilateral ganglia each with its own cell bodies and neuropile (Mobbs, 1985): the paired visual protocerebrum, the paired deutocerebrum which processes sensory information from the antennae, and the central tritocerebrum which integrates information from other systems (Figure 2.3B). Each region is composed of many neuropiles. Insect neurons are monopolar and have cell bodies distributed in a rind or cortex that surrounds the neuropile (Strausfeld, 1976). The general classification of

nervous system glia assigns the cells to different compartments of the CNS: 1) to the ganglionic surface around the brain, 2) to the cortex, and 3) amongst the synapses in the neuropile. Additional glial cell types such as wrapping glia exist in the peripheral nervous system (Stork *et al.*, 2008).

2.2.1.1 SURFACE GLIA

Flattened surface glia constitute the externalmost layer of the blood brain barrier (BBB) that isolates the nervous system from the haemolymph of the insect's open circulatory system. They are composed of two types of glia that can be distinguished by their location and cell shape: perineurial (apical) cells, which are covered by a thick extracellular matrix, the neural lamella, and subperineurial (basal) glia.

Perineurial glia lie on the ganglionic surface and have small elongate nuclei. These glia develop postembryonically, in a non-*glial cells missing* (*gcm*)-dependent manner (Awasaki *et al.*, 2008) and thus likely function only in the BBB of the adult. The exact function of the perineurial glia is not known. Subperineurial glia form an inner layer of large, sheet-like glia and are rich in septate junctions, which are proposed to be the principal component of the larval BBB (see: Bainton *et al.*, 2005; Schwabe *et al.*, 2005; Stork *et al.*, 2008). Awasaki *et al.* (2008) suggest that these two glial cell layers, with their differential patterns of gene expression, play non-overlapping complementary roles in regulating the permeability of the BBB. There has been some question in the literature whether the immature perineurial cells of embryos are actually glia and not haemocytes (Pereanu *et al.*, 2005). Unlike other glia, which are derived from the epithelium, the perineurial cells derive from the mesoderm (Edwards *et al.*, 1993) and do not express the glial cell marker *repo* early in their development (Hartenstein *et al.*, 1998). Yet, recent evidence suggests that perineurial cells are, in fact, a specialised subset of *repo* expressing glia which are developmentally delayed and which do inevitably express glial specific markers in the larva and early pupal stages (Awasaki *et al.*, 2008; Stork *et al.*, 2008). The identification of perineurial cells as glia is further supported by the fact that *repo* is never expressed in GCM-positive haemocytes (Lee and Jones, 2005).

TABLE 2.1 - SPECIFIC DRIVER LINES FOR GLIA OF THE *DROSOPHILA* CNS

GLIAL TYPE	DRIVER LINE	REFERENCE
LARVA		
eye disc, optic stalk, carpet glia	*M1-126*	Choi and Benzer, 1994
larval eye disc surface glia	*c527-GAL4*	Hummel *et al.*, 2002
larval eye disc wrapping glia	*Mz97-GAL4*	Hummel *et al.*, 2002
larval eye disc wrapping glia	*ptc-GAL4*	Murakami *et al.*, 2007
larval eye disc and optic stalk surface glia	*NP4702-GAL4*	Murakami *et al.*, 2007
larval eye disc surface glia and wrapping glia	*NP2109-GAL4*	Murakami *et al.*, 2007
larval eye disc surface and wrapping glia, optic lobe surface glia	*NP3053-GAL4*	Murakami *et al.*, 2007
PUPA and ADULT		
perineurial	*NP6293-GAL4*	Awasaki *et al.*, 2008
subperineural	*NP2276-GAL4*	Awasaki *et al.*, 2008
cortex	*NP577-GAL4*	Awasaki *et al.*, 2008
cortex	*NP2222-GAL4*	Awasaki *et al.*, 2008
astrocyte-like	*NP3233-GAL4*	Awasaki *et al.*, 2008
astrocyte-like	*NP1243-GAL4*	Awasaki *et al.*, 2008
ensheathing	*NP6520-GAL4*	Awasaki *et al.*, 2008
ensheathing and cortex (weakly)	*NP1243-GAL4*	Awasaki *et al.*, 2008
cortex (weakly)	*NP6520-GAL4*	Awasaki *et al.*, 2008
antenna perineural glia, antennal lobe commissure glia	*Mz317-GAL4*	Sen *et al.*, 2005; Yao *et al.,* 2007
antennal coeloconic independent glia	*GH146-GAL4*	Sen *et al.*, 2005
cortex glia, some neuropile glia, chiasm glia	*Nrv2-GAL4*	Oland *et al*., 2008; Górska-Andrzejak *et al*., 2009; Mayer *et al*., 2009
ensheathing glia of the antennal lobe	*Mz0709-GAL4*	Doherty *et al*., 2009
astrocyte-like glia of the antennal lobe	*dEAAT1-GAL4*	Doherty *et al*., 2009
astrocyte-like glia of the antennal lobe	*alrm-GAL4*	Doherty *et al*., 2009

2.2.1.2 CORTEX GLIA

Cortex glia are embedded amongst and maintain close contact with the somata of neurons in the cortex of the CNS (Freeman and Doherty, 2006). Anatomically they form a mesh in the cortex and one cortex glial cell can enwrap many neuronal cell bodies (Awasaki *et al.*, 2008). In the visual system all cortex glia are called satellite glia (Eule *et al.*, 1995; Tix *et al.*, 1997), of which there are two distinct types in the lamina, each surrounding the cell bodies of distinct classes of neurons. It is unknown if other neuropiles contain multiple types of cortex glia.

2.2.1.3 NEUROPILE GLIA

Neuropile glia have their nuclei in the synaptic neuropile, are associated with axons and axon fascicles, and extend sheath-like membranes around axon bundles. They help to isolate nerves and may promote neuronal survival through trophic support. Neuropile glia can be either: 1) ensheathing and fibrous; or 2) dendritic and astrocyte-like. Ensheathing glia are lamellar, extending processes along the outer surface of the neuropile to isolate neurons. Astrocyte glia, on the other hand, elaborate extensive processes in the neuropile where spatial considerations dictate that they must be associated with synaptic regions and thus could modulate neural connections. They were depicted from Golgi impregnation in early accounts (e.g., Sánchez y Sánchez, 1935) and have only recently been referred to as astrocyte-like (Awasaki *et al.*, 2008) although they differ genetically from their namesakes, the astrocyte glia of the vertebrate brain.

2.2.1.4 A PREVIOUSLY UNCLASSIFIED SUBTYPE: TRACT GLIA?

Another subset of glia wraps axon tracts which project between neuropiles. The tracts in the adult insect brain are too numerous to list comprehensively, but include the outer (between lamina and medulla) and inner (between medulla and lobula neuropiles) optic chiasmata in the visual system; and in the olfactory system, the commissure connecting the two antennal lobes (Yao *et al.*, 2007), multiple antennocerebral tracts that connect the antennal lobes to the mushroom bodies, or the protocerebrocalycal tracts that connect the α- and β-lobes of the mushroom bodies to the calyx through the peduncle (Strausfeld, 1976).

While glia have long been known to surround these tracts they are categorized in only a single study (Tix *et al.*, 1997) as their own subtype within the CNS. Their singularity lies in the fact that they lack characteristics that would allow them to be grouped with any of other known glial subtypes. They are not surface glia because they do not lie on the surface of the brain. Although their cell bodies lie near the cortex they are not cortex glia because they are not restricted to the cortex and do not surround neuronal cell bodies. Nor are they neuropile glia. While they are often classified as neuropile glia, and are similar to the ensheathing subtype, their cell bodies are not within the neuropile nor are they associated with synapses. Some of these glia may be considered equivalent to the interface glia which line axon tracts along the embryonic ventral nerve cord, while the glia of the optic chiasms have drawn comparison to the midline glia of the ventral nerve cord (Tix *et al.*, 1997). The tract glia may, in fact, be two distinct types of glia with the same enwrapping, lamellar morphology, distinguished by those which form chiasms and those which do not. Tract glia within the adult CNS are likely distinct from wrapping glia in the PNS associated with afferent sensory neurons or the *GH146-GAL4*-expressing nerve layer glia of the antenna (Sen *et al.*, 2005).

2.2.1.5 Invertebrate Glia May Have Functional Similarities to Mammalian Glia

Glia of the insect brain, while distinct from their mammalian counterparts, do share some common features. The most obvious difference between mammalian and insect glia is simply in their numbers in the CNS, with glia being the most abundant cell type in the mammalian brain, yet comprising as few as 10-25% of the cells in the insect brain (Ito, pers. comm; Pfrieger and Barres, 1995). Furthermore, *gcm* is essential for glial specification in *Drosophila* (Jones *et al.*, 1995), but not in mammals (Kim *et al.*, 1998). While axon bundles in insects are ensheathed by glia, the axons themselves are not associated with any type of Schwann cell or oligodentrocyte-like myelin sheath, although *Drosophila* glia express Neurexin, a key junctional protein component required for vertebrate myelination (Baumgartner *et al.*, 1996; Bhat *et al.*, 2001). Similarities also exist in glial structure. Astrocyte-shaped glia exist within the synaptic neuropiles of *Drosophila* (Awasaki *et al.*, 2008). Similarly, neuropile glia could be considered oligodendrocyte-like in that they wrap and guide individual axons during development (Chotard and Salecker, 2004) but astrocyte-like in that they are involved in the regulation

of neurotransmitter recycling in the adult (Borycz *et al.*, 2002; Richardt *et al.*, 2002; Richardt *et al.*, 2003). Immune-associated microglia have not been reported in *Drosophila*. Instead the neuropile ensheathing glia, with cell bodies at the cortex/neuropile border, are responsible for engulfing degenerating axons (Doherty *et al.*, 2009). For a more comprehensive review of the similarites between mammalian and *Drosophila* glia see Freeman and Doherty (2006).

2.3 SYSTEMS GLIA

Glia can be further subdivided according to the neuropile with which they are associated and by the locations they occupy within that neuropile.

2.3.1 OPTIC LOBE GLIA

The glia of the fly's visual system have several distinct morphological subtypes that have been described in extensive detail for the first optic neuropile, or lamina (Figure 2.1), of *Musca* (Saint Marie and Carlson, 1983b) as well as the second optic neuropile, or medulla, and the associated chiasmata of the optic lobe in *Drosophila* (Tix *et al.*, 1997).

2.3.1.1 FUNCTIONAL ANATOMY OF IDENTIFIED GLIA IN THE LAMINA

The compound eye of *Drosophila* is composed of approximately 800 unit ommatidia, each containing a fixed complement of cells. These include eight photoreceptor neurons as well as the pigment and cone support cells (Wolff and Ready, 1993). Each photoreceptor axon terminates in one of three different strata of the optic lobe, depending upon the opsin expression of its soma and thus its spectral sensitivity. Photoreceptors R1-R6 have axons that terminate in the lamina, sorting at the distal face of the lamina so as to converge upon a unit column, or cartridge, along with other R1-R6 axons that signal the same point in visual space according to a principle of neuronal superposition (Braitenberg, 1967). The terminals of R1-R6 release the neurotransmitter histamine (Hardie, 1987; Sarthy, 1991) and thereby signal to lamina monopolar neurons L1-L3 and amacrine cells (Burkhardt and Braitenberg, 1976; Nicol and Meinertzhagen, 1982; Meinertzhagen and O'Neil, 1991). To optimize spatial resolution the cartridges are

electrically and chemically isolated by the highly organised system of glial barriers which surrounds each cartridge (Shaw, 1984a).

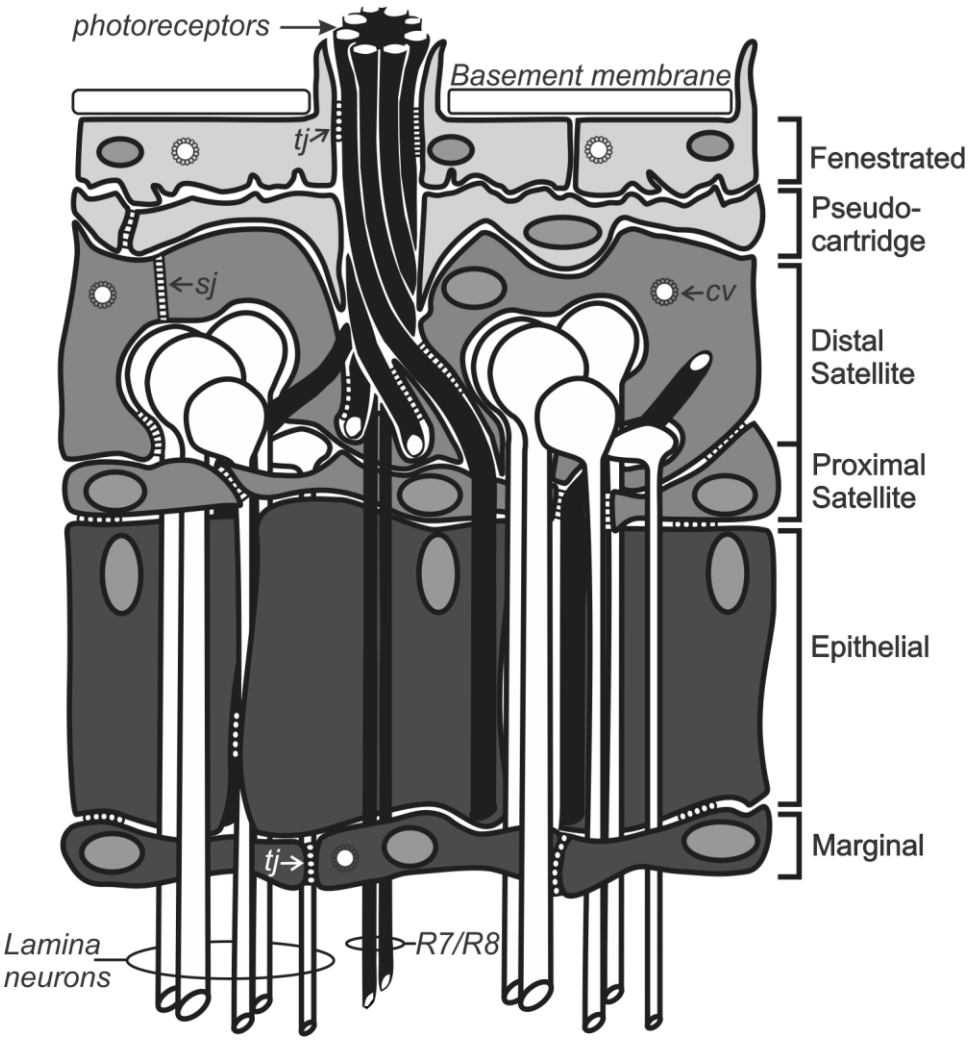

FIGURE 2.1 - GLIA IN THE ADULT FLY LAMINA.

The lamina of the adult optic lobe of the fly is populated by six distinct classs of glia. These include (from distal to proximal) two types of surface glia - the fenestrated and pseudocartridge glia; two types of cortex glia - the distal and proximal satellite glia; and two types of neuropile glia - the epithelial and marginal glia. Septate junctions (*sj*) connect the distal satellite glia and are an integral part of the blood brain barrier. Tight junctions (*tj*) are more common in the proximal glial layers, although their presence between photoreceptors and fenestrated glia has been disputed (Shaw, 1984a). The outermost glia also contain clathrin coated vesicles (*cv*) and engage in clathrin-mediated endocytosis. Figure modified from Saint-Marie and Carlson (1993a).

Within the lamina six morphologically distinct classes of glial cell form successive populations, arranged from distal to proximal, as follows: the fenestrated glia, pseudocartridge glia, distal and proximal satellite glia, epithelial glia and marginal glia. The functions and expression patterns of some of these subtypes are presented below, followed by an evaluation of their developmental origins. The migration pathways into the lamina and the origins of these cells, as determined by clonal mosaic analysis, suggests that at least some of the subtypes have distinct identities from early in development (Winberg *et al.*, 1992; Perez and Steller, 1996; Dearborn and Kunes, 2004).

2.3.1.1.1 FENESTRATED GLIA

Fenestrated and pseudocartridge glia, as originally described in *Musca* (Saint Marie and Carlson, 1983a), are often incorrectly grouped into a single class called the sub-retinal glia (Winberg *et al.*, 1992). However, these two surface glial layers are separate subtypes that are anatomically unique and have distinct functions. In *Musca*, fenestrated glia are evenly distributed in an array, one per ommatidium (Saint Marie and Carlson, 1983a) so as to form a monolayer with a highly involuted membrane surface. They extend processes which not only ensheathe photoreceptors and tracheae but also penetrate the basement membrane and enter the retina (Saint Marie and Carlson, 1983a).

Their location likens them to a type of surface glia, the perineurial glia. Although sometimes proposed to be a part of the BBB their principle function is not as a barrier because they allow the longitudinal passage of colloidal lanthanum (Saint Marie and Carlson, 1983a). While these glia do contain pleated septate junctions, which can provide a barrier to diffusion of solutes through the extracellular space (Juang and Carlson, 1992), those junctions are located principally between the glia and the photoreceptor axons they ensheathe, and not between the glial cells themselves, which are connected only by adhering junctions such as desmosomes or intercellular gap junctions (Chi and Carlson, 1980). Tight junctions have also been reported to exist between glia and photoreceptors in *Musca* (Saint Marie and Carlson, 1983b), a finding that Shaw (1984a) was unable to replicate, however.

Instead of an insulating role, the undulated apical surface, presence of coated vesicles, and ability to take up colloidal lanthanum (Saint Marie and Carlson, 1983a) together suggest that fenestrated glia in *Musca* have pinocytotic activity and may be involved in clearing neurotransmitter or toxins from the extracellular space and in controlling ion fluctuations (Saint Marie and Carlson, 1983a; Carlson and Saint-Marie, 1990). While the fenestrated glia of *Musca* contain coated vesicles (Saint Marie and Carlson, 1983a), those in *Drosophila* express coated-vesicle associated genes such as the clathrin binding AP-3β adaptin gene *ruby* (Kretzschmar *et al.*, 2000) and are immunoreactive for the vesicular monoamine transporter vMAT (Romero-Calderón *et al.*, 2008). A distinct band of immunolabelling to histamine, presumably of photoreceptor origin, is found in the fenestrated glia in wild-type *Drosophila* (Borycz *et al.*, 2002; Romero-Calderón *et al.*, 2008). This, along with a lack of the histamine synthesis enzyme *histidine decarboxylase* (*hdc*; Burg *et al.*, 1993; Thimgan *et al.*, 2006) suggests that histamine may enter these glia by means of endocytotic uptake. These glia may not have completely identical functions in different Dipteran species, however, since fenestrated glia in *Drosophila* contain pigment granules (Kretzschmar *et al.*, 2000) while those in *Musca* do not (Saint Marie and Carlson, 1983a).

2.3.1.1.2 PSEUDOCARTRIDGE GLIA

In adult *Musca domestica*, the pseudocartridge glia can be identified by their position beneath the fenestrated glia and by their abundant horizontal microtubules, long nuclei, and larger cells, which are up to 15μm wide and 2 to 10μm deep, sufficient to enwrap the axons from neighbouring rows of ommatidia. These glia also contain coated vesicles suggesting that they too partake in endocytosis (Saint Marie and Carlson, 1983a), but unlike the fenestrated glia this cell layer contains many more septate junctions, especially between the cells' long interdigitating processes. Both the presence of septate junctions and the increased surface area of these glia that results from interdigitation (Saint Marie and Carlson, 1983b) suggest that these glia are equivalent to the subperineurial glia found elsewhere on the surface of the brain, and thus may form the 'barrier' layer of the eye-brain barrier, as suggested by Shaw and Varney (1999).

In the pseudocartridge region, septate junctions are found not only between pseudocartridge glia themselves but also between the axons of photoreceptors which enter the lamina (Saint Marie and Carlson, 1983b). The role of pseudocartridge glia as

the most external boundary of the BBB is supported by an inability of colloidal lanthanum to penetrate deeply into their septate junctions (Saint Marie and Carlson, 1983b). Despite forming such a barrier, the surfaces of fenestrated and satellite glia that abut the pseudocartridge glia on either face are connected by gap junctions, as are the pseudocartridge glia among themselves (Saint Marie and Carlson, 1983b), suggesting that an intercellular network exists between these three classes of glia, at least in *Musca*.

2.3.1.1.3 SATELLITE GLIA

Satellite glia are a class of cortex glia divisible into two distinct types, distal (or rind) glia that ensheathe the cell bodies of monopolar neurons in the lamina cortex, and proximal (or interface) glia that invest the photoreceptor axon bundles and the necks of monopolar neurons (Saint Marie and Carlson, 1983a). Both subtypes can also be distinguished in *Drosophila* (Eule *et al.*, 1995). In *Musca*, only the distal-most glia contain endocytotic coated vesicles, but both subtypes are part of the glial network by virtue of forming gap junctions with their glial neighbours. They form septate junctions, desmosomes and occluding tight junctions, with more septate junctions found proximally, where the glia wrap axonal bundles of photoreceptors and monopolar neurons (Saint Marie and Carlson, 1983b). As a result of their extensive septate junctions the satellite glia may act as a second layer of the BBB.

2.3.1.1.4 EPITHELIAL GLIA

Epithelial glia are neuropile glia which extend throughout the depth of the lamina neuropile. They constitute the sole class of cells with nuclei in the distal neuropile proper, a unique diagnostic characteristic. Groups of lamina neurons are surrounded by a triad of epithelial glia to form a cartridge, and any one glial cell also ensheathes the three neighbouring cartridges, as first identified in *Musca* (Boschek, 1971) and later confirmed in *Drosophila* (Meinertzhagen and O'Neil, 1991). Both tight and gap junctions are found at epithelial glia membrane appositions as well as at their base and apex where they contact marginal and satellite glia respectively (Saint Marie and Carlson, 1983b).

Epithelial glia differ from other lamina glia in exhibiting two anatomically distinct organelle junctions: 1) capitate projections, dynamic invaginations from glia with a spherical head (Trujillo-Cenóz, 1965); and 2) bulbous projections called gnarls (Campos-Ortega and Strausfeld, 1973), which are planar in *Drosophila* (Meinertzhagen and O'Neil, 1991), and extend into the β neurites of T1 neurons. These glia also insinuate themselves at plaque contacts between T1 and photoreceptor terminals and are also occasional postsynaptic elements at histaminergic tetrad synapses (Meinertzhagen and O'Neil, 1991).

Epithelial glia that insert at gnarl junctions between the α processes of amacrine cells and the β neurites of T1 neurons are also technically postsynaptic to those α processes in both *Lucilia* (Shaw, 1984a) and *Drosophila* (Meinertzhagen and O'Neil, 1991). While the transmitter of amacrine cells is still not known, these cells strongly express immunoreactivity to vesicular glutamate transporter, vGluT (Sinakevitch and Strausfeld, 2004; Kolodziejczyk *et al.*, 2008), while T1 neurons at the same synapse are identifiable with an Excitatory amino acid transporter (EAAT) driver line, *dEAAT-GAL4* (Hamanaka and Meinertzhagen, 2010), also compatible with a glutamate phenotype. Thus, it is possible that epithelial glia respond to and regulate clearance of at least two neurotransmitters: histamine at the photoreceptor tetrads, and glutamate at gnarl contacts. Histamine acts as an inhibitory (sign-reversing) neurotransmitter at the former, and glutamate would most probably act as an excitatory neurotransmitter at the latter.

The membranes of the epithelial glia are deeply infolded as well as highly branched amongst the neurons they ensheathe (Saint Marie and Carlson, 1983a) features that contribute to the glia's ability to form individual electrical barriers around each cartridge as well as to produce the high electrical resistance that exists between the retina and lamina (Shaw, 1975). The glia themselves signal their postsynaptic location at the histaminergic tetrad synapses of the photoreceptor (Shaw, 1984a; Meinertzhagen and O'Neil, 1991) by expressing the first of two histamine-gated chloride receptor channel proteins, called variously HA-Cl I (Witte *et al.*, 2002), HisCl1 (Zheng *et al.*, 2002) or HclB (Gengs *et al.*, 2002) on their surface (Gao *et al.*, 2008). These "gliapses" and the presumed Cl^- influx that results from histamine activation of their receptor appear to play a role in shaping the 'on' transient component of the electroretinogram (ERG; Figure 2.4C; Shaw, 1984a; Meinertzhagen and O'Neil, 1991; Sinakevitch and Strausfeld, 2004; Kolodziejczyk *et al.*, 2008; Pantazis *et al.*, 2008). Finally, epithelial glia are reported to

have phagocytic properties, as revealed by their role in engulfing profiles of R1-R6 terminals that undergo degeneration in the *Drosophila* mutant *retinal degeneration B* (Stark and Carlson, 1982), and in experimentally induced photoreceptor degeration in *Musca* (Brandstätter *et al*., 1991).

2.3.1.1.5 MARGINAL GLIA

The lamina is bounded on its proximal surface by a layer of overlapping marginal glia, one per cartridge (Saint Marie and Carlson, 1983a; Eule *et al.,* 1995). At their apices these extend processes into the lamina neuropile, enveloping all axons and tracheae as they exit or enter the lamina. Thus, they seal off the lamina extracellular space from the underlying optic lobe. The marginal glia of *Musca* also contain coated vesicles (Saint Marie and Carlson, 1983a) just like the glia of the distal lamina and may thus have endocytotic properties.

Tight junctions are particularly abundant in marginal glia of *Musca* and can be found between the glia themselves and between glia and axons. Desmosomes and occasional gap junctions also connect the marginal glia but they lack the septate junctions typical of the BBB in the more distal glia of the lamina (Saint Marie and Carlson, 1983b). Functionally, the marginal glia with their extensive tight junctions form the seat of the resistance barrier that exists in the lamina (Saint Marie and Carlson, 1983b).

2.3.1.1.6 GLIA OF THE DEEPER OPTIC LOBE REGIONS

The glia of the inner optic neuropiles have been less well characterised using *LacZ* enhancer trap lines (Eule *et al.,* 1995; Tix *et al.*, 1997) that are no longer available. Nonetheless, they reveal numerous major glial classes (Figure 2.3C): 1) giant optic chiasm glia which are arranged in rows between successive dorsoventral sheets of intercrossing fibres of the outer and inner chiasmata; these have an early origin (Eule *et al*., 1995; Tix *et al.*, 1997) and are visible in the larval brain (Meinertzhagen, 1973; Tix *et al.*, 1997); 2) small outer optic chiasm glia associated with the the axon bundles; 3) cortex glia of the medulla (medulla satellite glia), and lobula complex (lobula plate satellite glia); and, 4) other neuropile glia such as the medulla neuropile glia, that form an interface layer with cell bodies in the medulla cortex and have processes that extend deep into the neuropile, and the lobula and lobula plate neuropile glia (Eule *et al*., 1995;

Tix *et al.*, 1997). No distinction has yet been made between the ensheathing and astrocyte-like glia in these neuropiles. Chandelier cells have been consistently described as lying at the limit of the medulla and the inner optic chiasm in some Diptera, Odonata and bees, but have not yet been identified in *Drosophila*. These are astrocyte-like neuropile glia with a cell body near the chiasma and arbors that extend distally, up into the columns of the medulla (Sánchez y Sánchez, 1935; Cantera and Trujillo-Cenóz, 1996).

2.3.1.2 THE DEVELOPMENTAL ORIGINS OF LAMINA OPTIC LOBE GLIA

The distinction between the three proximal-most layers of lamina glia, the satellite, epithelial and marginal glia, can be observed early in development from the positions these cells occupy in the developing optic lobe (Winberg *et al.*, 1992; Perez and Steller, 1996; Dearborn and Kunes, 2004; Chotard *et al.*, 2005). Epithelial and marginal glia cells originate from the dorsal and ventral glial precursor cell areas, which lie near the bilaterally located lamina furrows of the outer optic anlage (Chotard *et al.*, 2005). This region of the glial precursor zone (GPZ), alternatively known as subdomain I, can be distinguished in the larva by its expression of *wingless*, *optomotor blind* and *dachsous* (Dearborn and Kunes, 2004). While recent reports do not discuss an origin for the satellite glia from these glial precursor cell areas (Dearborn and Kunes, 2004; Chotard *et al.*, 2005), a group of satellite glia does in fact label with green fluorescent protein (GFP) and bromodeoxyuridine (BrdU) in glial mitotic clones that also label epithelial and marginal glia (Winberg *et al.*, 1992; Perez and Steller, 1996). *MARCM* (Mosaic Analysis with a Repressible Cell Marker) analysis of glial origins in other areas of the *Drosophila* brain suggests that neuropile glia and cortex glia have distinct origins, with cortex glia precursors originating during embryogenesis and neuropile glial precursors developing during larval and pupal stages (Awasaki *et al.*, 2008). If this generalisation were to hold true for the visual system as well, then the distal satellite glia should have a separate origin from the epithelial and marginal glia. The uncertainty regarding the origin of satellite glia, either deriving from subdomain I along with the neuropile glia or from a distinct source, may derive from BrdU incorporation into distinct subsets of simultaneously dividing cells. Thus, it is quite likely that satellite glia have distinct origins with all marginal, epithelial, and satellite glia originating concurrently as development of the visual system proceeds from the late second-instar stage onward. For a more

extensive review of optic lobe glial development, see: Chotard *et al*., (1995), Chotard and Salecker (2007) and Perez and Steller (1996), who indicate the developmental origins of these three layers of glia.

For the satellite glia, most researchers have not distinguished between the proximal (or interface) and distal (or rind) subtypes previously identified in *Musca* (Saint Marie and Carlson, 1983a) and *Drosophila* (Eule *et al.,* 1995). These not only have distinct anatomical features (Saint Marie and Carlson, 1983a; Eule *et al.,* 1995) but also have distinct genetic identities with the proximal satellite glia expressing Ebony (Wagner *et al.*, 2007; interpreted from their figure 4D) and the distal satellite glia expressing the Na^+/K^+-ATPase *Nervana2* (Górska-Andrzejak *et al.*, 2009). They may also have distinct origins in the larva. It might be that only the proximal, or interface, satellite glia originate in the brain, if their proposed *ebony* expression were to ally them to their possible developmental kin, the epithelial glia, which also express *ebony* (Richardt *et al.*, 2002). The distal satellite glia, on the other hand, may be derived from a population of glia migrating from the eye disc. It is quite possible that the border between those glia that derive from the eye disc and those that derive from the optic lobe may thus fall between the distal and proximal satellite glia. Resolution of these subtypes and their likely separate developmental origins awaits the isolation of appropriate markers.

Distal to these lamina glia, the nomenclature and developmental origins of the remaining two classes of adult lamina glia, fenestrated and pseudocartridge, are yet more ambiguous. In fact, much of the current literature frequently makes no distinction between these two surface glial layers of the adult lamina, those underlying the basement membrane of the retina. This has resulted in confusing terminology in reference to them, the most common shortcoming of which is referring to them by a single classification – the subretinal glia. Nevertheless, these two layers contain different glial subtypes that are in fact separate entities, possibly, with distinct origins (Winberg *et al.*, 1992; Perez and Steller, 1996). We will start with a review of the terminology in current usage, before proceeding to a suggested resolution.

2.3.1.2.1 Naming Schemes of the Larval Visual System Glia: An Historical Perspective

Various names have been applied to glial cells that come to underlie the developing retina. Thus, retinal basal glia (RBG) are reported in the larva to arise from the optic

stalk and migrate centrifugally into the eye disc (Choi and Benzer, 1994) where they then help guide outgrowing photoreceptor axons towards the optic stalk (Hummel *et al.*, 2002). Another glial cell type, the subretinal glia, is also reported at the distalmost surface of the larval optic lobe (Perez and Steller, 1996). Mitotic clones of glial cells originating in the larval optic stalk give rise to labelled cells in the eye disc, optic stalk and developing distal lamina, suggesting a single origin for these 'subretinal glia', 'optic stalk glia' and 'retinal basal glia' and yet, when the optic stalk and supposed source of glial cells is eliminated, as in *disconnected (disco)* mutants, some RK2-(Repo) expressing glia persist on the brain's surface, suggesting that there may be two populations of 'subretinal glia' and that at least some of these cells have a distinct origin (Perez and Steller, 1996). Reasons that invoke embryonic explanations for how some distal lamina glia may survive despite the loss of the larval optic stalk in *disco* mutants can be advanced. As the larval photoreceptors in Bolwig's organ develop, their axons navigate a path through the brain along a series guidepost cells and this path is lined by three genetically distinct types of glia (Schmucker *et al.*, 1997). The optic stalk develops around the axons of Bolwig's organ and becomes externalized as the eye disc evaginates from the brain (Younossi-Hartenstein *et al.*, 1993). While the fate of glial cells within the embryonic optic stalk is not known they are likely to be the precursors of the larval optic stalk glia. When the axons of Bolwig's organ mistarget in the *disco* mutant, the glial cells remain in their appropriate positions along the presumptive embryonic optic stalk (Schmucker *et al.*, 1997). It is possible that in the absence of an optic stalk these glia persist in the brain and are capable of dividing to produce glia that occupy a position at the distalmost surface of the optic lobe. These possible explanations for the action of *disco* are not mutually exclusive and the validity of each would require separate investigation.

One further distinction needs to be made with respect to the larval subretinal glia. The subretinal glia of the optic lobe (Winberg *et al*., 1992; Perez and Steller, 1996) are distinct from subretinal cells that contain pigment granules and are described as originating later in development from the pupal eye disc (Cagan and Ready, 1989a). Their naming schemes make it easy to confuse these glial terminologies despite the fact that the larval subretinal glia (Winberg *et al*., 1992; Perez and Steller, 1996) are found in the larval brain while the subretinal cells are found in the eye disc (Cagan and Ready, 1989a). Furthermore, there is no evidence in the current literature to support the existence of a true glial cell type in the eye disc with any origin other than the optic stalk

(Rangarajan *et al.*, 2001; Hummel *et al.*, 2002; Silies *et al.*, 2007). Despite the terminologies and possibly also their identification being frequently interchanged in the literature (see: Winberg *et al.*, 1992; Xiong *et al.*, 1994), there is no evidence to suggest that larval subretinal glia of the optic lobe that derive, in part, from the optic stalk (Perez and Steller, 1996) and the pupal subretinal cells of the eye disc (Cagan and Ready, 1989a) are one and the same. To complicate matters, both the fenestrated and pseudocartridge glia of the adult are grouped as subretinal glia, and yet there is no evidence that either the larval subretinal glia or subretinal cells corresponds to the fenestrated or pseudocartridge glia of the adult. For all these reasons we advocate the abandonment of the term subretinal glia in reference to adult lamina glia as both confusing and inaccurate. To clarify the nomenclature of *Drosophila* optic lobe glia at various stages of development, we therefore include a table of recommended terminologies (Table 2.2).

2.3.1.2.2 THE GLIA OF THE EYE DISC AND OPTIC STALK

The photoreceptors, which differentiate in a posterior to anterior sequence, secrete Decepentaplegic (Dpp) and Hedgehog (hh) to influence both the proliferative and migratory behaviour of basally located surface glia (Rangarajan *et al.*, 2001). Studies on glial migration in the casein kinase mutant *gilgamesh* as well as of flies that overexpress *tramtrack69,* which can repress mitosis in surface glia, support the finding that glia of the eye disc originate in the optic stalk and that they migrate into the disc so as to first occupy positions from the posterior edge of the eye, then more anterior locations (Hummel *et al.*, 2002). Further support comes most recently from the work of Silies *et al.* (2007) which reveals that glia migrate into the eye disc along large carpet glia, a type of subperineurial glia that expresses *moody* and otherwise restricts the premature anterior migration of glia. Distinct enhancer trap lines reveal moreover that the eye disc contains at least two types of glial cells, surface and wrapping glia (Hummel *et al.*, 2002), while analysis of glial mitotic clones using *repoFLP* transgenic flies suggests that throughout the different stages of eye disc development no less than six anatomically distinct glial types can be distinguished (Figure 2.2; Silies *et al.*, 2007). These are: 1) fusiform-shaped optic stalk glia; 2) perineurial surface glia which lie along the basal surface of the eye disc and migrate anteriorly; 3) wrapping glia that lie above the outgrowing photoreceptor axons and ensheathe bundles of axons; 4) an undifferentiated

population of glia that lies close to the morphogenetic furrow and has filopodia; 5) peripherally located marginal glia cells at the margins of the eye disc, that have an elongated clapboard-like shape; and 6) two large, flat, basally-located, carpet glia, each with a large nucleus and containing septate junctions (Silies *et al.*, 2007). Other surface glia can be detected between the photoreceptor cell bodies and their axons by the *c527-GAL4* reporter line (Hummel *et al.,* 2002). The marginal glia in the larval eye disc (Silies *et al.*, 2007) are not to be confused with the neuropile marginal glia at the base of the lamina in the adult.

Wrapping glia differ from surface glia, in that they are delayed in migrating to the eye disc, and are not involved in directing photoreceptor axons toward the optic stalk. This delay occurs because wrapping glia derive from a subpopulation of mitotically active surface glia that delaminate and migrate inward. Migrating glia, triggered by Fibroblast Growth Factor (FGF) Receptor activation, differentiate when they reach the anterior edge of the carpet glia and come into contact with the epithelium and newly differentiated photoreceptors (Silies *et al.*, 2007; Franzdóttir *et al.*, 2009). Choi and Benzer's (1994) findings that RBG/wrapping glia labelled by *M1-126* do not migrate into the eye in eyeless mutants (*eyes absent* and *sine oculus*) may not actually indicate a failure of glia to migrate, but instead a failure of glia to differentiate from perineurial surface glia into *M1-126-LacZ* labelled wrapping glia, since this would normally occur only when these glia contact photoreceptors expressing the FGF8-like ligand Thisbe (Franzdóttir *et al.*, 2009).

FLP-out clonal analysis of glial cell types (Rangarajan *et al.*, 1999) suggests that the large carpet glia are clonally related to the 'retinal basal glia' since both are labelled, although carpet cells are not yet anatomically recognized as a distinct glial subset, in a GFP labelled cell lineage derived from a single clone. Furthermore, Choi and Benzer (1994) report two, and only two, large *M1-126-LacZ* positive nuclei in the optic stalk of the second-instar larva, which could correspond to the large carpet glia nuclei. Only later in development, at about the third-instar stage, do more *M1-126-LacZ* positive RBG, with a wrapping glial morphology, appear in the optic stalk. These continue to increase in number over time (Choi and Benzer, 1994). Therefore, the glia referred to as RBG (Choi and Benzer, 1994) appear to correspond to two different types of glia now identified as wrapping glia and carpet glia (Silies *et al*., 2007). The fact that wrapping glia appear to be clonally related to carpet glia (Rangarajan *et al.*, 1999), and are yet

known to form as a result of delamination from surface glia (Silies *et al.*, 2007), suggests that all three glial types (carpet, wrapping and surface) originate from a single precursor type. Again, confirmation of this suggestion must await the availability of suitable markers.

Two further observations on optic stalk glia are pertinent. First, in addition to a population of fusiform perineurial glia (the optic stalk glia) that forms a dense mesh of cells surrounding the photoreceptor axons, the optic stalk also contains an inner glia cell population. While the perineurial glia form a component of the blood brain barrier, the inner glia separate the fascicles of ommatidial axons from those of the unwrapped Bolwig's neuron photoreceptors (Silies *et al.*, 2007). The fate of these inner glia in the adult is unknown since they have not been traced through pupal metamorphosis. Optic stalk glia can also be distinguished by expression of the glial driver line *NP7402*, even in second-instar larvae, before photoreceptor axons enter the brain (Murakami *et al.*, 2007). As more and more photoreceptor axons grow down into the optic stalk and penetrate the brain, the optic stalk enlarges to accommodate them, but *sine oculis* mutants demonstrate that the photoreceptors are not required for this enlargement to take place. Glia not only increase in number but the diameter of the optic stalk also increases even before photoreceptor axon ingrowth occurs (Murakami *et al.*, 2007). Glial cell division in the optic stalk depends upon glia-glia intercellular signalling by the FGF8-like ligand Pyramus and activation of its receptor Heartless (Franzdóttir *et al.*, 2009). Expansion of the optic stalk also requires the Focal Adhesion Kinase *fak56D* and *cdGAPr*, a GTPase-activating protein domain homologous to that of mammalian CdGAP, for proliferating surface glial cells to migrate in an anteroposterior direction and come to occupy the stalk (Murakami *et al.*, 2007).

2.3.1.2.3 The Eye Disc Glia Likely Correspond to Adult Lamina Glia

It is, as yet, possible to propose only rather tentative correspondences between these glia identified in the developing visual system and those known in the distal lamina of the adult. The wrapping glia of the larval eye disc are presumed to correspond, in part, to Choi and Benzer's RBG on the following grounds: their smaller numbers, 80 RBG corresponding to 800 ommatidia, and because the RBG actually enwrap photoreceptor axons, about 10 fascicles apiece (Choi and Benzer, 1994). The relatively sparse wrapping glia which extend processes along the surface of developing photoreceptor cell

axons (Hummel *et al.*, 2002; Silies *et al.*, 2007) may correspond to the large, sparse, septate junction-rich subperineurial pseudocartridge glia. The pseudocartridge glia ensheathe photoreceptor axons extensively as they enter the brain, branching and interdigitating among the axons (Saint Marie and Carlson, 1983a). *M1-126* labels both an unidentified glial layer near the lamina of the larval brain and an unidentified layer in the adult lamina (Choi and Benzer, 1994), suggesting perhaps that these unidentified glial cell types in the lamina of larvae and adults are related. The wrapping glia marker *Mz97-GAL4* (Hummel *et al.*, 2002) also appears to label some as yet unidentified cells in the adult brain (Savarit and Ferveur, 2002), suggesting a possible relationship between glia of the eye disc and those of the adult lamina. The issue of pupal glial reconfiguration is complicated by the fact that carpet glia, not wrapping glia, form the septate-junction-rich subperineurial glia layer in the larva (Silies *et al*., 2007). However, since wrapping glia far outnumber carpet glia, they seem the most likely candidate to be reconfigured into adult pseudocartridge glia. What becomes of carpet glia in the adult is not known.

Alternatively, the outer surface glia (a subset of the perineurial glia) are more numerous than inner wrapping glia, with one glial cell nucleus associated with each ommatidium, and these cells are involved in photoreceptor axon guidance (Hummel *et al.*, 2002). Their exteriormost location, as well as their abundance, makes surface glia a likely candidate for the adult perineurial fenestrated glia.

In summary, we propose that at least some populations of adult lamina glia, fenestrated and pseudocartridge, are derived from glia of the eye disc and that the fenestrated glia may in fact correspond to larval surface glia and pseudocartridge glia to wrapping glia. Again, confirmation of this proposal must await the availability and careful deployment of suitable markers.

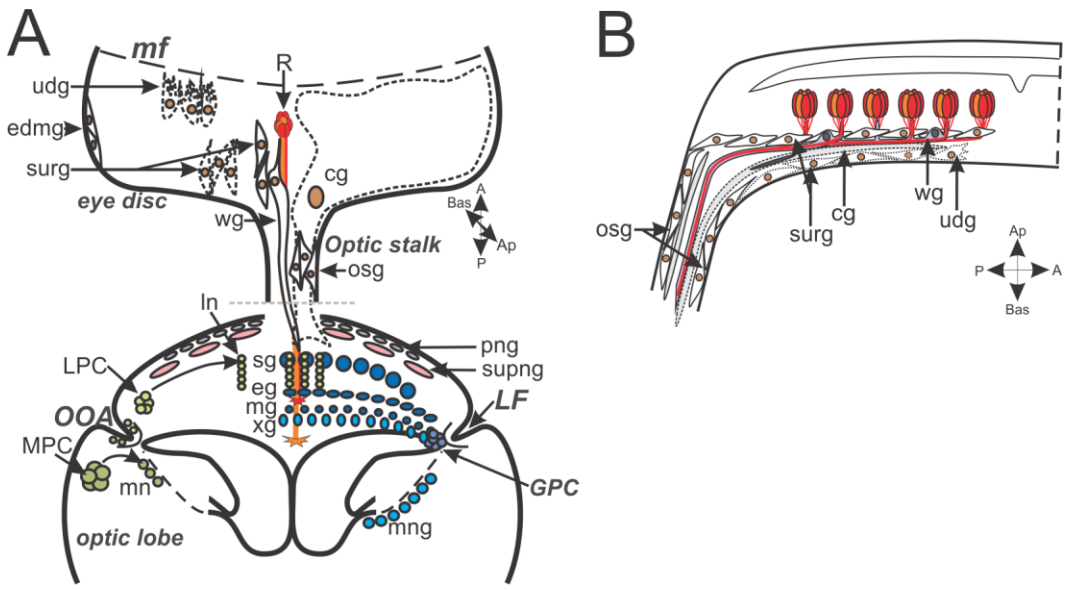

FIGURE 2.2 - GLIA IN THE LARVAL VISUAL SYSTEM.

The larval visual system becomes populated by glia from two different sources, the eye disc and, in the developing optic lobe, the glial precursor centre (GPC). **A**: The glia of the eye disc (brown nuclei) originate in the optic stalk (osg) and migrate into the eye disc. There are four types of differentiated glia in the eye disc: two large basally-located carpet glia (cg, outline in dashed lines), the eye disc marginal glia (edmg; not to be confused with the lamina marginal glia), wrapping glia (wg) and surface glia (surg). Undifferentiated glia (udg, outline in dashed lines) migrate along the basal surface of the eye disc, below the carpet glia, until they contact newly differentiated photoreceptors (R) just posterior to the morphogenetic furrow (*mf*). Differentiating glia then migrate apically and develop extensions to surround photoreceptor axons, becoming wrapping glia. A grey dashed line indicates a rotation of the brain relative to the optic lobe for illustration purposes, but both wrapping and carpet glia extend into the optic lobes. In the optic lobe, glia are derived from GPC which lie proximal to the lamina furrow (*LF*) and the Outer Optic Anlage (*OOA)*, from whence neuronal precursors arise. Three types of lamina glia (dark blue) derive from the GPC; these may include at least some of the satellite glia (sg), as well as the epithelial (eg) and marginal glia (mg). The GPC also gives rise to the glia lining the medulla neuropile (light blue), including the outer chiasmal glia (xg) and the medulla neuropile glia (mng). Cells underlying the larval marginal glia are usually labelled medulla glia in the literature, failing to acknowledge that in the adult an additional layer of glia, those of the outer chiasm 'small' and 'giant' glia (Tix *et al*., 1997), lies between the marginal glia and medulla glia. Lamina precursor cells (LPC) are displaced to the lamina where, as lamina neurons (ln), their cell bodies come to lie between the satellite and the epithelial glia. Medulla precursor cells (MPC), possibly ganglion mother cells, give rise to medulla neurons (mn). Subperineurial glia (supng; pink nuclei) derived from the epithelium and mesodermally derived perineurial glia (png; grey nuclei) surround the entire optic lobe as a sheath to form distinct components of the blood brain barrier. The inner glia of the optic stalk and the medulla cortex glia are not illustrated. **B**: A cross section of the eye disc shows the relative apical (Ap)/basal (Bas) locations of the glia and their locations in relation to the photoreceptors. Figures modified from originals in Chotard *et al*. (2005) and Silies *et al*. (2007).

TABLE 2.2 - CORRESPONDING GLIAL CELL TYPES FROM THE *DROSOPHILA* LITERATURE

PREFERRED GLIAL CELL NAME	CORRESPONDS TO	SUBTYPE
LARVAL EYE DISC/ OPTIC STALK		
wrapping glia Rangarajan *et al*., 2001; Hummel *et al*., 2002	retinal basal glia Choi and Benzer, 1994	peripheral glia?
carpet glia Silies *et al*., 2007	retinal basal glia Choi and Benzer, 1994	subperineurial glia
eye disc surface glia Hummel *et al*., 2002	subretinal glia; retinal basal glia Cagan and Ready, 1989a ;Choi and Benzer, 1994	perineurial glia
optic stalk surface glia Silies *et al*., 2007	-	perineurial glia
shingle glia *	marginal glia Silies *et al*., 2007	unknown
optic stalk inner glia Silies *et al*., 2007	-	peripheral glia?
LARVAL BRAIN		
distal satellite glia	subretinal glia Winberg *et al*., 1992; Perez and Steller, 1996	cortex glia
satellite glia Winberg *et al*., 1992	-	cortex glia
epithelial glia Winberg *et al*., 1992	-	neuropile glia
marginal glia Winberg *et al*., 1992	-	neuropile glia
outer chiasm large glia Tix *et al*., 1987	medulla glia	tract glia
ADULT FIRST OPTIC NEUROPIL		
fenestrated glia Eule *et al*., 1995	sub-retinal glia Winberg *et al*., 1992	perineurial glia
pseudocartridge glia Eule *et al*., 1995	sub-retinal glia Winberg *et al*., 1992	subperineurial glia
distal satellite glia Eule *et al*., 1995	satellite glia, rind glia Strausfeld, 1976; Wigglesworth 1959	cortex glia
proximal satellite glia Eule *et al*., 1995	satellite glia, interface glia Strausfeld, 1976; Wigglesworth 1959	cortex glia
epithelial glia	-	neuropile glia
marginal glia Eule *et al*., 1995	-	neuropile glia

*Renamed edging glia by their discoverers (Silies *et al.*, 2010)

2.3.2 GLIA OF THE OLFACTORY SYSTEM

Much as the eye conveys spatial information into the brain, the olfactory receptor neurons (ORNs) of the insect antenna project information to distinct glomeruli of the antennal lobe to form a spatial map of odour-specific signalling (Vosshall *et al.*, 2000). The general design of the olfactory network is the same in all insects, with most peripheral sensory neurons synapsing in the antennal lobe and uniglomerular projection neurons from the antennal lobe then conveying this sensory information to higher-order centres in the brain, such as the mushroom bodies and the lateral horn (Galizia and Rössler, 2010).

In *Drosophila* specifically, the dendrites of the bipolar ORNs expand into sensilla on the third antennal segment and the maxillary palp of the proboscis, with between one and four ORNs per sensillum. Each sensillum is electrically isolated from its neighbour by surrounding support cells that include glia (Venkatesh and Naresh Singh, 1984). ORNs are defined by their specific combination of odorant receptors. These are members of either the G-protein coupled receptor gene family (the ORs; Vosshall *et al.*, 1999) or the ionotropic glutamate receptor gene family (the IRs; Benton *et al.*, 2009). In *Drosophila* there are 1200 ORNs in each antenna (Vosshall and Stocker, 2007), each expressing a combination of between one and four receptor molecules (Couto *et al.*, 2005; Fishilevich and Vosshall, 2005; Goldman *et al.*, 2005) from a group of 45 adult-expressed odorant receptor genes (Clyne *et al.*, 1999; Gao and Chess, 1999; Vosshall *et al.*, 1999). Yet another class of ORN in the coeloconic sensilla expresses a combination of up to five of 15 recently discovered ionotropic receptor genes, some of which are expressed in combination with ORs (Benton *et al.*, 2009). ORNs project to one of the glomeruli in the antennal lobe, with those expressing the same odorant receptor projecting an axon to the same glomerulus to form a chemotopic map (Gao *et al.*, 2000). ORNs expressing 45 unique OR receptor combinations converge on approximately 36 of the 43 distinct glomeruli in the antennal lobe (Laissue *et al.*, 1999) and some of the newly discovered IRs, have been found to project to a subset of glomeruli previously unaccounted for (Benton *et al.*, 2009). Further details are reviewed in Vosshall and Stocker (2007).

While the arrangement and number of sensory neurons may change from species to species, along with a corresponding change in the arrangement of glomeruli in the antennal lobes, the general design of the olfactory system remains the same (Galizia and Rössler, 2010).

2.3.2.1 GLIA OF THE ANTENNA

In the adult *Drosophila* antenna there are at least two distinct subsets of glia (Sen *et al.*, 2005). The first is a small population of glia labelled by *GH146*, which originates in the brain and migrates into the antenna along the ORNs but has no role in patterning the trajectories of ORN axons (Jhaveri *et al.*, 2000; Sen *et al.*, 2005). Once in the antenna these glia, also called the coeloconic independent glia, ensheathe the ORNs, segregating them into groups as their axons enter the brain (Sen *et al.*, 2005). The second group of glia (labelled by *MZ319*), constitute the majority of glia in the antenna and form an outer sheath around the ORNs and *GH146*-expressing glia, as well as ensheathing the cell bodies of peripheral sense organs (Sen *et al.*, 2005). These glia are derived from an *atonal*-dependent coeloconic sensory-order lineage and are involved in sorting ORN axons (Jhaveri *et al.*, 2000; Sen *et al.*, 2005). Despite their role in axon sorting, they do not correspond to the sorting zone glia of the moth *Manduca*, which arise from the antennal lobe and are located in the brain where the antennal nerve enters the lobe. It is there that axons are sorted into the fascicles which project to distinct glomeruli (Rössler *et al.*, 1999). In fact, because they originate in the brain, at the base of the antennal lobe, the coeloconic independent glia are more likely to be akin to *Manduca*'s sorting zone glia despite the fact that these cells in *Drosophila* play no role in sorting the ORNs as they enter the antennal lobes (Sen *et al.*, 2005).

2.3.2.2 GLIAL ORGANISATION IN THE ANTENNAL LOBES OF *MANDUCA* VS *DROSOPHILA*

The tobacco hornworm *Manduca sexta* has been a model species for many studies on insect antennal lobe development, structure and function (Tolbert and Hildebrand, 1981). In the adult antennal lobe of *Manduca* there are five major classes of glia, grouped by the position of their cell bodies: the perineurial and subperineurial glia which ensheathe the antennal nerve and the brain surface, the cortical (or cortex) glia associated with the cell bodies of neurons, the nerve-layer glia (including the sorting zone glia), and the neuropile glia (Oland *et al.*, 1999).

On the way to the first-order olfactory neuropile, the antennal lobe, axons in the antenna are ensheathed by nerve layer glia with long processes having multiple expansions that enwrap the fascicles of the ORNs. Neuropile glia that surround the olfactory glomeruli fall into two categories. The first are complex glia with large cell bodies and branching

astrocyte-like arbors that are associated with axon fascicles as they enter the glomeruli. There are between one and five apically located complex glia per glomerulus. The second are simple glia: small glia with multiple, mostly unbranched processes that form a glomerular envelope with only shallow projections into the neuropile. Each simple glial cell is associated with no more than two or three glomeruli (Oland *et al.*, 1999). Insofar as they lie at the interface between the cell body cortex and the underlying neuropile these are speculated to be modified from interface glia (Edwards and Tolbert, 1998), also known as neuropile cover glia (Cantera, 1993) that have been recognised by various workers (Strausfeld, 1976; Meyer *et al.*, 1987; Cantera, 1993; Ito *et al.*, 1995). Glial cells of a single subtype, such as those of the complex neuropile glia can have different shapes depending on their location in the antennal lobe, while the simple neuropile glia can have irregularly shaped nuclei (Oland *et al.*, 1999). Regional subtypes of these glia may also exist, but have not yet been designated.

Drosophila differs from *Manduca* in that all glial cell bodies remain exclusively in a rind surrounding the glomerulus, and in that the *Drosophila* glial network is more sparse (Tolbert and Hildebrand, 1981; Oland *et al.*, 1999; Oland *et al.*, 2008). Furthermore, in *Drosophila* there are no known spatial relationships between the positions of the glial cell bodies and the individual glomeruli (Oland *et al.*, 2008). There are about 80 glial cells in each adult *Drosophila* antennal lobe. These include the four to six glia that gate and ensheathe tracts on both sides of the antennal commissure (Yao *et al.*, 2007; Oland *et al.*, 2008) and another two-to-four glial cells, possibly nerve layer glia, that encircle the lateral cluster of the antennocerebral tract (Oland *et al.,* 2008) and extend processes around the ORN axons as they enter the lobe (Sen *et al.*, 2005; Oland *et al.*, 2008). Glia have not been indentified at the base of the antennoprotocerebral tract that could ensheathe the efferent projection neurons.

The neuropile glia have been reported to project extensions in three directions. They extend: 1) some processes external to the neuropile to ensheathe incoming olfactory receptor neurons of the antennocerebral tract; 2) out of the antennal lobe to ensheathe projection neuron axons as they extend towards higher-order processing centres in the mushroom bodies; and 3) into the central neuropile to ensheathe large dendrites (Oland *et al.*, 2008). Within the neuropile, these glia insinuate between the glomeruli to form a sparse network around each glomerulus and shallowly invade the synaptic neuropile itself.

Both cortex (Pereanu *et al.*, 2005) and neuropile glia contribute to the sheath surrounding the neuropile. Neuropile glia extend a thin net of velate or branched processes around each glomerulus, which also extend, in a random fashion and at different densities, into the interior of the glomerulus (Oland *et al*., 2008). Analysis at both the light microscopic and EM levels reveals that glia never completely separate adjacent glomeruli, unlike the situation in the *Manduca* antennal lobe (Oland *et al.*, 1999); yet individual glomeruli are still able to process distinct odorant information in the absence of any isolating barrier provided by glia (Oland *et al.*, 2008). The glial investment of the neuropile varies in an anterior to posterior direction, with glomerular borders and neuropile investment becoming less visible towards the posterior (Oland *et al.*, 2008).

Using a *GAL4/FLP*-out based system, Awasaki *et al.* (2008) identified a number of glial cell types in the CNS of *Drosophila*. Based on cellular location and morphology these constitute the three broad categories: surface, cortex or neuropile, which are further subdivided into distinct groups of surface and neuropile glia (Awasaki *et al.*, 2008). Two types of neuropile glia have been reported: one that preferentially outlines the neuropile compartments and another that fills the interior. Glia specific to the antennal lobes of *Drosophila* have been defined by similar *FLP*-out techniques: cell body glia with a nucleus in the cortex, and two types of neuropile glia, ensheathing and astrocyte (Figure 2.3D; Doherty *et al.*, 2009). Ensheathing glia are flattened and line the borders of the neuropile to separate it from the cortex. They have processes which surround but do not invade the glomeruli, thus acting to separate these units. Astrocyte-like glia, by contrast, extend membranes into the neuropile to surround synaptic rich regions (Doherty *et al.*, 2009). Thus on morphological grounds these *Drosophila* glia correspond, respectively, to the simple lamellar glia, and the complex astrocyte-like glia, as described earlier for the antennal lobes of *Manduca* (Oland *et al.*, 1999).

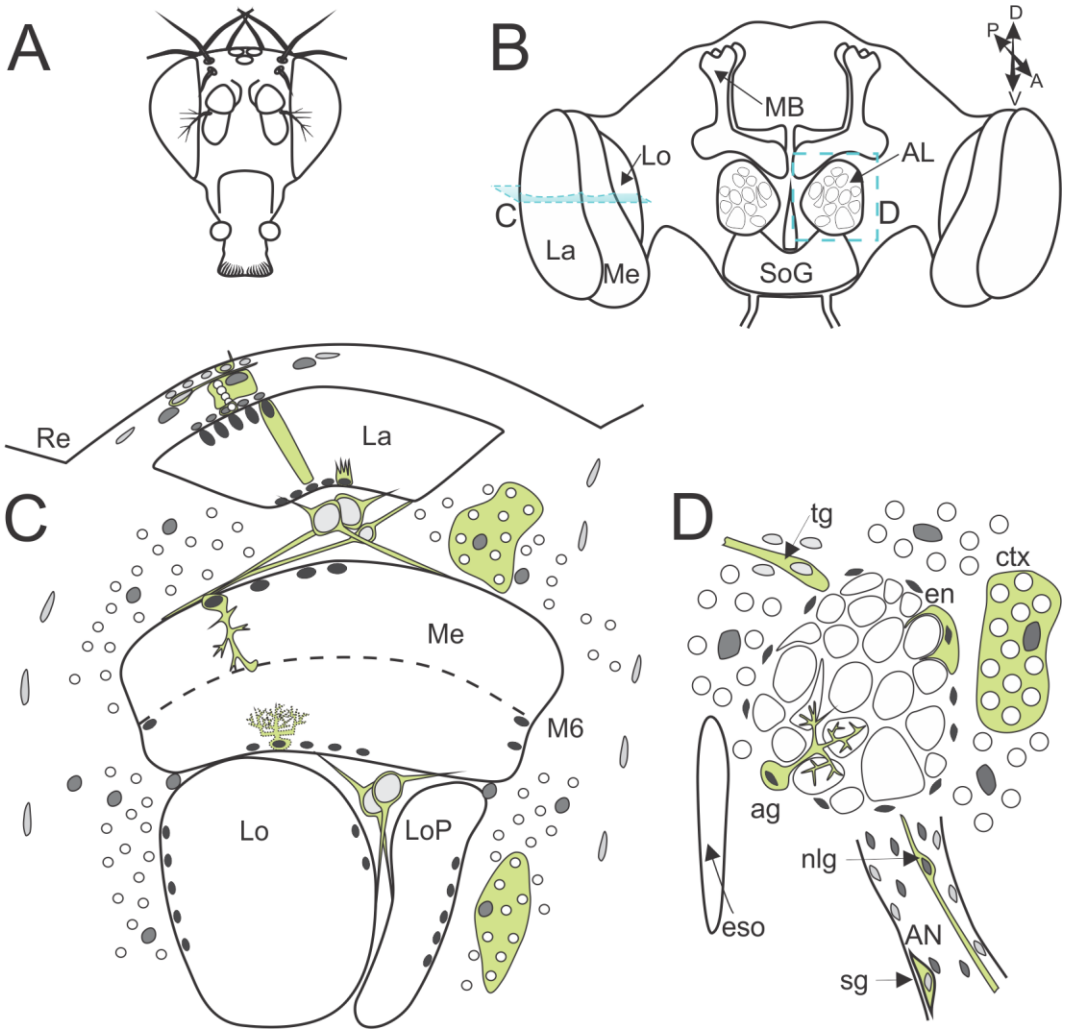

FIGURE 2.3 - THE GLIAL ANATOMY OF *DROSOPHILA*.

There are three identified classes of glia in the insect brain, surface, cortex and neuropile. Figures A and B depict a frontal view of (**A**) the *Drosophila* head and (**B**) underlying brain neuropiles. The lamina (La), medulla (Me), lobula (Lo) and lobula plate (LoP) together constitute the optic lobes of the visual protocerebrum (B and C) which underlie the retina (Re). The antennal lobes (AL) and mushroom bodies (MB) constitute the deutocerebrum, while all other neuropiles (not illustrated here) including the subesophogeal ganglion (SoG) belong to the tritrocerebrum. A horizontal section through the visual neuropiles (**C**, section plane C in B) shows the nuclear location of surface (light grey), chiasm (light grey), cortex (medium grey) and neuropile (dark grey) glia relative to their respective neuropiles and their associated neurons (nuclei in white). Subperineurial surface glia and cortex glia (called satellite glia when associated with the visual system) are sparse and only a few satellite glia are required to surround many neuron cell bodies in the cortex. Chiasm glia lie in two locations: between the lamina and medulla neuropile (first optic chiasm) and the medulla and lobula/lobula plate neuropiles (second optic chiasm), in both cases forming an anterior to posterior glial boundary. Within the first optic chiasm two types of glia can be distinguished, small and

(FIGURE 2.3 - CONTINUED, 2 OF 2)

giant. Neuropile glia lie amongst the axon terminals but for some optic lobe neuropiles no distinction has yet been made between their ensheathing and astrocyte-like glia. Chandelier glia, which have been detected in the neuropile of other Diptera, but have not yet been described in *Drosophila,* are illustrated in dotted outline at the base of the medulla. In chapter 3 (Figure 3.2), I confirm the presence of chandelier glia in the *Drosophila* medulla, as well as identify other medulla neuropile glia that have not been previously described in *Drosophila*. On the other hand, within the antennal lobes (**D**) both types of neuropile glia (dark grey nuclei): ensheathing (en) glia, which wrap the neuropile, and astrocyte-like glia (ag), which extend processes amongst the glomeruli, can be distinguished using different *GAL4* driver lines. Outside the neuropile, neuronal cell bodies (white) are ensconced in extensions from cortex glia (ctx; medium grey nuclei) which separate the antennal lobe from neighbouring neuropiles and the oesophagus (eso). Nerve layer glia (nlg) lie at the base of the antennal nerve (AN) where the nerve enters the antennal lobe, while surface glia (sg) ensheathe the nerve, and tract glia (tg) lie at the edge of the antennal lobe commissures.

2.3.2.2.1 ANTENNAL LOBES OF BEES

Embedded within the somata of the antennal lobe cortex, and restricted to this area, are large multipolar glial cells with numerous cytoplasmic processes that branch amongst the neuronal cell bodies and extend to the surface to form the glomerular envelope. The external and lateral sides of the antennal lobe glomeruli in the honeybee are covered by a cap of glia with flat, spindle-shaped nuclei. These have long lamellar extensions which enwrap the glomeruli with several layers of a glial sheath. As in the *Drosophila* antennal lobes, glial cell processes fail to invade the neuropile, so that individual glomeruli are not separated by a glial sheath. However, unlike *Drosophila* a few glial cell bodies can be detected in the neuropilar core of the antennal lobes (Hähnlein *et al.*, 1996). Extensions of these also invade antennoprotocerebral tracts containing the antennal lobe projection neurons (Hähnlein and Bicker, 1996). Thus, much as in the antennal lobes of *Drosophila* and *Manduca*, three types of glia can again be identified in bees: a single type of cortex glia and two kinds of neuropile glia, ensheathing and astrocyte-like.

2.3.2.3 MUSHROOM BODY GLIA

Outputs from the antennal lobes include multiple antennoprotocerebral tracts which project to the lips of the mushroom bodies and the lateral horn (Mobbs, 1985; Galizia and Rössler, 2010). The mushroom body plays a role in higher-order sensory integration, learning, and, in particular, odour-related learning (de Belle and Heisenberg, 1994). The mushroom bodies themselves comprise the calyx input neuropiles, the pedunculus, and the α-, β- and γ-lobes. In social hymenopterans the calyx can be further divided into the lip (olfactory input), collar (visual input) and basal ring (Galizia and Rössler, 2010). Intrinsic neurons, the Kenyon cells, extend dendrites into the calyx. Depending upon the subtype of Kenyon cell the axon may extend through the pedunculus and branch into the α and β lobes (Class I), or just the γ lobe (Class II; (Fahrbach, 2006). We will next summarise the glial organisation of these regions for three different insect systems.

In the *Drosophila* mushroom body, glia can be detected in the cell body clusters of the cortex (Ito *et al.*, 1997). Glia also ensheathe the calyx, pedunculus and lobes. Neuropile glia extend throughout the calyx, not in an organised way that reflects the quadripartite origins of this neuropile, but instead so as to form a loose, unorganised

meshwork. Furthermore, they do not enwrap the synaptic microglomeruli (Leiss *et al.*, 2009) and thus are unlikely to have a role in neurotransmitter recycling in this neuropile. Still other glia can be detected between the four fascicles of the pedunculus (Ito *et al.*, 1997).

In the cricket *Acheta domestica*, at least, the mushroom body cortex is not very rich in glia (Cayre *et al.*, 1996). At the cortex-neuropile interface, glia with large nuclei that are immunoreactive to MAb 5B12 (Glionexin), outline the neuropiles at the bottom of the calyx and extend between the columnar rows of Kenyon cells. The neuropile also contains a distinct subset of microglia labelled by MAb 3G6 (Cayre *et al.*, 1996).

Ethyl gallate staining in the honeybee reveals both cortex and neuropile glia in the mushroom body. Glial cells of varying shapes lie amongst and wrap around the Kenyon cell bodies in the cortex. The size, position and number of glia enwrapping Kenyon cell bodies differ in drones and workers, yet both have small glia which extend processes to wrap around the neuronal somata as well as around the tops of Kenyon cell axons that project towards the calyces. The mushroom body neuropile is completely lined by an envelope of spindle-shaped glia, separating it not only from the cortex but also from the surrounding protocerebral neuropile. Internally, the mushroom body neuropile is divided up into compartments by numerous astrocyte-like glia. These delineate the three columns of the pedunculus that correspond to the lip, collar, and basal ring. There is also a network of mushroom body intrinsic glial cells. They separate the α-lobe from the β-lobe where these branch, as well as separating the lobes from the pedunculus. Although tracheae in the calyces are also ensheathed by glia, glia in the calycal neuropile itself are rare, lying only at the border of the collar and basal ring (Hähnlein and Bicker, 1996).

The α- and β-lobes have three horizontal strata, with a high density of astrocytic glia in the ventral part of the α-lobe. Glia also occur at the boundaries between some of the six layers of the α-lobe and extend processes between the layers where extrinsic neurons arborize into bands. By contrast, only a glial septum-like structure splits the β-lobe into dorsal and ventral halves (Hähnlein and Bicker, 1996).

2.4 GLIAL FUNCTION

Glia fulfill many functions in the insect brain. Of these, their role in forming the blood brain barrier and in recycling neurotransmitters have received particular attention.

2.4.1 BLOOD BRAIN BARRIER

In vertebrates, tight junctions between endothelial cells of capillaries in the CNS form the primary barrier to extracellular flow, whereas in insects there is no closed circulatory system and the CNS must instead be isolated from the open circulation of haemolymph. This barrier is necessary to protect the brain from haemolymph fluctuations especially in K^+, such as those which occur after feeding in some insects (Treherne, 1985). Glia also surround the tracheoles by which air enters the brain (Cantera and Trujillo-Cenóz, 1996; Pereanu *et al.*, 2007). A role for glia in the BBB can be clearly demonstrated by the diffusion of extracellular tracers, which is blocked at glial sites (Shaw, 1977), an ability believed to be the principal function of occluding junctions such as the pleated septate junctions (Stork *et al.*, 2008). For an extensive review of insect junctions see Carlson *et al.* (2000).

2.4.1.1 IMPERMEABILITY TO DYES AND TRACERS

Septate junctions have been implicated in establishing an important diffusion barrier in the insect nervous system. Fly brains that lack glia, or normal glial function, such as in the *Drosophila* mutant *reversed polarity* (Repo) are not only permeable to extracellular tracers such as dextran (Stork *et al.*, 2008) but also have abnormal physiological properties such as the reversal in polarity of their ERG, for which they are named (Xiong *et al.*, 1994; Xiong and Montell, 1995). Embryos that are mutant for *neurexin IV*, a component of the septate junction, allow the diffusion of dextran into the CNS with similar kinetics to that of *gcm* flies which lack glia altogether, suggesting that the septate junction itself is a vital component of the BBB (Stork *et al.*, 2008).

In the lamina it appears as if the barrier that prevents influx of substances from the haemolymph into the brain is composed of septate junctions formed between pseudocartridge glia and their neighbours. Thus, when introduced to the circulating haemolymph, dyes never enter the optic lobes, and tracer substances such as ionic

lanthanum and dyes do not enter the optic lobe from the retina, but instead penetrate only a superficial layer of perineural cells – the fenestrated glia (Shaw, 1984a). At the EM level, colloidal lanthanum applied to the retina fails to penetrate deeply into the septate junctions of pseudocartridge glia (Saint Marie and Carlson, 1983b). These findings, along with the fact that tight junctions, the only other occlusive junctional contact, are not readily found in the pseudocartridge glia (Saint Marie and Carlson, 1983b), suggests that the pleated septate junctions of the pseudocartridge zone function principally to restrict movement of substances from the blood into the optic neuropiles.

2.4.1.2 MOLECULAR COMPONENTS OF THE SEPTATE JUNCTION

The septa of the septate junction act like a series of baffles to impede the passage of substances through the extracellular space between glia. In *Drosophila* embryos smooth and pleated septate junctions have been reported (Tepass and Hartenstein, 1994). These vary morphologically and have different tissue distributions, but are functionally equivalent (Lane *et al.*, 1994).

Pleated septate junctions contain NeurexinIV (Baumgartner *et al.*, 1996) and Coracle (Fehon *et al.*, 1994) which are believed to be components of the septa themselves. A myriad other genes also affects septate junction formation in different *Drosophila* tissues, including genes for structural proteins such as the polarity determining PDZ protein Scribble (Bilder and Perrimon, 2000); Membrane Associated Guanylate Kinases such as Discs large (Woods and Bryant, 1991; Hough *et al.*, 1997) and Varicose (Wu *et al.*, 2007; Moyer and Jacobs, 2008); the transmembrane claudins Sinuous (Wu *et al.*, 2004) and Megatrachea (Behr *et al.*, 2003); cell adhesion proteins Contactin (Faivre-Sarrailh *et al.*, 2004), Neuroglian (Genova and Fehon, 2003), Fasciclin III (Hortsch and Goodman, 1991; Hough *et al.*, 1997), Gliotactin (Genova and Fehon, 2003; Schulte *et al.*, 2003) and Lachesin (Llimargas *et al.*, 2004; Strigini *et al.*, 2006); the G-protein coupled receptor Moody (Bainton *et al.*, 2005; Schwabe *et al.*, 2005); the transcription factor Grainy head (Narasimha *et al.*, 2008), and the α and β subunits of the Na^+/K^+ ATPase Nervana 2 (Genova and Fehon, 2003). Gliotactin, Neuroglian and both subunits of Nervana 2 are all required to form a functioning paracellular barrier (Genova and Fehon, 2003) and yet the *nervana2* promoter does not drive expression in subperineurial glia (Mayer *et al.*, 2009), the primary cellular component of the BBB in insect nervous systems. It is instead limited to cortex and neuropile glia (Pereanu *et al.*,

2005), such as the cortical distal satellite glia of the *Drosophila* lamina (Górska-Andrzejak *et al.*, 2009), which lie just beneath the subperineurial pseudocartridge glia.

2.4.1.3 OTHER REQUIREMENTS FOR A PROPERLY DEVELOPED BLOOD BRAIN BARRIER

In addition to septate junction proteins, the G-protein coupled receptor Moody, which is expressed specifically by surface glia, is essential for proper barrier formation. Loss of *moody* results in both the reduced formation of septate junctions and a leaky blood–brain barrier because *moody* mutants purportedly fail to properly regulate the cortical actin cytoskeleton that assembles septate junctions (Bainton *et al.*, 2005; Schwabe *et al.*, 2005). The α and β proteins of Moody immunolocalise in the adult *Drosophila* brain to a wide band in the lamina that is proposed to include the pseudocartridge glia (Bainton *et al.*, 2005) but may also include the satellite glia which contain abundant septate junctions, at least in *Musca* (Saint Marie and Carlson, 1983b). Higher resolution studies are needed to clarify this point.

The ATP-binding cassette (ABC) transporter gene m*dr65* is another essential component of the BBB system with an important role in neuroprotection. Mdr65, which is immunolocalised to the apicalmost surface of the subperineurial glia, near the humoral interface, is able to change the inherent sensitivity of the blood brain barrier to toxic pharmaceuticals (Mayer *et al.*, 2009). Mutations of *mdr65* allow abnormal passage and accumulation of ABC transporter substrates, such as the lipophilic dyes Rho123 and RhoB, into the brain from the haemolymph, but do not affect accumulation of 3 kDa FITC-dextran or 10 kDa Texas Red dextran, which are not substrates for the ABC transporters. The selective transport of Rho123 and RhoB fluorophores, but not dextrans in *mdr65* mutants indicates that the mutation does not disturb the paracellular diffusion barrier. Mutations in *mdr65* also increase sensitivity to the anti-microtubule agent vinblastine, allowing mutant brains to accumulate significantly more dextran than wild-type brains or *mdr65* brains without co-application of vinblastine. Thus *mdr* loss of function increases the sensitivity of subperineurial glial cells to vinblastine, suggesting a neuroprotective role for the intact protein (Mayer *et al.*, 2009). The functions of an additional ABC transporter gene, *white*, and its binding partner genes *brown* and *scarlet*, are detailed below.

2.4.1.4 THE BLOOD BRAIN BARRIER CONTROLS THE FLOW OF NUTRIENTS FROM HAEMOLYMPH TO NEURONS

Occluding barriers have the consequence that fluid-borne ions and nutrients have limited access to the underlying avascular neuropile. A possible solution to this conundrum has been found among the lamina glia, where both the proximal (marginal) and distal (fenestrated, pseudocartridge) layers of glia contain clathrin-coated vesicles (Saint Marie and Carlson, 1983a). These indicate the cells' capacity for active endocytosis by which they may acquire nutrients.

2.4.1.4.1 TRANSPORT OF MATERIAL: THE ROLE OF TRANSPORTERS AND GAP JUNCTIONS

For ions, nutrients and metabolites to reach neurons, glia must be able to transport these components from the haemolymph to the brain and in the opposite direction, sometimes with great efficiency. For some components that move over short distances diffusion is sufficient, for which the interglial gap junctions that are reported to exist between all glia of the first optic neuropile may be utilized to form an intercellular network (Saint Marie and Carlson, 1983b). This glial intercellular network may be a means by which essential nutrients can be transported in, but also a means by which excess neurotransmitter can be cleared from the brain (Carlson and Saint Marie, 1990).

Not only have gap junctions been detected at the EM level between glia in some species of fly (Saint Marie and Carlson, 1983b) but their molecular components, the innexins, have also been localised to the developing and adult visual system of *Drosophila.* Thus, *innexin2*, *innexin3*, and *optic gangion reduced* (*ogre*) all express mRNA transcripts in a similar pattern at areas likely to correspond to glial cells (Stebbings *et al.*, 2002).

Altered function of innexins also has implications in the visual system. For example $ogre^{cb8}$ mutants have not only a reduced number of neurons in the optic lobes (Watanabe and Kankel, 1990) but also an abnormal ERG that lacks 'on' and 'off' transients (Curtin *et al.*, 2002a). The *ogre* promoter drives expression in photoreceptors and the presence of a functional form of Ogre in the photoreceptors is necessary for a normal ERG. Ogre does not form a homotypic dimer however (Curtin *et al.*, 2002a), so some other *innexin* must be expressed in the photoreceptors to create a functional gap junction. Shaking B (N1 and N2) mRNA is expressed in the lamina monopolar cells (Zhang *et al.*, 1999), where it has an effect on the lamina transients of the ERG (Homyk

et al., 1980). This leaves Innexin1 and 2 as the most likely subunits to constitute the gap junctions of the lamina glia. Their existence and function have yet to be confirmed at these sites, however.

2.4.2 Neurotransmitter Transport Functions of Glia

2.4.2.1 Optic Lobe Glial Functions

2.4.2.1.1 Histamine and the Role of Glia in the ERG Response: The HisCl Receptor

Drosophila photoreceptors release histamine as a neurotransmitter at their synapses (Hardie, 1987, 1989). Histamine is produced in the retina from L-histidine, in a single-step reaction regulated by the enzyme HDC (Burg *et al.*, 1993) then pumped into vesicles and released at the photoreceptor synapse (Figure 2.4A). Few of these steps are known in any detail, however. *Drosophila* photoreceptor synapses are uniformly tetrads, at which release occurs onto a cluster of four postsynaptic elements. These comprise lamina monopolar neurons L1 and L2, which are obligate partners at all tetrads and two other partners from some combination of amacrine cells, L3, or epithelial glia (Figure 2.4B; Meinertzhagen and O'Neil, 1991). Released histamine hyperpolarizes the lamina monopolar neurons (Hardie, 1987) when it binds to Ort (HClA, HisCl2), a histamine-gated chloride channel (Gisselmann *et al.*, 2002; Zheng *et al.*, 2002), allowing an influx of Cl^- ions into the postsynaptic neurons. The summed electrical response of both photoreceptor depolarization and the lamina response to histamine release together constitute the externally recorded ERG (Figure 2.4C). Depolarization of the photoreceptors produces the sustained negative response (Heisenberg, 1971) while hyperpolarization of monopolar cells has been reported to produce the ‘on’ transient and their depolarization the ‘off’ transient (Heisenberg, 1971; Coombe and Heisenberg, 1986). The evidence for this conclusion rests on the concurrent loss of ERG transients and L1 and L2 neurons in the mutant *vacuolar medulla*, a correlation that does not, however, take into account other possible changes that occur in the lamina with the loss of these cells. In support of the conclusion that the origin of ‘on’ and ‘off’ transients lies in lamina monopolar cells, null mutations of the histamine-gated Cl^- channel gene *hisCl2*

(*HClA*, *ort*) that express in these cells (Witte *et al.*, 2002) abolish the synaptic transients of the ERG (Pantazis *et al.*, 2008). The ERG response can, however, be modulated by neighbouring epithelial glia which express the second histamine-gated Cl- channel gene, *hisCl1* (Pantazis *et al.*, 2008), or by synaptic feedback from amacrine and monopolar neurons (Zheng *et al.*, 2006; Nikolaev *et al.*, 2009). When compared with wild-type flies, mutants of *hisCl1* show a slower rise time in intracellular recordings from monopolar neurons as well as a twofold increase in the amplitude of the "on" transients of their ERG (Pantazis *et al.*, 2008). A number of explanations have been advanced for this difference (Pantazis *et al.*, 2008). First, there is the possible contribution of epithelial glia to the extracellular field potentials that regulate transmitter release from R1-R6 (Shaw, 1984a). Second, activation of histamine-gated chloride channels on the epithelial glia may affect glial uptake of histamine, with the histamine remaining in the cleft exerting a prolonged action at the HisCl2/Ort channels of L1-L3 that co-occupy the tetrad. Third, HisCl1 channels on the glia compete for histamine with the HisCl2 channels on L1-L3, thus reducing the response of the monopolar cells (Pantazis *et al.*, 2008).

2.4.2.2 HISTAMINE CLEARANCE FROM THE SYNAPTIC CLEFT

After its release from the R1-R6 photoreceptor terminals, liberated histamine must then be cleared from the cleft. While it is not yet known how this clearance occurs there are two obvious routes: 1) direct reuptake into the photoreceptor terminal, or 2) uptake into the surrounding epithelial glia. The photoreceptors of barnacle nauplii *Balanus amphitrite* take up radioactively labelled histamine in a Na^+ dependent manner (Stuart *et al.*, 1996; Stuart *et al.*, 2002) but such studies do not clearly demonstrate that the uptake is direct, and not via an unidentified glial or pigment cell pathway. Corresponding evidence that dipteran photoreceptors can take up histamine directly is lacking. When barnacle eyes take up radioactive histamine, depolarized photoreceptor terminals take up the label more intensely in the light than do hyperpolarized, dark-adapted photoreceptors, and in dark-adapted nauplii it is the glia that label strongly (Stuart *et al.*, 1996). This finding is inconsistent with findings from other Na^+ dependent transporters, which take up their transmitter when the cell is relatively hyperpolarized (Tachibana and Kaneko, 1988; Cammack and Schwartz, 1993). Stuart *et al*. (1996) hypothesise that active uptake of histamine into depolarized photoreceptors may occur either because of the release itself, because the histamine is sequestered more actively into a vesicular

pool during transmitter recycling, or because of other presynaptic processes involved with transmitter release, such as ion or second-messenger changes.

The possibility that light-induced release of neurotransmitter might itself also induce or accelerate direct histamine reuptake by the photoreceptors should be seen in the light of two major characteristics of fly photoreceptors, their high gain and rapid rates of tonic neurotransmitter release (Laughlin, 1981; Shaw, 1984a; Uusitalo *et al.*, 1995a). From likely rates of vesicle shedding, quantum size, and the number of synaptic vesicles in each R1-R6 terminal, it has been calculated that without recycling the terminal's histamine would theoretically deplete within a matter of about 10 seconds (Borycz *et al.*, 2005). It may be possible that given the increased rate of histamine release during light exposure, both direct (into the R-cell) and indirect (via glial) reuptake mechanisms could be utilized, whereas tonic dark release may not utilize direct reuptake.

2.4.2.3 THE HISTAMINE/CARCININE RECYCLING PATHWAY: THE RECIPROCAL ROLES OF EBONY AND TAN

Borycz *et al.* (2002) were the first to propose that a histamine/carcinine (β-alanyl-histamine) recycling pathway exists at fly photoreceptors and this is now known to involve a shuttle between the photoreceptor terminals and their surrounding epithelial glia (Richard *et al*., 2003; True *et al.*, 2005; Wagner *et al*., 2007; as reviewed in Stuart *et al.* 2007). This recycling pathway utilizes the reciprocal actions of two proteins Ebony and Tan (Figure 2.4A), encoded by an evolutionarily ancient bacterial peptidase (*ebony*: Hovemann *et al.*, 1998) and a fungal isopenicillin-N N-acyltransferase (*tan*: True *et al.*, 2005) genes. The pathway was first demonstrated by the accumulation of [^{3}H]carcinine in *tan*, but not *ebony flies* (Borycz *et al.*, 2002), and can be explained by the reciprocal regulation of β-alanyl conjugation of histamine. Ebony, which is expressed in epithelial glia (Richardt *et al.*, 2002), confines histamine as the inactive conjugate, carcinine. Alternately, Tan protein in the photoreceptors (Wagner *et al.*, 2007) liberates the histamine from its conjugation to β-alanine as carcinine, an action that has been confirmed *in vivo* (True *et al.*, 2005).

2.4.2.4 HISTAMINE TRANSPORT

2.4.2.4.1 THE ROLE OF INEBRIATED AND WHITE IN CARCININE/HISTAMINE TRANSPORT

The proper function of the histamine cycling pathway is dependent on a means by which to transport histamine and carcinine. Histamine in the synaptic cleft may be transported directly back into the photoreceptors or into the glia where it is inactivated, while carcinine must be transported out of the glia and back into the photoreceptors where it can be recycled into histamine. β-alanine must be shuttled back and forth between both photoreceptors and glia as well. Missing from the equation, however, is the means by which histamine is taken up into the epithelial glia and the means by which carcinine is then returned from the glia to the photoreceptors, fluxes that must be rapid and for which the role of specific transporters would normally be invoked (Stuart *et al.*, 2007).

It has been proposed that *inebriated* (*ine*) plays a role in returning carcinine to the photoreceptor (Gavin *et al.*, 2007). Ine is a member of the Na^+/Cl^- dependent neurotransmitter transporter family which is expressed as multiple transcripts, two of which are characterised: a short form, Ine–RB with 12 transmembrane spanning domains and a long form, Ine–RA with an additional N-terminal domain (Burg *et al.*, 1996; Soehnge *et al.*, 1996). While it is not yet known if these two forms are functionally distinct, flies mutant for either the long form (ine^2) or both forms (ine^3) have an abnormal ERG characterised by oscillations during the retinal 'sustained negative' response and a loss or reduction of both 'on' and 'off' lamina transients (Burg *et al.*, 1996; Gavin *et al.*, 2007). Two pieces of evidence implicate a relationship between Ine function and carcinine: 1) retinal oscillations are missing in $ine^2;ebony^{11}$ double mutants but not in $tan^1;ine^2$ double mutants, suggesting that the product of *ebony* gene action, carcinine, contributes to these oscillations; and 2) feeding flies carcinine can act partially to mimic the ine^2 ERG phenotype, implying that these oscillations result from an excess of carcinine.

Glial specific rescue of the short transcript, *ine-RB,* in an ine^3 mutant background fully restores the 'on' and 'off' transients to the ERG and eliminates the oscillations, while photoreceptor-specific rescue eliminates the oscillations (Gavin *et al.*, 2007). Gavin *et al.* (2007) hypothesise that carcinine accumulates in the extracellular cleft of *ine* mutants because non-functional Ine cannot transport carcinine into photoreceptors. They

conclude that an excess of carcinine causes the retinal oscillations, while the loss of transients is said to be due to a consequent reduction in histamine. If flies are able to clear histamine from the cleft via uptake into the glia but are then unable to liberate the inactive carcinine for return to the photoreceptors, as is proposed to occur when *ine* is defective, histamine recycling would be effectively blocked.

Four major obstacles remain to this hypothesis of *ine* function. First, *ine* mRNA has been localised to the retina (Burg *et al.*, 1996) but has yet to be directly localised to the photoreceptors or specifically to the epithelial glia. Second, although Ine functions as a transporter (Huang and Stern, 2002) and despite its ability to modulate the ERG (Gavin *et al.*, 2007) the protein itself has not yet been actually shown to transport carcinine or even histamine. Third, no distinction is made between possible functional differences of the two Ine transcripts, long and short. While mRNA of the long transcript is abundant in the head (Burg *et al*., 1996) and loss of the long transcript alone (via ine^2) can result in an ERG mutant phenotype, this phenotype can be rescued using the short version of the protein (Gavin *et al*., 2007). Fourth, rescue of *ine* exclusively in the glia should allow carcinine to be transported out of the glia but not back into the photoreceptor. Thus, there would be excess carcinine in the extracellular space and this, according to the model proposed above, should result in more oscillations in the retinal response, not fewer, as has been demonstrated (Gavin *et al.,* 2007).

The suggested action of Ine in the visual system relies on both the release of carcinine from glia as well as its uptake by photoreceptor neurons (Gavin *et al.*, 2007). Ine (as RosA) has been localised by means of *in situ* hybridisation to regions throughout the brain of *Drosophila*, including the retina (Burg *et al.*, 1996). An antibody against the *Manduca sexta* Ine protein, which has 55% identity with *Drosophila* protein, immunolocalises to glial cells, neuropiles and axons in the optic lobes of both *Manduca* and *Drosophila* (Chiu *et al.*, 2000). In *Drosophila*, Ine has been reported to localise to the cell bodies of photoreceptors as well as their axons in the lamina and medulla (Chiu *et al.*, 2000) although published data from this study can also be interpreted to suggest expression solely in areas corresponding to the fenestrated, and pseudocartridge glia. There is clearly room for a detailed study of Ine immunoexpression in the visual system, but available data already suggest that expression will be widespread and restricted neither exclusively to neurons, glia, nor to regions of histamine release.

Despite having an unknown substrate (Chiu *et al.*, 2000), the presence of Ine expression throughout the CNS of *Manduca sexta* and *Drosophila* (Burg *et al.*, 1996; Chiu *et al*., 2000), implies a much wider role than just carcinine transport in the photoreceptors and glia of the visual system. Not so far considered is β-alanine, a specific substrate for Ebony action that is presumably widely used as a means to inactivate biogenic amines (Richardt *et al.*, 2003). This also requires a transport mechanism that has so far eluded identification.

Mutants of ABC transporter genes *white*, *brown*, and *scarlet* that control eye pigmentation reveal an additional transport function implicating optic lobe glia. These mutants all have a reduced head content of histamine, as well as reduced levels of other biogenic amines (Borycz *et al.*, 2008) and a redistribution of these amines in head homogenates. In all such mutants less neurotransmitter, be it histamine, dopamine or 5-HT (5-hydroxytryptamine/serotonin), is detected in a vesicle-enriched pellet fraction and more remains in the supernatant. This change is consistent with a redistribution of neurotransmitter that reflects a function for White and its binding partners in pumping amine transmitters into some compartment contained within the pellet fraction of brain homogenates, most likely the synaptic vesicles (Borycz *et al.*, 2008). This explanation is weakened by the fact that histamine is found in photoreceptor terminals while White protein is only weakly expressed in the photoreceptors and is instead found far more obviously in the surrounding epithelial glia (Borycz *et al.*, 2008). A possible explanation can be invoked from this glial expression considering that these mutants also have fewer multiple-headed capitate projections. This is consistent with the possibility that mutants of ABC transporters have altered vesicle endocytosis, which occurs at the capitate projection (Fabian-Fine *et al.*, 2003).

A significant aspect of White function is that the *white* mutation alters the histaminergic phenotypes of *tan* and *ebony* flies. A *white,tan* double mutant effectively triples the head histamine content relative to single-mutant *tan* flies; conversely the *white*;;*ebony* double mutant has reduced histamine relative to *ebony* (Borycz *et al.*, 2008). How exactly does a glial-associated ABC transporter such as White affect photoreceptor specific Tan protein function in order to ultimately alter head histamine concentration? The answer may lie in the fly's ability to take up histamine into the glia and convert it to the inactive form carcinine. Thus, both single-mutant *white* and double-mutant *white*, *tan* are unable to convert tritiated histamine into carcinine whereas *tan* flies can convert tritiated

histamine into tritiated carcinine (Borycz *et al.*, 2008), essentially trapping all excess histamine as carcinine (Borycz *et al*., 2002; True *et al*., 2005). This difference suggests that *white* flies lack the ability to take up histamine into their glia for conversion to carcinine under the action of Ebony (Richardt *et al.*, 2002; Richardt *et al.*, 2003; Borycz *et al.*, 2008). However, this does not implicate White itself as an actual neurotransmitter transporter nor does it explain why ABC transporter mutants have an excess of non-vesicular neurotransmitter. More must be done to determine the transporters responsible for shuttling of histamine, carcinine and β-alanine into and out of neurons and the role played by the different optic lobe glia in this process.

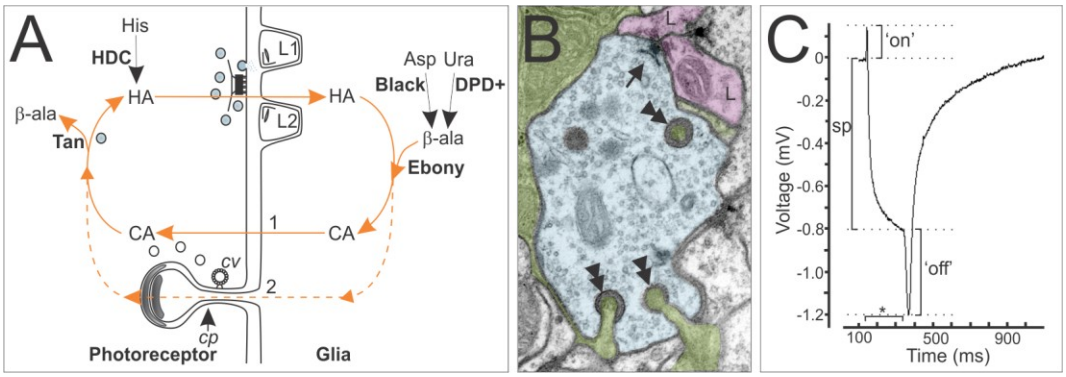

FIGURE 2.4 - VISUAL SYSTEM FUNCTION IS DEPENDENT UPON AN INTIMATE ASSOCIATION BETWEEN PHOTORECEPTORS AND GLIA.

A: Histamine (HA) is synthesized from L-histidine (His) in the photoreceptor by the enzyme Histamine decarboxylase (HDC). HA is released from vesicles at the photoreceptor T-bar ribbon. In the synaptic cleft it can act on HA-gated chloride channels at the surface of the monopolar cells (L1,L2) or the glia. Excess HA is taken up by the glia where it is then inactivated by conjugation to β-alanine (β-ala) by the protein Ebony. β-ala is produced in the glia from decarboxylation of aspartate (Asp) by Black, or by catabolism of uracil (Ura) along a dihydropyrimidine dehydrogenase (DPD^+) dependent pathway (Rawls, 2006). The HA- β-alanyl conjugate, called carcinine (CA), is shuttled from the glia back into the photoreceptor by an unknown mechanism (path 1) or possibly via the capitate projection (cp, path 2), where clathrin-mediated endocytosis of coated vesicles (cv) takes place. In the photoreceptor HA is liberated from CA by Tan. Liberated HA is then pumped back into recycled vesicles and prepared once again for release at the synapse. **B**: An EM cross-section of the *Drosophila* lamina. Photoreceptors (blue) synapse (arrow) onto paired monopolar neurons (L, magenta). Epithelial glia (green) surround the cartridge and invests areas close to synapses. Glia invaginate into photoreceptors at specialised sites called capitate projections (double arrowheads). **C**: The inverted extracellular response (ERG) recorded from the eye of *Drosophila* is triggered by a light flash (*) and consists of the combined negative sustained response (sp) of the photoreceptors and the hyperpolarizing ('on') and depolarizing ('off') responses of the lamina. The 'on' response is modulated by activation of HisCl1 receptors on the epithelial glia.

TABLE 2.3 - CELL SPECIFIC MARKERS FOR GLIA OF THE ADULT OPTIC LOBES

GLIAL CELL TYPE	GENE/PROTEIN/DRIVER	FUNCTION	REFERENCE
fenestrated glia	anti-dVMAT-B	vesicular monoamine transporter	Romero-Calderón *et al*., 2008
distal satellite glia; some medulla neuropile glia; outer/inner chiasm glia; most cortex glia	*Nrv2-GAL4*	Na+,K+ -ATPase β-subunit	Górska-Andrzejak *et al*., 2009; Oland *et al*., 2008
fenestrated glia; central brain glia	*CG33528*	VMAT-like	Thimgan *et al*., 2006
epithelial glia	*black*	aspartate/ glutamate decarboxylase, β-alanine production	Phillips *et al*., 1993
epithelial, and medulla neuropile glia	anti-Ebony	β-alanine-biogenic amine synthetase	Richardt *et al.*, 2002; Wagner *et al.*, 2007,
surface* and satellite glia	*P1478-GAL4*; Basigin	Extracellular Matrix MetalloPRotease Inducer	Curtin *et al*., 2007
fenestrated glia	*ruby*	clathrin binding AP-3β adaptin	Kretzschmar *et al*., 2000
epithelial glia	*HisCl1-GAL4*	histamine receptor	Pantazis *et al*., 2008; Gao *et al*., 2008
all lamina glia and medulla neuropile glia +	*B380-LacZ*	unknown	Winberg *et al*., 1992
epithelial glia	anti-White	ABC transporter subunit	Borycz *et al.,* 2008
surface*, satellite, epithelial, marginal glia +	*3-109 (loco)-LacZ*	regulator of G-protein signalling	Winberg *et al*., 1992; Xiong *et al*., 1994, Perez and Steller 1996

(+) also labels other glial subtypes in the brain

(*) glia labelled as surface are not distinguished as being either fenestrated or pseudocartridge

2.4.2.4.2 CAPITATE PROJECTIONS AS SPECIALISED RECYCLING ORGANELLES

Capitate projection organelles are sites at which epithelial glia make close invaginating appositions into photoreceptors (Figure 2.4A, B). Each is characterised by its spherical head, approximately 190 nm in diameter (Stark and Carlson, 1986) that contains a widened extracellular space between the glial and photoreceptor cell membranes. This space is filled with an unknown filamentous electron-dense substance (Saint Marie and Carlson, 1983a). Just beneath the glial cell membrane there also lies an intracellular electron-dense filamentous material (Stark and Carlson, 1986). The capitate heads are also characterised by particles on both glial and photoreceptor cell surfaces that have been visualized in freeze-fractured material (Stark and Carlson, 1986). None of these specialisations has been assigned a function. While it is not known what cytoskeletal proteins are associated with the capitate projection on the glial side, on the photoreceptor side the cell surface Extracellular Matrix Metalloprotease Inducer, Basigin, which interacts with Integrin to promote cytoskeletal rearrangement, is required to enable epithelial glia to enter the R1-R6 terminals to form a penetrating capitate projection (Curtin *et al.*, 2005).

Capitate projections, or structurally related organelles, also occur in the terminals of R7 and R8 in the medulla (Melamed and Trujillo-Cenóz, 1968; Takemura *et al.*, 2008) as well as in the terminals of photoreceptors in the ocellus (Stark *et al.*, 1989). These structures are all associated with histamine positive photoreceptors (Nässel *et al.*, 1988; Pollack and Hofbauer, 1991) but the glia that participate at these invaginations obviously differ at each of the three sites. Irrespective of the invaginating glial subtype, the photoreceptor controls the size of the capitate projection head (Edwards and Meinertzhagen, 2009). It is not known what role, if any, glial cytoskeletal proteins play in the formation, penetration, or maintenance of capitate projections but it is clear that photoreceptors and their cytoskeletal proteins play an important role in the shape, extension or maintenance of these specialised organelles, probably via an interaction between photoreceptors and glia that is initiated on the photoreceptor cell surface and requires Basigin (Curtin *et al.*, 2007).

Capitate projections are sites of vesicle endocytosis and the endocytotic proteins Clathrin and Endophilin localise to these organelles (Fabian-Fine *et al.*, 2003). Clathrin coated vesicles occur near capitate projections and endocytotic figures attached to the capitate projection stalk are seen during recovery from endocytotic arrest in the mutant

shibire, suggesting a role for the capitate projection in vesicle recovery and a postulated role in direct histamine recovery (Fabian-Fine *et al.*, 2003). The mechanism for the latter lacks evidence, however, and is suggested mostly from the economy of linking vesicle retrieval with histamine recyling in a single organelle and by the intimacy there between epithelial glia, which produce carcinine, and the photoreceptor terminal, which hydrolyses it to liberate trapped histamine. Capitate projections are dynamic and their various stages of development, from shallow to multiheaded, can be identified in a short series of EM sections. Furthermore, the numbers of capitate projections in a photoreceptor terminal can change dependent upon light conditions (Rybak and Meinertzhagen, 1997), pharmacological treatment (Pyza and Górska-Andrzejak, 2004), temperature (Brandstätter and Meinertzhagen, 1995), or genetic mutation - including mutations of *tan* and *ebony* (Meinertzhagen and Wang, 1997).

2.4.2.5 A POSSIBLE ROLE FOR OTHER GLIA

Tan protein localises exclusively to photoreceptors (Wagner *et al.*, 2007) and the fly's rapid histamine recycling pathway in the lamina has been proposed to work via a shuttle pathway between photoreceptor terminals and *ebony*-containing epithelial glia (Borycz *et al*., 2002; Richardt *et al*., 2002; True *et al*., 2005; Wagner *et al*., 2007) as reviewed in Stuart *et al.* (2007). However, histamine immunolabelling itself localises not only to the photoreceptors but also to a narrow band beneath the basement membrane of the eye that corresponds to the fenestrated and/or pseudocartridge glia (Romero-Calderón *et al.*, 2008) as well as to a band beneath the lamina neuropile that corresponds to the location of marginal glia (Borycz *et al.*, 2002; Romero-Calderón *et al.*, 2008). These glia contain neither HDC nor Tan and thus neither produce histamine on their own nor recycle it from carcinine. We propose that marginal glia may act as a sink for excess histamine which cannot be quickly transported back to photoreceptors at sites along the length of their terminals. However, this possibility poses two problems. First, it is not known how marginal glia which are not intimately associated with the R1-R6 terminals at sites of their histamine release, acquire histamine. Two possibilities exist: 1) excess histamine pools at the bottom of the lamina neuropile and is taken up at marginal glia either by transporters or by endocytosis, given that in *Musca* these glia also contain coated vesicles (Saint Marie and Carlson, 1983b); and 2) in *Musca* marginal glia are reported to connect to epithelial glia via gap junctions (Saint Marie and Carlson, 1983b), which allow

the passage of dyes up to at least 2 kDa in size (Phelan and Starich, 2001), and so could allow excess carcinine to pass from the epithelial glia into the marginal glia for storage. The second problem may thus simply be the reverse of the first, namely how carcinine then finds its way back to the photoreceptor terminal.

Ebony protein localises not only to the epithelial glia but also to medulla neuropile and chiasmal glia (Richardt *et al.*, 2002). In addition, close inspection of previously published confocal microscopy data (Wagner *et al*., 2007) reveals possible additional sites of Ebony expression in the lamina proximal satellite glia. Table 2.3 provides a list of cell markers and *Drosophila GAL4* lines which drive expression in glia and may be used to correctly identify which adult optic lobe glia express Ebony or other histamine-related proteins.

The wide range of Ebony expression suggests that other glia may be involved in histamine recycling and, in addition, a storage function for lamina glia can be suggested in one further example. Mutant *ebony* flies, which cannot produce carcinine from histamine and have 50% less total head histamine than wild-type flies, lack the wild-type band of histamine immunolabelling beneath the basement membrane (Borycz *et al.*, 2002). This band corresponds to the location of the fenestrated and pseudocartridge glia, two glial subtypes which do not normally express Ebony protein (Richardt *et al.*, 2002). It is unclear how an *ebony* mutation affects histamine expression in glia which do not normally express *ebony* unless we consider these glia a barrier to, or storehouse for, excess histamine, a storehouse not otherwise needed in an *ebony* fly because of its failure to effectively recycle histamine through the epithelial glia pathway. It is not known how histamine reaches the fenestrated and pseudocartridge glia which in *Musca* are separated from the lamina neuropile, and thus from the source of histamine, by a band of pseudocartridge and satellite glia rich in occluding junctions (Saint Marie and Carlson, 1983b).

One way in which histamine could enter the fenestrated and pseudocartridge glia is via the vesicular monoamine transporter DVMAT-B, which has been identified in the fenestrated glia in *Drosophila* (Thimgan *et al.*, 2006; Romero-Calderón *et al.*, 2008). VMAT transporters normally mediate the transport of monoamine neurotransmitters into secretory vesicles, and *Drosophila* variants of this protein recognise and possibly transport the biogenic amines, dopamine, 5-HT, octopamine, tyramine and histamine (Greer *et al.*, 2005). DVMAT-A is immunolocalised to dopaminergic and serotinergic

neurons, as well as to octopaminergic type II terminals at the neuromuscular junction (Greer *et al.*, 2005), while DVMAT-B immunolocalises to the fenestrated glia (Romero-Calderón *et al.*, 2008). This site is unusual because it is glial and because the fenestrated glia, while they are probable sites of endocytosis, are not known to have vMAT-associated secretory vesicles. vMAT must therefore be associated with the plasma membrane of fenestrated glia, as has been observed *in vitro* with vMAT-B transcripts in *Drosophila* S2 cells (Greer *et al*., 2005). Further implicating a role for *dVMAT-B* in histamine uptake/recycling in the visual system is the finding that mutants $dVMAT^{P1}$ and $dVMAT^{\Delta 14}$ have reduced head histamine concentrations as well as reduced histamine immunolabelling in the distal lamina, decreases that are restored by glial specific rescue of *vMAT-B* (Romero-Calderón *et al.*, 2008). Three main interpretations have been proposed for these VMAT-B containing fenestrated glia: 1) that they store carcinine produced by epithelial glia before transferring it back to the photoreceptor in some way, 2) that they buffer 'spillover' between adjacent cartridges, and 3) that they store histamine as a reserve for use under conditions of intense signalling (Romero-Calderón *et al.*, 2008). Direct evidence is available for none of these, however, and must await future analysis.

2.4.2.6 OTHER NEUROTRANSMITTERS

Even though Ebony function has been characterised as a β-alanyl-histamine synthetase within the glia of the visual system (Hovemann *et al.*, 1998; Richardt *et al.*, 2002; Richardt *et al.*, 2003), Ebony in fact expresses in glia throughout the CNS (Hovemann *et al.*, 1998). Biochemically it acts to conjugate β-alanine to other biogenic amines in addition to histamine; the requirement for β-alanine is essentially absolute, but many amines can act as a substrate (Richardt *et al.*, 2003). Despite this *in vitro* evidence, Ebony's role is confirmed only for histamine and visual system functioning (Borycz *et al.*, 2002; Richardt *et al.*, 2002; Richardt *et al.*, 2003) and, apart from its regulation of dopamine in the cuticle and in locomotor behaviour (Suh and Jackson, 2007), there is no other indication for what additional neurotransmitters Ebony might act upon *in vivo.*

Glia not only take up and inactivate amine neurotransmitters, they also play a vitally important role in clearing other neurotransmitters, such as glutamate, from the extracellular space. As evidence of its importance, loss of the *Drosophila* glial protein Excitatory Amino Acid Transporter (dEAAT) induced by means of RNA interference

(RNAi) shortens lifespan and results in brain neuropile degeneration, apparently as the outcome of glutamate-mediated neurodegeneration resulting from oxidative stress (Rival *et al.*, 2004; Liévens *et al.*, 2005). Finally, in addition to uptake, at least one enzyme for neurotransmitter synthesis is expressed in glia. Thus the gene for dopa decarboxylase, which is required to synthesize dopamine and 5-HT, is expressed in a subset of glia in the larval CNS (Beall and Hirsh, 1987; Mastick and Scholnick, 1992).

In addition to, and possibly associated with, uptake of neurotransmitters, glia also have endocytotic activity. When the temperature-sensitive allele of *shibire*, which codes for Dynamin and is required for clathrin-mediated endocytosis (e.g., Artalejo *et al.*, 1995), is expressed in most glia of the *Drosophila* adult by means of a *repo-GAL4* driver, lethality ensues after only three days at the restrictive temperature (Doherty *et al.*, 2009). Thus, adult glia engage in a number of endocytotic functions which are essential for survival (Doherty *et al.*, 2009). Note, however, that this interpretation rests exclusively on the role played by Dynamin in endocytosis, and does not take into account Dynamin's other functions in cells, especially as a microtubule-associated protein (Shpetner and Vallee, 1989). Evidence for the latter comes from *shibire* mis-expression, which results in microtubule bundling and signs of degenerative changes in photoreceptor and lamina neurons (Gonzalez-Bellido *et al.*, 2009).

2.5 Neurotransmitter Uptake Functions of Glia, and Glial Involvement in Behavioural Regulation

Glia play an important role in neurotransmitter clearance and this, ultimately, affects vision, locomotion, sexual behaviour, survival and other behaviours as we now detail.

The ability of insect glia to take up neurotransmitters and clear them from the extracellular space has been long established. Cockroach glia take up glutamate at the neuromuscular junction (NMJ; Faeder and Salpeter, 1970) and in the locust glia surrounding the NMJ absorb tritiated GABA (van Marle *et al.*, 1985). GABA transporters have been immunocytochemically localised to neuropile glia within the antennal lobes of *Manduca* where they are believed to regulate the extracellular GABA levels within that neuropile (Oland *et al.*, 2010). In flies, so too, do the satellite, epithelial and marginal glia take up GABA in the lamina (Campos-Ortega, 1974), although in that neuropile endogenous sources of GABA are apparent only for two types of centrifugal neuron (Kolodziejczyk *et al.*, 2008). In addition, as previously discussed, epithelial glia take up

histamine released from photoreceptors, clearing it from the cleft (Borycz *at al*., 2002) and may possibly take up glutamate at sites, known as gnarls, where these glia lie in close association with amacrine cells (Meinertzhagen and O'Neil, 1991).

2.5.1 The Role of Glia in Glutamate Transport and Courtship

In *Drosophila*, glutamate is an essential neurotransmitter in normal adult sexual courtship, and glia play an essential role in the regulation of both glutamate and sexual behaviour. A mutation in the glial cysteine/glutamate amino acid transporter *genderblind* results in male flies courting other males with the same probability as that with which they would court females (Grosjean *et al.*, 2008).

Genderblind is not only expressed throughout development in a subset of larval CNS glia and in perineurial glia along peripheral nerves (Augustin *et al.*, 2007), but it is also abundant in glia of the adult CNS (Grosjean *et al.*, 2008). While it is difficult to study the exact mechanism of Genderblind action in the adult, its action in the larval PNS provides some clues as to how it may regulate glutamate levels in the adult CNS. At the larval NMJ, perineurial glia take up secreted glutamate and then release it into the haemolymph, thus regulating the amount of glutamate available at the synapse (Augustin *et al.*, 2007). Reduction of Genderblind function in larvae ultimately results in reduced extracellular glutamate (Augustin *et al.*, 2007) and other amino acids (Piyankarage *et al.*, 2008). Furthermore, mutations of the *genderblind* transporter affect not only the concentration of glutamate but also the number of glutamate receptors at the NMJ. A 50% reduction in extracellular (haemolymph) glutamate coincides with a 2-3 fold increase in postsynaptic GluRIIA and GluRIIB receptors in *genderblind* larval NMJs. This receptor phenotype consequently affects synaptic transmission in the larvae which can, in turn, be rescued by the addition of glutamate (Augustin *et al.*, 2007).

Reducing Genderblind function exclusively in the adult glia using RNAi alters courtship behaviour (Grosjean *et al.*, 2008) suggesting that this behaviour is dependent on adult regulation of neurotransmitter. Indeed, altered courtship behaviours in male *genderblind* mutants result because changes in adult ambient extracellular glutamate levels and receptor clustering, in turn, cause improper information processing of a repelling odorant, 7-tricosine, which is emitted by other male flies (Grosjean *et al.*, 2008).

2.5.2 Glutamate Transport Via Glia dEAATs Affects Dopaminergic Neuron Survival, and Ultimately Motor Control

Glial regulation of glutamate concentration is required to prevent neurodegeneration in the brain. In adult *Drosophila,* EAATs that transport both glutamate and aspartate (Donly *et al.*, 1997; Seal and Amara, 1999; Besson *et al.*, 2000) localise to Repo-expressing glial cells in the protocerebral bridge, the optic lobes, and to glial extensions that project close to synaptic areas. Loss or reduction of the glutamate buffering capacity, which requires dEAAT, is neurotoxic, thus revealing the necessity of this glial transporter (Rival *et al.*, 2004).

Flies expressing *dEAAT1* RNAi walk normally but have deficits in flying and escape behaviour (Rival *et al.*, 2004). These behavioural deficits are believed to be central in origin since no electrophysiological disruption of synaptic transmission at NMJs is obvious nor does expressing *dEAAT1* RNAi in peripheral glia, surrounding the motor neurons, elicit the same behavioural phenotype. Locomotor deficiencies are significantly rescued by expressing human EAAT2 under the control of the *Drosophila* promoter, suggesting that the behavioural phenotype results in part from a glutamate transport deficiency. Ultrastructural analysis of the CNS in *dEAAT* flies reveals neurons that appear to be undergoing degeneration. It is proposed that a lack of glial *dEAAT* results in an accumulation of glutamate in the extracellular space and that this excess glutamate induces oxidative stress in neighbouring neurons, with dopaminergic neurons showing increased vulnerability to degeneration. Flies having reduced dEAAT1 function ultimately exhibit reduced survival, living on average 10-13 days compared with 20-29 days for controls (Rival *et al.*, 2004).

2.5.3 The Role of Glia in Circadian Rhythmicity

In *Drosophila,* circadian rhythms are controlled by two interconnected molecular loops involving the clock genes *timeless*, *period, cycle*, and *dclock* (Boothroyd and Young, 2008; Helfrich-Förster, 2009). Sites of *period* expression and function are widespread and include glia as well as neurons (Ewer *et al.*, 1992). Some clock neurons also express the neuropeptide Pigment Dispersing Factor (PDF), which is released to regulate cells downstream in the circadian pathway (Helfrich-Förster and Homberg, 1993; Helfrich-Förster, 1995; Lear *et al.*, 2005; Mertens *et al.*, 2005). The following text summarises the involvement of glia in the fly's circadian clock mechanisms.

2.5.3.1 EBONY AND THE CLOCK GENES

In the adult, Ebony protein localises exclusively to glia, at areas close to the projections of clock neurons in the optic lobe, protocerebrum and thoracic ganglion (Richardt *et al.*, 2002), with a subset lying close to 5-HT and dopamine-positive neurons (Suh and Jackson, 2007). Some of these Ebony-expressing glia contain clock genes, others do not, and yet *ebony* RNA, which itself displays robust circadian cycling (Ueda *et al.*, 2002), is not dependent upon PDF, suggesting the internal control of *ebony* cycling by clock genes in some glia and indirect control by clock neurons in others (Suh and Jackson, 2007).

2.5.3.1.1 EBONY PERTURBS *DROSOPHILA* LOCOMOTOR ACTIVITY

The likely involvement of glia in aspects of circadian regulation is immediately obvious in the case of *ebony* because of this gene's exclusively glial pattern of expression. However, an explanation for the ability of Ebony expressing glia to modulate locomotor behaviour is more elusive and depends upon the proximity of subsets of glia to neurons controlling locomotion.

Mutations in the *ebony* gene perturb *Drosophila* locomotion, causing the normally 'day active' rhythmic pattern of locomotor activity to become arrhythmic (Newby and Jackson, 1991). On the other hand, *ebony* mutations do not affect the circadian pattern of eclosion, suggesting that these two circadian behaviours are regulated by different mechanisms, only one of which requires *ebony* function (Suh and Jackson, 2007). The *ebony* RNA exhibits circadian cycling with peak expression at 5 hours after zeitgeber time, ZT5 (Claridge-Chang *et al.*, 2001), and cycling both in a normal light:dark cycle and in total darkness (Suh and Jackson, 2007). The spatial distributions of the dopamine-producing enzyme Tyrosine Hydroxylase, as well as of PDF and Timeless proteins, are the same in *ebony* mutants as in controls. The proximity of Ebony-expressing glia to clock cells, on the one hand, and to 5-HT and dopamine containing neurons on the other, as well as *ebony*'s genetic interactions together indicate that *ebony* acts downstream of the clock to regulate the fly's circadian behavioural rhythms (Suh and Jackson, 2007). However, Ebony has not yet been shown to modify 5-HT or dopamine in the nervous system *in vivo.*

Ebony function is required for high levels of daytime activity (Suh and Jackson, 2007). Furthermore, not only is Ebony expression circadian, but the responsiveness of the dopamine receptor-mediated modulation of motor behaviour is, itself, also under circadian control. Ebony protein production increases concurrently with a decrease in postsynaptic dopamine receptor sensitivity, both of which occur during the subjective day (Andretic and Hirsh, 2000; Suh and Jackson, 2007). The gene *black*, which codes for an aspartate/glutamate decarboxylase responsible for the production of Ebony's substrate, β-alanine (Phillips *et al.*, 1993), also cycles during a normal light–dark cycle. However, somewhat contradicting an increase in Ebony during the day is the finding that *black* peaks during the night, around ZT16 (Ceriani *et al.*, 2002). While dopamine concentrations have not been shown to cycle throughout the day, a simultaneous increase in the concentration of dopamine-inactivating Ebony protein in the glia and a decrease in dopamine receptor sensitivity suggest a means to offset possible changes in dopamine concentration (Andretic and Hirsh, 2000). Together, this evidence suggests Ebony as a candidate in modulating the dopaminergic control of locomotor behaviour.

2.5.3.2 Rhythmic Changes in Epithelial Glial Size

Not only does *ebony* mRNA expression display circadian rhythmicity but some *ebony*-expressing glia also exhibit circadian changes in size (Pyza and Górska-Andrzejak, 2004). Multiple cellular compartments of the fly's lamina cartridge exhibit rhythmic size changes. In *Musca* the cross-sectional areas of the lamina monopolar L1 and L2 axon profiles normally expand during the day and shrink at night, with the rhythm for L2 being circadian (Pyza and Meinertzhagen, 1996, 1999). The phase of corresponding size changes in L1 and L2 is reversed in *Drosophila* from that in *Musca* (Pyza and Meinertzhagen, 1999), although the phenomenon probably shares a similar mechanism in both flies. At least in *Musca*, the axon size changes are counteracted by opposite changes in the profile area of the epithelial glia, which expand in the night and shrink during the day (Pyza and Górska-Andrzejak, 2004).

Glia, presumably epithelial glia, obviously exert some form of control over the circadian modulation of L1/L2 axon diameter because injecting glial metabolic toxins such as fluorocitrate and iodoacetate increases these day/night size changes, suggesting that the glia normally act to inhibit their extremes (Pyza and Górska-Andrzejak, 2004). However, this interpretation rests on the specificity of these toxins in fly glia and the

localisation of their action to epithelial glia. On the other hand octanol, which closes gap junctions, has the opposite effect. It disrupts the circadian changes of L2 in *Musca*, preventing L2's swelling during the day, while L1 axons are less affected. Octanol also decreases the profile areas of the epithelial glia, preventing their swelling during the subjective night (Pyza and Górska-Andrzejak, 2004). This suggests that inter-glial communication via gap junctions is necessary for epithelial glia to modulate changes in axon profile size, however it fails to rule out any possible contribution from the gap junctions that exist between neurons (Saint Marie and Carlson, 1985). In addition, both octanol and iodoacetate also have an effect on the number of the glial/photoreceptor specific capitate projection organelles. These findings suggest that the glial cells mediate circadian information from the clock neurons to the lamina neurons to modulate processing of visual information during the day and night (Pyza and Górska-Andrzejak, 2004).

2.6 CELLULAR AND METABOLIC FUNCTIONS OF GLIA

2.6.1 GLIA AND HOMEOSTASIS: ION BUFFERING AND TROPHIC SUPPORT

A number of studies indicate that functioning glial cells are required for neuronal survival. For example, glia surround photoreceptor axons in the lamina neuropile and cortex, and if these cells are dysfunctional, as in *repo*, there is increased photoreceptor cell death (Xiong and Montell, 1995). In the embryonic insect's CNS, loss of glial cells, either by targeted glial ablation or by mutantion of *gcm,* leads to excess neuronal apoptosis among follower neurons (Booth *et al.*, 2000).

Other cases of trophic dependence of neurons have recently been reviewed (Zhu *et al.*, 2008) but in most cases an exact glial source has neither been inferred nor closely demonstrated. Recently, a neurotrophin has been discovered which is released from glia and is responsible for the maintenance of dopaminergic neurons, but expression has so far only been demonstrated during development (Palgi *et al.*, 2009). On the other hand, the *Drosophila* neurotrophin superfamily members DNT1, DNT2 and Spätzle may play a role in neuronal survival of adults (Zhu *et al.*, 2008). *DNT1* transcripts are expressed in the CNS throughout development as well as in the optic lobes and central brain of the adult. A loss of function *DNT1* induces a significant increase in apoptosis

after embryonic stage 17, while over-expressing *DNT1* in all neurons is able to suppress naturally occurring apoptosis. However, it is not clear in this particular case whether these neurotrophins have a glial origin. Loss of function of any one of DNT1, DNT2 or Spätzle results in slow, uncoordinated movements in the adult. Yet these motor defects likely stem from abnormalities in development and it is not known if the neurotrophins in question continue to promote cell survival after metamorphosis (Zhu *et al*., 2008).

It is not exactly known why glial malfunction results in the cell death of its neighbouring neurons. A general proposal is that glia are essential to buffer K^+ in the extracellular space and are involved in metabolic signalling to their associated neurons. In *repo* mutants, adult flies can be identified by a reversal in the polarity of the ERG (Xiong *et al.*, 1994). This reversal has been attributed to defects in the ability of fenestrated, pseudocartridge and satellite glia, which lie between the eye and the lamina neuropile, to buffer K^+ correctly. Lamina glia fail to buffer K^+ released by the lamina neurons they surround, thus increasing the lamina's response to light to twice that recorded from wild-type flies (Xiong *et al.*, 1994). When the small corneal negative response is summed with an enhanced positive lamina response an overall positive response is recorded. Thus, it is possible that the reversed-polarity ERG observed in *repo* results from a combined deficiency in K^+ buffering and impaired resistance to current flow in the lamina. The ultimate result of this loss of lamina glia is the death of both lamina monopolar neurons and photoreceptors (Xiong and Montell, 1995).

2.6.2 GLIOTROPHIC FACTORS

The above examples document neuronal responses to glial malfunction. In contrast, we also include documentation of the cases in which neurons exert positive influence on the survival, growth or maintenance of glia. Thus, neurons in the developing CNS midline secrete gliotrophic factors, such as Spitz (Kim and Crews, 1993) and Vein (Hidalgo *et al.*, 2001), which activate Epidermal Growth Factor Receptors on the surface of glial cells (reviewed in Hidalgo, 2002). In addition, PVF and PVR promote midline glial survival through ATK and extracellular-regulated kinase (ERK) pathways (Learte *et al.*, 2008).

2.6.3 GLIA AND NEURONAL METABOLISM

The honeybee's retina has proved an excellent model system to study the metabolic relationship between photoreceptor neurons and their glial counterparts in the retina, the pigment cells. These two cell types exhibit a clear separation of metabolic functions, with photoreceptor neurons being aerobically very active and containing a large number of mitochondria, and pigment cells lacking mitochondria but possessing large quantities of glycogen (Tsacopoulos and Poitry, 1982).

In steady-state dark conditions pigment cells transform glucose, stored as glycogen, to phosphorylated glucose-6-phosphate (Tsacopoulos *et al.*, 1988; Tsacopoulos and Magistretti, 1996), which is then converted to pyruvate and ultimately alanine (Tsacopoulos *et al.*, 1994). Light conditions increase glial glycogen turnover and alanine production (Brazitikos and Tsacopoulos, 1991; Evêquoz-Mercier and Tsacopoulos, 1991). Alanine is then released from the pigment cells and taken up by neighbouring photoreceptors where it is converted to pyruvate that enters the Krebs cycle and in the process drives the production of NH_3 from the conversion of glutamate to α-ketoglutarate (Tsacopoulos *et al.*, 1994). Exogenous proline also enters the Krebs cycle and is likewise converted to glutamate and α-ketoglutarate with the production of NH_3 (Tsacopoulos *et al.*, 1994).

Photoreceptors must first signal in order for pigment cells to increase glycolysis and produce alanine, because these cells themselves fail to respond directly to light stimulation (Tsacopoulos *et al.*, 1987). In the honeybee's retina, metabolically active photoreceptors produce and release glutamate and NH_3 which immediately becomes NH_4^+ at physiological pH (Tsacopoulos *et al.*, 1987). NH_4^+ is then transported along with glutamate into the neighbouring pigment cells via a member of the K^+-Cl^- co-transporter family, which is selective for NH_4^+ over K^+ (Marcaggi *et al.*, 1999; Marcaggi and Coles, 2000). Glutamate uptake by the pigment cells regulates the concentration of this potentially toxic amino acid in the extracellular space, in a role that is adopted by glia elsewhere in nervous systems (Seal and Amara, 1999). A rise in the intracellular concentrations of NH_4^+ and glutamate in the pigment cell triggers glycolysis by acting directly on the enzymes phosphofructokinase, alanine aminotransferase and glutamate dehydrogenase, leading to the production and release of alanine (Tsacopoulos *et al.*, 1987). While some may not consider pigment cells to be glia, this system still implicates an important role for neuronal support cells in assisting the proper function of neurons.

The system remains to be validated in *Drosophila*, but already provides evidence for a nutritive function of glia in maintaining neurons that is both novel and comprehensive.

2.7 Glial and Neuronal Interactions During Growth and Neurodegeneration

Neurons and glia engage in reciprocal signalling so that whenever the integrity of one is threatened, the other may show reactive changes. In addition to these interactions, there are also interactions among the glial cells themselves. For example, after a chemical gliaectomy in the abdominal connective of the cockroach that spares the neighbouring neurons, the surviving glia undergo division (Smith *et al.*, 1990). In adult *Drosophila*, however, there appears to be only a finite period of time during early adulthood when glia are able to divide in response to degeneration of their neuron neighbours (Kato *et al.*, 2009) and, in this respect, insect glia are unlike their vertebrate counterparts. Thus, although capable of division to replace the loss of their own kind, most glia fail to divide in response to axonal lesions and neuronal death in mature adults. Instead they manifest changes that have received particular attention in *Drosophila*. We will consider these below, first as the death of neurons when glial function is impaired and then the more intensively studied changes in glia when their neuronal partners are damaged and undergo degeneration.

2.7.1 Neuron Death From Glial Cell Dysfunction

Glia are required for the proper development and survival of neurons. The role of glia in development is well understood and their ability to provide developing axons with localisation signals has been extensively studied in *Drosophila* (for reviews see: Tayler and Garrity, 2003; Chotard and Salecker, 2004). The importance of glia in the adult brain is readily revealed by a number of *Drosophila* mutants including but not limited to: *drop dead* (Buchanan and Benzer, 1993), *swiss cheese* (*sws;* Kretzschmar *et al.*, 1997), and *repo* (Xiong and Montell, 1995). It can also be demonstrated by overexpression of mammalian proteins such as the polyglutamine polypeptides of *ataxin-3* (Kretzschmar *et al.*, 2005).

Adult *drop dead* flies survive into adulthood but anatomical abnormalities exist even before the behavioural phenotype manifests itself. Upon eclosion the neuronal morphology appears normal, yet glial cells are stuck in the early stages of development

and their stunted processes fail to form a complete glial sheath. As flies age the brain begins to degenerate (Buchanan and Benzer, 1993) and an acceleration of age-related markers that appear to suggest that theses flies age more rapidly (Rogina *et al.*, 1997). While the early onset mortality phenotype of *drop dead* may in part result from digestive abnormalities (Blumenthal, 2008), the aberrant shape of glia in the adult suggests rather obviously a role for proper glial development in the maintenance of nervous system function and neuronal survival (Buchanan and Benzer, 1993).

Glial hyperwrapping, as it occurs in the *Drosophila* mutant *sws*, was also thought to be associated with age-related neuronal apoptosis beginning at approximately three-to-four days of adulthood (Kretzschmar *et al.*, 1997). In these mutants glial hyperwrapping is observed during pupariation and precedes neuronal cell death. Anatomical features of neuronal cell death are followed, except among marginal and epithelial glia of the lamina, by signs of glial cell death (Kretzschmar *et al.*, 1997). Mutations of the *sws* gene may affect cell death by one of two means. The *sws* gene is a homologue of the Neuropathy Target Esterase (NTE; Zaccheo *et al.*, 2004) protein that codes for a brain-specific phospholipase (Mühlig-Versen *et al.*, 2005). Both SWS and NTE regulate the deacylation of phosphatidylcholine (PtdCho; Zaccheo *et al.*, 2004), a major lipid of cell membranes which is elevated in *sws* mutants (Mühlig-Versen *et al.*, 2005), and this altered lipid composition can be deleterious (Klein, 2000). SWS is expressed in the endoplasmic reticulum of neurons and some glia, and it is in the endoplasmic reticulum where most PtdCho is processed (Mühlig-Versen *et al.*, 2005). In addition, the SWS protein acts as an inhibitor for the C3 catalytic subunit of cAMP activated protein kinase (PKA-C3). It has been proposed that normal SWS regulates, via inhibition, the localisation of kinase activity within the membranes and that an excess of PKA-C3 results in neurodegeneration (Bettencourt da Cruz *et al.*, 2008). Despite the finding that *sws* acts cell autonomously in both neurons and glia, neuron-specific rescue of the vacuolization phenotype is effective but incomplete, while glial hyperwrapping can be prevented with glial specific rescue and thus the neurodegenerative phenotype may still be affected by dysfunction in the glia (Mühlig-Versen *et al.*, 2005).

In the adult visual system *repo* is expressed in all lamina and medulla glia, including the fenestrated and pseudocartridge glia that underlie the retina. In the visual system of *repo*^{1} mutants, the survival of lamina neurons and photoreceptor cells depends upon *repo* expression in the associated glia. The photoreceptors degenerate in a retrograde

fashion, possibly as a result not only of the loss of their synaptic partners, the lamina monopolar cells, but also the loss of their supporting lamina glia (Xiong and Montell, 1995) but these details need to be elucidated.

In addition, in a *Drosophila* model of polyglutamate expansion diseases, such as Huntington's disease, overexpression of polyglutamine (polyQ) polypeptides from the C-terminus of human *ataxin-3* has been found to reduce life span in a way that correlates with the length and expression level of the polyQ tract. Flies with neuronal overexpression show no signs of degeneration but those with glial expression reveal progressive glial degeneration and apoptosis as well as more severe defects in phototactic behaviour (Kretzschmar *et al*., 2005). This correlation further demonstrates the necessity of proper glial function for adult neuronal survival.

2.7.2 The Glial Response to Neurodegeneration

Two kinds of neuronal degeneration are generally acknowledged: developmental degeneration, for example axonal pruning or removal of entire cells by apoptosis, and Wallerian degeneration, damage to a cell that appears in its distal extremities and proceeds in an anterograde direction (Griffin *et al.*, 1995). Neuronal degeneration, either natural or injury induced, elicits reactive gliosis as a response from neighbouring glia that involves changes in gene expression and morphology, so that the glia extend processes to invade the injury site and become actively involved in the clearance of degenerating neurites. In some species, such as ants, experience- dependent axonal pruning can occur for up to 60 days post-eclosion (Seid and Wehner, 2009), but most glial phagocytosis of axons in adult insects is in response to neuronal malfunction and axonal injury.

2.7.2.1 Wallerian Degeneration: Physical Features of the Glial Response to Neuronal Degeneration

The genetic pathways required to induce glial responses exhibit several key differences when these occur either in response to neurite pruning or to injury-induced degeneration. In studies utilizing flies, Wallerian degeneration has been induced by acute transection of antennal lobe neurons (ORNs) or by damage to photoreceptors. Injured ORN axons and their clearance from the CNS have been visualized by their

expression of fluorescent fusion gene markers. These reveal changes in glial cell morphology within 24 hours and complete removal of neuronal GFP from the site of injury within 5 days (MacDonald *et al.*, 2006).

2.7.2.2 REACTIVE GLIOSIS IN THE VISUAL SYSTEM

Degeneration among photoreceptor axons becomes apparent in only 2-5 minutes after mechanical lesions to the Dipteran retina (Griffiths and Boschek, 1976) and this degeneration has been quantified as a series of timed ultrastructural changes in the lamina, from 1 hour to 8 days. Photoreceptor axons that have been injured by photoablation of their cell bodies reveal non-synchronised degeneration of their synaptic terminals that starts within minutes, followed by changes among the surrounding epithelial glia (Brandstätter *et al.*, 1991). Slower changes follow retinal degeneration in mutant *Drosophila* (Stark and Carlson, 1982, 1985) and in flies exposed to high intensity blue irradiation (Stark and Carlson, 1984). Reactive gliosis and glial hypertrophy accompany these changes in the lamina, becoming obvious within the first week of degeneration as epithelial glia insinuate themselves at postsynaptic sites of former tetrads when these are vacated by the normal L1 and L2 target dendrites (Brandstätter *et al.*, 1992). Gliosis also occurs among the glia of the medulla, after lesion of the central photoreceptor neurons R7 and R8, such that over a six-day period the number of glial profiles increases to occupy a greater portion of the column cross section (Campos-Ortega and Strausfeld, 1972).

Parallel findings come from studies of retinal degeneration mutants. In flies mutant for *retinal degeneration A* (*rdgA*^{PC47}) photoreceptors degenerate after one week yet, in the lamina, both the monopolar neuron and glial somata are reported to be ultrastructurally normal (Stark and Carlson, 1985). Gliosis is nevertheless presumed to take place because glia expand into the area occupied by damaged photoreceptors (Stark and Carlson, 1985). In a second retinal degeneration mutant *rdgB*^{KS222}, there is no obvious change in epithelial glial morphology one week after eclosion even though degenerative changes such as electron dense photoreceptor axons and swollen lamina interneurons are readily evident. Gliosis becomes apparent by 21 days post-eclosion when the lamina contains scattered electron-dense profiles of cells presumed to be R1-R6 axons and other axons have been completely phagocytosed (Stark and Carlson, 1982). While Stark and Carlson (1982) suggest that glial cells multiply and fill the areas left by

degenerating axons, they provide no evidence of actual glial cell division and so expansion alone may account for the increased glial volume.

Concurrent with the degenerative changes in the photoreceptor neurons R1-R6, and the expansion of epithelial glial cell profiles, cortex satellite glia which surround the somata of lamina cells also respond quickly by increasing their production of the lysosomal marker, enzyme acid phosphatase (AcPase), at first in the endoplasmic reticulum, then to extracellular sites between the satellite glia and photoreceptor axons, and finally within the synaptic terminals. The glial cells are thought to export hydrolytic enzymes via the golgi-endoplasmic reticulum-lysosome complex to the photoreceptor axon interface (Griffiths, 1979).

2.7.2.3 GLIAL FACTORS MEDIATING THE RESPONSE TO DEGENERATION OF NEURONS

2.7.2.3.1 DRAPER

The glial response to neural degeneration is characterised by dramatic changes in glial cell shape. Early reports (Stark and Carlson, 1982; Shaw, 1984a) revealed the phagocytotic activity of lamina epithelial glia after photoreceptor degeneration. In mature adult flies, glia respond by increasing their surface area and extending projections into the site of injury rather than by proliferation or migration (MacDonald *et al.*, 2006). These changes are accompanied by an upregulation of the glial transmembrane protein Draper (Drpr), a *Drosophila* homologue of the *C. elegans* cell corpse engulfment gene *ced-1* (Freeman *et al.*, 2003). Injured axons fail to be cleared in *drpr* mutant flies. Furthermore, after ablating antennal segments in $drpr^{\Delta 5}$ mutants, noticeable changes in glial cell morphology are lacking. Glial processes do not accumulate in antennal lobe glomeruli housing severed axons and the intensity of GFP labelling in glia does not increase. A similar finding has been obtained in *drpr* RNAi flies. Both mutant and knock-down findings indicate a failure of glia to respond to axonal damage (Freeman *et al.*, 2003).

The Drpr protein itself may act as a glial receptor for molecular cues from severed axons, and it can drive recruitment of glial processes to injured axons for engulfment. Drpr is localised to severed axons four hours after ablation or axotomy, is concurrent with the appearance of the GFP puncta characteristic of degenerating axons, and is

maintained at high levels until all traces of GFP from degenerating axons are eliminated from the CNS (MacDonald *et al.*, 2006).

2.7.2.3.2 SIX MICRONS UNDER

The *Drosophila* phagocytosis receptor Six Microns Under (SIMU) is another member of the *ced-1*/*drpr* family of genes that is expressed in phagocytosing glia and is required to clear apoptotic profiles of degenerating cells from the nervous system (Kurant *et al.*, 2008). Like Drpr, the SIMU protein has a large extracellular EMILIN-like N-terminal domain required for protein recognition and binding but unlike Drpr has only a short intracellular cytoplasmic tail at the C-terminus.

CNS glia appear morphologically normal in *SIMU* mutants, yet the number of apoptotic cell particles increases twofold and these are less likely to be engulfed by glia. A clue to the role of SIMU is revealed from the behaviour of phagocytes, which have normal search behaviour and mobility, and bind some apoptotic particles, but do not engulf them. Affinity purified HIS-MYC-SIMUΔTM protein readily binds to apoptotic S2 cells, while cells transfected to express SIMU take up more apoptotic cell particles than cells transfected to express only GFP (Kurant *et al.*, 2008).

SIMU and Drpr expression patterns strongly overlap each other, although expression of SIMU appears more patchy. Both *SIMU* and *drpr* mutants show a twofold increase in apoptotic particles, which in *drpr* mutants are found inside phagocytic cells such as glia and macrophages, while *SIMU* mutants display a three-fold increase in non-engulfed particles relative to wild-type (Kurant *et al.*, 2008). These findings indicate that *SIMU* mutants fail to recognize and/or engulf apoptotic cells, and because *SIMU*;*drpr* double-mutants resemble the *SIMU* mutant it appears that SIMU acts upstream of Drpr. Despite this conclusion, there is no interaction between SIMU and Drpr in co-immunoprecipitation studies, suggesting that an intermediary factor acts between the two to control engulfment, at least during developmental apotosis (Kurant *et al.*, 2008).

2.7.2.3.3 SHARK, SRC42A, AND CED-6

The downstream effectors of engulfment in glia are just beginning to emerge. Two examples are the kinases Shark and Src42A (Ziegenfuss *et al.*, 2008). Shark is a non-

receptor tyrosine kinase that binds Drpr at its intracellular domain, an immunoreceptor tyrosine-based activation motif. Shark is essential for Drpr-mediated signalling events that result in reactive gliosis. Drpr receptor activation initiates Src family kinase, Src42A, activity, which in turn phosphorylates Drpr. This allows Drpr's association with Shark and ultimately results in phagocytosis. RNAi knockdown of both Shark and Src42A suppresses glial hypertrophy, phagocytosis of damaged axons and interferes with the upregulation of Drpr that is associated with glial phagocytosis (Ziegenfuss *et al.*, 2008). As a member of the CED family of corpse engulfment proteins, Drpr may act in a similar manner to *C. elegans* CED-1 (see Awasaki *et al*., 2006), by mediating actin-dependent cytoskeletal reorganisation via Rac1 (Kinchen *et al.*, 2005) and Dynamin (Ziegenfuss *et al.*, 2008).

In *C.elegans* Ced-6 acts downstream of the Drpr homologue Ced-1 in response to apoptotic cell death (Liu and Hengartner, 1998). Similarly, in *Drosophila* Ced-6 is upregulated in response to cell death, both by apoptosis and Wallerian degeneration (Awasaki *et al.*, 2006; Doherty *et al.*, 2009). *Drosophila* dCed-6 and Drpr co-immunolocalise to both neuropile ensheathing glia and cortex glia in the adult, and both proteins are also recruited to the glial surface during degeneration of ORN axons. Furthermore, *drpr* and *dced-6* appear to interact genetically since transheterozygotic animals containing a single copy of both mutations display impaired clearance of degenerating axons, whereas the respective single-mutant heterozygotes are both able to clear degenerating debris. Thus, it is not surprising that *repo*-driven glial knockdown of *dced-6* via RNAi in *Drosophila* suppresses the recruitment of Drpr to the site of injury and the clearance of degenerating axons (Doherty *et al.*, 2009). What is novel, however, is the finding that in *Drosophila* the genetic interaction is reversed compared with *C. elegans*, with *drpr* acting downstream of *dced-6*.

2.7.2.3.4 ENSHEATHING GLIA PHAGOCYTOSE DEGENERATING AXONS

Drpr-mediated engulfment of degenerating neuron profiles, at least in the antennal lobes of *Drosophila,* is the responsibility of the ensheathing glia which surround the neuropile. Both Drpr and dCed-6 antibodies immunolocalise to the *mz0709-GAL4* expressing ensheathing glia, as well as the cortex glia, but only expression of *UAS-draper*^{RNAi} and *UAS-shark*^{RNAi} in ensheathing glia completely blocks clearance of GFP labelled axonal debris. Blocking *shibire*-mediated endocytosis specifically in ensheathing, but not

astrocyte-like glia also suppresses glial clearance of degenerating axons (Doherty *et al.*, 2009). Although antennal lobe cortex glia also express Drpr, it appears that these glia do not engage in the phagocytic engulfment of debris following axotomy, since they fail to compensate for the specific role of ensheathing glia in Drpr knockdown experiments.

2.7.2.4 NEURONAL FACTORS MEDIATING THE GLIAL RESPONSE TO DEGENERATION OF NEURONS

Expression of the mouse anti-apoptotic factor Wallerian degeneration slow (Wld^S) in *Drosophila* neurons prevents the glial response to Wallerian degeneration, i.e. changes in glial morphology and Drpr accumulation, that accompanies the removal of transected neurons but plays no role in developmental axon pruning (Hoopfer *et al.*, 2006). Wld^S is a fusion protein composed of 70 amino acids from the polyubiquitination protein UDF2/E4 (required for both developmental pruning and injury induced degeneration) and the full-length nicotinamide mononucleotide adenyltransferase (Nmnat) which facilitates nicotinamide adenine dinucleotide (NAD) synthesis. While Wld^S is not reported in *Drosophila* its component systems, the ubiquitin-proteasome system (Zhai *et al.*, 2003) and NAD biosynthetic pathway (Sasaki *et al.*, 2006), are both active in flies (Watts *et al.*, 2003; MacDonald *et al.*, 2006). The ubiquitin activating enzyme *Uba1* (E1) and the 19S proteasome regulatory particles *Mov34* and *Rpn6* have all been implicated in neuronal protein degradation, at least in developmental axon pruning (Watts *et al.*, 2003). Inhibiting the ubiquitin-proteasome system and thereby protein degradation in axons can delay Wallerian degeneration (Zhai *et al.*, 2003). *dNmnat1* acts in an opposite sense to the ubiquitin-proteasome system, with overexpression suppressing self destruction of transected ORNs, although at a reduced rate relative to full-length Wld^S overexpression. This suggests that the neuroprotective effects of Wld^S may proceed via an Nmnat-dependent mechanism (MacDonald *et al.*, 2006). The fact that protective factors elicit molecular signals from transected axons implies that these unknown signals have a role in eliciting the glial response that eventually engulfs the degenerating axons (Hoopfer *et al.*, 2006; MacDonald *et al.*, 2006).

In fact, sensory axons do not need to be transected to undergo Wallerian degeneration. A loss of cell autonomous activity is sufficient to induce degeneration in antennal lobe neurons (Chiang *et al.*, 2009). Antennal sensory neurons must express odorant receptors on their surface in order to transmit signals to the glomeruli of the antennal

lobe. When odorant receptors are mistargeted, such as in the *or83b* mutant, then odour-evoked neuronal activity is lacking and these neurons begin to degenerate concurrent with a glial response. Degeneration also occurs when sensory neurons transduce odorant stimuli but are unable to transmit that information to their postsynaptic partners by release of neurotransmitter, as occurs with light chain tetanus toxin (teTxLC) or *shibire*^{K44A} overexpression in ORNs (Chiang *et al.*, 2009), or when photoreceptor neurons fail to synapse with lamina monopolar neurons in *disco* mutants (Campos *et al.*, 1992). This degeneration is not caspase-dependent and cannot be rescued by overexpressing Wld^{s}, but is dependent upon the ubiquitin protease pathway, since expression of UBP2 can rescue the degeneration phenotype. Modulation of Glycogen synthase kinase-3β (GSK-3β) levels affects degeneration, thus suggesting that neuronal activity mediates its effect by inhibiting activity of this kinase in neurons. How GSK-3β modulates these changes is not known, but is likely to occur via a *wnt*-dependent pathway since *wnt* overexpression can also reduce degeneration in otherwise inactive neurons (Chiang *et al*., 2009).

2.7.2.5 The Glial Response to Degenerating Axons is Age Dependent in *Drosophila*

While glial cell division in response to the loss of glial cells has been long established (e.g., Smith *et al*., 1990), whether glia divide in response to axonal injury has been debated. Heat shock inducible mitotic recombination as well as BrdU incorporation labelling reveals low levels of mitotic activity in healthy adult flies, at least up to six days after eclosion. Most of these mitosing adult cells do, in fact, become glia and these glia are concentrated in an area ventrolateral to the antennal lobes, where the antennal nerves enter the brain (von Trotha *et al.*, 2009). Despite a prior lack of evidence for glial mitosis after neuronal lesions, a recent study shows that for the olfactory system and central brain, at least, the ability of glia to divide in response to neuronal degeneration depends on the fly's age. Naturally occurring programmed cell death (PCD), antennal neuron axotomy, and manual damage from stab-injury can all induce glial mitoses in young flies (Kato *et al*., 2009). This age discrepancy may be the reason why, during axonal degeneration of sensory neurons in the antennal lobes of *Drosophila*, glia have previously been shown only to expand into the spaces surrounding damaged axons, but not to multiply (MacDonald *et al*., 2006).

In the *Drosophila* brain, PCD occurs in a consistent spatiotemporal manner. It is detected at the root of the antennal nerve in a location where BrdU incorporation occurs during the first 10 days post-eclosion but not later (Kato *et al.*, 2009; von Trotha *et al*., 2009). The glial response is the same following axotomy and BrdU incorporation, but is not detected if flies are older than 8 days (Kato *et al.*, 2009). This suggests that glial cell division can only occur during specific periods of adult life. BrdU positive glial cells are located within or very close to neuropiles but not deep in the cortex or along the brain surface (Kato *et al.*, 2009), suggesting that they are neuropile glia, of which there are two types: ensheathing and astrocyte-like (Awasaki *et al.*, 2008). Thus, it is likely that only a distinct subset of glia responds to PCD, much as how only ensheathing glia respond to Wallerian degeneration (Doherty *et al*., 2009). Within the visual system, the epithelial glia, also a type of neuropile glia, fill the space occupied by dying photoreceptors and lamina interneurons and are suspected to undergo division (Stark and Carlson, 1985; Carlson and Saint Marie, 1990).

If PCD in neurons is disrupted by overexpressing the caspase inhibitor gene *p35*, then glia also fail to incorporate BrdU. This suggests that glia must respond to some signal from dying neurons themselves and not a cell-death signalling cascade that precedes cell death (Kato *et al.*, 2009). It is still not known, however, what the exact signal from dying neurons is that triggers mitosis, or the Shark- (Ziegenfuss *et al.*, 2008) and Drpr- (MacDonald *et al.*, 2006) mediated engulfment responses of glia. Within glia, the tumor necrosis factor Eiger may be the cell autonomous signal promoting cell-death induced mitotic division (Kato *et al.*, 2009). In *eiger* mutants PCD remains the same as in wild-type, yet glia fail to undergo mitosis. When *eiger* is rescued in the glia of *eiger* homozygous mutants, there is a significant increase in the number of BrdU positive glia around PCD or damaged neurons, supporting a cell-autonomous role for Eiger in the glial mitotic response to neuronal degeneration (Kato *et al.*, 2009).

2.8 CONCLUSIONS

In this review we have annotated and categorised the glia of adult *Drosophila* and their developmental origins in the optic lobe. This task is essentially complete only for the fly's optic lobe lamina. Given the wealth of glial cell types in the simple optic lamina, equal to the numbers of the co-populating neurons, we may only speculate as to how many glial cell types must exist in the rest of the brain. Most of this diversity remains to

be discovered, however, and will presumably be matched by a corresponding diversity of glial cell functions.

Glia have widespread functions in the insect brain, analysed most completely in *Drosophila*. We have enumerated examples in which glia act to modulate and inactivate neurotransmitters, thus modulating behaviour. They also clear neurotransmitter from the extracellular space, so as to modulate neurotransmitter concentration at the receptors of some populations of neurons and reduce oxidative stress in others. In addition they provide nutritive and support functions to maintain their neighbouring neurons and, in the case of Wallerian degeneration, are responsible for disposing of the very neurons they once helped maintain. Glia provide a barrier both to, and within, the CNS, isolating it from the haemolymph in the form of the blood brain barrier and selectively transporting substances into and out of the brain. Glia are active and responsive; capable of changing their shape, size and numbers to deal with alterations in their neuronal environment, and to perform these various janitorial, regulatory and policing functions.

These functions may seem disproportionate to the small number of glial cells in insect brains but glial cell function should perhaps be thought of in terms of the numbers of glial cell types, as well as their volume and shape, which in the neuropile is highly elaborated (Strausfeld, 1976). Although progress has been made in the optic lobe, where different glial cell types are clearly distinguishable, we are generally poorly informed on the partition of glial functions in different glial cell types. Thus, while the analysis of glial cell function in insect brains has, as in vertebrate brains, lagged behind the analysis of neuronal function, much progress has been made in recent years in *Drosophila* because mutants of such function have appeared in genetic screens. In addition to documenting that progress, this review also highlights areas in which future progress can be expected.

2.9 ACKNOWLEDGEMENTS

The authors' work reported in this review was supported by National Institutes of Health grant EY-03592 (to I.A.M.), a Killam Fellowship from the Canada Council (to I.A.M.), and by a postgraduate scholarship from NSERC, and a stipend from the Lett Fund of the Dalhousie University Biology Department (to T.N.E). We would like to thank C. Groh (University of Würzburg), W. Rössler (University of Würzburg) and D.A. Hopkins

(emeritus, Dalhousie University) for their careful reading and recommendations on the manuscript.

2.10 TRANSITION TO CHAPTER THREE

Chapter three continues with the themes explored in Chapter two, namely the structure and function of glia. Using different glia-specific transgenic lines I have visualized and further characterised the six distinct layers of glia which lie in the vicinity of adult lamina, as well as described at least four types of glia that reside within the underlying neuropile, the medulla. Using these same transgenic lines I examine how the glia just mentioned in the previous chapter arise during development of the adult fly from its antecedent larval and pupal stages. This was done partly with the aim of resolving the developmental origins of cells that are poorly reported in the literature and have often been confused amongst themselves and also with the glia of the larval stage of the life cycle. There is a divide within the visual system, with all three layers of glia lying above the lamina cortex deriving from the eye disc, and all three layers of glia lying within and below the lamina cortex having their origins in the brain. This work has been prepared as a manuscript for *Development*.

CHAPTER 3

THE METAMORPHIC DEVELOPMENT AND STRUCTURE OF *DROSOPHILA* VISUAL SYSTEM GLIA

Tara N. Edwards and Ian A. Meinertzhagen

3.1 ABSTRACT

The visual system of *Drosophila* is an excellent model for determining the types of interactions responsible for the differentiation of unique cell types. However, such a model is only useful if we can accurately and reliably identify the cells that engage in these interactions. Glia are important players not only in the development of the nervous system, but also in the function of neurons with which they associate in the adult. There must not only be a means by which to accurately identify the glial subtypes, but a correlation must also be made between the glial subtypes that exist in the larva and those previously described for the adult. We have traced subsets of the larval eye disc glia through the earliest stages of pupal development to determine their correlates in the adult. Two distinct populations of glia exist in the adult *Drosophila* lamina: those that arise from precursors in the eye-disc/optic stalk and those which arise from precursors in the brain. In both cases, one larval source gives rise to at least three unique types glia, some of different cellular classifications. Cell signalling events which differentiate glial subtypes of the lamina appears to continue through the earliest stages of pupal development but the signals which determine these sub-types are not known. Furthermore, analysis of glial cell types in the medulla has identified at least three types of astrocyte-like glia in this neuropile. The cellular interactions during development which establish different sub-types of glia, albeit of similar class, will be an interesting topic for future research.

3.2 INTRODUCTION

Glia are important partners of neurons not only in neural development but also for neuronal function. The diversity of glial cell types and their importance have been slow to emerge. In mammalian brains, glia can account for up to 90% of brain cells (Blinkov and Glezer, 1968), but in the less highly populated central nervous system of the fruit fly *Drosophila melanogaster* they may constitute only 10% of all cells (Ito, pers. comm.), most of which are not individually identified. Even so, in the ventral nerve cord and peripheral nervous system of *Drosophila*, the development (Beckervordersandforth *et al.*, 2008; von Hilchen *et al.*, 2008), structure (Ito *et al.*, 1995) and functions of glia (Battye *et al.*, 1999; Sepp *et al.*, 2000, 2001; Parker and Auld, 2004) have been addressed. The same cannot be said for the developing glia of the adult brain. Even within well studied regions of the brain such the visual system, for which intimate details

of neuronal circuits are now well known (Meinertzhagen and O'Neil, 1991; Takemura *et al.*, 2008), little is understood about the development or functions of the many subtypes of co-populating glial cells.

In *Drosophila*, glia are grouped into three general classes: surface, cortex and neuropile. Surface glia, which surround the brain and function as the barrier between it and the haemolymph of its open circulatory system, are of two kinds. Small, numerous perineurial glia lie at the periphery and are likely to engage in endocytosis, but do not themselves form a barrier to the passage of substances into the brain (Chi and Carlson, 1981; Awasaki *et al.*, 2008). Underlying the perineurial glia are large, flat subperineurial glia (Eule *et al.*, 1995). These contain numerous septate junctions which impede the flow of substances between cells, and thus serve as a component of the blood brain barrier in various insect species (Shaw, 1978; Saint Marie and Carlson, 1983a; Shaw and Henken, 1984; Stork *et al.*, 2008).

Insect neurons are monopolar, with cell bodies that lie in a rind or cortex around their respective neuropiles, wherein projections from their axons form synapses (Bullock and Horridge, 1965). Cortex glia have cell bodies that co-occupy the cortex with the cell bodies of neurons, while neuropile glia lie within the neuropile itself (Freeman and Doherty, 2006; Awasaki *et al.*, 2008).

Although the basic anatomy of glia in the *Drosophila* larval brain and eye disc has been described in detail (Winberg *et al.*, 1992; Choi and Benzer, 1994; Hummel *et al.*, 2002; Dearborn and Kunes, 2004; Silies *et al.*, 2007), as has adult optic lobe glial anatomy (Eule *et al.*, 1995; Tix *et al.*, 1997), it is still hard to match the identities of glia in the larva with those in the adult visual system. In the larva there are at least four identified subtypes of glia within the eye disc alone (Silies *et al.*, 2007) and another four subtypes within an area of the brain at, or distal to, the lamina (Winberg *et al.*, 1992; Choi and Benzer, 1994; Perez and Steller, 1996). These numbers are not consistant with the numbers of glia in the adult lamina, for which only six identified types are reported (Eule *et al.*, 1995).

In the lamina of the adult visual system, the glia are subdivided on the basis of location and shape. Each class of glia has two subtypes, as first identified in the housefly (Saint Marie and Carlson, 1983b). The lamina's fenestrated glia are equivalent to the perineurial glia while pseudocartridge glia are a type of subperineurial surface glia, as first hypothesized by Shaw and Varney (1999). Both lie at the surface of the brain, just

beneath the retina. In the lamina, unlike other regions of the *Drosophila* brain, there are two distinct and identifiable types of cortex glia (Eule *et al.*, 1995). The distal satellite glia have large nuclei at the distal edge of the cortex and extensions from their cell bodies branch to embrace the somata of L1-L4 from neighbouring lamina cartridges. Proximal satellite glia lie at the neuropile border and embrace the somata of L5 neurons only. The lamina neuropile is divided into modules called cartridges, each containing a single set of R1-R6 photoreceptor terminals and lamina neurons that process information from a single point in visual space (Trujillo-Cenóz, 1965; Braitenberg, 1967; Kirschfeld, 1967). A set of three epithelial glia surrounds and isolates each cartridge (Boschek, 1971), while marginal glia at the proximal edge of the lamina separate this neuropile from the underlying axonal chiasm and medulla cortex (Trujillo-Cenóz, 1965; Saint Marie and Carlson, 1983a, Saint Marie and Carlson, 1983b).

The axons passing between the lamina and medulla in the external chiasm are ensheathed by large and small chiasm glia (Eule *et al.*, 1995). The glia of the medulla are not as well defined as those in the lamina but satellite glia surround cell bodies in the cortex while a single type of neuropile glia has been reported which has its cell body in the distal medulla and branches among the terminals of the R7 and R8 axons (Eule *et al.*, 1995; Tix *et al.*, 1997; Richardt *et al.*, 2002). A second glia-like cell has also been identified in the distal medulla, based on its expression of the histamine receptor gene *ort* (Gao *et al.*, 2008), that extends a vellate-like sheath down a number of individual columns; this cell has yet to be definitively identified as glial, however.

The visual system commences development in the third-instar larva, and the origins of the optic lobe neuropile glia and the glia of the eye disc are now both well described. The epithelial and marginal glia originate in subdomain I, a region within the paired dorsal and ventral glial precursor zones of the larval brain. Subdomain I is distinguished from other areas of glial cell division by its expression of *wingless*, *optomotor blind* and *dachsous* (Dearborn and Kunes, 2004). The marginal, epithelial and satellite glia are easily identified in the larval brain from the linear arrangement of their nuclei in successive layers (Perez and Steller, 1996). No distinction has yet been made between two subsets of lamina satellite glia in the larva, however. Furthermore, the origins of the satellite glia themselves are unclear. While some reports have shown labelling of all of the marginal, epithelial and satellite glial cell types with Green Fluorescent Protein (GFP) and bromodeoxyuridine (BrdU) in mitotic clones (Winberg *et al.*, 1992; Perez and Steller,

1996), more recent reports make no mention of satellite glia (Dearborn and Kunes, 2004; Chotard *et al.*, 2005). *MARCM* analysis has meanwhile revealed that for other areas of the brain, at least, the cortex and neuropile glia arise at different stages, with cortex glia originating in the embryo and neuropile glia not developing until larval stages and beyond (Awasaki *et al.*, 2008).

In the eye disc, which lies distal to the brain, there are four distinct types of differentiated glia. All originate during late larval and early pupal life from glia of the larval optic stalk, which connects the eye disc to the brain. The optic stalk glia themselves likely have their origins in the embryonic CNS (Schmucker *et al.*, 1992; Silies *et al.*, 2010). During late larval life, glia divide and migrate from the optic stalk into the eye disc where they continue their development (Choi and Benzer, 1994; Silies *et al.*, 2007). Surface glia line the periphery of the entire optic stalk and extend into the eye disc where they surround photoreceptor axons at both their apical and basal surfaces (Rangarajan *et al.*, 1999; Hummel *et al.*, 2002; Silies *et al.*, 2007). Two large, flat, septate junction-rich carpet glia lie just above the basal surface glia and extend projections into the optic stalk and the brain (Silies *et al.*, 2007). Wrapping glia are derived from migrating surface glia that come into contact with FGF8-like expressing photoreceptors at the anterior edge of the carpet glia (Franzdóttir *et al.*, 2009). Their cell bodies lie above the photoreceptor axons and extend lamellae which wrap bundles of photoreceptor axons, approximately eight axons per glia, thus ensheathing the axons as they course through the optic stalk and into the brain (Hummel *et al.*, 2002). Finally, the marginal edges of the eye disc contain a layer of clapboard shaped “marginal glia” (Silies *et al.*, 2007), since renamed edging glia by their discoverers (Silies *et al.*, 2010).

Despite the many reports of these glia in larval stages, we are not yet able to accurately equate those glia that exist in the larval brain and eye disc to the known glial types which they may give rise to in the adult. For this, the first requirement is to identify and characterise appropriate markers that will allow glia to be traced through wild-type or mutant development in the intervening stages of the pupa.

3.3 METHODS

3.3.1 FLY STRAINS

Flies were raised on standard cornmeal molasses agar at 24°C. The following lines were used in this study: *R.29.A12*, *R.32.H04*, *R.25.A01*, *R.43.H01*, *R.10.D10*, and *R.19.C02* are glial *GAL4* lines provided by Drs. G. Rubin and A. Nern (HHMI, Janelia Farm). Additional lines include: (BL#8474) *w[*]; P{w[+mW.hs]=GawB}17A/CyO*, (BL# 9488) *w[*]; P{GawB}Mz97 P{UAS-Stinger}2, w[*]; (BL# 8849) P{EAAT1-GAL4.R}2*, (BL# 23881) w^{1118}*; Mi{ET1}ths*^{MB02475}, (BL# 6796) *P{Nrv2-GAL4.S}3 P{UAS-GFP.S65T}T2; P{Nrv2-GAL4.S}8 P{UAS-GFP.S65T}T10*, (BL#5136) *P{UAS-mCD8::GFP.L}LL4, y[1] w[*]; Pin[Yt]/CyO,* (BL# 6317) *w[*]; P{w[+mC]=lacW}J29*, *UAS-HRP::CD2*/*CyO* (C.H. Lee - NIH, Bethesda) and *gli*^{rL82}*-GAL4* (V. Auld – UBC, Vancouver).

3.3.2 IMMUNOCYTOCHEMISTRY

The brains of larvae and the heads of pupal and adult flies were fixed in a solution of 4% formaldehyde [from paraformaldehyde (PFA)] in 0.1 M phosphate buffer (PB) for 4 h or overnight at 4°C. Brains were washed in 0.1 M PB, mounted in 7% agarose, and sliced in the horizontal plane at 80–100 µm thickness by means of a Vibratome 1000. Brains were permeabilized in successive treatments of 0.2% and 2% Triton X (Tx) in 0.01 M phosphate buffered saline (PBS) and then blocked with 5% normal goat serum (NGS) in 0.2% PBS-Tx. Tissues were incubated 24-48 h at 4°C in antibody diluted in 5% NGS-PBS-Tx. The following primary antibodies were used at these dilutions: 1:20 mouse anti-β-gal 40-1a, 1:20 mouse anti-chaoptin (24B10), 1:10 anti-Fasciclin II (FasII), 1D4 (Grenningloh *et al.*, 1991); 1:100 rabbit anti-β-gal (Molecular Probes, Eugene, OR, USA) 1:20 -1:50 mouse anti-repo (8D12), 1:1000- 1:1500 rabbit anti-GFP (Invitrogen, Carlsbad, CA, USA). After at least six washes in 0.2% PBS-Tx, tissues were incubated overnight in some corresponding combination of the following secondary antibodies: 1:400 goat anti-mouse Cy3, 1:400 goat anti-rabbit Cy3, 1:400 goat anti-mouse Cy5 (Jackson ImmunoResearch, West Grove, PA, USA); 1:400 goat anti-rabbit Alexa 488 or 1:400 goat anti-mouse Alexa 488 (Invitrogen). Tissues were washed at least six times in 0.01M PBS before being mounted in Vectashield (Vector Laboratories) and images

captured using an LSM 510 or LSM Meta confocal microscope, with software (Carl Zeiss GmbH, Jena, Germany).

3.3.3 ELECTRON MICROSCOPY

To identify marginal glia by electron microscopy (EM) *R.19.C02-GAL4* was crossed with a *UAS-HRP::CD2* reporter line to drive expression of Horse Radish Peroxidase (HRP) at the plasma membrane (Larsen *et al.*, 2003). Sites of HRP expression were confirmed from an electron-dense precipitate formed in the presence of 3,3'-diaminobenzidine (DAB) (Graham and Karnovsky, 1966; Larsen *et al.*, 2003). Heads were fixed on ice in 4% PFA and 0.5% glutaraldehyde in 0.1M PB. To increase penetration of DAB, heads were sliced at 100 µm using a Vibratome. After two washes in PB, tissue sections were treated for 20 min with fresh 1% sodium borohydride in 0.01M PBS followed by four washes in 0.01M PBS. Tissue was pre-incubated in filtered 0.5mg/ml DAB solution (Cat. No. D5905: Sigma, St. Louis, MO, USA) with 6mg/ml of nickel ammonium sulfate in 0.01M Tris Buffered Saline (pH 7.6) for 1 hr. They were then incubated for 27 minutes in DAB that was made reactive by the addition of 0.03% H_2O_2, at a final dilution of 3-6 X 10^{-6} v/v. Visibly labelled brains were washed three times in TBS and post-fixed in 0.5% aqueous osmium tetroxide (Cat. No.19150: Electron Microscopy Sciences, Hatfield, PA, USA) for 30 min, dehydrated, embedded in PolyBed 812, sectioned at 50-60 nm, and stained with uranyl acetate. Sections were viewed at 80kV in a Philips Tecnai 12 electron microscope and images captured with a Gatan 832 Orius SC1000 CCD camera using Gatan DigitalMicrograph software.

TABLE 3.1 - ANTIBODY DOCUMENTATION AND SPECIFICITY

ANTIGEN	TARGET	SEQUENCE	SPECIES	SOURCE	SPECIFICTY CHARACTERISED BY	REFERENCES
Chaoptin	Sensory neurons	Head homogenates	mouse	DSHB (24B10: Benzer)	Western blot	Zipursky *et al*., 1984; Van Vactor *et al*., 1988
β-gal	β-gal	E-coli β-galactosidase 116kDa	mouse	DSHB (40-1a:, Sanes)	Failure to label in flies lacking lacZ expression construct. (personal observation)	
β-gal	β-gal	Unknown	rabbit	Molecular Probes	Failure to label in flies lacking lacZ expression construct. (personal observation)	
Repo	glial nuclei	AAs 218-612 of *Drosophila* Repo protein	mouse	DSHB (8D12: Goodman)	Detects Repo transgene expression. Similar labelling as *repo-LacZ* reporter genes, other antibodies and *in situ* probes that target *repo* gene products.	Alfonso and Jones, 2002; Lee and Jones, 2005; Xiong *et al*., 1994; Halter *et al*., 1995
FasII	L1/L3	Complete ORF *D.m.* fusion protein	mouse	DSHB (1D4: Goodman)	Failure to label in FasII null mutants	Grenningloh *et al*., 1991
GFP	Transgenic GFP	GFP from *Aequorea victoria*	rabbit	Molecular Probes/ Invitrogen - A11122	Cytological staining (by Molecular Probes) and absence of signal in flies lacking GFP expression construct. (personal observation)	

3.4 RESULTS

The glial cell types of the adult optic lobe are illustrated in Figures 3.1 and 3.2, and their developmental origins pursued in later figures.

3.4.1 THE GLIA OF THE ADULT LAMINA

In order to visualize the development and structure of the lamina glia in the adult, we selected markers for each of the six distinct glial cell types. *GAL4* driver lines were identified that allowed us to identify five of the previously described glial cell types. We initially lacked a driver line which expressed in the fenestrated glia or in their CNS equivalent, the perineurial glia, so these glia were therefore identified by their nuclear location from the pattern of immunoreactivity to Repo which expresses in the nuclei of all adult glial cells (Campbell *et al*., 1994) and by exclusion from labelling with other *GAL4* drivers. This identification was confirmed by the serendipitous discovery that the *thisbe* P-element line, w^{1118}*; Mi{ET1}ths*^{MB02475}, from the Bloomington Stock Center expresses GFP in fenestrated glia of the adult, as well as in photoreceptors of the eye imaginal disc, as previously described (Franzdóttir *et al*., 2009; Figure 3.1A). GFP is also expressed in glial cells which have nuclei lying near the distal edge of the lamina but which extend a glial sheath proximally, alongside the lateral edges of the lamina.

The structure of the five glial cell types for which we had specific drivers was visualized in the adult using a membrane bound *UAS-mCD8::GFP*. *P{17A}-GAL4* expresses in the pseudocartridge glia (Figure 3.1B). Pseudocartridge glia enwrap photoreceptor fascicles as they enter the lamina from the retina (Figure 3.3F). They also surround tracheae. A layer of glia that express *UAS-mCD8::GFP;P{17A}-GAL4* also branches down along the lateral edges of the lamina neuropile but does not contact the subperineurial glia, in which *P{17A}-GAL4* also drives expression. Thus the subperineurial glia, and their functional equivalent in the lamina – the pseudocartridge glia, do not themselves together form a complete glial sheath surrounding the optic lobe.

Driver lines with wider expression patterns also allowed visualization of the pseudocartridge glia. *Mz97-GAL4*, which lies within the promoter of the gene *CG5473/ SP2637* (Beckervordersandforth, 2007), drives expression not only in the pseudocartridge glia but also in the distal satellite glia and the outer and inner chiasmal giant glia of the adult (Figure 3.4F), while *gliotactin* (*gli*^{rL82}*-GAL4)* drives expression in the

adult pseudocartridge and proximal satellite glia, with weaker expression in the distal satellite glia (Figure 3.5F).

A screen of more than 5,000 *GAL4* lines conducted at the Janelia Farm Research Campus of Howard Hughes Medical Institute uncovered drivers for other glia of the lamina (Table 3.2). These distinguished the two types of unique cortex glia. *R.10.D10* (Figure 3.1C) drives expression in the distal satellite glia, at a location previously identified using the driver line *Nrv2-GAL4* (Górska-Andrzejak *et al.*, 2009; Mayer *et al.*, 2009). *R.10.D10* also drives expression in the neuropile marginal glia. These two glial subtypes are separated by two layers of Repo positive glial nuclei, representing the proximal satellite and epithelial glial layers. A few, large, distal satellite glia encase the cell bodies of lamina monopolar neurons L1-L4. The driver line *R.32.H04* consistently labelled the proximal satellite glia (Figure 3.1D), and also labelled some of the epithelial and marginal glia in a mosaic pattern. As in the housefly *Musca domestica* (Saint Marie and Carlson, 1983b), the proximal satellite glia were confirmed to enwrap the cell bodies of only a single type of lamina monopolar neuron in the proximal cortex, most likely L5. Another driver, *R.43.H01*, also strongly labelled both subtypes of lamina cortex glia, but expression with this line was not limited to cortex glia, as GFP was also detected in the outer chiasm glia beneath the lamina (Figure 3.1I).

The lamina neuropile also contains two distinct subsets of glia. Epithelial glia enclose a group of six photoreceptors and their lamina target neurons, in an isolated cartridge (Trujillo-Cenóz, 1965; Saint Marie and Carlson, 1983a, Saint Marie and Carlson, 1983b). These glia are identified using the driver *R.29.A12* which labels astrocyte-like glia throughout the brain (Figures 3.1E, G and 3.2A). The features of epithelial glia have been reported in great detail elsewhere (Saint Marie and Carlson, 1983b; Meinertzhagen and O'Neil, 1991; Richardt *et al.*, 2002; Gao *et al.*, 2008; Pantazis *et al.*, 2008). The anatomy of marginal glia has not, however, been reported in any detail for *Drosophila*. As revealed by means of the driver lines *R.19.CO2* (Figure 3.1F) and *R.10.D10* (Figure 3.1C), their appearance in *Drosophila* is similar to that described for *Musca* (Saint Marie and Carlson, 1983b), although they extended branches much higher into the lamina than expected, so as to contact the terminals of R1-R6 (Figure 3.1H), and branch around the epithelial glia (Figure 3.1J, K). From electron microscopy, the more distal extremities of the marginal glia were seen to lie close to the monopolar cell axons and other axon bundles, but not to surround the terminals of R1-R6 completely. They did invaginate

photoreceptors at some sites of contact (Figure 3.1K), but failed to form specialised structures, such as the capitate projections that form when epithelial glia invaginate the R1-R6 terminals. Close examination of the marginal glia at EM level revealed that they contain clathrin coated vesicles (Figure 3.1L, L'), as had been previously reported for the marginal glia of the housefly *Musca* (Saint Marie and Carlson, 1983b).

The locations of lamina glia are summarised in Figure 3.1M'.

3.4.2 Other Glia of the Optic Lobes

Surface, cortex and neuropile glia populate all neuropiles of the optic lobe (Figure 3.1M). Underlying the lamina and extending to the surface of the medulla neuropile are outer chiasm giant glia (Figures 3.1I and 3.7) with cell bodies that lay in a single row aligned in a dorsal to ventral direction. A number of driver lines labelled these glia including *Nrv2-GAL4* (not shown), *Mz97-GAL4* (Figure 3.4), *R.43.H01* (Figure 3.1I), and specifically *R.25.A01*, which we have used to trace the developmental origins of these glia (Figure 3.7). The outer chiasm giant glia are easily distinguished in the adult (Tix *et al.*, 1997) but they are often incorrectly labelled as medulla glia in the larva (Poeck *et al.*, 2001; Suh *et al.*, 2002; Chotard *et al.*, 2005).

Both cortex and neuropile glia are also present in the medulla, lobula and lobula plate (Eule *et al.*, 1995; Tix *et al.*, 1997). While the lamina has two types of cortex glia and two types of neuropile glia, the glia of the medulla cortex and neuropile have not been shown to comprise morphologically distinct subtypes. This is despite the fact that most neuropiles contain two types of glia, an outer ensheathing variety, and an inner astrocyte-like variety (Awasaki *et al.*, 2008; Doherty *et al.*, 2009). Using the *EAAT-GAL4* and *Mz97-GAL4* lines we distinguished two kinds of glia at the interface of the medulla neuropile: those that had driver-based expression of mCD8::GFP and those that did not (Figure 3.2D, E). This split pattern of expression could represent incomplete driver expression or may alternatively reflect a partition between driver-expressing astrocyte-like glia, and non-driver-expressing ensheathing glia.

The structure of astrocyte-like neuropile glia which lay at the distal surface of the medulla was revealed by rare mosaic driver expression in some specimens using the *R.29.A12* line (Figure 3.2C). A single, distal, medulla astrocyte-like glia extended

branches into 4-5 columns of the medulla and occasional branches in a centrifugal direction, along the chiasmal axons or glia that approach from the lamina.

The same astrocyte-like glia driver, *R.29.A12*, also revealed chandelier glia deeper in the medulla, at its base (Figure 3.2A, A'). This cell type has been previously reported as a class of neuropile "cover glia" in other muscid flies, Odonata and the honeybee (Sánchez y Sánchez, 1935; Cantera and Trujillo-Cenóz, 1996). Chandelier glia have Repo expressing nuclei which lie outside the neuropile, immediately distal to the inner chiasm giant glia (Figure 3.2A'). They extend astrocyte-like branches in an area above stratum M10 and beneath the serpentine layer M7. The *R.29.A12-GAL4* line also reveals astrocyte-like glia in the lobula and lobula plate (Figure 3.2A), but we have not characterised these further.

Another previously undescribed medulla glial cell type lies at the margins of the serpentine layer. These large, amorphous "serpentine glia" were occasionally revealed in at the posterior margin of the serpentine layer using *R.29.A12* (Figure 3.2F). Insofar as they express the β-alanyl-Histamine/Dopamine synthase protein Ebony (Figure 3.2G; Richardt *et al.*, 2003) these cells are similar to the epithelial (Richardt *et al.*, 2002) and proximal satellite glia of the lamina (see Chapter 4), the medulla neuropile glia (Richardt *et al.*, 2002), and the outer chiasm giant glia (Ziegler and Hovemann, 2010). The serpentine glia extend thin branches distally towards the terminals of R7 photoreceptor terminals in M6 (Figure 3.2F, G), as well as into M8, which lies beneath the serpentine layer.

3.4.3 Development of the Optic Lobe Glia

The two subsets of adult lamina neuropile glia have their origins in the dorsal and ventral glial precursor zones which lie under the lamina furrows of the outer optic anlage (Winberg *et al.*, 1992; Perez and Steller, 1996; Dearborn and Kunes, 2004; Chotard *et al.*, 2005). Unlike these two, the larval origins of the remaining subtypes of adult lamina glia, including both types of cortex and surface glia, are at best inconclusive. To address this issue, I used *GAL4* driver lines and morphological analysis were used to trace the known larval subtypes through pupal metamorphosis to determine their adult counterparts.

3.4.3.1 THE PSEUDOCARTRIDGE GLIA

Based on their shape and position at the distal border of the lamina, the adult pseudocartridge glia appear to be a type of subperineurial glia. Corresponding glial cell types are lacking at the distal face of the presumptive lamina in both the larva and early pupa. Instead, subperineurial glia, labelled by *P{17A}-GAL4,* surrounds the entire brain except for a small area through which the photoreceptors enter the optic lobe via the optic stalk (Figure 3.3A). GFP expression in the subperineurial glia surrounding the entire brain was maintained throughout pupal development (Figure 3.3A-D) and into the young adult (Figure 3.1B). *P{17A}-GAL4* driven GFP expression was not detected in the eye disc and optic stalk of the larva (data not shown) or P+5% pupa (Figure 3.1A) and first appeared in the eye disc only at about P+10 % pupal development (data not shown), just after head eversion. Early in development the strongest mCD8::GFP expression was in the posteriormost regions of the eye disc, and then extended anteriorly, so that a posterior to anterior gradient of GFP expression underlay the retina by P+20%. Weaker expression occurred in lamellar extensions that enwrap photoreceptor axon bundles in the anterior, as seen at P+20% (Figure 3.3B). At this stage of development *P{17A}-GAL4* driven GFP expression overlapped a subset of the *Gli-lacZ* expressing nuclei, specifically those which lie closest to photoreceptor cell bodies (Figure 3.3E). There was a large, non-GFP expressing area around the lateral margins of the lamina in the early pupa, suggesting a non-continuous glial barrier at this stage of development (Figure 3.3B, C). Alternatively, it may be that these lateral borders were surrounded by glia which were not labelled by the driver line. By P+40%, GFP expression was uniform along the basal surface of the developing eye, in an area that corresponds to the pseudocartridge glia of the adult (Figure 3.3C). Glia marked by *P{17A}-GAL4* driven GFP expression continued to enwrap photoreceptor fascicles while other GFP expressing glia extended branches down from the eye and along the lateral margins of the lamina neuropile (Figure 3.3D), so that in the adult the glia from the eye disc came into close contact with the subperineurial glia of the brain (Figure 3.1B). In the adult the pseudocartridge glia with *P{17A}-GAL4*-driven expression were definitively identified as lying between anti-Repo labelled fenestrated glia and distal satellite glia at the edge of the lamina cortex. Their wrapping morphology was also observed in selected sections of the adult brain (arrowheads, Figure 3.3F).

3.4.3.2 THE SATELLITE GLIA

The subsets of satellite glia were revealed in the adult by various drivers, including *NRV2-GAL4*, *Mz97-GAL4*, *R.43.H01*, *R.10.D10*, *R.32.H04* and *J29/gli^{rL82}*. *Mz97 -GAL4*, *R.43.H01* and the gliotactin drivers were expressed in subsets of the satellite glia throughout pupal life. *Mz97-GAL4* has been described as a marker for wrapping glia in the larval eye disc (Hummel *et al.*, 2002; Silies *et al.*, 2007; Franzdóttir *et al.*, 2009). In the larva, stinger-GFP expression in wrapping glia is restricted to cells with nuclei in the eye disc (not shown). At P+20% pupal development, this line drove GFP expression in two types of lamina glia: at the base of the eye disc in a location, and with a morphology, corresponding to the pseudocartridge glia (Figure 3.4C); and in the optic stalk and brain at a location corresponding to the distal satellite glia (Figure 3.4A). These glial identities are confirmed at P+40% pupal development (Figures 3.4D, E), when the lamina adopts a structure similar to that in the adult (Figure 3.4F).

The *gliotactin* drivers *gli^{rL82}-GAL4* and *J29-lacZ* both expressed in glia of the larval eye disc, the optic stalk and at the postero-lateral surface of the presumptive lamina. *J29-lacZ* expression in the larval eye disc is similar to the expression pattern described for retinal basal glia (Choi and Benzer, 1994), and thus labels not only wrapping glia but also the two large bilateral carpet glia nuclei (Figure 3.5A). It also drives β-gal expression, albeit weakly, in one large nucleus which lies at the posterior surface of the optic stalk at P+20% development (Figure 3.5B).

Repo labelling was detected in the proximal satellite glia from the onset of pupal metamorphosis but these cells were rarely visible at stages up to P+20% using the *gliotactin* drivers (Figure 3.5D, H). By P+40%, however, two layers of glia labelled by the *gliotactin* driver *J29-lacZ* were clearly distinguished (Figure 3.5E). One layer was sparse and lay beneath the eye disc; the other layer contained many labelled nuclei and corresponded to the location of proximal satellite glia. This expression pattern survived in the adult (Figure 3.5C).

GFP labelling using *UAS-mCD8::GFP*; *gli^{rL82}-GAL4* revealed the gross structure of the developing pseudocartridge and satellite glia (Figure 3.5G-I), thus confirming the identification of cells expressing *J29-lacZ*. In the adult, the GFP expressing glial subtypes were identified by their position relative to Repo labelling (Figure 3.5F, F') in the fenestrated glia, which lay above the GFP-labelled pseudocartridge glia, and the epithelial glia, which lay below the GFP-labelled proximal satellite glia. GFP expression

was strong in the distal satellite glia of the young pupa (Figure 3.5G-I), but in the adult (Figure 3.5F, F') was almost undetectable except in a few newly-eclosed flies (not shown).

Since *gli*^{rL82}*-GAL4* did not allow visualization of the developing proximal satellite glia at stages prior to P+40%, I analyzed the developmental expression of the driver *R.43.H01* (Figure 3.5J-L), which expresses in both the distal and proximal satellite glia of the adult. *R.43.H01* driven mCD8::GFP expression patterns were then compared with developmental expression of *gli*^{rL82}*-GAL4 and Mz97-GAL4*.

Anatomy alone only partially resolves the issue of whether the proximal satellite glia have a peripheral origin in the eye disc or a central one in the Glial Precursor Zone (GPZ). The lamina develops in a posterior to anterior direction (Figure 3.6B) and this developmental progression is revealed in the horizontal plane (Figure 3.6A) by the length of photoreceptor axons extending into the brain (Meinertzhagen and Hanson, 1993; Huang and Kunes, 1996, 1998; Huang *et al.*, 1998). At the anterior, and "newest" edge of the developing lamina, the photoreceptor axons (Figure 3.6C) were shortest and the nuclei of proximal satellite glia lay closer to the optic stalk and farther from the source of neuropile glia, the GPZ. As the lamina continues to develop, and the proximal satellite glia get older, their nuclei come to lie closer to the lamina plexus. From their appearance alone, and their proximity to the optic stalk in some section planes (Figure 3.4D), this arrangement suggests that the nuclei of the proximal satellite glia migrate in from the eye disc via the optic stalk (Figure 3.6C, D). However, at dorsal and ventral areas, close to the GPZ, a few *R.43.H01* expressing cells were found that suggested a central origin for the proximal satellite glia (Figure 3.6E).

3.4.4 Other Glia in the Lamina Cortex

No other glia besides satellite glia have previously been described in lamina cortex, yet, a small population of Repo-positive glia reside amongst the otherwise *Mz97-GAL4;Stinger-GFP*-labelled distal satellite glia. These were seen from P+40% development through to adulthood (Figure 3.4D', D", and F). While numerous large glial nuclei resided near the pupal optic lobes, one, at the anterior edge of the lamina cortex/neuropile interface, expressed both Repo and *Mz97-GAL4* at P+40% pupal

development (Figure 3.4D). The larval origin and, ultimately, the adult fate of this cell remains unknown.

3.4.5 The First Optic Chiasm Glia

Chiasm glia have been described for the larva in early reports (Meinertzhagen, 1973; Tix *et al.*, 1997), and while these cells are easily identified when lying between the lamina and medulla of the adult, they have been grossly misidentified as medulla glia in the larva. A *GAL4*-driver line, *R.25.A01* readily labels these glia from third-instar larvae (Figure 3.7A) into the adult (Figure 3.7F). A ventral view of whole-mount larval optic lobes shows the location of the chiasm glia relative to the nuclei of other, anti-Repo labelled, glia in the lamina and medulla (Figure 3.7A). A view in section of the P+10% pupa reveals that these glia extend lamellae in an antero- and ventro-lateral direction towards the lamina (Figure 3.7B) and in a posterior and medial direction, towards the medulla, where they terminate just below the medulla neuropile glia (Figure 3.7B, and D-E). Even at this early stage of development, the outer chiasm glia are clearly distinct from the marginal and epithelial glia that lie in successively distal rows, and the medulla glia that lay scattered medially (Figure 3.7C).

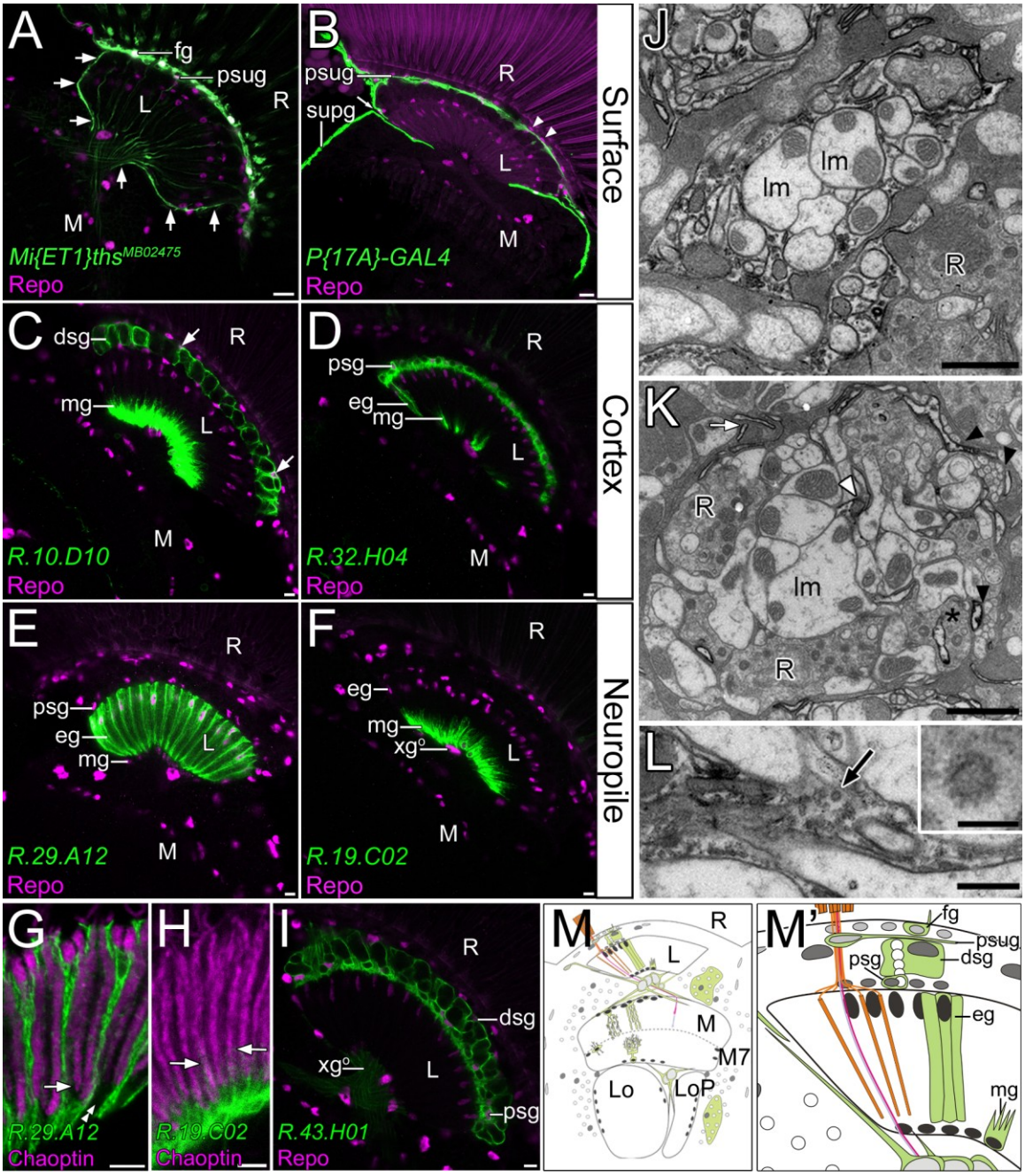

FIGURE 3.1 - SUMMARY OF GLIAL CELL TYPES IN THE ADULT *DROSOPHILA* LAMINA.

Confocal images of horizontal slices of adult brains expressing mCD8::GFP (green) under the control of different glial-specific *GAL4* drivers were visualized relative to glial nuclear Repo immunoexpression (magenta in A-F, I) or photoreceptor specific Chaoptin (magenta in G,H). These reveal three types of glia, surface (A,B), cortex (C,D,I) and neuropile (E,F). **A-B**: There are two layers of surface glia. **A**: Fenestrated glia (fg) visualized using the line w^{1118}; *Mi{ET1}ths*^{MB02475}. Expression also occurs in photoreceptors R7 and R8, as well as in glia lining the lateral edges of the lamina (arrows). **B**: Pseudocartridge glia (psug) visualized using *P{17A}-GAL4* driven

(FIGURE 3.1 - CONTINUED 2 OF 2)

mCD8::GFP. A single layer of Repo positive glial nuclei (arrowheads) corresponding to the location of fenestrated glia lie above the *P{17A}-GAL4* labelled pseudocartridge glia, enabling the separate identification of the two glial cell types. *P{17A}-GAL4* also drives expression in the subperineurial glia (supg) which lines the entire surface of the brain. Pseudocartridge and subperineurial glia do not meet at the lamina – medulla interface (arrow). **C-D**: Two layers of cortex glia are clearly distinguished. **C**: The driver line *R10.D10* label the distal satellite glia (dsg) and their nuclei (arrows), as well as the marginal glia; while **D**: *R.32.H04* drives expression in the more numerous proximal satellite glia (psg), as well as occasional epithelial and marginal glial cells. **E-H**: The lamina neuropile contains two types of glia, epithelial (eg, E,G) and marginal (mg, F, H). **E**: The astrocyte-like glial driver *R.29.A12* reveals epithelial glia (eg) that extend throughout the lamina neuropile, between proximal satellite and marginal (mg) glia. **G**: The epithelial glia (green) extend beyond the proximal tips of the R1-R6 photoreceptor terminals, which are visualized by anti-Chaoptin (magenta, arrow in G), and they leave the lamina column “open” at its proximal surface (arrowheads). **F,H**: The *R.19.CO2* driver expresses in marginal glia in the proximal lamina; and these marginal glia extend branches (arrows in H) toward the distal surface of the lamina neuropile. Comparison between glial labelling in G and H reveals overlap between the spread of epithelial (G) and marginal (H) glia. **J-L**: The ultrastructure of lamina glia revealed in 50 nm thin EM sections by a DAB reaction on *R.19.CO2* - *GAL4*-driven HRP. **J**: Marginal glia extend widely in the proximal lamina to surround the axon bundle, which includes the lamina monopolar cell axons (lm). **K**: At a slightly more distal level in the lamina, marginal glia are associated with axon bundles (arrowheads), with epithelial glia (arrow), and are found at the centre of the cartridge cross section (open arrowhead), or associated with and penetrating the photoreceptors (R, asterisks) without forming capitate projections. **L**: The marginal glia contain Clathrin coated vesicles (arrow, enlarged in inset). **M**: Diagram showing the location of the retina relative to the optic neuropiles, as well as the locations ofsurface (light grey nuclei), cortex (medium grey nuclei) and neuropile (dark grey nuclei) glia contained within the optic lobes. **M’**: Enlarged diagram of the lamina itself showing the locations of the fenestrated, pseudocartridge, distal satellite, proximal satellite, epithelial and marginal glia, and their relationship to the lamina monopolar neurons (nuclei in white) and photoreceptor axons. Other abbreviations: xg^{o} - outer chiasm giant glia, mng - medulla neuropile glia, xg^{i} - inner chiasm giant glia, R - retina, L - lamina, M - medulla, Lo - lobula, LoP - lobula plate. Scale bars A,B, 10 μm; J,K, 1 μm; L, 500 nm; inset 100 nm; C- I, 5 μm.

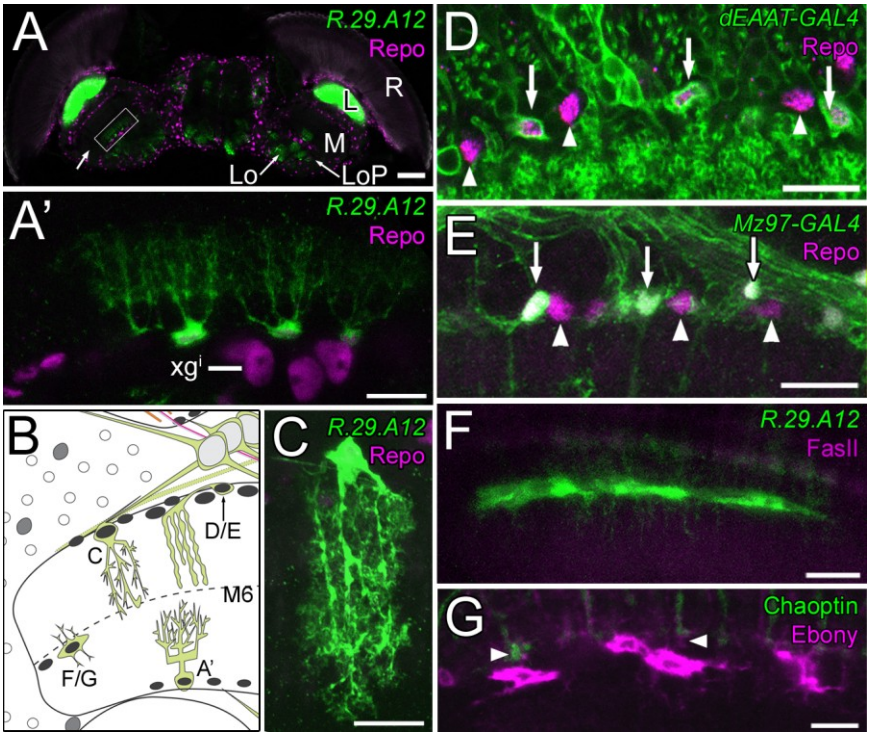

FIGURE 3.2 - DRIVER LINES EXPRESS IN GLIA OF THE DEEPER OPTIC LOBE NEUROPILES.

A-C,G: *R.29.A12* drives GFP expression in astrocyte-like glia. **A**: Chandelier glia (box, enlarged in A') are visible at the proximal-most surface of the medulla (M), just above the inner chiasm giant glia (xg^l). These have an astrocyte-like morphology and branch up almost to the serpentine layer. **B**: The relative locations of at least four types of distinct medulla neuropile glia identified in *Drosophila* are marked with the locations of image panels that illustrate these. Two different types of glia at the distal-most surface of the medulla are illustrated in C, D and E. **C**: In the distal medulla, another type of astrocyte-like glia displays an extensive branching pattern that spans at least five medulla columns. **D**: Some glia label with *dEAAT-GAL4* (green, arrows); and **E**: *Mz97-GAL4* (green, arrows, from a 6 µm projected image stack), while others do not (arrowheads in D and E). The latter, nuclei expressing only Repo (magenta), are likely to be ensheathing glia, which are described for other neuropiles but not the medulla. At the margins of the medulla serpentine layer (arrow in A) lies a subset of previously undescribed astrocyte-like glia which we name serpentine glia. **F**: These are visualized with both the *R.29.A12* line, seen here as a projected image stack 10.5 µm deep; **G**: and with anti-Ebony immunolabelling (magenta). Their cell bodies lie in the serpentine layer but extend branches in both proximal and distal directions to come into the vicinity of the R7 terminals in M6 (arrowheads in G, anti-Chaoptin, green). Scale bars A, 50 µm; A'-G, 10 µm.

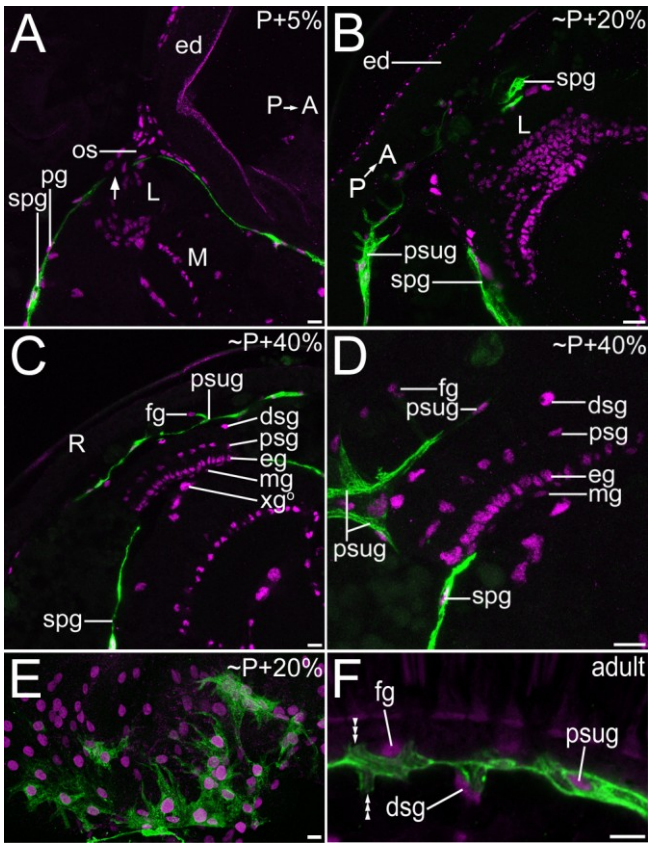

FIGURE 3.3 - DEVELOPMENTAL ORIGINS OF THE LAMINA SURFACE GLIA.

All images show *P{17A}-GAL4* driven expression of mCD8::GFP (green) relative to Repo (magenta in A-D, F) in Vibratome sectioned brains, or *gliotactin* driven β-gal (magenta in E) in whole mounts. **A**: Surface glia lack GFP in the larval and early pupal eye disc, at P+5% (ed). Expression is exclusively in the subperineurial glia (spg) except for where the photoreceptors enter the brain via the optic stalk (os, arrow). All other glia expressed nuclear Repo. **B,E**: By 20% pupal development the pseudocartridge glia (psug) is visible in the eye disc/retina (R), with a posterior to anterior gradient in the strength of GFP expression (B). This glial layer does not contact the sub-perineurial glia, as seen near the posterior lamina. *P{17A}-GAL4* driven GFP expression overlaps, in part, with *J29-lacZ* (gliotactin, magenta) driven nuclear β-gal expression in the eye disc (seen as a 53 µm projected image stack, E). **C-D**: By ~P+40% pupal development) the pseudocartridge glia extend across the entire breadth of the retina (C). Within the retina, the nuclei of fenestrated glia (fg) sit atop columns of photoreceptor-ensheathing pseudocartridge glia (22 µm projected image stack in D). mCD8::GFP is also detected in glia that extend from the pseudocartridge zone, towards the proximal regions of the lamina (L), to eventually approximate the subperineurial glia. **F**: In the adult, nuclei of the fenestrated, pseudocartridge and distal satellite glia (dsg) lie in close proximity, but can be distinguished here by a centrally located sheath of pseudocartridge glia labelled by *UAS-mCD8::GFP;P{17A}-GAL4*. The wrapping morphology of pseudocartridge glia is still visible in the adult (chained arrowheads). Other abbreviations: psg- proximal satellite glia, eg - epithelial glia, mg - marginal glia, xg^{o} - outer chiasm giant glia, pg - perineurial glia, M - medulla. Scale in A-E is 10 µm, in F is 5 µm.

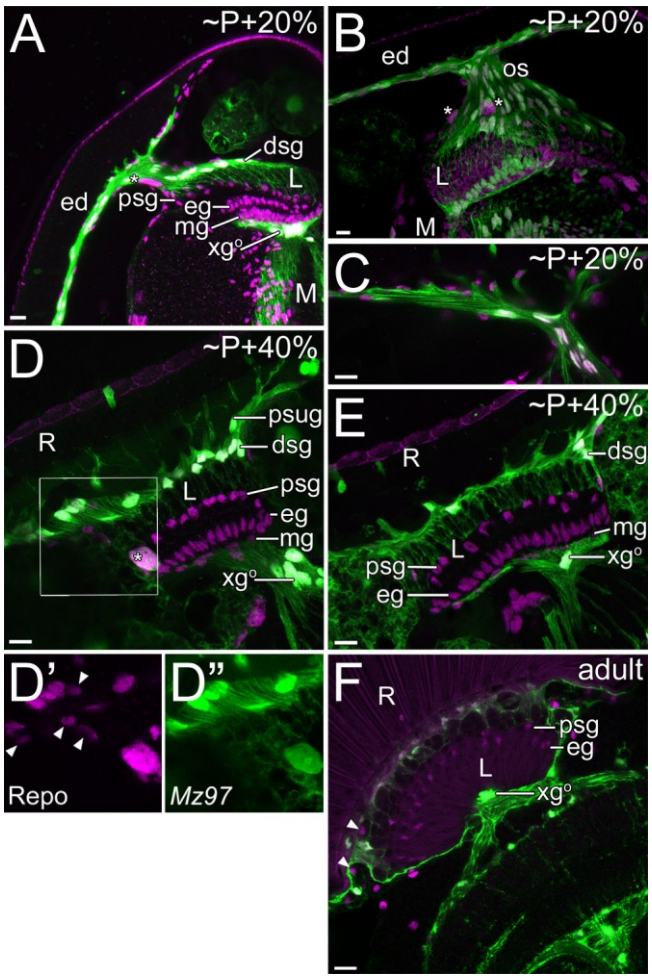

FIGURE 3.4 - WRAPPING GLIA OF THE LARVAL EYE DISC GIVE RISE TO THE PSEUDOCARTRIDGE AND DISTAL SATELLITE GLIA OF THE ADULT.

In the larva, *Mz97-GAL4* drives expression in the wrapping glia exclusively in the eye disc (ed). Glial cell nuclei are labelled by anti-Repo (magenta in all panels). **A-C**: In the P+20% pupa *Mz97-GAL4* drives expression of Stinger-GFP in pseudocartridge glia (psug) along the surface of the eye disc; and in distal satellite glia (dsg) with nuclei in the optic stalk and in the postero-lateral regions of the optic lobe [as viewed in projected image stacks from: a dorsal (A: 10 µm deep, and C: 8 µm deep); or postero-lateral (B: 30 µm deep) direction]. Extensions from the distal satellite glia reach towards the cell bodies of proximal satellite glia (psg), but do not enwrap them. **D,E** (both 8 µm projected image stacks): This arrangement is apparent at P+40% development when the positions of glial nuclei in the lamina are similar to those in the adult. **D',D":** Not all glia in the distal cortex express *Mz97-GAL4*,and the identities of three types of glia: small *Mz97*-negative glia (D"; cf Repo, arrowheads in D'); large *Mz97*-negative glia (asterisks in A,B); and large *Mz97*-positive glia (asterisks in D) in the adult is not known. **F**: By emergence, *Mz97-GAL4* driver expression is weak and Stinger-GFP is reduced. Still, in the nuclear layer immediately beneath the pseudocartridge glia there remain some *Mz97*-negative glial nuclei (arrowheads). Other abbreviations: eg - epithelial glia, mg - marginal glia, xg^{o} - outer chiasm giant glia, pg - perineurial glia, spg - subperineurial glia, os - optic stalk, R - retina, L - lamina, M - medulla. Scale in all is 10 µm.

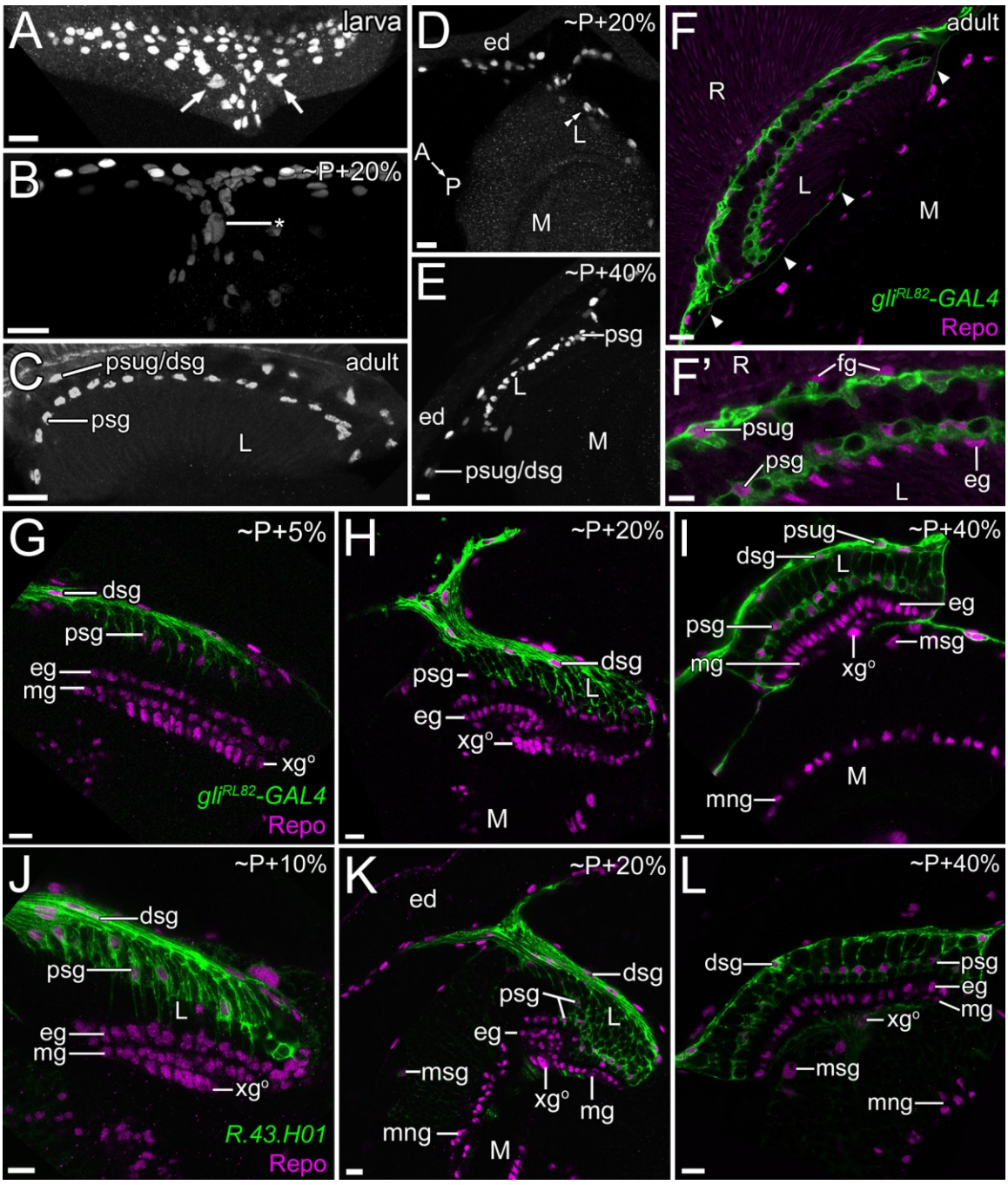

FIGURE 3.5 - THE DEVELOPMENTAL ORIGINS OF ADULT SATELLITE GLIA.

Various driver lines label satellite glia in the adult lamina (L), including *gliotactin* (*J29-lacZ* - A-E; *Gli*^{RL82}*-GAL4* – green in F-I) and *R.43.H01* (green in J-L). All other glial nuclei are visualized with Repo (magenta in F-L). **A**: In a 23 µm projected image stack of the larval eye disc (ed), most *J29-lacZ* driven β-gal expression is in nuclei that correspond to larval wrapping glia and in the two larger carpet glial nuclei (arrows in A). **B,D**: At P+20% development *J29-lacZ* drives β-gal expression in glia near the postero-lateral surface of the brain (arrowheads, viewed as a 66 µm projected image stack from

(FIGURE 3.5 - CONTINUED, 2 OF 2)

the lateral surface in B and from the ventral surface of a 20 µm projected image stack in D) and in a single large glial nucleus near the optic stalk (asterisk in B). **E**: β-gal expression in the proximal satellite glia (psg) was identified at P+40% development (E, 16 µm projection) and persists into the adult (**C**, 15 um projection). **F-I**: Using a different *gliotactin* driver, *Gli^{RL82}-GAL4* with *UAS-mCD8::GFP gliotactin* expression is definitively localised to the pseudocartridge (psug) and proximal satellite glia in the adult (F, enlarged in F') and in these plus the distal satellite glia in the pupa (G-I). An extension from the pseudocartridge glia branches under the lamina (arrow heads in F). Although they cannot be seen in the early pupa with a gliotactin driver, the proximal satellite glia are, indeed, present during the early stages of pupal development at P+5% (G), P+10% (J), and P+20% (H,K), and were visualized in horizontal Vibratome slices of the pupal brain using Repo or *GR.43.H01* (J-K). **G, J**: At ~ P+5% to P+10% the nuclei of the proximal satellite glia are arranged in a band running from the base of the optic stalk to the lamina neuropile. **I,L**: By P+40%, the nuclei of proximal satellite glia are spaced equidistant from the epithelial glia (eg), similar to their arrangement in the adult. Other abbreviations: R - retina, M – medulla, fg - fenestrated glia, mg - marginal glia, mng - medulla neuropile glia, msg - medulla satellite glia, xg^{o} - outer chiasm giant glia. Scale is 10 µm, except in A,D which are both 20 µm.

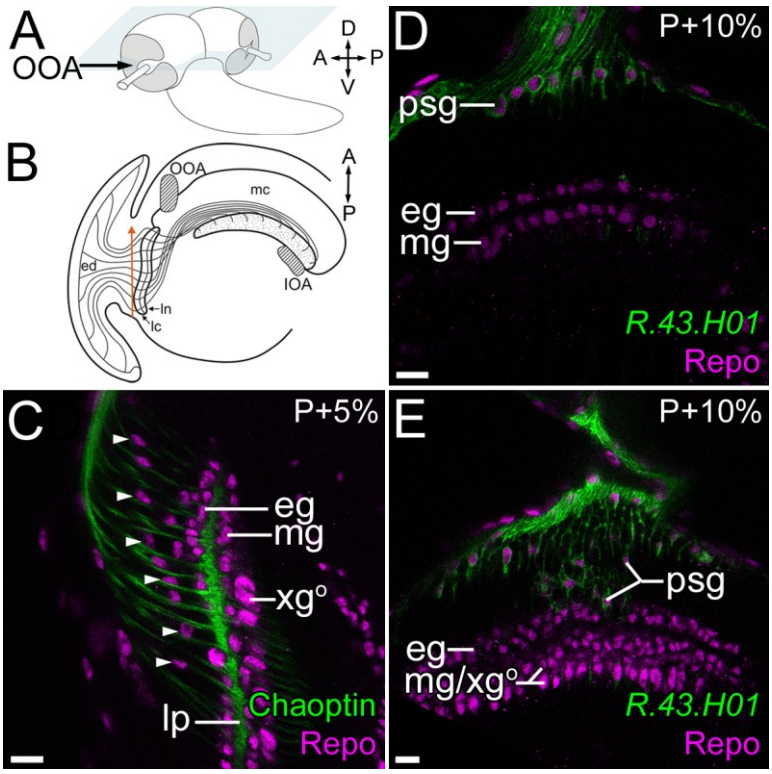

FIGURE 3.6 - PROXIMAL SATELLITE GLIA ORIGINATE IN THE CENTRAL NERVOUS SYSTEM.

A: Larval central nervous system showing the approximate section plane for slices of early pupal brains. The glial precursor zones are found under dorsal and ventral portions of the Outer Optic Anlage (OOA). **B**: The position of the OOA is illustrated in a section of the larval brain that shows the relative locations of the ingrowing photoreceptors, lamina, and medulla neuropiles. The lamina and its associated glia develop in a posterior to anterior direction, as indicated by the orange arrow, following the ingrowth of photoreceptor axons from the eye disc (ed). **C**: A single image from a Vibratome slice of a P+5% pupal brain shows the relative locations of proximal satellite (arrowheads), epithelial (eg), marginal (mg) and outer chiasm giant (xg^o) glia (Repo, magenta) in relation to the photoreceptor terminals (Chaoptin, green) in the lamina plexus (lp). **D**: At section planes close to the entry point of the optic stalk, the *R.43.H01* expressing proximal satellite glia (GFP, green) of the P+10% pupa are distally located - close to the optic stalk, while other lamina glia (Repo, magenta) lie deeper in the brain. **E**: At dorsal and ventral locations of the P+10% pupal brain a subset of the *R.43.H01* expressing proximal satellite glia (GFP, green) lie in proximity to the epithelial glia (Repo, magenta) which derive from the glial precursor zones. Other Abbreviations: IOA – inner optic anlage, lc – lamina cortex, ln – lamina neuropile, mc – medulla cortex. Figure A redrawn from Meinertzhagen and Hanson (1993). Figure B redrawn from Meinertzhagen (1975). Scale in C-E is 10 µm.

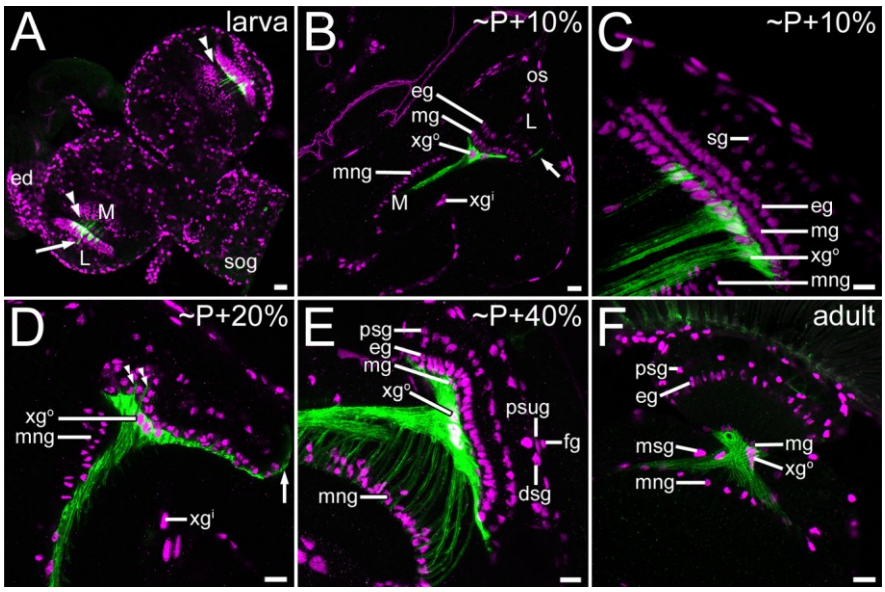

FIGURE 3.7 - THE OUTER CHIASM GIANT GLIA LIE IMMEDIATELY BENEATH THE LAMINA THROUGHOUT DEVELOPMENT.

The driver line *R.25.A01* was used to trace the outer chiasm giant glia (xg^o) from the third-instar larvae to emergence. **A**: A 17 µm projected view from the ventral surface of a whole mount larval brain shows outer chiasm giant glia (GFP, green) lying just under the nuclei of the marginal glia (mg; Repo, magenta) of the developing optic lobes. A space (arrowheads in A) exist between the nuclei of the outer chiasm glia and those of the medulla neuropile (M). Most chiasm glia send extensions into the medulla, but some also extend projections along the antero- and ventro-lateral surface of the lamina (arrows in A, B, D). **B-C**: Vibratome slices through a pupal brain at P+10% (10 µm projection in C) shows the location of the large chiasm glia relative to the marginal neuropile glia (mng), and a different perspective (4 µm projection in B) reveals that projections from the chiasm glia lie below the glia of the medulla neuropile. They do not contact the neuropile glia which line the surface of the medulla. **D**: When the medulla begins to rotate, at P+20%, chiasm glia come into closer contact with neuropile glia at the proximal regions of the medulla. Some chiasm glia also extend small projections distally between the nuclei of marginal glia in the lamina (arrowheads in D). **E**: After the medulla rotates, at about P+40% development, the ends of the chiasm glia still lie below the nuclei of the medulla neuropile glia in a 9 µm projected image stack. **F**: By adulthood (3 µm projected image stack) the first optic chasm shortens, the medulla lies closer to the lamina and the chiasm glia terminate above the medulla neuropile glia. Other abbreviations: R - retina, dsg - distal satellite glia, ed - eye disc, eg - epithelial glia, fg - fenestrated glia, msg - medulla satellite glia, psg- proximal satellite glia, psug - pseudocartridge glia, sog - sub-esophageal ganglion, xg^i - inner chiasm giant glia. Scale in A is 20 µm, in B-F is 10 µm.

TABLE 3.2 - DEVELOPMENTAL PROFILES FOR THE EXPRESSION OF GLIAL DRIVER LINES

FLY LINE	DRIVER LOCATION	LARVA	PUPA	ADULT
R.43.H01	**intron or 5' *of pointed*∞**	wg, psg	dsg, psg, xg^o	dsg, psg, xg^o
R.29.A12	**intron of *netrin-B*∞**	no	expression by ~P+20 in eg	eg, mdag*, mcg, mspg*, loag, lopag
R.32.H04	**intron of *swiss cheese*∞**	no	not tested	psg*, mg*
R.19.C02	**5' of *dachsous*∞**	no	expression by ~P+20 in mg	mg
R.25.A01	**intron of *wnt oncogene analogue4*∞**	xg^o	xg^o	xg^o
R.10.D10	**5' of *dimm*∞**	neurons	expression by ~P+80 in dsg and mg	dsg, mg
nrv2-GAL4; UAS-EGFP	***nervana2***	non-lamina cortex and neuropile glia	some cortex and neuropile glia, not in dgs prior to P+40%	dsg
P{17A}-GAL4	**unknown on 2nd chromosome**	spg	spg, expression in psug by ~P+10%	spg, psug
Mz97-GAL4, UAS-stinger	***SP2637*** Δ	wg, xg^o, xg^i	psug, dsg, xg^o, xg^i	psug, dsg, xg^o, mdag, mcg, xg^i
J29-lacZ	***gliotactin***	cg, wg	psug, dsg, expressed in psg at ~P+40%	psug, psg, dsg*
gli^{RL82}-GAL4	***gliotactin***	cg, wg	psug, dsg, expressed in psg at ~P+40%	psug, psg, dsg*

ΔBeckervordersandforth (2007)
∞A. Nern (HHMI, Janelia Farm)

eg - epithelial glia; cg - carpet glia; dsg - distal satellite glia; fg - fenestrated glia; loag - lobula astrocyte-like glia; lopag - lobula plate astrocyte-like glia; mcg - medulla chandelier glia; mdag - medulla distal astrocyte-like glia; meng - medulla ensheathing glia; mg - marginal glia; msg - medulla satellite glia; mspg - medulla serpentine layer glia; psg - proximal satellite glia; psug - pseudocartridge glia; spg - subperineurial glia; wg - wrapping glia; xg^i - inner chiasm giant glia; xg^o - outer chiasm giant glia; * - incomplete driver expression

3.5 DISCUSSION

My observations indicate that at least six distinct types of glia surround and populate the lamina neuropile and another five distinct types of glia do the same within the medulla. Each glial subtype has its own unique structure and is positioned in such a way that it is in contact with a unique set of optic lobe neurons, suggesting that each plays a specific role within its region of the optic lobe. Thus, the diversity of neurons within the brain is mirrored by diversity in the glia which surround or contact them, emphasizing the need to recognize glial identity and diversity with the same assiduity as for classes of neurons (Edwards and Meinertzhagen, 2010). Each class of glia also has its own pattern of gene expression, confirming that the different glial subtypes we recognize from morphological criteria coincide with genetic decisions made in the fly during its development, as revealed by *GAL4* or epitope expression, and as previously compared for lamina neurons (Meinertzhagen *et al.*, 2009).

3.5.1 PUPAL DEVELOPMENT OF ADULT LAMINA GLIAL CELLS

3.5.1.1 THE PUPAL ORIGIN OF LAMINA PSEUDOCARTRIDGE GLIA

The origin of the lamina's pseudocartridge glia is difficult to identify because we lack a marker that exclusively labels these prior to P+10% of pupal development. Pseudocartridge glia are a subtype of subperineurial glia which form a major component of the blood brain barrier in the *Drosophila* CNS (Bainton *et al*., 2005), the critical functioning of which has been clearly demonstrated at all stages of development (Baumgartner *et al.*, 1996; Carlson *et al.*, 2000; Banerjee *et al.*, 2008; Stork *et al.*, 2008; Edwards and Meinertzhagen, 2010). In the larva, the role of subperineurial glia in the eye disc is subsumed by the two, large, basally located carpet glia which are bound by septate junctions (Silies *et al.*, 2007). In the adult, the fenestrated and pseudocartridge glia together form unique components of the eye-brain barrier, and the expression patterns of glial driver lines analysed herein, specifically gliotactin which is required for the formation septate junctions (Genova and Fehon, 2003; Schulte *et al.*, 2003) and the function of the blood nerve barrier in the larval PNS (Auld *et al.*, 1995), indicate that the pseudocartridge glia are strategically equivalent to subperineurial glia that surround the rest of the CNS. This correspondence might, as a result, suggest that the larval carpet

glia divide and migrate to give rise to the pseudocartridge glia of the adult, and they do indeed serve a similar function and express some of the same genes (Bainton *et al.*, 2005; Silies *et al.*, 2007). The ultimate fate of carpet glia in the adult remains unknown, however. We will examine the evidence that either the carpet glia or a subset of the eye disc wrapping glia, may be give rise to the pseudocartridge glia in the adult.

Starting at about P+10% of pupal development, *P{17A}-GAL4* first begins to drive mCD8::GFP expression in the pseudocartridge glia. It is unclear if these cells are determined prior to P+10% or if driver expression is concurrent with cell fate specification. It is clear, however, that the subperineurial glia derive from a subset of *gliotactin* expressing glia since, at P+20%, *P{17A}-GAL4* driven mCD8::GFP co-expresses with *J29-lacZ* specific β-gal in some apically located glia of the eye disc. Given that *gliotactin* and *Mz97* drive in a similar pattern in the eye disc, it would appear as if the pseudocartridge glia may arise from a subset of the wrapping glia. This conclusion is preliminary, however, because *gliotactin*, unlike *MZ97*, expresses in carpet glia as well as the wrapping glia. It therefore remains possible that the two large carpet glia, whose nuclei lie at the posterior edge of the eye disc, begin to divide after pupariation to give rise to the multiple pseudocartridge glia seen at P+20%, although their position in the eye disc - basal to the wrapping glia - makes this unlikely. In the adult, the pseudocartridge glia lie immediately above the wrapping glia-derived distal satellite glia. In order for carpet glia to give rise to pseudocartridge glia they would therefore need not only to divide but also to migrate apically. It is thus more likely that a subset of the wrapping glia, those closest to the fenestrated glia and photoreceptors, receive an additional signal to trigger differentiation into pseudocartridge glia, as opposed to maintaining a default state and becoming distal cortex glia.

3.5.1.2 The Pupal Origin of Cortex Glia

Even though the lamina monopolar neurons they surround derive from a single source, the outer optic anlage (Trujillo-Cenóz and Melamed, 1973; Meinertzhagen and Hanson, 1993; Huang and Kunes, 1996, 1998; Huang *et al.*, 1998), the lamina contains at least two distinct types of cortex glia. Each of these has a different developmental origin, with all glia distal to L4 coming from the eye disc and all glia proximal to it, most likely deriving from the GPZ in the brain. L5 is unique amongst the lamina monopolar neurons in having a soma ensheathed by its own glial subtype - the proximal satellite glia. It is

possible therefore that the development and differentiation of these neurons and glia is in some way linked. Since L5 cells do not differentiate in topological sequence with L1-L4 (Huang and Kunes, 1998), and since ectopic L5 neurons can be induced along the medial lateral axis by expressing a constitutively active form of Spitz, it has been proposed that some signal, coming from a local source such as glia, might determine the L5 fate (Huang *et al.*, 1998). Similarly, *gliotactin* expression in the proximal satellite glia is delayed until after P+12.5%, when all L5 somata are clearly discernable in the lamina cortex (Meinertzhagen and Hanson, 1993), suggesting that L5 may trigger the specification and continued development of its glial partner, or vice versa.

Prior studies on the origins of glia in the developing optic lobes have indicated that two populations of cortex glia exist in the optic lobe: a population on the surface of the brain that is clonally related to glia in the eye disc and optic stalk, and a population of glia in the cortex area, which are clonally related to the neuropile glia populations derived from the GPZ (Perez and Steller, 1996). By tracing the expression of cell-specific driver lines through the early stages of pupal development we have provided evidence to suggest that the distal satellite glia that surround the somata of L1-L4 derive from wrapping glia in the larval eye disc. Thus, the wrapping glia are the likely precursor for two types of adult lamina glia, the pseudocartridge and the distal satellite glia. The signal which allows the differentiation of wrapping glia into two distinct subtypes during pupal development is not yet known.

The distal and proximal satellite glia may not be the sole glial subtypes residing in the lamina cortex. In the developing pupa, and even in the young adult, a population of small, round, Repo-expressing nuclei exist at the distal edge of the lamina cortex. These cortex glia do not express *Mz97-GAL4*, a marker for the distal satellite glia and pseudocartridge glia, which also lay near this area of the cortex. They may appear unique simply because *Mz97-GAL4* driver expression is incomplete, but at least three other possibilities exist. First, their position at the edge of the lamina cortex suggests that they may be a type of surface glia, possibly perineurial in origin, for which we, personally, do not have a cell-specific marker or driver-line. Preliminary results from tracing the pupal development of larval surface glia with the driver *c527-GAL4* indicates the presence of a population of surface glia-like cells in the adult which have cell bodies restricted to the the lateral edges of the retina and the lamina (Appendix A). These, and the *Mz97*-negative glia of the cortex, have yet to be shown definitively to be one-and-

the-same, however. Second, they could be a population of incompletely differentiated glia that undergoes cell division in order to clean up apoptotic neurons (Doherty *et al.*, 2009; Kato *et al.*, 2009). Engulfing glia would be necessary in the lamina if L5 were to differentiate from one of two supraneuropile cells, leaving the other to undergo apoptosis and be removed from the cortex. Cell death is common in the lamina cortex during the first half of pupal development (Trujillo-Cenóz and Melamed, 1973; Hofbauer and Campos-Ortega, 1990; Meinertzhagen and Hanson, 1993). Such a role is supported by the finding that cortex glia of the adult express the engulfment proteins Draper and dCed-6, however, in other parts of the adult brain this duty falls to the ensheathing glia (Doherty *et al.*, 2009). Third and lastly, they could be a unique and previously undescribed type of cortex glia.

3.5.1.3 The Origin and Fate of Other Optic Lobe Glia

Yet other glia, previously unidentified, are found within the developing visual system. Large glial nuclei are located around the perimeter of the lamina neuropile of the pupa. The nuclei of some of these express *Mz97-GAL4*, while others do not. Were they to persist into the adult, both expressing and non-expressing forms would represent additional subtypes of previously undescribed glia. Their origins are also unclear. They may be glioblasts or derivatives from the carpet glia of the larval eye disc. The single *Mz97*-expressing glial cell in the P+20% optic stalk is unlikely to be one of the two carpet glia, however. Based on its position and singularity it may correspond to the inner glia which separate the axons of Bolwig's organ from other photoreceptor axons in the optic stalk (Silies *et al*., 2007).

Another type of lamina glia, the "subretinal glia" (Winberg *et al.*, 1992), has been previously identified within the brain of the larva. These glia lie at the posterior-lateral surface of the ingrowing photoreceptor axons, where axon bundles of the optic stalk enter the anlage. "Subretinal glia" invariably express all of the same drivers as wrapping glia, including *Mz97*, *R.43.H01* and *gliotactin*. Furthermore, their positions anticipate those of the distal satellite glia as detected with *Mz97-GAL4;UAS-stingerGFP* in the P+20% pupa. For these reasons we have previously advocated abandoning the term subretinal glia (Edwards and Meinertzhagen, 2010) and adopting the more definitive terms wrapping glia in the larva and distal satellite glia in the pupa and adult.

3.5.2 Astrocyte Glia are Not Created Equal

The *R.29.A12* driver line labels astrocyte-like glia throughout the adult brain in areas including, but not limited to, the medulla, lobula, lobula plate and antennal lobes. Most, if not all, of the cells labelled are astrocyte-like in structure. Within the lamina, *R.29.A12* drives mCD8::GFP expression in the epithelial but not marginal glia, suggesting that despite their unusual columnar shape, the epithelial glia are in fact a type of astrocyte-like glia, while the marginal glia are not. Considering their locations within the neuropile this is a reasonable assumption. To the extent which astrocyte-like glia are defined by their extensions into other neuropiles (Awasaki *et al.*, 2008), epithelial glia can be similarly classified because they extend into the synaptic regions of the lamina. They are postsynaptic at photoreceptor tetrad synapses, as well as the gnarls of T1 (Meinertzhagen and O'Neil, 1991); a functional role at tetrad synapses is implied by their expression of the histamine receptor protein HisCl1 (Gao *et al.*, 2008; Pantazis *et al.*, 2008) and their expression of Ebony, an enzyme which inactivates histamine (Richardt *et al.*, 2002).

Marginal glia, while they project into the basal-most layers of the lamina are, on the other hand, not intimately associated with synapses. Apart from their nuclear localisation (Eule *et al.*, 1995), marginal glia have not been well described in adult *Drosophila*, and we rely instead on anatomical descriptions based on EM studies in *Musca* (Saint Marie and Carlson, 1983b, a). There, from stratification of their lateral processes, the marginal glia are reported to have a shingled appearance with a flat basal surface. The apical surface has processes extending into the neuropile that envelop the tracheoles, the axons of the R7 and R8 photoreceptors, and the perimeter of the optic cartridge (Saint Marie and Carlson, 1983b). Their position lining the bottom of the lamina, and the fact that they fail to express GFP under the *R.29.A12* driver, both point to the marginal glia being a subtype of ensheathing glia rather than astrocyte-like neuropile glia.

Within the medulla, *R.29.A12* expresses in three unique types of glia. Although rarely expressed in the distal medulla glia, when it does express there it reveals an astrocyte-like glia with many branches that extend into at least five neighbouring medulla columns and as deep as stratum M7, the serpentine layer. Their branching is more elaborate than the pattern of branching visualized by Ebony immunolabellling in glia of the distal medulla (Richardt *et al.*, 2002; Wagner *et al.*, 2007). The distal medulla glia are therefore positioned so as to be associated with the medulla's input terminals from R7

and R8 and L1-L5, all of which synapse in this region (Takemura *et al.*, 2008). They are also well qualified to be the glial partners at small, club-headed capitate projections which invaginate the terminals of photoreceptors R7 and R8 in the distal medulla (Melamed and Trujillo-Cenóz, 1968; Takemura *et al.*, 2008; Edwards and Meinertzhagen, 2009).

Unlike the glia of the distal medulla, chandelier glia, which have cell bodies outside the medulla neuropile's proximal-most surface, frequently express *R.29.A12*. They extend astrocyte-like branches that extend distal to stratum M10 and beneath the serpentine layer, in a location similar to the dendrites of medulla tangential neurons such as Mt5, or the neurons T3 and T4 (Fischbach and Dittrich, 1989). Their location and branching pattern suggest that they are associated with a completely different set of neurons than the astrocyte-like glia which branch in M1-M6. They are thus likely to have different genetic expression profiles even though they both share expression of some of the limited set of drivers utilized in this study, including *R.29.A12* and possibly even d*EAAT-GAL4* and *Mz97-GAL4*, which both drive broad expression of GFP in the proximal medulla.

While the *R.29.A12* driver reveals the many types of astrocyte-like glia, we were not able to detect or confirm the presence of ensheathing glia-like cells with cell bodies in the cortex and lamellae that appear to wrap axons in several photoreceptor containing columns in the medulla neuropile, as described using *ort-GAL4* driver (Gao *et al.*, 2008). The distal medulla does, however, contain at least two distinct types of glia, as revealed by the presence of two types of Repo-expressing nuclei there. One subtype is the asytocyte-like glia described herein using *R.29.A12,* and elsewhere using Ebony immunoexpression (Richardt *et al.*, 2002; Wagner *et al.*, 2007). *Mz97-GAL4;UAS-stinger* appears to express in astrocyte-like glial of the medulla, as determined by the similarity of their extensions to those of Ebony-expressing medulla neuropile glia. However, another subset of glial cells in the distal medulla do not express *Mz97-GAL4*, and because we have not isolated a driver which expresses in these cells we cannot determine their structure. They may be ensheathing glia, with lamellae which lie almost entirely outside of the neuropile, and/or they may be similar in appearance to the *ort-GAL4* expressing glia-like cells (Gao *et al.*, 2008), as illustrated in Figure 3.2. It is entirely possible that the distal medulla has three, or even four, distinct types of glia. The discontinuous expression of *dEAAT-GAL4* driven GFP in glial cells at the distal

medulla is further support for the presence of at least two distinct types of glial cells in this area of the brain.

3.5.3 The Glia of the Adult Blood-Brain and Blood-Eye Barrier

No blood-eye barrier exists in the eye disc of the *Drosophila* third-instar larva (Carlson *et al.*, 1998). As previously mentioned, the eye-brain barrier that lies just above the lamina is distinct from that surrounding the rest of the CNS, and consists of two glial cells types that develop during pupal metamorphosis: the fenestrated and pseudocartridge glia (Eule *et al.*, 1995), of which only the pseudocartridge glia is occluding (Shaw, 1978). These are essentially equivalent to the perineurial and subperineurial glia which form the blood brain barrier lining the rest of the nervous system in the larva and adult (Shaw, 1978; Chi and Carlson, 1981; Carlson *et al.*, 2000; Bainton *et al.*, 2005; Stork *et al.*, 2008).

In the adult, the occluding subperineurial glia surround the entire CNS except for a small space at the outer optic chiasm where axons project between the lamina and medulla. Thus, the surface glia lining the base of the retina do not contact the surface glia around the rest of the CNS. Instead, glia with nuclei lying beneath the basement membrane of the retina, at a location similar to the fenestrated and pseudocartridge glia, extend their lamellae in a proximal direction to surround the lateral borders of the lamina. Although GFP expression in these cells is driven by the same promoters as for fenestrated and pseudocartridge glia, they are morphologically different in that they project extensions into the brain instead of along the underside of the eye, thereby navigating along a unique surface. GFP expression in the fenestrated glial line w^{1118}*; Mi{ET1}ths*^{MB02475} allows visualization of glia that line the lateral margins of the lamina, and their driver expression suggests that these differ from a similarly located glia labelled using the pseudocartridge and subperineurial glia specific driver *P{17A}-GAL4.* These glia that line the lateral borders of the lamina are not, however, the lateral most glia around the lamina. Other small, round, Repo-expressing glial nuclei are detected just outside the lamina glia borders. These may correspond to a previously undescribed class of adult surface glia which express *c527-GAL4* and which have cell bodies restricted to the lateral edges of the cortex and an area around the lateral edges of the retina (Appendix A). I have identified these glia but do not describe them here, requiring additional time to characterise them more completely and trace their development.

In *P{17A}-GAL4* expressing flies there is a small space left unoccupied between the GFP labelled pseudocartridge glia and the subperineurial glia at the anterior edge of the adult lamina. However, proximal extensions from w^{1118}; $Mi\{ET1\}ths^{MB02475}$-expressing perineurial-like glia and distal extensions from the outer chiasm giant glia reach out towards this space from both directions and may act as a part of the blood brain barrier or provide a means for proximal-distal transport of substances along the edges of the lamina .

3.5.4 What Promoter Expression Reveals About Glial Subtypes

The genes that a cell expresses can reveal a lot about its function. As indicated in Table 3.1, the promoter or enhancer for each of the expression lines provided from the Rubin collection at Janelia Farm has been mapped to the sequence level. Fenestrated glia in the adult express a driver for the FGF8-like ligand *thisbe*, despite its previously reported pattern of expression having been limited to the photoreceptors in the larva. Over-expression of *thisbe* in larval photoreceptors induces the formation of supernumerary wrapping glia, resulting in the hyperwrapping of photoreceptor axons (Franzdóttir *et al.*, 2009). Is it possible that late-onset Thisbe expression in fenestrated glia is the signal which triggers the differentiation of their neighbouring pseudocartridge glia from the larval wrapping glia? Determining a timeline for the onset of *thisbe* expression in fenestrated glia would be a good first step in establishing its candidacy in this role.

Gliotactin driver expression in pseudocartridge glia supports the suggestion that these are indeed septate junction-containing glia (Auld *et al.*, 1995; Genova and Fehon, 2003; Schulte *et al.*, 2003), as has been demonstrated in other species (Shaw, 1978; Chi and Carlson, 1981; Saint Marie and Carlson, 1983a). While the complete series of intercellular junctions has not yet been resolved for the lamina of *Drosophila*, in the housefly all of the pseudocartridge, distal and proximal satellite glia form septate junctions (Saint Marie and Carlson, 1983a). The expression of a *gliotactin* driver in all of these glial subtypes goes someway to suggest a similar junctional arrangement in *Drosophila*. Both *gliotactin* and *nrv2* are necessary for the proper development of septate junctions (Genova and Fehon, 2003) and both are expressed in the distal satellite glia, at least in the late stages of pupal development and up until eclosion. In the adult, it is the pseudocartridge glia and the proximal satellite glia which express *gliotactin*, but not *nrv2*, suggesting that, at least in these cells, *nrv2* is not necessary to

form septate junctions. It is intriguing to think that the septate junction barrier extends as deep as the proximal satellite glia in the adult. Perhaps a barrier is needed to prevent the extracellular passage of ions and substances from the lamina and in a distal direction towards the eye, or to contain the large quantities of histamine that are released from the photoreceptor terminals, and corral these for local recycling in the lamina.

The distal satellite glia also express promoters/enhancers for all of *pointed*, *dimmed* and an N-terminal Asparagine amidohydrolase coded by *SP2637*, implicating these cells in regulating apoptosis (Ditzel *et al.*, 2003) as well (dimmed) as being associated with a neuroendocrine phenotype (Hamanaka *et al.*, 2010). The *dimmed* associated driver line *R.10.D10* also drives expression in the marginal glia, wide-field neurons near the medulla (data not shown), and elsewhere in the brain. The transcription factor *pointed* regulates the expression of various genes necessary for glial development (Klämbt, 1993; Klaes *et al.*, 1994; Granderath *et al.*, 2000).

Both of the proximal satellite glia and the outer chiasm giant glia also express drivers for *pointed*, but differ in that the proximal satellite glia express *swiss cheese* and *gliotactin*, as previously discussed, while the chiasm glia express a driver for the *wnt oncogene analogue4* and the protocadherin *dachsous,* which is expressed as early as glial establishment within subdomain I (Dearborn and Kunes, 2004). Of the glia examined here, no two had identical patterns of driver expression. The presence of a *swiss cheese* driver (*R.32.H04*) in both the proximal satellite and marginal glia implicates these cells in the maintenance of their neighbouring neurons (Kretzschmar *et al.*, 1997; Mühlig-Versen *et al.*, 2005; Bettencourt da Cruz *et al.*, 2008), however, Swiss cheese is immunolocalised to the lamina surface glia, distal satellite glia and medulla neuropile glia (Mühlig-Versen *et al.*, 2005). Thus, caution must be utilized because driver expression does not necessarily dictate protein expression.

Finally, the epithelial and astrocyte-like glia express a driver for *netrinB (R.29.A12)*, which is required for axon and dendrite guidance (Mitchell *et al.*, 1996). While Netrins are not involved in targeting photoreceptor axons to the lamina during development, they do express at targets within the lamina (Gong *et al.*, 1999). In this case NetrinB may be involved in fine scale targeting of cells.

3.5.5 The Nomenclature of Optic Lobe Glia

Two major sources of confusion over glial identities are reflected in the nomenclature these cells have received in the literature. First, genetic markers may fail to distinguish between glial subtypes that can be distinguished by other criteria. This was the case when subretinal glia of the adult visual system were first designated by enhancer trap line 3-109 (Winberg *et al.*, 1992) that expressed in both fenestration and pseudocartridge glia. Second, glia have received the same names at the larval and adult stage without any evidence that one transforms into the other. The latter case is true for subretinal glia in the larval eye disc and larval optic anlage and the subretinal glia of the adult optic lobe, which bear no confirmed relation to each other (Edwards and Meinertzhagen, 2010). Although the situation of the respective nomenclatures is now largely resolved, all systems rely on markers and are only as reliable as the marker in question. A third class of confusion has arisen when glia are incorrectly identified, even when markers exist to reveal the identity of the cells in question. Thus, the glia of the first optic chiasm (Meinertzhagen, 1973; Tix *et al.*, 1997) are often incorrectly identified as medulla cortex glia (Poeck *et al.*, 2001; Suh *et al.*, 2002; Chotard *et al.*, 2005), apparently because chiasm glia have not been widely recognized in previous glial developmental studies.

The complexity of glial subtypes is belied by their current naming schemes and the way they have been grouped into subclasses. Our current analysis of glial subtypes suggests that the structure of both surface and astrocyte-like glia in a single neuropile varies, usually depending upon the location of the glia within that neuropile. These differing structures are likely to represent the different genetic programming during development and slightly different mature functions of similarly categorized glial subtypes in the adult. In the larval brain most of these glia are just categorized as “medulla glia” and the means by which they migrate to their final location and differentiate into a structurally unique subtype is unknown and itself merits further investigation. During the development of the lamina, at least, it appears as if a series of chronologically timed signalling events between photoreceptors and their underlying eye disc glia ultimately give rise to three distinct types of glia. Photoreceptors initiate the differentiation of migrating surface glia-like cells into a distinct larval subtype, wrapping glia, using the FGF8-like ligand Thisbe (Franzdóttir *et al.*, 2009). Then, during pupal development, these larval wrapping glia differentiate into two unique subtypes, the

pseudocartridge and distal satellite glia. While the signal which triggers this change is not known, the transformation from wrapping glia to pseudocartridge glia is probably due to further interplay of signals between photoreceptors and glia at later stages of development. Although all glia of the wrapping subtype may be competent to receive further signals for differentiation, only those which lie closest to the photoreceptors begin to express the pseudocartridge glia specific marker *P{17A}-GAL4* during the early stages of pupal development. *P{17A}-GAL4* also labels the subperineurial glia surrounding the entire larval brain but these cells divide and differentiate before larval hatching (Awasaki *et al*., 2008), not during pupal development , which is when *P{17A}-GAL4* driven GFP expression becomes apparent in pseudocartridge glia.

A similar mode of glial differentiation may also take place within the medulla to result ultimately in the creation of different astrocyte-like glial cell types. While all may be competent to become any of the astrocyte-like glial types described herein, it is ultimately their final location, and thus their interactions with surrounding neurons that determines the adult structure of the particular glial subtype. Development of glia in the medulla is still a vastly understudied field and so many of the interactions which may occur between the developing neurons and glia that lie within must await discovery. Many more cell signalling pathways may yet be elucidated for deeper regions of the *Drosophila* optic lobes. The discovery of unique glial cell types within the adult medulla is a foundation upon which studies of neuron and glial interaction during development can be based.

3.6 ACKNOWLEDGEMENTS

Antibody 24B10 was developed by Dr. Seymour Benzer, 40-1a by Dr. Joshua Sanes,and 8D12 by Dr. Corey Goodman. All were obtained from the Developmental Studies Hybridoma Bank, University of Iowa. Anti-Ebony was provided by Dr. Bernhardt Hovemann (Ruhr-Universität Bochum, Germany). The *c527-GAL4* stock was generously provided by Dr. Christian Klämbt (Westfälische Wilhelms Universität; Münster, Germany); the *Gli*^{rL82}*-GAL4* stock by Dr. Vanessa Auld (University of British Columbia, Canada) and the *UAS-HRP::CD2* lines by Dr. Chi-Hon Lee (NIH, Bethesda). Special thanks to Dr. Gerry Rubin and Dr. Aljoscha Nern (HHMI, Janelia Farm) for the R. stocks. All other stocks were provided by the Bloomington Stock Center. I would also like to thank Zhiyuan Lu for his assistance with sectioning and electron microscopy and

Andrea Nuschke and Qurat-ul-ain Haider for their help with immunocytochemistry and imaging.

3.7 TRANSITION TO CHAPTER FOUR

The liberation of histamine from its β-alanyl derivative carcinine is essential to return histamine to the photoreceptor, and thus sustain continued light-evoked release. Identification of the gene *tan* that regulates this liberation and its expression in fly photoreceptors, as well as its function in liberating histamine from exogenous sources of carcinine are all essential aspects of histamine metabolism that are covered in the next chapter. This work has been published, in part, in *PLoS Genetics* (2005). Tan is the *Drosophila* homologue of fungal isopenicillin-N N-acyltransferase coded for by the gene *CG12120*, that plays an important role in both cuticle pigmentation and histamine recycling. In this chapter I localise *tan* to the cytoplasm of photoreceptors, as well as to areas outside the central nervous system. Using whole-head measurements of histamine contents I was able to demonstrate that the quantity of available Tan protein determines the whole-head histamine contents of assorted *tan* mutants, as published in PLoS. While *tan* expression in the photoreceptors is shown to be essential for the liberation of histamine from carcinine, Tan in the body is also capable of hydrolysing carcinine.

CHAPTER 4

TAN EXPRESSION AND CARCININE HYDROLYSIS IN THE BRAIN AND BODY OF *DROSOPHILA*

TARA N. EDWARDS AND IAN A. MEINERTZHAGEN

CONTAINS SECTIONS FROM A MANUSCRIPT SUBMITTED JULY 5, 2005, ACCEPTED OCTOBER 14, 2005 AND PUBLISHED NOVEMBER 19, 2005. PUBLISHED IN PLOS GENETICS 1(5):E63.

© JOHN R. TRUE, SHU-DAN YEH, BERNHARD T. HOVEMANN, TOBIAS KEMME, IAN A. MEINERTZHAGEN, TARA N. EDWARDS, SHIAN-REN LIOU, QIAN HAN AND JIANYONG LI

4.1 ABSTRACT

Vision in *Drosophila* depends on efficient recycling of the photoreceptor neurotransmitter histamine. This recycling pathway involves the reciprocal action of two enzymes in the visual system, Tan in the photoreceptors and Ebony in surrounding epithelial and medulla neuropile glia. Here we characterise Tan's action in photoreceptor terminals. Within the head, Tan is expressed specifically in the cytoplasm of photoreceptors and both the concentration of histamine and the magnitude of 'on' and 'off' transients of the ERG change in proportion with the levels of *tan* mRNA. After drinking a solution containing the β-alanyl conjugate of histamine, called carcinine, there is an excess of histamine in fly heads which immunolocalises to surface glia that form the blood brain barrier. Other glia within the visual system such as the marginal glia, the distal satellite glia and the fenestrated glia probably also play a role in regulating the amount of histamine that is accessible to the visual system. However, Tan protein in the body has influence on the measurable concentration of histamine in the head. While histamine and its inactivated β-alanyl conjugate, carcinine, are able to be transported through the blood brain barrier, their limited access to the visual system is likely determined by the requirements of the nervous system.

4.2 INTRODUCTION

Vision is arguably the most important sensory modality for a flying insect. The insect must be able to navigate its way through a three-dimensional space, avoiding danger through quick up, down, and side-to-side movements, adjusting its flight trajectory to avoid threats or obstacles. The first requirement for rapid behavioural responses is a visual system with high temporal resolution to light stimuli. Light-evoked responses from photoreceptors signal at high frequencies (Tatler *et al.*, 2000) that are adapted to the insect's visual environment (Laughlin and Weckström, 1993), and require rapid transmission at photoreceptor synapses (Laughlin *et al.*, 1987) and circuits for the efficient extraction of information on motion that drive optomotor pathways (Srinivasan *et al.*, 1999). The fly's compound eye is composed of many individual ommatidia, each containing eight photoreceptors (Ready *et al.*, 1976). Six of these, R1-R6, express a single rhodopsin (Rh1) and are responsible for motion detection (Ostroy *et al.*, 1974; Hardie, 1985; Mismer and Rubin, 1987; Rister *et al.*, 2007) while the other two, R7 and R8, have different spectral peaks (R7 in the UV and R8 in the blue-green; Hardie and

Kirschfeld, 1983; Chou *et al.*, 1996; Huber *et al.*, 1997; Chou *et al.*, 1999), and are used to distinguish biologically relevant colours (Heisenberg and Buchner, 1977; Gao *et al.*, 2008). R1-R6 terminate in the first optic neuropile, or lamina, while the axons of R7 and R8 penetrate the lamina and terminate in the second neuropile, the medulla (Braitenberg, 1967; Fischbach and Dittrich, 1989; Takemura *et al.*, 2008). Despite these differences in opsin expression and axon trajectory, all utilize the same neurotransmitter - histamine - at their synapse (Hardie, 1987; Nässel *et al.*, 1988; Pollack and Hofbauer, 1991).

The efficiency of the visual system of the fly's compound eye, in particular its sensitivity to motion (Borst, 2000) derives from the synaptic circuits in the underlying optic neuropiles. The inputs to these are provided by the R1-R6 photoreceptors, one each from beneath neighbouring ommatidial facets, which terminate alongside, and synapse upon, a set of lamina monopolar neurons in a single lamina cartridge (Braitenberg, 1967; Meinertzhagen and O'Neil, 1991). The photoreceptors that converge upon a unit cartridge are exactly those that view a single point in visual space according to the principal of neural superposition (Kirschfeld, 1967). When stimulated by light, the soma of the photoreceptor depolarises and its terminal releases histamine onto a tetrad of postsynaptic partners. These always include two lamina monopolar neurons, L1 and L2; with some combination of the lamina monopolar neuron L3, amacrine cells or epithelial glia comprising the remaining pair of elements in the postsynaptic tetrad (Meinertzhagen and O'Neil, 1991). All four postsynaptic partners express one of two histamine gated Cl^- channels on their surface, with the neurons expressing a receptor, HisCl2, that is distinct from the HisCl1 receptor expressed on the epithelial glia (Gisselmann *et al.*, 2002; Witte *et al.*, 2002; Zheng *et al.*, 2002; Pantazis *et al.*, 2008). The release of histamine is tonic (Uusitalo *et al.*, 1995a) and light modulates the rate of release. Histamine then activates the postsynaptic receptors to trigger an influx of Cl^- into the postsynaptic partners, and ultimately, the hyperpolarization of L1 and L2 neurons (Uusitalo *et al.*, 1995b). These neurons are claimed to be the major contributors to the 'on' and 'off' transients of the ERG (Coombe, 1986). When the light stimulus diminishes or extinguishes, the inevitable release from inhibition - visualized as the 'off' transient - follows shortly afterwards (Heisenberg, 1971; Hardie, 1989; Pantazis *et al.*, 2008). Activation of HisCl1 in the epithelial glia modulates the HisCl2-derived response of their lamina monopolar cell neuronal partners in the tetrad (Pantazis *et al.*, 2008).

Once histamine is released it must immediately be cleared from the synaptic cleft and inactivated to enable further release to be signalled, and thus preserve the temporal resolution of visual transmission. In fact, given the tonic nature of histamine release, all signalling must reflect a balance between release and clearance (Stuart *et al.*, 2007). Given the high rates of release, histamine must also be shuttled back to the photoreceptor for re-use. It has been estimated that, should all of the synapses of a single *Drosophila* photoreceptor terminal release simultaneously in bright light, the terminal's population of synaptic vesicles and their associated histamine would deplete at a rate of ~5000 vesicles/sec (Borycz *et al.*, 2005). Compensatory vesicle endocytosis and histamine reuptake are thus required to avoid synaptic depletion from the loss of histamine and its vesicles, and to clear released histamine from the synaptic cleft.

Histamine recycling is accomplished, in part, through a shuttle pathway which involves both the epithelial glia and the photoreceptors in the lamina (Borycz *et al.*, 2002; Richardt *et al.*, 2002; True *et al.*, 2005; Stuart *et al.*, 2007; Wagner *et al.*, 2007). The N-β-alanyl dopamine producing (NBAD) enzyme, Ebony, which is responsible for the cuticle pigmentation phenotype in mutants of the corresponding gene, is also responsible for inactivating histamine by mediating its conjugation to β-alanine, thus forming β-alanyl-histamine, originally known as carcinine (Richardt *et al.*, 2003). Ebony, however, is expressed in the epithelial glia (Richardt *et al.*, 2002), and so histamine released at the synapse must first be taken up by glia in order to be inactivated. Inactivated histamine must then be shuttled back as carcinine from the glia to the photoreceptor for re-use. The transport functions for these steps have yet to be discovered, but they must be fast and operate with a high capacity. Production of carcinine is rapid (Borycz *et al.*, 2002), and the structural intimacy between the R1-R6 photoreceptor terminals and the surrounding epithelial glia in the lamina suggests that the Ebony shuttle pathway is the first means by which histamine is cleared from the cleft.

In order to be "recycled", however, there must be a means to liberate histamine from carcinine. In neurons that use other monoamines, either the amine itself is taken up directly into new synaptic vesicles endocytosed from the presynaptic membrane, or the vesicle takes up the amine precursor so that the amine itself is produced only within the vesicle's lumen. Thus mammalian dopaminergic neurons have vesicles that directly pump dopamine from the cytosol by means of a vesicular amine transporter (Liu *et al.*, 1992), and although the *Drosophila* transporter of dopamine differs from the mammalian

transporter in its pharmacological profile, it is also involved in direct uptake of dopamine (Pörzgen *et al.*, 2001). In mammalian noradrenergic neurons of sympathetic nerves the final β-hydroxylase synthesis of noradrenaline from dopamine occurs within the vesicle itself, which then co-releases its contents, noradrenaline and β-hydroxylase (Weinshilboum *et al.*, 1971), with the latter being recycled. Either situation could, in principle, apply in the *Drosophila* photoreceptor terminal, depending on whether its vesicles take up carcinine or histamine, and whether they contain Tan or not.

At the onset of this research it was known only that the protein encoded by the mutant pigmentation gene *tan* played an integral role in histamine recycling (Borycz *et al.*, 2002), but neither the corresponding gene nor its site of action were known. Upon discovery that *tan* corresponded to *Drosophila* gene *CG12120*, a homologue of fungal isopenicillin-N N-acyltransferase, a collaborator from the Hovemann lab in Bochum and I were simultaneously able to localise *CG12120* transcripts to the retina (True *et al.*, 2005). Thus, histamine is liberated from carcinine by Tan protein in the photoreceptors. The Tan protein itself was confirmed to catalytically cleave carcinine into its components, histamine and β-alanine both *in vivo* and *in vitro* (True *et al.*, 2005), and the production and immunoreactivity of an antibody confirmed that Tan protein is localised exclusively to the cytoplasm of photoreceptors in the CNS of *Drosophila* (Wagner *et al.*, 2007). The presence of Tan in the photoreceptors meant that a shuttle system for histamine, carcinine and β-alanine must exist between the photoreceptors and their surrounding epithelial glia.

Despite the clear identification of reciprocal Ebony/Tan enzymatic activity, it is unlikely that the histamine/carcinine recycling pathway functions in complete isolation within the cartridges of the *Drosophila* lamina. Ebony is expressed in glia throughout the central nervous system (Richardt *et al.*, 2002; Suh and Jackson, 2007) and both Tan and Ebony action are required for proper cuticle melanization (Hovemann *et al.*, 1998; True *et al.*, 2005; Aust *et al.*, 2010), indicating their function outside the CNS. The photoreceptor axons of R7 and R8, which terminate in the medulla, also release histamine at their synapses and are themselves in close association with Ebony-expressing medulla neuropile glia (Wagner *et al.*, 2007). Histamine is not only the neurotransmitter at photoreceptors, however, but also at mechanosensory neurons in the head and the PNS (Buchner *et al.*, 1993) and at interneurons within the CNS (Nässel *et al.*, 1988; Pollack and Hofbauer, 1991). Histamine is also immunolocalised to the fenestrated glia, which

lie just below the surface of the retina (Pollack and Hofbauer, 1991; Melzig *et al.*, 1998; Borycz *et al.*, 2002) and its presence in these glia can change depending upon the genetic background of the fly (Borycz *et al.*, 2002; Romero-Calderón *et al.*, 2008).

Here, I will consider the localisation of Tan to the cytoplasm of *Drosophila* photoreceptor and the effect of differing mutant *tan* alleles on determinations of the whole-head contents of histamine. After feeding carcinine to flies in which the *tan* mutation is exclusively restricted to the eyes, our measurements of whole-head histamine suggest that the lamina recycling pathway alone cannot account for all of the histamine found in the fly's head after these types of generalized feeding experiments. A possible role for factors outside the lamina in the recycling and mobilization of histamine must therefore be considered. These factors include the role of non-epithelial glia of the visual system in the isolation and storage of histamine, as well as factors outside the CNS itself, which can affect current measurements of whole-head histamine content.

4.3 METHODS

4.3.1 FLY STRAINS

Flies were raised on a standard cornmeal molasses agar medium at 24°C (or 23°C for analysis with high performance liquid chromatography – HPLC) with a 12 h light:12 h dark cycle. For carcinine feeding experiments, flies were isolated for 2 h and then given either an aqueous solution of 4% glucose or 0.5% carcinine in glucose for 16 h under their normal L:D cycle.

The following lines were used in this study: *R.29.A12*, *R.43.H01*, *R.10.D10*, *R.19.C02* which are glial *GAL4* lines provided by Drs. G. Rubin and A. Nern (HHMI, Janelia Farm). These lines were crossed to (BL#5136) *P{UAS-mCD8::GFP.L}LL4, y[1] w[*]; Pin[Yt]/CyO* to identify glial expression.

For tan^1 rescue and EGUF-hid analysis tan^1 (BL#130) was recombined with (BL#1709) *P{neoFRT}19A; ry[506]* on the X chromosome. This tan^1 *neoFRT19A* line was then crossed with the EGUF-hid line (BL#5248) *P{GMR-hid}SS1, y[1] w[*] P{neoFRT}19A; P{GAL4-ey.H}SS5, P{UAS-FLP1.D}JD2* to generate flies which were mutant for *tan* exclusively in the eye. The offspring of *neoFRT19A* and *neoFRT19A-EGUF-hid* was

used as the wild-type control vs *tan-EGUF-hid* flies. The *tan*^{1} *neoFRT19A* line was also used as the background for R1-R6 photoreceptor-specific rescue using *Rh1-GAL4* (BL#8691) and *UAS-CG12120* (on II). The protocol for establishing these lines is described in Appendices B and C).

For HPLC analysis of histamine concentration in *tan* mutants four excision and four revertant lines were used, all of which were derived from the P-element line *w*^{1118}*,P{XP}CG12120*^{d07784}. Excision lines with deletions of the *CG12120* gene include *20A*, *37C*, *27A* and *42A*. Revertant lines, which had removal of part of the P-element, but had no *tan* deletions of the *CG12120* gene and no *tan* phenotype, were *19A*, *17B*, *38B*, and *51C* (Appendix D; True *et al*., 2005).

Wild-type *OR*, *w*^{1118} and *w*^{1118}*tan*^{1} were used as controls.

4.3.2 IMMUNOCYTOCHEMISTRY

For standard immunocytochemistry the heads of adult flies were fixed in a solution of 4% formaldehyde [from paraformaldehyde (PFA)] in 0.1 M phosphate buffer (PB) for 4 h or overnight at 4°C. For histamine immunolabelling adult heads were fixed in a solution of 4% 1-Ethyl-3-[3-dimethylaminopropyl] carbodiimide Hydrochloride (EDAC, Sigma, St. Louis, MO, USA) in 0.1M PB for 3 h at 4°C. For cryostat sectioning, fixed heads were cryoprotected in 12% sucrose in PBS for 30 min followed by an overnight treatment in 25% sucrose/PBS at 4°C. Heads were then embedded in Tissue-Tek OCT (Andwin Scientific, Addison IL, USA) and instantly frozen in liquid nitrogen. Horizontal sections were cut at 10 µm, collected on Superfrost Plus Gold slides (Fisher Scientific, Pittsburgh, PA, USA) and allowed to dry before rehydration in PBS. Alternatively, brains were washed in 0.1 M PB, mounted in 7% agarose, and sliced in the horizontal plane at 80–100 µm thickness by means of a Vibratome 1000.

For immunolabelling, sectioned brains were permeabilized in successive treatments of 0.2% and 2% Triton X (Tx) in 0.01 M PBS and then blocked with 5% normal goat serum (NGS) in 0.2% PBS-Tx. Tissues were incubated 24-48 h at 4°C in primary antibody diluted in 5% NGS-PBS-Tx. Primary antibodies were used at the following concentrations: 1:20 anti-Futsch (22C10, DSHB), 1:500 rabbit anti-Ebony (B. Hovemann), 1:100 rabbit anti-Tan supernatant (B. Hovemann), 1:500 rabbit anti-Histamine (H+L; ImmunoStar, Hudson, WI, USA), 1:1000 mouse anti-GFP (3E6,

Molecular Probes, Eugene, OR, USA; A11120). The immunogen source and characterization of primary antibodies is summarised in Table 4.1. After at least six washes in 0.2% PBS-Tx, tissues were incubated overnight in some combination of the following secondary antibodies: 1:400 goat anti-rabbit Cy3 (Jackson ImmunoResearch Inc: West Grove, PA, USA); 1:400 goat anti-mouse Alexa 488 (Invitrogen, Carlsbad, CA, USA) or 1:400 goat anti-rabbit Alexa 488 (Invitrogen, Carlsbad, CA, USA). Tissues were washed at least six times in 0.01M PBS before being mounted in Vectashield medium (Vector Labs, Burlingame, CA, USA) and images were captured using a LSM 510 confocal microscope and associated software (Zeiss, Jena, Thüringen, Germany).

4.3.3 High Performance Liquid Chromatography - Histamine Assays

As previously reported (True *et al*., 2005): "Flies for histamine determinations were aged for at least 3 d prior to preparation for high performance liquid chromatography (HPLC) to ensure the completion of the critical period for lamina development (Barth *et al.*, 1997), when histamine content has stabilized (Hamilton, 2004). To determine *tan* allele function by carcinine conversion to histamine, flies were analysed after two feeding protocols. Flies were either collected from standard *Drosophila* medium and immediately frozen, or were dehydrated for 2 h prior to feeding with aqueous solutions of 4% glucose or 0.5% carcinine in glucose overnight for 16 h. These flies were collected 2 h after lights on, then rapidly frozen and stored at -80°C until assayed by HPLC. In all cases, histamine determinations were performed on groups of 20–50 isolated heads using HPLC with electrochemical detection as reported for *D. melanogaster* (Borycz *et al.*, 2000; Borycz *et al.*, 2002; Borycz *et al.*, 2005), and values are reported for the means of 3 - 12 such samples."

To determine the ability of tissue-specific Tan protein to hydrolyse carcinine to histamine we measured histamine concentration in fly heads after feeding flies an aqueous solution of carcinine in 4% glucose for 1-3 h or 16 h. Histamine accumulation was then measured in an *EGUF-hid* line which expresses Tan only in the body, but not in the eye where it would be necessary for vision. The control for this experiment was the F1 offspring of *a neoFRT 19A; EGUF-hid* cross with a fully functioning allele of *tan*. These were then compared with an eye-specific rescue tan^{1}*neoFRT19A/*tan^{1}*neoFRT19A; UAS-CG12120/+; Rh1-GAL4/+*, and w^{1118} or w^{1118},tan^{1} controls. A tan^{1}*;GMR-GAL4* driven rescue cross was also created but this was not eye-specific and drove expression in

various locations throughout the body, and thus was not used in this study. For Statistical analysis for HPLC measurements of histamine content were compared by ANOVA between groups within treatments and between treatments. A post-hoc Bonferroni correction was performed at 95% confidence between individual data sets.

For whole body measurements of histamine, flies were collected directly from standard corn meal/agarose medium and frozen. The heads were separated from frozen bodies by agitation, and heads vs bodies were processed for HPLC by the standard protocol given above.

4.3.4 TISSUE *IN SITU* HYBRIDIZATION

The complete *CG12120* cDNA was obtained from the *Drosophila* Genomics Resource Center (http://dgrc.cgb.indiana.edu/) as clone *RH41996* (barcode 17763), consisting of the 2,009-bp *CG12120* cDNA in plasmid vector *pFLC-1*. To create *in situ* probes the vector was digested with BamH1 or Xho1 (MBI Fermentas, Glen Burnie, MD, USA). Linearized DNA was purified with a GFX-PCR, DNA and gel band purification kit (Amersham Biosciences, Sweden, 27-9602-01, now GE Healthcare). Purified, linearized, vector DNA was then incubated at 37°C for 2.5 h in Digoxygenin (DIG)-conjugated UTP (Roche Applied Science, Mannheim, Germany, 1-227-073), polymerase-specific transcription buffer and either T3 (for BamH1 digested vector) or T7 (for Xho1 digested vector) polymerase (MBI Fermentas) to create DIG-labelled RNA probes. The probes were precipitated in 2.5 µl of 4.0M lithium chloride in 75 µl of prechilled 100% ethanol, chilled at -80°C for 30 min, centrifuged at 13,000 g for 15 min at 4°C, and then washed in 70 % ethanol. The dehydrated pellet was then dissolved in 100 µl of dd-RNAse free H_20, aliquoted and stored at -80°C for later use.

For *in situ* hybridization adult heads were dissected in 4% PFA in 0.1M PBS, then fixed in two 20-min washes of 4% PFA at 4°C. For cryostat sectioning, fixed heads were cryoprotected in 12% sucrose in PBS for 30 min followed by an overnight treatment in 25% sucrose/PBS at 4°C. Heads were pre-treated and embedded in Tissue-Tek OCT (Andwin Scientific, Addison IL, USA) then instantly frozen in liquid nitrogen. Horizontal sections were cut at 10 µm, collected on Superfrost Plus Gold slides (Fisher Scientific) and allowed to dry before rehydration in PBS. Sections were immediately post-fixed for 30 min at 4°C, treated with 1:500 proteinase K in PBS for 5 min, then washed twice each

for 15 min in acetylation solution followed by two 15-min washes in 5X-SSC. Tissue was prehybridized for 2 h at 58°C in hybridization solution and then hybridized in 400 ng/ml of probe in hybridization solution for ~40 h at 58°C

Hybridized tissue was then acclimated to PBS with successive washes in a decreasing concentration of sodium chloride/ sodium citrate solution (SSC) as follows: 30 min in 5X-SSC at RT, 1 h in 2X-SSC at 65°C, 30 min in 1X-SSC at 65°C, 30 min in 0.1X-SSC at 65°C, and 30 min in a 50/50 solution of 0.1X-SSC/PBS. This was followed by blocking with two 20-min washes in 1% BSA in PBS, then three 10-min washes in 0.5% blocking solution in PBS. Tissues were incubated overnight at 4°C in 1:5000 pre-adsorbed AP-conjugated sheep anti-DIG antibody (Roche Applied Science, 11 093 274 910) in 0.5% block in PBS, then washed three times each for 15 min in PBS. For DIG labelling, tissue was washed three times each for10 min in stain solution and then incubated in BM purple (Roche Diagnostics GmbH, Mannheim, Germany, 11 442 074 001) until developed. After two 5-min washes in TE, sections were mounted on slides with 90% glycerol in PBS.

All solutions for *in situ* labelling were made in Diethylpyrocarbonate (DEPC) water and are given in Appendix E.

4.3.5 CG12120::EGFP VECTOR CONSTRUCT AND EXPRESSION

A 1198bp fragment containing the complete *tan* coding region was cloned from the RH41996-containing *pFLC-1* vector by PCR using the Omniscript RT kit (Qiagen, Alameda, CA, USA) and the forward primer 5'-ATG TCG ACG AAC CCC GAA CCC ATT TTA-3' with a Sal1 restriction site (underlined) and a reverse primer 5'-TGC CGC TGA TCT ACA AGT AAC CGG TAT-3' with a BshT1 restriction site (underlined). All DNA was purified with a GFX-PCR, DNA and gel band purification kit (Amersham Biosciences). Using T4 DNA ligase (Invitrogen), the cloned fragment was directionally ligated between Sal1 and BshT1 in the MCS of the mammalian expression vector pEGFP-N1 (Clonitech, Palo Alto, CA, USA), which was treated with Calf intestinal alkaline phosphatase (CIAP; MBI Fermentas, D0428) after restriction digest. This places *tan* between the Human CytoMegaloVirus Promoter (P-CMV IE) and the enhanced GFP. Following ligation a restriction digest with Xho1 was performed to determine the correct directional placement of *tan* within the vector. All vectors were

transformed into subcloning efficient DH5α competent cells (Invitrogen) on kanamycin-selective plates, amplified in LB broth, and purified using a standard mini-prep protocol (Appendix F).

DNA was run at 85-110 V in a 1.0 - 1.2% agarose gel (Sigma) using an Owl Easycast horizontal minigel system. All PCR products and restriction digests were monitored by comparison with a GeneRuler 1kb DNA Ladder (MBI Fermentas, D0428) and after exposure to 1:770 (1.3 µl in 1 ml) SYBR Green I or GelStar nucleic acid stain (Cambrex Bio Science Rockland Inc, Rockland, ME, USA) in 1xTBE for 30 min, followed by visualization and image capture with a FisherBiotech Ultraviolet Transilluminator and digital camera or using a Gel Doc 1000 (Bio-Rad Laboratories, Hercules, CA, USA) and Molecular Analyst Software, v. 1.5 (Bio-Rad Laboratories)

The *tan-pEGFP-N1* vector was chemically transfected into mammalian COS1 cells using SuperFect transfection reagent (Qiagen) and cells were raised in kanamycin-selective DMEM. Cells were fixed in 4% PFA for 20 min, washed in 1xPBS and mounted in Vectashield (Vector Labs). *Tan-pEGFP-N1* expressing cells were visualized at 488 nm emission using a Zeiss inverted confocal microscope and LSM 510 software (Zeiss, Jena, Thüringen, Germany).

TABLE 4.1 - ANTIBODY DOCUMENTATION AND SPECIFICITY

ANTIGEN	TARGET	SEQUENCE	SPECIES	SOURCE	SPECIFICTY CHARACTERISED BY	REFERENCES
Histamine (19C)	histaminergic neurons	Histamine conjugated to succinylated keyhole limpet hemocyanin with EDCDI	rabbit	immunostar	Dot blot, Failure to label in *hdc null* flies	Panula *et al*., 1988; Nässel *et al*., 1990; Melzig *et al*., 1996
Futsch	sensory neurons	Head homogenates	mouse	DSHB (22C10: Benzer)	Failure to label in *futsch*^{K68} heads	Zipursky *et al*., 1994; Hummel *et al*., 2000
Ebony	glia	221 AAs from Gly-438 to Asp-658	rabbit	B. Hovemann	Failure to label in western blots from *In(3R)e*^{AFA} heads	Richardt *et al*., 2002
Tan	photoreceptors and other tissues	Peptide NH2-CPSETEPHCRLPLLYK-COOH	rabbit	B. Hovemann	Failure to label in *P{g1557} tan* flies	Wagner *et al*., 2007
GFP (3E6)	transgenic GFP	GFP from *Aequorea victoria*	mouse	Molecular probes/ Invitrogen	Cytological staining (by Molecular Probes) and absence of signal in flies lacking GFP expression construct (personal observation)	
DIG	DIG-tagged mRNA	Digoxygenin from *Digitalis*	sheep	Roche	Failure to label in tissue lacking DIG (Roche).	

4.4 RESULTS

Histamine production and inactivation utilizes a cycle which involves both the R1-R6 photoreceptors and the epithelial glia that surround their terminals in the lamina. To understand how *tan* functions and to establish a more accurate model for its action in the visual system, it was important to determine which cells express this gene and in particular to establish whether its protein is associated with membranes or is cytoplasmic.

4.4.1 TAN IS EXPRESSED IN THE CYTOPLASM OF PHOTORECEPTORS

In order to determine whether *tan* was expressed in the photoreceptors, glia, or both, and prior to the immunocytochemical demonstration of Tan protein expression in photoreceptors (Wagner *et al.*, 2007), tissue *in situ* hybridization was performed using a DIG-labelled anti-sense probe generated from the full-length CG12120 sequence in the RH41996 vector. The DIG-labelled sense probe was copied from a template of up to 1164 bp at the 5' end of the CG12120 gene. Although *tan* transcripts were difficult to detect using these probes, the anti-sense probe consistently gave a signal after hybridization. It labelled a region at the distal margins of the eye, at a location near the nuclei of the R1-R7 photoreceptors, cone cells, and the cell bodies of retinal pigment cells (Figure 4.1). This suggested that, provided this probe actually bound *tan* mRNA, it was doing so in the retina, not in the lamina glia. The sense probe displayed no specific labelling. *In situ* hybridization against CG12120 transcripts, as performed by our collaborators in the Hovemann lab, showed distribution of transcripts throughout the retina, and not localized solely to the distal margins of the retina (True *et al.*, 2005).

The finding that *tan* is expressed in the retina, likely in the photoreceptors, suggested an interesting mechanism for recycling in which histamine is inactivated in the glia, transferred to the photoreceptor as carcinine, and then liberated therein. This raised an additional question of whether histamine is liberated from carcinine at the plasma membrane immediately upon its entrance to the photoreceptor, within the cytoplasm, or within the vesicle. Distinction between these possibilities was determined, in part, by elucidating whether the Tan protein was associated with membranes or the cytoplasm. To do this 1200 bp of the full length *tan* transcript was fused upstream of EGFP in the pEGFP-N1 vector (Figure 4.2A). The directionality of the insert was determined by

digestion with Xho1, which cuts once in the MCS before the Sal1 insertion site of the pEGFP-N1, and once ~982 bp into the cloned *tan* gene (Figure 4.2A, B). When transfected into COS1 cells, the Tan::EGFP fusion construct was detected in both the cytoplasm and in the nucleoplasm but not in the membranes (Figure 4.2C).

4.4.2 *TAN*-LIKE P-EXCISION LINES HAVE REDUCED HEAD HISTAMINE AND IMPAIRED CONVERSION OF CARCININE TO HISTAMINE

As previously reported (True *et al*., 2005): "Flies from the four *tan*-like P excision lines (*20A*, *37C*, *42A*, and *27A*) were given either 4% glucose to drink or 4% glucose laced with 0.5% carcinine. After drinking 4% glucose, all lines except *27A* had reduced head histamine contents compared with corresponding w^{1118} control flies (Figure 4.3). The reductions were to between 0.7% (*37C*) and 7.3% (*20A*) of w^{1118} histamine levels. Line *27A* had, by contrast, 13% more head histamine than w^{1118}. After the flies drank glucose plus carcinine, the head histamine contents were much larger than in flies that drank only glucose. These differences were significant for all excision lines ($p < 0.05$, t-test). The increases were not in proportion to the original head histamine content. The accumulated histamine levels after carcinine feeding in all P excision lines were far less than for the corresponding control w^{1118} flies, in which the differences were 2.15 times greater than in the tan-like excision line *27A*. The differences between all excision alleles and w^{1118} were significant ($p < 0.001$) in carcinine-fed flies. However, there was no significant difference in head histamine contents between the excision lines *20A*, *37C*, and *42A* and flies from a control $tan^{1};w^{1118}$ double-mutant line that also drank a 0.5 % carcinine solution ($p > 0.005$). After ingesting carcinine, w^{1118} flies had a histamine head content 47 times greater than the $tan^{1};w^{1118}$ controls, confirming the defective ability of flies mutant for *tan* to liberate histamine from exogenous carcinine."

4.4.3 REVERTANT P-EXCISION LINES EXHIBIT PARTIALLY RESTORED HEAD HISTAMINE CONTENTS AND CONVERSION OF CARCININE TO HISTAMINE

As previously reported (True *et al*., 2005): "Flies from the four revertant P excision lines (*019A*, *051C*, *038B*, and *017B*) were also fed carcinine and control solutions. Control head histamine contents in flies that drank a 4.0% glucose solution were either similar to (*019A* and *051C*: $p > 0.05$) or even slightly greater than (*017B* and *038B*: $p < 0.005$) those in w^{1118} control flies (Figure 4.3). After drinking carcinine, the head histamine

increased in all revertant lines. The increases were significant compared with controls that did not drink carcinine ($p < 0.005$). Compared with w^{1118} control flies that also drank carcinine, the increases in head histamine were less, by between 16% (*019A*) and 63% (*017B*) of w^{1118} levels. The rank order in head histamine increases was roughly the same as the rank-ordered original head histamine contents in control flies before drinking carcinine. Thus, fly lines in which *tan* function was rescued most completely with respect to control head histamine content also had the largest histamine increases after drinking carcinine."

4.4.4 The Histamine Recycling Pathway in the Visual System Involves More Cells Than Just the Photoreceptors and Their Nearest-Neighbour Neuropile Glia

In order to localise histamine and Ebony more definitively to sites within the lamina, their antibody expression patterns were compared with those of newly identified *GAL4* lines which were used to drive *UAS-mCD8::GFP* expression in specific subsets of glia. A strong band of anti-Histamine immunolabelling was localised to the marginal glia at the base of the lamina and to the surface glia, as previously described (Figure 4.4). Histamine did not co-localise with mCD8::GFP in epithelial glia (Figure 4.4B), but was sometimes detected in the distal satellite glia, although this expression was weak (Figure 4.4C). Ebony, as expected, overlapped mCD8::GFP in the epithelial glia (Figure 4.5C), but also immunolabelled the proximal satellite glia. Ebony expression in the proximal satellite glia was weaker than in the epithelial glia and so it did not appear to co-localise with *R.43.H01* driven mCD8::GFP expression in these glia (Figure 4.5B), even though immunolabelling was visible immediately above the epithelial glia (Figure 4.5D) and immediately beneath the distal satellite glia (Figure 4.5A). Ebony was not detected in the marginal glia as seen by a lack of co-localisation to mCD8::GFP at the base of the lamina in both *R.10.D10* and *R.19.C02* flies.

4.4.5 Tan and Histamine Both Express in the Body

HPLC determinations of histamine in combined samples of male and female wild-type OR flies are variable but indicate that, on average, the body has 6.21 ng (±1.98, N=5) of histamine, approximately 2.5 times more than head samples (2.53 ± 0.11 ng, N=6, $p < 0.005$) that were processed simultaneously.

Given that there is so much histamine in the body, it is reasonable to question whether Tan also localised to histamine-expressing mechanosensory neurons (Buchner *et al.*, 1993), or if it was solely localised to those areas near the cuticle that are required for melanization (True *et al.*, 2005). In the thorax (Figure 4.6A, B), Tan antibody immunolabelled tissues near the cuticle but never co-localised with the neuronal marker anti-Futsch (Zipursky *et al.*, 1984; Hummel *et al.*, 2000). In the abdomen, punctuate expression of Tan was detected around the digestive system and female reproductive organs (Figure 4.6C, C', D). The strongest expression was in tissue at the posterior-most regions of the abdomen (Figure 4.6E) and in parts of the ovary, especially around individual germline cysts and in structures associated with the dorsal appendage at the anterior end of mature eggs (Figure 4.6D).

4.4.6 Tan Proteins and Histamine Liberation in the Body Both Influence Whole-Head Histamine Determinations

The wild-type fly head can have variable histamine contents but on average contains about 2 ng (Borycz *et al.*, 2000). In this study, using OR wild-type heads, an average of 2.53 ng histamine per head was obtained. Many factors, from dietary conditions (Appendix G) to genetic background, can influence head histamine, however (Borycz *et al.*, 2008). In order to determine the effect of wild-type Tan expression in the body on whole-head histamine contents we measured the ability of *tan-EGUF-hid* flies to hydrolyse histamine from fed carcinine (Figure 4.7A). Thus, whole-head histamine (in ng/head) was compared between flies which were mutant for *tan* exclusively within the eye, as seen by their lack immunolabelling with Tan antibody (Figure 4.7C, E), and *neoFRT19A-EGUF-hid* control flies which have normal Tan immunolabelling (Figure 4.7B, D). After short periods of feeding, up to 3 h, *tan-EGUF-hid* flies hydrolysed a fed solution of carcinine into histamine no less than control flies. Although measurements recorded after 1 hr showed control flies (1.11 ± 0.0005 ng/head) had more head histamine than *tan-EGUF-hid* flies (0.90 ± 0.05 ng/head; $p < 0.005$), while those recorded after 2 h of feeding showed that *tan-EGUF-hid* flies (1.98 ± 0.13 ng/head) had more head histamine than *neoFRT19A-EGUF-hid* (1.56 ± 0.1 ng/head, $p<0.005$) flies (Figure 4.7A).

As an alternative approach, flies were generated which are mutant for *tan* in the whole body but have tissue-specific rescue of this protein in just the *Rh1-GAL4* expressing R1-

R6 photoreceptors. w^{1118} was chosen as a wild-type control because this mutation is present in the background of most transgenic *Drosophila*, even though it itself has an obvious histamine phenotype (Borycz *et al.*, 2008). The double-mutant $w^{1118}tan^{1}$ served as the negative control (Figure 4.7F). Thus some flies, such as the *tan*-rescue lines have a red eye, while others have a *white* eye (as illustrated in Figure 4.7), and this provides confounding variables within our experiment. Furthermore, the *Rh1-GAL4* line, which is used to drive eye-specific rescue, has a baseline level of histamine that is greater than in wild-type OR flies (data not shown), which may contribute to the histamine phenotype in *tan* rescue flies.

In flies that were fed 4% glucose, the baseline measurements of head histamine were elevated for tan^{1}*;UAS-tan*;*Rh1-GAL4* -rescue flies (2.7 ± 0.22 ng/head). *tan-EGUF-hid* flies had less head histamine (0.81 ± 0.08 ng/head) than wild-type averages but these did not differ significantly from the w^{1118} control (0.87 ± 0.03 ng/head) nor from a *neoFRT19A-EGUF-hid* control (0.83 ± 0.13 ng/head, data not graphed). Both *tan-EGUF-hid* flies and Tan-rescue flies, as well as controls, had more head-histamine ($p < 0.001$) than the $w^{1118}tan^{1}$ mutant (0.14 ±0.05 ng/head).

After drinking an aqueous solution of 0.5% carcinine in glucose, all of w^{1118}, the rescue line tan^{1}*;UAS-tan;Rh1-GAL4*, *tan-EGUF-hid* and the alternative control *neoFRT19A-EGUF-hid* (not shown), had significant increases ($p < 0.001$) in head histamine relative to their glucose fed controls (Figure 4.7F). The eye-specific rescue line, tan^{1}*;UAS-tan;Rh1-GAL4*, could produce up to 18.74 ± 5.16 ng histamine/head. Despite having similar baseline levels of head histamine ($p > 0.05$), the w^{1118} flies had more histamine after drinking carcinine (13.51 ± 1.15 ng/head, $p < 0.001$) than did *tan-EGUF-hid* flies (7.52 ± 1.07 ng/head), suggesting that they were better able to hydrolyse histamine from carcinine. There was no significant difference between contol *neoFRT19A-EGUF-hid* (6.75 ± 0.7 ng/head) and *tan-EGUF-hid* flies. Perhaps the most telling differences however, were seen for the ratio changes of head histamine in flies after drinking glucose vs a solution of carcinine in glucose (Figure 4.7G). Control w^{1118} flies had a 15.5 times increase in measureable head histamine, greater than both tan^{1}*;UAS-tan;Rh1-GAL4* (6.9 times increase) and *tan-EGUF-hid* (9.3 times increase). The sum change in head histamine content from carcinine conversion in the body (*tan-EGUF-hid*) and the eye (tan^{1}*;UAS-tan;Rh1-GAL4*) was similar to the ratio change in head histamine for w^{1118}*,* which has wild-type expression of *tan*. Alternatively, the negative control,

w^{1118}tan^{1}, had only a 2 times increase in head histamine. The final concentration of histamine after feeding carcinine (0.29 ± 0.04 ng/head) was low enough to be accounted for by spontaneous breakdown of carcinine.

To determine where histamine was localised after its liberation by hydrolysis from carcinine, immunolabelling was performed on the heads of flies fed either 4% glucose or 0.5% carcinine in 4% glucose, identical to the feeding protocol used for HPLC analyses of head histamine (Figure 4.7H-K). Wild-type flies that consumed only glucose had histamine immunolabelling in the photoreceptors and their terminals in the lamina and medulla as well as in the fenestrated and marginal glia (Figure 4.7H). Histamine was concentrated within neurons of the ventro-lateral protocerebrum and the median protocerebrum in the central brain (Figure 4.7J), as previously reported (Nässel, 1999). After consuming a solution of 0.5% carcinine, more histamine was detected in the surface glia surrounding the CNS while antibody signal became less apparent in histaminergic neurons of both the visual system and central brain (Figure 4.7I, K).

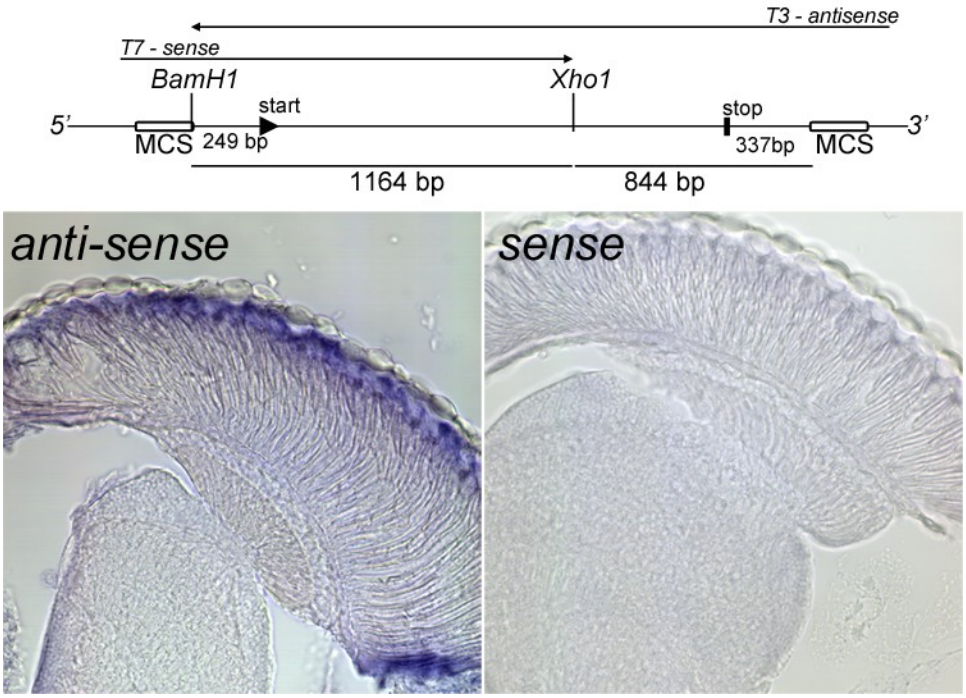

FIGURE 4.1 - *TAN* TRANSCRIPTS LOCALISE TO THE E YE BY *IN SITU* HYBRIDIZATION.

A DIG-labelled anti-sense probe to detect *tan* mRNA was generated by digesting the *RH41996* vector with *BamH1*, which lies within the MCS of *pFLC1,* at the 5'end of the full length *CG12120* gene. Digested vector was incubated with T3 polymerase to manufacture a probe of up to 2008 bp. A DIG-labelled sense probe was made from a 1164 bp fragment of the *CG12120* gene by digesting *RH41996* with *Xho1* and incubating the cut vector with T7 polymerase. The anti-sense probe detects transcripts at the surface of the retina in horizontal sections of wild-type OR heads. The control sense probe does not show significant staining.

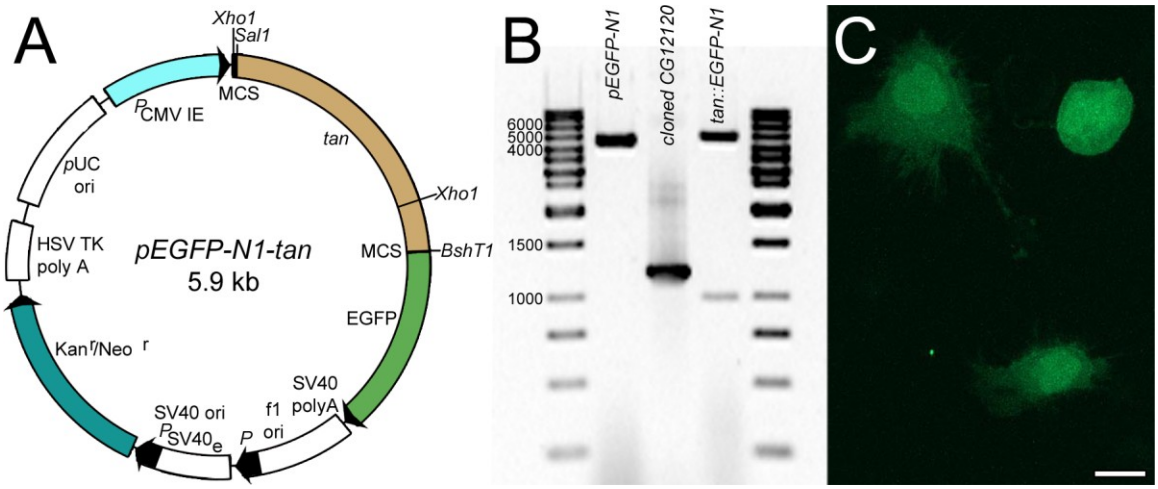

FIGURE 4.2 - TAN::EGFP IS EXPRESSED IN THE CYTOPLASM OF COS1 CELLS.

A: The full-length *tan* sequence cloned from the *CG12120* containing vector RH41996 and spliced into the pEGFP-N1 vector between Sal1 and BshT1. The directionality of insertion can be confirmed by excision with Xho1. **B**: The full-length *pEGFP-N1* vector cuts once with Xho1 in the MCS to form a single band at 4700 base pairs (lane 2). The cloned *tan* sequence (lane 3) is 1200 bp. The *tan::EGFP-N1* vector is cut twice with Xho1, once in the 1st MCS and once near the 3' end of the *tan* gene (lane 4) to generate two bands of ~982 bp and 4918 bp. The GeneRuler 1kb DNA Ladder is in lanes 1 and 5. **C**: COS1 cells transfected with *tan::EGFP-N1* express EGFP throughout the cytoplasm and in the nucleus (C). Scale bar C,10 µm.

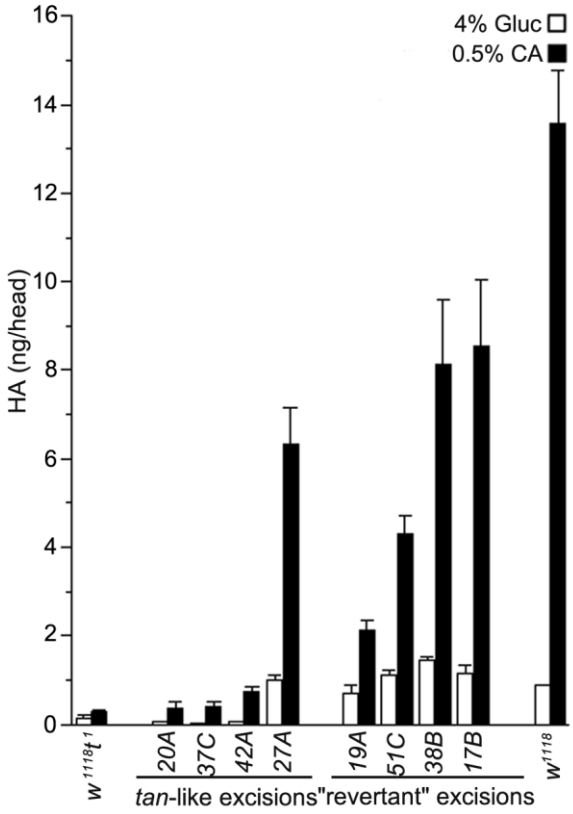

FIGURE 4.3 - HEAD HISTAMINE CONTENTS VARY IN A GRADED FASHION IN *TAN*-LIKE AND REVERTANT P-EXCISION LINES RELATIVE TO CONTROL FLIES.

Head histamine increased in all flies that drank 0.5% carcinine in 4% aqueous glucose (black bars), relative to controls that drank only 4% glucose (open bars). Revertant and *tan*-like excision lines are arranged in rank order. Note that excision line flies that drank only 4% glucose have histamine contents too small to show above the abscissa. Mean ± sem, CA fed, N= $w^{1118}t^{1}$ (3); 20A(6), 37C(12), 42A(11), 27A(10), 19A(4), 51C(6), 38B(9), 17B(8), w^{1118}(9); Glucose fed, N= $w^{1118}t^{1}$ (4), 20A(4), 37C(6), 42A(6), 27A(6), 19A(4), 51C(5), 38B(5), 17B(7), w^{1118}(8). Figure and legend from True *et al*. (2005).

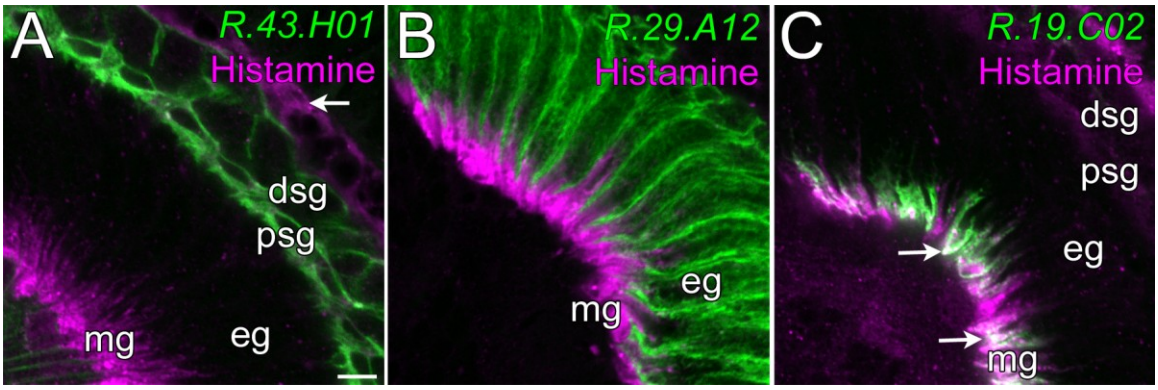

FIGURE 4.4 - HISTAMINE POOLS IN THE MARGINAL GLIA.

A: Histamine (magenta) is immunolocalised to an area immediately above the distal and proximal satellite glia, (dsg, psg; arrow in A) corresponding to the location of surface glia, and immediately above the outer chiasm giant glia, which label with mCD8::GFP (green) in *R.10.D10* flies. **B**: There is no histamine in the epithelial glia (eg) of mCD8::GFP-expressing *R.29.A12* flies, but instead the signal lies immediately below the epithelial glia. **C**: Histamine co-localises (white; arrows in C) with mCD8::GFP only to the marginal glia (mg) shown by driver line *R.19.C02*. Scale in A as in all, 5µm.

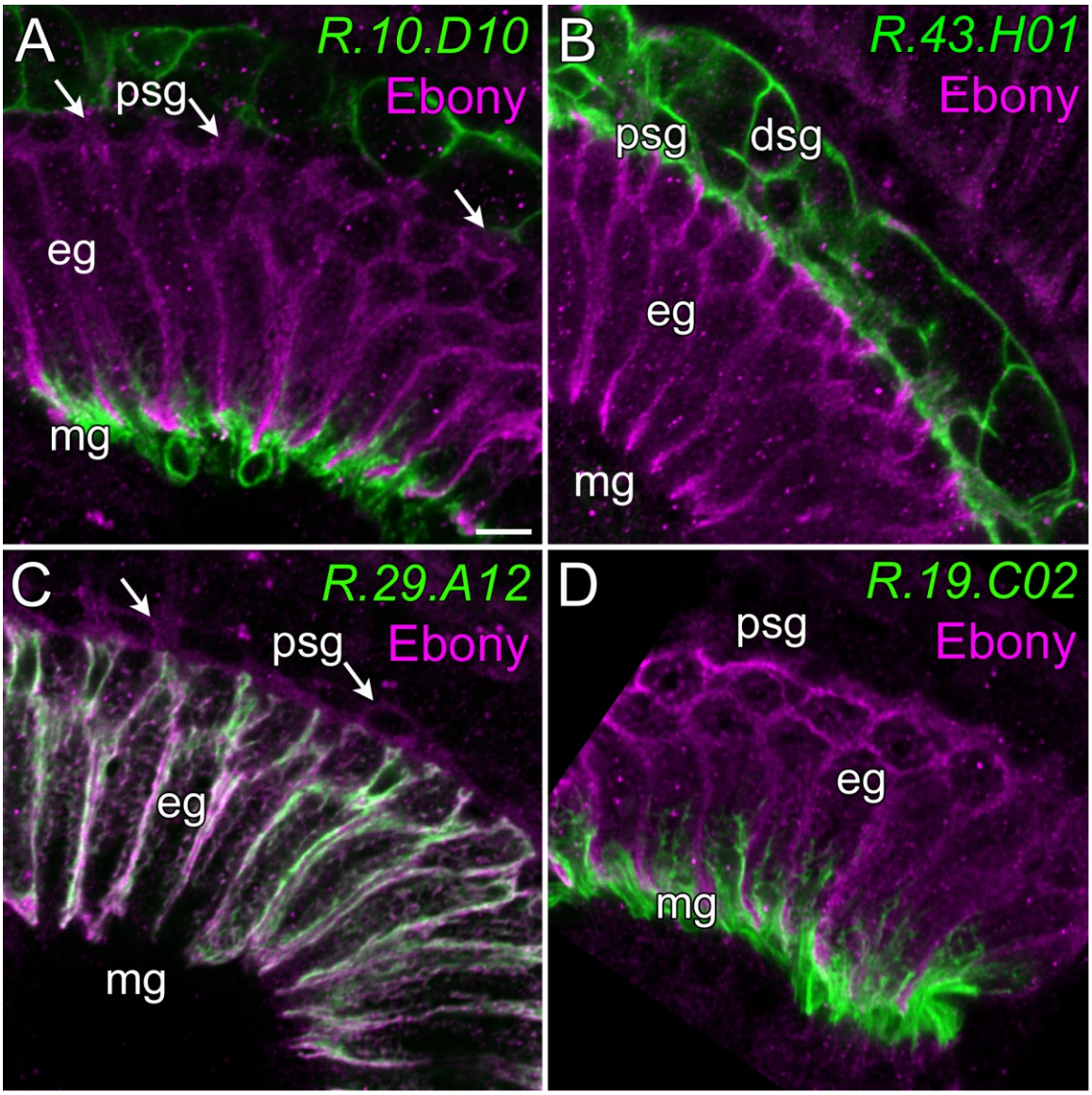

FIGURE 4.5 - EBONY IS EXPRESSED IN PROXIMAL SATELLITE AND EPITHELIAL GLIA.

A-D: Using mCD8::GFP labelling (green) to identify glia in the lamina definitively identifies Ebony immunoreactivity (magenta) in proximal satellite glia (psg; arrows in A and C) and epithelial glia (eg), but neither the distal satellite (dsg) nor marginal glia (mg). **A**: Single image views of Vibratome sliced brains viewed at 63x/1.4 show Ebony immunolabelling sandwiched between the mCD8::GFP expressing distal satellite glia and marginal glia in *R.10.D10* expressing flies. **C**: Ebony is also detected in (white), as well as just above, the epithelial glia in *R.29.A12* expressing flies. This suggests the presence of Ebony protein in the proximal satellite glia despite the fact that Ebony does not appear to co-localise to either type of GFP-expressing satellite glia in the *R.43.H01* line (**B**). **D**: Ebony does not co-localise with *R.19.C02* driven GFP-expression in marginal glia. Scale in A as in all, 5µm.

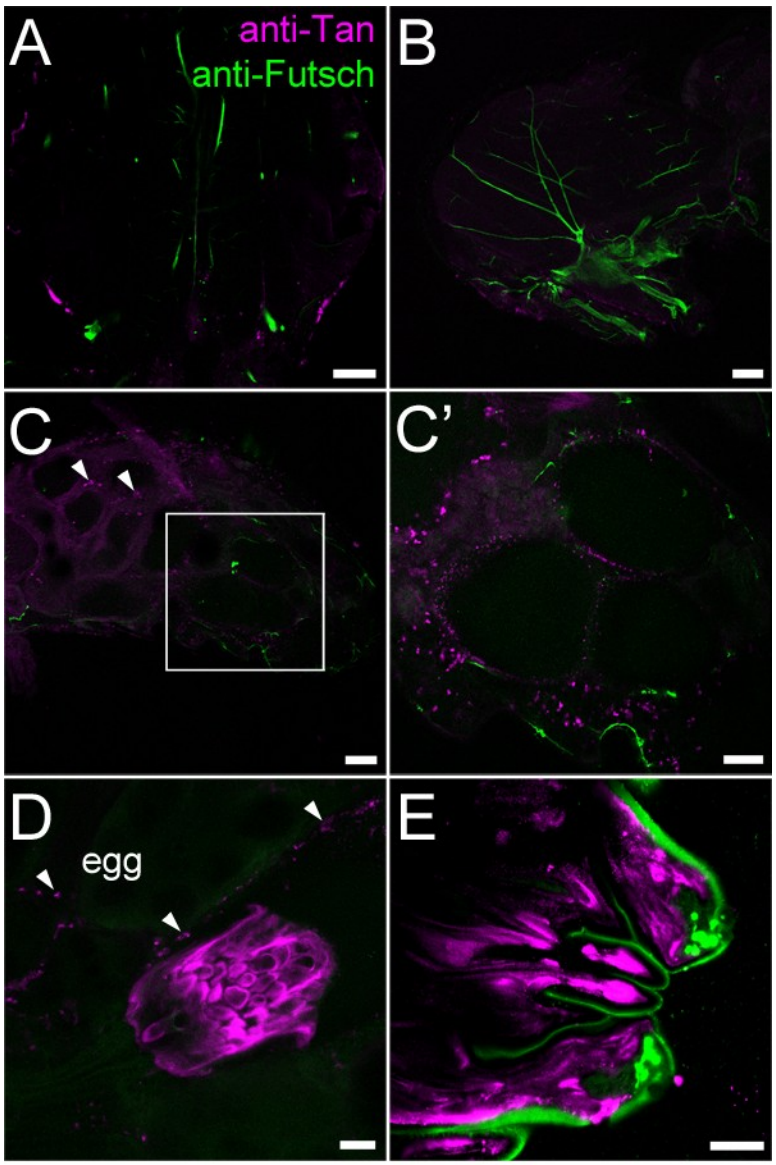

FIGURE 4.6 - TAN PROTEIN IS EXPRESSED THROUGHOUT THE BODY OF WILD-TYPE FLIES.

Double labelling with anti-Tan (magenta) and the neuronal marker anti-Futsch (green) in wild-type flies. Co-localization is absent in the thorax (A, B - 25 µm projection) or abdomen (C-E). **A-B**: In the thorax Tan is localised to areas near the cuticle in both frontal (A) and sagittal (B) sections. **C**: In a sagittal section of the abdomen, punctate expression of Tan occurs around the reproductive organs of the female (arrowheads in C, magnified in C') and surrounding the developing eggs (arrowheads in D). **D-E**: Follicle cells near the dorsal appendage of mature eggs display strong Tan immunolabelling (D, 20 µm projection), as do tissues at the distalmost region of the abdomen (E). Green fluorescence in panel E may not reflect Futsch expression, but autofluorescence in the cuticle. Scale in A - C, 100 µm; C', 50 µm; D - E, 20 µm.

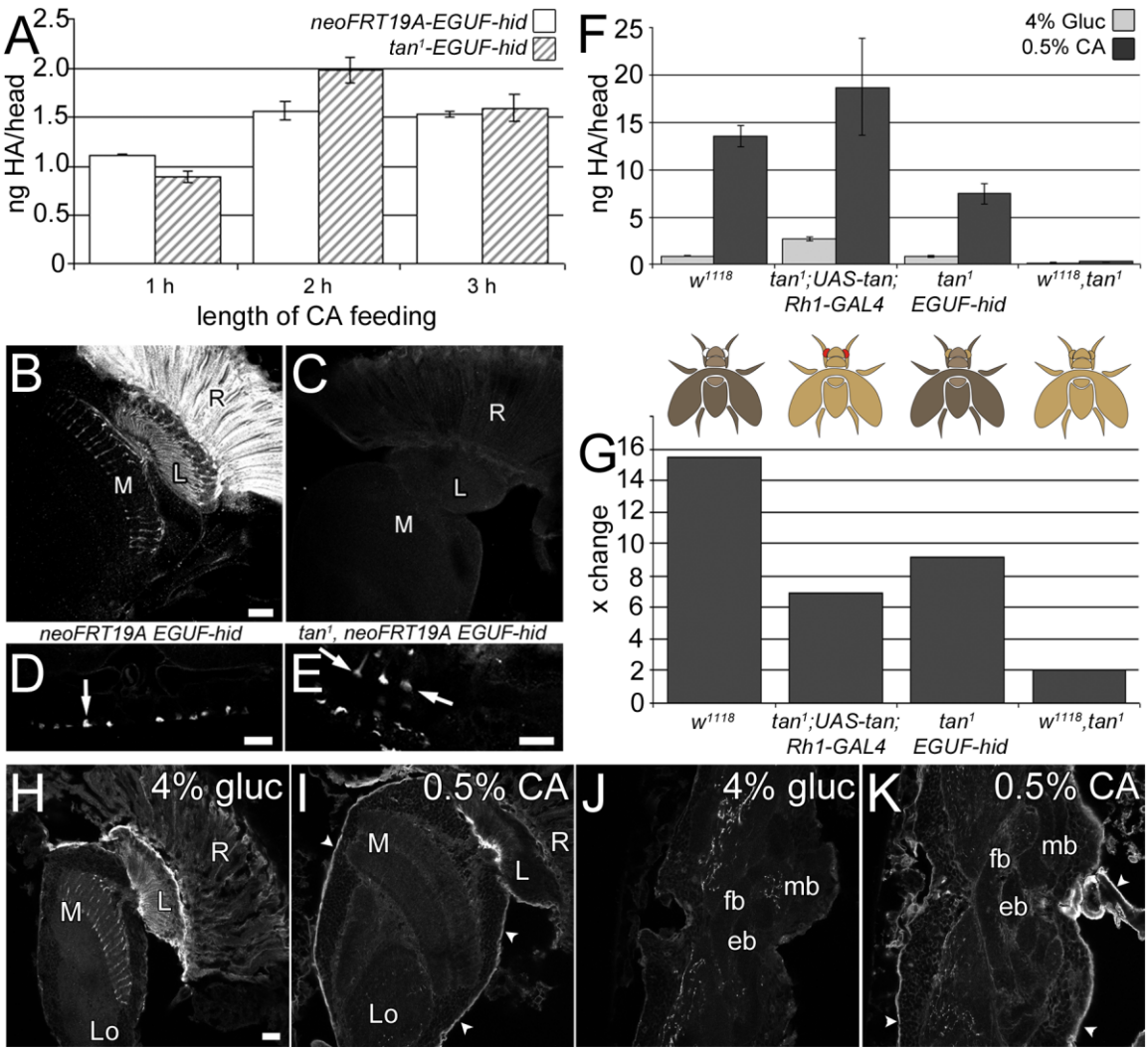

FIGURE 4.7 - TAN PROTEIN IN THE BODY CONTRIBUTES TO WHOLE-HEAD HISTAMINE MEASUREMENTS DETERMINED FROM HPLC.

A: Histamine content in the heads of control *neoFRT19A-EGUF-hid (open bars) and tan-EGUF-hid* (hatched bars) that drank a solution of 0.5% carcinine (CA) in 4% aqueous glucose for 1-3 h. **B,D**: In horizontal Vibratome sections of *neoFRT19A-EGUF-hid* fly heads, Tan is immunolocalised to photoreceptors, with cell bodies in the retina (R) and terminals in the lamina (L) and medulla (M); and near the cuticle at the posterior portion of the head (arrow in D). **C,E**: *tan-EGUF-hid* head sections lack Tan immunoreactivity in their photoreceptors but Tan expression is maintained near the cuticle (arrows in E). **F**: Histamine content in the heads of flies after drinking a solution of either 4% glucose or 0.5% carcinine (CA) in 4% glucose. Note the 10-fold difference in the scale of the ordinate relative to A. Much like the control w^{1118} fly, both tan^{1}*;UAS-tan;Rh1-GAL4* flies - which have *tan* rescue expression exclusively in the eye, and tan^{1} *EGUF-hid* flies – with wild-type expression of *tan* in the body but mutant expression in the eye, make histamine naturally (light grey bars) as well as liberate it from carcinine when they drink it (dark grey bars). The $w^{1118}tan^{1}$ control cannot liberate histamine from carcinine. Flies in which *tan* has been rescued in the eye have more 'natural' histamine in their heads than

(FIGURE 4.7 – CONTINUED, 2 OF 2)

do flies which are mutant for *tan* exclusively in the eye. The location of the *tan* mutation in mosaic animals is indicated by a colour-coded cartoon for each corresponding genotype of the fly shown in F and G. **G**: The efficiency with which a fly liberates histamine from carcinine is illustrated by the ratio of the change in the histamine content after drinking a solution of carcinine in glucose. **H-K**: Histamine immunolabelling in cryostat sections of wild-type fly heads after drinking a solution of 4% glucose or 0.5% CA in glucose. Horizontal sections through the visual system (H,I) and the central brain (J,K), at the level of the fan-shaped body (fb), ellipsoid body (eb), and mushroom bodies (mb) are illustrated. More histamine immunolabelling is found at the surface glia, surrounding the brain (arrowheads), after drinking a solution of 0.5% carcinine. Scale in all = 20 μm. Error bars represent SD.

4.5 DISCUSSION

Current models of histamine metabolism and recycling in the visual system involve the expression and action of specific genes in both the photoreceptors and their surrounding glia in the lamina or medulla (Borycz *et al.*, 2002; True *et al.*, 2005; Stuart *et al.*, 2007). One problem with these models, however, is that the visual system is assumed to be closed and histamine recycling is often considered only within the context of the R1-R6 terminals and epithelial glia of the lamina cartridge. The reason for this focus is of course because 71% of the head's total histamine content is contained in the paired, bilateral compound eyes and underlying laminas, with most (51.6%) in the eyes (Borycz *et al.*, 2005).

The full extent of histamine sources in the body is not entirely known, however. Histamine is not only a neurotransmitter for photoreceptors but also a candidate neurotransmitter in head mechanosensory neurons in flies, and has been immunolocalised to 18 cell bodies located in the ventral regions of the thoraco-abdominal ganglia, as well as in peripheral locations such as the leg nerves (Nässel *et al.*, 1990; Buchner *et al.*, 1993). Histamine also probably occurs in the standard *Drosophila* food medium, as the likely product of bacterial metabolism there (Borycz *et al.*, 2002), from which it could be taken up (Melzig *et al.*, 1998) and, thus, should also be present in the gut.

Neither whole-head histamine measurements, nor neuropile-specific measurements, take into consideration the possibility that histamine may be circulating in the haemolymph between these various sources. The possibility that histamine could be present in the circulating haemolymph was initially the subject of speculation during characterization of the Panula histamine antibody 19C, when histamine immunoreactive terminals were identified outside the blood brain barrier of *Calliphora* (Nässel *et al.*, 1990). If this possibility is correct, then endogenous sources of histamine from elsewhere in the body are likely to contribute to whole-head determinations of histamine. However, any histamine that is present in the haemolymph has restricted access to the brain because the insect brain is surrounded by a specialised sheath of surface glia that forms a blood brain barrier (Shaw, 1977; Shaw, 1978; Shaw and Henken, 1984; Bainton *et al.*, 2005; Stork *et al.*, 2008). The histamine content of the visual system has previously been measured using whole-head HPLC methods, even though histamine, as well as Ebony and Tan, are all expressed elsewhere in the body (Nässel *et al.*, 1990;

Richardt *et al.*, 2002; True *et al.*, 2005; Suh and Jackson, 2007), and thus could influence the histamine content of haemolymph in the body which also circulates through the head.

To clarify the situation we present a model of histamine recycling within the confines of the visual system and then expand this to include parameters outside the visual system.

4.5.1 HISTAMINE RECYCLING IN THE VISUAL SYSTEM

Both tissue *in situ* hybridization and antibodies against Tan peptide localise expression of *tan* expression to the photoreceptors (True *et al.*, 2005; Wagner *et al.*, 2007). Isolated Tan protein liberates histamine from carcinine *in vitro* (True *et al.*, 2005) offering confirmation for the measurements of carcinine hydrolysis analysed *in vivo* here for various *tan* mutants. The cytoplasmic localization of Tan has also been confirmed by western blots on head fractions separated by centrifugation in sucrose gradients (Wagner *et al.*, 2007), but its presence in the nucleoplasm has yet to be confirmed by centrifugation experiments.

Within the visual system, the histamine recycling pathway is dependent on the complementary expression of Ebony in the glia and Tan in the photoreceptors. Upon being taken up into the glia, histamine must immediately be converted to carcinine by Ebony (Richardt *et al.*, 2002; Richardt *et al.*, 2003), presumably accounting for the rapid appearance of ^{3}H carcinine 5 sec after head injections of ^{3}H histamine in the large fly *Sarcophaga* (Borycz *et al.*, 2002). After its synthesis, carcinine is transported out of the glia and into the photoreceptors before its conversion back into histamine by Tan. The fact that Tan is localised to the cytoplasm means that histamine is liberated by Tan somewhere between its entry into the photoreceptors and its being packaged into vesicles. Thus, the liberation of histamine from carcinine is decoupled from the process of carcinine transport into the photoreceptor, which is proposed to be regulated by the putative neurotransmitter transporter Inebriated (Gavin *et al.*, 2007), as well as both vesicle endocytosis and vesicle pumping within the terminal. These steps are part of a constant trafficking of histamine through the terminal at a rate sufficient for tonic signalling. Studies from the eye of the giant barnacle, *Balanus nubilus,* also support the conclusion that recycling of neurotransmitter is more important than *de novo* synthesis of histamine from L-histidine (Morgan *et al.*, 1999). In *Drosophila*, the dominance of the

recycling pathway may explain why *tan*^{1} mutants have significantly more capitate projections penetrating in their photoreceptor terminals than wild-type flies (Meinertzhagen and Wang, 1997). Capitate projections are sites at which Ebony-expressing epithelial glia penetrate into the Tan-expressing photoreceptors, and the endocytotic recovery of new synaptic vesicles occurs at the base and shaft of this organelle. It is because of their intimacy, and their role in vesicle recycling, that capitate projections are proposed sites of histamine recycling (Fabian-Fine *et al.*, 2003). Thus, an increase in the number of capitate projections may be seen as a compensatory reaction to the decreased availability of histamine via recycling. This possibility will require careful examination however.

4.5.2 The Quantity of Tan Protein Controls the Extent of Carcinine Hydrolysis and the Size of the ERG Transients

The *tan* "excision" and "revertant" mutants used in this study represent a graded series of Tan's action and have been analysed, using quantitative real time-PCR, for the quantity of *tan* mRNA that they express (True *et al*., 2005; Appendix H). There is a direct correlation between the amount of *tan* mRNA and the quantity of naturally occurring histamine present in the head of flies reared on cornmeal molasses medium, which we can presume indicates that if a fly transcribes more *tan* it makes more Tan protein. This then moves the balance of carcinine hydrolysis towards the production of more histamine. No direct correlation between the amount of naturally occurring histamine and the size of either the 'on' and 'off' transients of the ERG has previously been reported, but the data reported in True *et al.* (2005) indicate that when a fly's head has more histamine these transients are larger. The increased magnitude of the transients indicates, if all other factors remain unchanged, that histamine release during transmission is enhanced. This in turn would suggest that light-evoked histamine release is limited by available histamine stores in the terminals of R1-R6, supporting the importance of histamine recycling, as opposed to synthesis, in photoreceptor synaptic transmission.

As noted in the study by True *et al.* (2005), the dependence of the transients of the ERG, as measured by the Hovemann lab in Bochum, Germany, on histamine concentration, as measured in this study, differ slightly between the 'on' and 'off' transients. The 'off' transients are more sensitive to histamine content than are the 'on' transients,

supporting the hypothesis of a separable origin for these transients (Smith *et al.*, 1998; Rajaram and Nash, 2004). However, the size of the 'on' transient can be modulated by epithelial glia (Pantazis *et al.*, 2008), and so differences in the ratios of the 'on' and 'off' transients may not represent separable origin so much as they represent separable modification.

4.5.3 A Role for Multiple Glial Cell Types in the Histamine Cycle

The retina and lamina together contain 71% of the head's total measurable histamine (Borycz *et al.*, 2005), and until now the sole histamine recycling pathway that has been given serious attention in the lamina has been the Ebony/Tan shuttle operating between the epithelial glia and the R1-R6 photoreceptor terminals. However, within the visual system itself, histamine is not exclusively contained in the photoreceptors. It is also immunolocalised to the fenestrated glia which lie immediately beneath the retina (Borycz *et al.*, 2002), and to marginal glia beneath the lamina neuropile. There is little to no histamine immunosignal in the epithelial glia, presumably because any histamine at that site is immediately converted to carcinine under the action of Ebony (Borycz *et al.*, 2002). Ebony is not expressed in the marginal glia, however, which may explain, in part, why histamine can accumulate there. What is not obvious, however, is how histamine gets into marginal glia, since these glia are not associated with synapses or areas of histamine release. There are two possible explanations: first, that the marginal glia act as a sink to collect free histamine which has accumulated in the extracellular space of the lamina; or second, that excess histamine that cannot be deactivated by Ebony passes from the epithelial glia into the marginal glia. How this histamine is returned to the photoreceptors or eliminated from the visual system is currently not known.

Ebony immuno-expression in the proximal satellite glia means that these glia are equipped to deactivate histamine by conjugating it to β-alanine rather than to simply store it. Any excess histamine which diffuses through the extracellular space in a distal direction towards the eye could readily be taken up at the base of the cortex and inactivated. Transport functions for this histamine uptake are likewise not known.

The presence of histamine in the surface glial layers of the lamina, the fenestrated and pseudocartidge glia, is explained by the blood brain barrier function of these glia. When flies are fed a solution of carcinine in glucose they convert this to histamine not only in

the brain, but also in the torso. There, histamine has access to the haemolymph and can be circulated throughout the body. However, substances in the haemolymph have restricted access to the brain. Thus, flies that have drunk a solution of carcinine generate excess histamine, which then appears as an enhanced immunocytochemical signal in the surface glia surrounding the entire brain, but not necessarily to those glia that underlie the eye. In wild-type flies fed on cornmeal-molasses medium or 4% glucose, a strong band of histamine labels in what are presumably the fenestrated glia, as observed elsewhere (Borycz *et al.*, 2002). The fenestrated glia are equivalent to the perineurial glia of the blood-brain barrier and thus are likely to act as a blockade, absorbing excess histamine from the haemolymph and preventing its access to the visual system, or storing it for later use. It seems more plausible that the pathway runs in a direction from the haemolymph to the eye than assuming that histamine, released from photoreceptor terminals in the lamina, diffuses towards the eye through two-to-three layers of glia, especially given that some of these not only express histamine-inactivating Ebony, but in the housefly, at least, also form septate junctions (Saint Marie and Carlson, 1983a) that act as extracellular barriers.

4.5.4 Tan in the Body

Tan is a multifunctional protein that can act in different tissues on different substrates, for which the best known function in the body is cuticle pigmentation. Tan protein hydrolyses N-β-alanyl dopamine (NBAD), the precursor to tan coloured pigment, into dopamine, the precursor for melanin, in the epidermal cells underlying the pupal cuticle. An excess of NBAD results in the unusual pigmentation phenotype of *tan* mutants (True *et al.*, 2005). Thus, Tan protein expression in epidermal cells of the thorax and in otherwise heavily pigmented areas such as the posterior abdomen is not surprising. However, it was not known initially if Tan expression is associated with histaminergic neurons throughout the body (Nässel *et al.*, 1990; Buchner *et al.*, 1993), as it is in the visual system (Wagner *et al.*, 2007). We found that Tan does not co-localise to Futsch-expressing neurons in the CNS and PNS, but does express strongly in tissues associated with the female reproductive system. Thus, there are much more accessible sources of Tan protein in the body than in the nervous system itself, and these are not only available to hydrolyse exogenous carcinine, but are also more conveniently located to do so.

The presence of Tan in non-neural tissues near the cuticle, and throughout the abdomen, provides an explanation for why *tan-EGUF* hid flies are able to hydrolyse carcinine to histamine. They do so at a rate comparable to controls despite a lack of *tan* expression in the eye, where histamine is naturally abundant (Borycz *et al.*, 2005). This finding also serves as a cautionary reminder that model systems, such as the visual system, do not function in isolation. Standard measurements of histamine liberated from fed carcinine do not simply measure histamine in the eye, but histamine in the entire head, much of which, as shown here using *tan-EGUF-hid* mosaic flies, is liberated by Tan protein outside the eye. Whole-head measurements of histamine do not solely reflect the contents in the visual system because converted histamine is abundant in the surface glia surrounding the brain after carcinine feeding, and this histamine almost certainly comes, via the haemolymph, from non photoreceptor sources.

4.5.5 CARCININE PENETRATES THE BLOOD BRAIN BARRIER

To determine whether exogenous carcinine can penetrate the glial blood brain barrier and access to the eye we used R1-R6 photoreceptor specific *Rh1-GAL4* to drive expression of *tan* in an otherwise mutant *tan* fly. Tan-rescue flies also hydrolyse exogenous carcinine into histamine, indicating that carcinine must be taken up by glia in the blood brain barrier, transferred into the brain and ultimately hydrolysed in the photoreceptors. Head histamine under these conditions was greater than in *tan-EGUF-hid* flies and w^{1118} controls that drank carcinine, a difference that indicates that photoreceptors alone are very efficient at converting carcinine to histamine. The ratio of the change in head histamine content in flies with and without carcinine feeding is more revealing. Tan mutants, irrespective of the location of enzymatic deficiency, have less effective resources for carcinine hydrolysis than flies with no *tan* mutation, as indicated by a reduction in the fold-change in histamine contents after consuming exogenous carcinine. Thus, whole-head determinations of histamine in carcinine-fed wild-type flies appear to reflect the combined effects of hydrolysis by Tan in both the body and the visual system. Although alternative pathways for the hydrolysis of carcinine are not reported, our interpretation relies on the assumption that a fly does not use alternative pathways to compensate for the loss of gene function when this is procured by genetic means in specific cells. The interpretation of our results in is, moreover, complicated by the presence of w^{1118} in the background of some of the flies examined and by our

utilization of w^{1118} and w^{1118}, tan^{1} as controls. The ATP-binding cassette (ABC) transporter mutants *white* and its binding partners, *brown* and *scarlet,* all have reduced head contents of the biogenic amines histamine, dopamine and serotonin. Furthermore, the mutant w^{1118} ameliorates the effects of *tan* on whole-head histamine, presumably by limiting the transport of histamine into the epithelial glia and reducing the efficiency of histamine recycling (Borycz *et al.*, 2008). As these various genetic effects accumulate, they make it difficult to compare flies with complex genotypes, because more than one variable effects changes in histamine concentration.

4.5.6 CONCLUSION

Here we have shown that Tan protein in the eye hydrolyses carcinine to liberate histamine, but that factors extrinsic to the visual system affect histamine concentration, and thus may affect the interpretation of results from carcinine feeding experiments. As an example, the glia of the blood brain barrier act to impede the influx of histamine into the brain, and thus "whole-head" determinations of histamine reflects histamine which lies not only inside the brain, but also in the surface glia, and in the haemolymph. Thus, such determinations need not directly reflect histamine concentration in the visual system. Model systems, such as the histamine recycling pathway of the *Drosophila* visual system, are treated as simplified systems that operate in isolation and that we can use as a test bed to assay gene or protein function. In fact, results presented in this study indicate that the visual system does not function in isolation. Further progress will require reduction of the number of factors extrinsic to the visual system that come into play when analysing visual system function.

4.6 ACKNOWLEDGEMENTS

This work was supported by a National Institutes of Health Grant EY-03592 (I.A.M.). The antibody 22C10, developed by Seymour Benzer, was obtained from the Developmental Studies Hybridoma Bank (University of Iowa, Iowa City, IA). *R.29.A12*, *R.43.H01*, *R.10.D10*, *R.19.C02* were provided by Dr. Gerald Rubin and Aljoscha Nern (HHMI, Janelia Farm, Chevy Chase MD, USA), *20A*, *37C*, *27A, 42A, 19A*, *17B*, *38B*, *51C* and *UAS-CG12120* were provided by Dr. John True (NYU Stony Brook, Stony Brook NY, USA). All other stocks were provided by the Bloomington Stock Center. The P-EGFP-

N1 vector was a generous donation from the lab of Dr. Vett Lloyd (Dalhousie University, Halifax, NS) and COS1 was provided by Dr. Tom MacRae (Dalhousie University, Halifax, NS). I would like to thank Dr. William MacDonald and Dr. Andrew Haigh for their assistance and advice with cloning, *in situ*, and PCR techniques and Tanya Villeneuve for assistance with cell culture techniques. I am also especially grateful to Dr. Janusz Borycz, Jacek Panek and Dorota Tarnogorska for their assistance with HPLC techniques, to Dr. Jola Borycz for advice on Histamine and Ebony immunolabelling and to Jane Anne Horne for her assistance with statistical analysis.

4.7 TRANSITION TO CHAPTER FIVE

The termination of transmitter action at the synaptic cleft is as essential a function as the speed of neurotransmitter release, because only when transmitter is cleared can the next signal be transmitted. At photoreceptor synapses of the fly, terminating the action of histamine is an important determinant of the temporal frequency of visual signalling. Uptake of neurotransmitter generally occurs by means of uptake transporters, but mechanisms for the termination of histamine action are not reported at histaminergic synapses, and no such transporter specific for histamine is known. The mechanisms by which histamine, β-alanine and their subsequent conjugate, carcinine, are shuttled between the photoreceptors and the glia remains a mystery. In the following chapter I examine three classes of gene for their potential as a candidate transporter. These include the organic cation transporters - *orct1* and *2*, the gap junction subunit innexins – *inx1* and *inx*2, and the uncharacterised gene *no on nor off transient C*.

CHAPTER 5

CANDIDATE TRANSPORTERS OF HISTAMINE, CARCININE AND β-ALANINE: ABSENCE OF EVIDENCE IS NOT EVIDENCE FOR ABSENCE

5.1 ABSTRACT

Vision is an essential sensory modality in the life of the flying insect. In order to function properly the eye must not only be correctly wired to interneurons in the brain, but it must also release vast amounts of neurotransmitter from its photoreceptors and have a means to recycle this neurotransmitter efficiently. *Drosophila melanogaster* releases histamine at the photoreceptor synapse and recycles this neurotransmitter through the epithelial glia using the reciprocal action of two proteins, Tan and Ebony. An inert metabolite, carcinine is produced by Ebony in the glia and must be transported back into the photoreceptor for the liberation of histamine by Tan. This beautifully models the efficiency of fly photoreceptor physiology, yet it lacks one thing – a means by which histamine and its associate metabolites are transported into, and out of, the neurons and glia involved in the recycling pathway. In this study I examine three types of genes for their candidacy, in some role, as a transporter in the histamine recycling pathway: *organic cation transporters* (*orct1* and *orct2*), *innexins* (*1* and *2*) and *no 'on' or 'off' transient C* (*nonC*). *orct1* and *2* are expressed throughout the cortex of the CNS, and *orct1* can be localised to both glia and neurons in cortical regions throughout the brain, but its widespread expression makes it unlikely to be exclusive to the histamine recycling pathway. The Innexin proteins are localised to the lamina optic neuropile. Innexin2 is expressed in the epithelial glia and other non-identified cells in the lamina. Innexin1 was more difficult to localise but may be expressed in the photoreceptors. Neither Innexin has been shown to act as a hemichannel for osmotic transport of histamine metabolites, however. The gene that codes for the mutant allele *nonC* has a number of visual system phenotypes. Further analysis of these phenotypes hinges on localisation of this mutation to the corresponding gene on the X chromosome, and so deficiency mapping was utilized in an attempt to isolate the gene that codes for *nonC.*

5.2 INTRODUCTION

Histamine is a ubiquitous aminergic messenger that is well recognized for triggering an inflammatory response in the mammalian immune system (Siraganian, 1983; Schneider *et al.*, 2002). However, its actions are much more widespread. Histamine, by its aminergic nature, also acts as a neurotransmitter in a wide variety of species, both vertebrate and invertebrate (Schwartz *et al.*, 1980; Hardie, 1987; Panula *et al.*, 1989; Buchner *et al.*, 1993; Nässel, 1999; Burns *et al.*, 2003; Stuart *et al.*, 2007). In

Drosophila, as in other arthropods, histamine is the principal neurotransmitter released at the photoreceptor (Hardie, 1987; Sarthy, 1991). It is present throughout the brain and thoracic ganglia (Nässel *et al.*, 1990; Pollack and Hofbauer, 1991; Nässel, 1999) and in *Drosophila* is also utilized as a mechanosensory neurotransmitter (Buchner *et al.*, 1993).

In fly photoreceptors, histamine is synthesized from L-histidine by the enzyme Histidine decarboxylase (Burg *et al.*, 1993; Melzig *et al.*, 1996). Once released from the synapse, histamine is recycled through a pathway which involves reciprocal inactivation of the neurotransmitter by Ebony in the epithelial glia to produce a β-alanyl-histamine conjugate called carcinine, and the subsequent dissociation of histamine from β-alanine by Tan in the photoreceptors (Borycz *et al.*, 2002; Richardt *et al.*, 2002; Richardt *et al.*, 2003; True *et al.*, 2005; Wagner *et al.*, 2007). Consequently, a system of transporters is predicted to allow histamine and β-alanine to move into the glia, as well as the movement of carcinine into, and β-alanine out of, the photoreceptors.

In general, neurotransmitter transporters clear neurotransmitter from the extracellular space after its regulated release at the synapse (Torres *et al.*, 2003; Blakely *et al.*, 2005). Transmembrane transporters are found either in the neuron that releases neurotransmitter (Demchyshyn *et al.*, 1994; Pörzgen *et al.*, 2001; Gainetdinov and Caron, 2003; Hasegawa *et al.*, 2006), or in the surrounding glia (Rival *et al.*, 2004; Rival *et al.*, 2006; Eulenburg and Gomeza, 2010; Eulenburg *et al.*, 2010) from where they take up neurotransmitter, clearing it from the extracellular space and thus maintaining low baseline concentrations of these signalling molecules. Any mutation that affects neurotransmitter transporters at the plasma membrane can be expected to affect clearance of its neurotransmitter from the synaptic cleft and thereby to affect behaviour (Gainetdinov *et al.*, 2002; Gainetdinov and Caron, 2003; Grosjean *et al.*, 2008) and, ultimately, survival.

Many unique types of transporter proteins have been characterised in invertebrates. *Drosophila* alone contains at least 49 genes predicted to encode neurotransmitter and/or amino acid transporters/permeases (Romero-Calderón *et al.*, 2007). The potential candidates for histamine transport have been narrowed down on the basis of what we already know about histamine transport in the lateral ocellus of another invertebrate species, the barnacle *Balanus amphitrite*. In both the larval and adult barnacle, photoreceptors utilize a Na^+ dependant transporter to take up radioactive histamine, but not serotonin or GABA, from the extracellular environment (Stuart *et al.*, 1996; Stuart *et*

al., 2002). Furthermore, the ability of both larval and adult photoreceptors to take up histamine is blocked by the action of the antagonists chlorpromazine and phenoxybenzamine, both of which block aminergic transport (Stuart *et al.*, 1996; Stuart *et al.*, 2002). Taken together this suggests that a histamine–specific transporter is expressed in the lateral eyes of the barnacle.

There are many types of Na^+ dependent transporters in *Drosophila*, some of the best characterised of which are members of the solute-linked carrier (SLC) family, and these are classified into two groups: SLC1 and SLC6. Most SLC transporters use electrochemical gradients of sodium, chloride or potassium to drive transport of neurotransmitters and amino acids across the plasma membrane and into the cytosol (Masson *et al.*, 1999; Chen *et al.*, 2004), thus making them likely candidates for the transport of histamine or carcinine.

The SLC1 family of Na^+/K^+ dependant transporters includes the excitatory amino acid transporters (EAATs) which are responsible for glutamate and aspartate transport (Neckameyer and Cooper, 1998; Seal *et al.*, 1998; Besson *et al.*, 2000). A mutation in EAAT results in an excess of glutamate which has neurotoxic effects, both in *Drosophila* (Rival *et al.*, 2004) and in mammals (Mbungu *et al.*, 1995; Seal and Amara, 1999).

Twenty-one SLC6 family genes have been identified in *Drosophila* (Thimgan *et al.*, 2006), many of which have been localised to the CNS. The SLC6 transporters are subdivided into multiple classes including, but not limited to: 1) the Na^+ /Cl^- dependant monoamine transporter group which transport serotonin (SerT; Corey *et al.*, 1994; Neckameyer, 1998), dopamine (DAT; Pörzgen *et al.*, 2001), and GABA (GAT; Neckameyer and Cooper, 1998) back into the presynaptic neuron; 2) the “orphan” amino acid transporters, represented in *Drosophila* by *inebriated* (Burg *et al.*, 1996; Soehnge *et al.*, 1996) and *bloated tubules* (Johnson *et al.*, 1999); and 3) the nutrient amino acid transporters such as DmNAT1 and Lithium-inducible SLC6 transporter (*list*; Thimgan *et al.*, 2006; Miller *et al.*, 2008; Kasuya *et al.*, 2009). Yet, of all the SLC family transmitters described, only *inebriated* has been linked to the histamine recycling pathway (Gavin *et al.*, 2007), even though, as explained later, the evidence for *inebriate*’s role in histamine recycling is not definitive.

Another well-described class of transporters are the vesicular neurotransmitter transporters which, in general, are localised to the synaptic vesicles into which they shuttle neurotransmitter (Daniels *et al.*, 2006; Fei *et al.*, 2007; Grygoruk *et al.*, 2010).

Vesicular GABA transporters (vGATs) are responsible for the storage of GABA and its transport into the vesicle (Fei *et al.*, 2010), while *Drosophila* vesicular glutamate transporter (dVGLUT) pumps glutamate (Daniels *et al.*, 2004; Daniels *et al.*, 2006; Mahr and Aberle, 2006). Vesicular monoamine transporters (vMATs), in particular DVMAT-A, transports all of dopamine, serotonin, octopamine, tyramine, and histamine (Greer *et al.*, 2005). Yet, none of these vesicular transporters is expressed in the photoreceptors or the neuropile glia (Kolodziejczyk *et al.*, 2008), and thus they are unlikely to be candidate transporters for any of histamine, carcinine or β-alanine in the recycling pathway. Despite the seeming incongruity in their function, vMATs have been linked to histamine uptake and are localised to cells within both the *Drosophila* lamina and medulla (Romero-Calderón *et al.*, 2008). DVMAT-A is expressed in dopaminergic and serotinergic neurons, modulating behaviours as varied as grooming, locomotion and sexual activity, yet despite expression in the optic lobes, it has no apparent association with histaminergic neurons (Chang *et al.*, 2005). An alternatively spliced variant of the gene, DVMAT-B is expressed in the fenestrated glia of the *Drosophila* lamina (Romero-Calderón *et al.*, 2008). Here, DVMAT-B is likely to be expressed within the glial plasma membrane, since it is associated with the plasma membrane in *Drosophila* S2 cell culture (Greer *et al.*, 2005). Consistent with a role in pumping histamine, mutants of $vMAT^{\Delta 14A}$ show a reduction in both DVMAT-B and head histamine immunolabelling, especially in the fenestrated glia (Romero-Calderón *et al.*, 2008). Considering that fenestrated glia are isolated from the lamina neuropile it is most likely that they are not involved in direct recycling but are instead involved in the recovery of histamine and other substances from the haemolymph.

So far, only two transporters are definitively known to affect the histamine recycling pathway, but their means of action in this system have not yet been fully elucidated. These are the ABC transporter White, and the Na^+/Cl^- dependant transporter Inebriated. Mutants of the gene *white* have reduced contents of histamine in the head, whereas *tan* mutants have an excess of carcinine (Borycz *et al.*, 2002) because they cannot liberate histamine in the photoreceptor (True *et al.*, 2005; Wagner *et al.*, 2007). Yet, when combined, the *white,tan* double mutant fails to produce carcinine (Borycz *et al.*, 2008). White is immunolocalised to the glia, and this, combined with the absecnce of carcinine in *white,tan* mutants, implies that histamine, once released from synaptic vesicles at the photoreceptor synapse, does not have access to the carcinine producing enzyme, Ebony, in the glia (Borycz *et al.*, 2008). It is not known whether White acts in

conjunction with other ABC transporters, if it acts alone, or if it is simply required for homeostatic regulation in epithelial glia which otherwise affects the function of neighbouring transporters.

In the second case, *inebriated* functions in both the photoreceptors and glia, and has been proposed to act as the carcinine transporter in the photoreceptors (Gavin *et al.*, 2007). Inebriated has three separable phenotypes of the electroretinogram (ERG), a reduction of the 'on' and 'off' transients, a hyperpolarization response, and an oscillation in the photoreceptor's sustained negative response, which is triggered when a photoreceptor is depolarized by a light flash (Burg *et al.*, 1996). Ebony's action, and hence the production of carcinine, is required for *inebriated* mutants to have an oscillation in the sustained negative response of the ERG (Gavin *et al.*, 2007). Furthermore, it has been found that an excess of carcinine mimics the ERG phenotype of *inebriated* mutants, specifically the abnormal oscillations that appear during the retinal response to a light flash. However, the severity of the oscillations after carcinine ingestion is nowhere near as severe as those seen in the ine^2 mutant, and even then, oscillations appear in only 35% of the wild-type animals tested. Given these findings Gavin *et al.* (2007) suggest that uncleared carcinine acts on some synaptic receptor to cause the oscillation phenotype, an unresolved hypothesis.

There are many reasons why Inebriated is likely not a transporter for carcinine. First, Inebriated has not been shown to transport carcinine either *in vivo* or *in vitro*. Second, its expression is too widespread, implying a more generalized physiological function, as indicated by its hyperexcitability phenotype (Stern and Ganetzky, 1992; Huang and Stern, 2002). Carcinine is relatively limited in the brain and is not clearly detectable by HPLC in head homogenates from wild-type samples (Borycz *et al*., 2002). Inebriated, on the other hand, is expressed throughout the CNS (Chiu *et al.*, 2000; Huang *et al.*, 2002), as well as in the eyes (Burg *et al.*, 1996), at the neuromuscular junction (Huang *et al.*, 2002; Huang and Stern, 2002), in the gut and malphigian tubules (Romero-Calderón *et al.*, 2007), in the embryo (Soehnge *et al.*, 1996), and is even important in the development of perineurial glia in the PNS (Yager *et al.*, 2001). It is more likely that Inebriated functions, as reported, by negatively regulating neuronal sodium channels (Huang and Stern, 2002), and this alone would affect ionic gradients across the membrane and the function of many other transporters that may exist nearby.

5.2.1 UNLIKELY TRANSPORTER CANDIDATES

A screen for all known transporter genes described in the *Drosophila* genome has failed to yield a transporter which expresses (by *in situ* hybridisation) in locations surrounding histaminergic neurons or in histaminergic neurons themselves (Thingam, 2006). It is thus possible that proteins not traditionally thought of as neurotransmitter or amine transporters could play some role in the movement of histamine and its inert conjugate, carcinine, between photoreceptors and glia in the lamina cortex. It is because of this that we have chosen to investigate a number of unconventional genes, and the possibility that these may play a role in histamine/carcinine transport. I have attempted to localise *Drosophila organic cation transporter* (*orct*) expression, as well as the expression patterns of two gap junction proteins, Innexin1 and Innexin2. I have also examined the effect that eye-specific mutants for these gap junction genes have on head histamine content. Finally, I attempted to determine which gene on the X chromosome corresponds to "*no on or off transient C*" (*nonC*), which has a histamine and ERG phenotype (Heisenberg, 1979; Stephenson and Pak, 1980; Meinertzhagen *et al.*, 2000).

5.2.1.1 ORGANIC CATION TRANSPORTERS

Of the candidates described above, the genes deemed most likely to play a role in histamine and/or carcinine transport are the organic cation transporter-like genes *orct1* (*CG6331*) and *orct2* (*calderón*). The mammalian organic cation transporters (OCTs) transport carnitine, a product of fatty acid metabolism (Bremer, 1983) and, when expressed in cultured cells or *Xenopus* oocytes, the OCTs transport monoamine neurotransmitters such as histamine, dopamine, serotonin, and epinephrine as well (Enomoto *et al.*, 2002; Amphoux *et al.*, 2006; Ogasawara *et al.*, 2006). Mammalian OCT-3 is also thought to function as a histamine transporter *in vivo*, since mice mutant for this gene display a significant increase in the histamine contents of their spleen (Ogasawara *et al.*, 2006).

The *Drosophila orct1* gene is alternatively spliced to code for two forms: a large protein with 12 transmembrane-spanning domains and a smaller protein with 6 transmembrane spanning domains (Taylor *et al.*, 1997). Transcripts from *orct1* have been localised to all cells of the *Drosophila* embryonic midline primordium (Kearney *et al.*, 2004), but not much else is known about its pattern of expression or its role in the fruit fly. A similar

Drosophila organic cation transporter gene, *orct2* (*calderón*), encodes a downstream effector of the insulin receptor pathway and is required for the normal growth of larval tissues (Herranz *et al.*, 2006).

5.2.1.2 *NONC*

In order to better understand the role that *nonC* plays in visual system function, and to determine if it may code for a transporter, I set out to localise and characterise the *nonC* gene using complementation mapping and standard ERG recording techniques.

The *nonC* gene was first identified in a screen for mutants that affect the ERG (Heisenberg, 1979). Among its known phenotypes are a loss of transients of the ERG (Heisenberg and Götz, 1975; Pak, 1975), impaired optomotor response, reduced spatial resolution, reduced fixation in flight (Heisenberg and Götz, 1975), and impaired fixation in a Y-maze (as alleles X37, X61, X72; Bülthoff, 1982). Previous work from the Meinertzhagen lab identified an excess of histamine in the heads of *nonC* flies, approximately 2.5 times more than the histamine content of wild-type OR fly heads (Meinertzhagen *et al.*, 2000), thus implicating a possible role for *nonC* in the histamine cycle. *nonC* mutants not only have altered histamine contents but they also have smaller photoreceptor terminals with fewer vesicles and a lower vesicle packing density than wild-type CantonS flies. As a result of an increased histamine content and reduced vesicle pool, the distribution of histamine within the optic neuropiles and even between the vesicles and cytoplasm is altered (J.A. Borycz, unpublished data.). Furthermore, $nonC^{P37}$ flies have altered numbers of capitate projections compared with Canton S flies (M. Shimohigashi and Meinertzhagen, unpublished data), and show lethality when crossed with deficiency lines in the 11A region of the X chromosome (M. Loubani, unpublished data).

5.2.1.3 INNEXINS

In the vertebrate retina, glycine is able to move from rod amacrine cells, the source of its synthesis, to nearby cone bipolar cells, which store the glycine (Vaney *et al.*, 1998). The transfer does not occur by high-affinity uptake but by means of gap junctions. The chief evidence is that glycine replenishment in bipolar cells is reduced by the connexon blocker carbenoxolone (Vaney *et al.*, 1998). Also in the retina, a negative feedback

pathway from horizontal cells to cones is mediated by hemichannels. At this synapse, connexin26 forms hemichannels on horizontal cell dendrites near the glutamate release site of the cones (Pottek *et al.*, 2003), and blocking these hemichannels with carbenoxolone abolishes feedback mediated responses (Kamermans *et al.*, 2001). These data suggest that a current flows through the hemichannels to modulate the output of the cones (Kamermans *et al.*, 2001). This wholly counter-intuitive idea requires that the neurons leak current constantly, but also suggests an alternative to the reuptake of histamine from fly photorececptors by high-affinity transporters.

In *Drosophila, innexins* code for gap junction proteins (Phelan, 2005), the invertebrate functional equivalent to vertebrate connexins. Each gap junction consists of a hemichannel unit of six subunits on one cell, associated with a hemichannel in a neighbouring cell, and together these form a channel through which small molecules can pass. We considered the possibility that invertebrate innexins, like their vertebrate counterparts the connexins and pannexins (Vaney *et al.*, 1998; Kamermans *et al.*, 2001; Pottek *et al.*, 2003; Ye *et al.*, 2003; Parpura *et al.*, 2004; Zoidl *et al.*, 2004; Iglesias *et al.*, 2009; Scemes *et al.*, 2009), may act in the fly lamina as hemichannels to allow the passage of histamine or carcinine through the cell membrane, and thus mediate the shuttle between photoreceptor terminals and epithelial glia.

In order to be considered as a potential histamine transporter candidate in the visual system, innexins must fulfill at least three criteria: 1) they must be expressed in the visual system, specifically the photoreceptor cell terminals and/or the epithelial glia; 2) mutations of these genes must affect histamine recycling thus altering synaptic function at the photoreceptor synapse; and 3) they must allow transport of molecules at least as large as the histamine or carcinine.

There are eight innexin genes in *Drosophila*: *inx1* (also known as *optic ganglion reduced*, *ogre*), *inx2*, *inx3*, *inx4* (also known as *zero population growth*, *zpg*), *inx5*, *inx6*, *inx7*, and *Shaking B* (*shakB*, also known as *passover*, *pas*). Of these, only *ogre*, *inx*^{2}, *inx3* and *shakB* are expressed in the visual system. Transcripts for *ogre, inx2* and *inx3* have been localised to the lamina of the developing pupa using tissue *in situ* hybridization (Stebbings *et al.*, 2002), and both *shakB* and *ogre* mutant flies have abnormalities in their ERGs (Curtin *et al.*, 2002b). *ShakB* is expressed in the photoreceptors (Stebbings *et al.*, 2002) and in the lamina, presumably at photoreceptor terminals, as visualized with an antibody against ShakB (reported in Shimohigashi and

Meinertzhagen, 1998; Phelan *et al.*, 1996). There is also a reduction in the number of close membrane appositions in TEM preparations of *ShakB* mutant brains (Shimohigashi and Meinertzhagen, 1998) and from its developmental expression profile (Stebbings *et al.*, 2002). While *ogre* appears to be expressed in the glia during development (Stebbings *et al.*, 2002), expression of an *ogre-promoter-GAL4* driver implies that *ogre* is also expressed in some photoreceptors in the adult (Curtin *et al.*, 2002b). Furthermore, a photoreceptor specific mutation of the gene results in an abnormal ERG, suggesting that *ogre* must also be present in the photoreceptors, although the ERG is only partially rescued by expressing *ogre* in all neurons using *ELAV-GAL4* (Curtin *et al.*, 2002b). The possibility that *ogre* expresses in both photoreceptors and glia is intriguing even though this protein does not form functional channels with itself, at least not in a *Xenopus* oocyte expression system (Phelan and Starich, 2001). It is interesting because, in *Musca,* gap junctions have been described which lie at the heads of capitate projections (Chi and Carlson, 1981), which form between photoreceptors and epithelial glia and which are proposed sites of neurotransmitter recovery (Fabian-Fine *et al.*, 2003). However any gap junctions that form there could also be between a combination of Ogre/Inx1 and Inx2 or Inx2 and Inx3, which interact to form functional heteromeric channels (Stebbings *et al.*, 2000; Keane *et al.*, 2009), and are appropriately located in the visual system (Stebbings *et al.*, 2002).

The fact that *innexins* are expressed in the visual system, and mutations of at least two of these genes results in altered transmission at the photoreceptor synapse, fulfills two of our criteria required for a potential histamine and/or carcinine transporter.

In order to assess the candidacy of the preceding genes as players in the histamine/carcinine/β-alanine recycling pathway I first determined where these genes are expressed in the visual system and then whether they have any effect on the histamine content of the head.

5.3 METHODS

5.3.1 FLY STRAINS

Deficiency and P-element lines were crossed to $nonC^{P37}$ for complementation analysis of the $nonC^{P37}$ ERG phenotype. The *nonC* alleles: $nonC^{P37}$, $nonC^{mc45\pi}$, $nonC^{mc47\pi}$, and

nonC$^{mc46\pi}$ were generous donations of Dr. W. Pak (Purdue University, West Lafayette, Indiana, USA). All deficiency lines were obtained from the Bloomington *Drosophila* stock center and additional details for these lines are described in Table 1. P-element stocks for genes in the 6D3-6E2 region included (CG4547, BL# 18418) *w*^{1118} *PBac{WH}Atx-1*^{f01201}, (*CG3044*, BL#18540) *w*^{1118} *PBac{WH}Cht11*^{f02328}, (*CG14434,* BL#16645) *y*^{1}*w*^{67c23}*P{EPgy2}CG14434*^{EY05245}, *CG4557*^{c03783}*, CG4558*^{c03129}*, CG12796*^{c02956}, *CG14435*^{f07374}*, CG3044*^{c03148}, *CG33692*^{f00206}, all originally from the Exelixis collection at Harvard Medical School. An excision mutation in the gene *pod1* (BL#8750, *w* pod* $^{\Delta 96}$ *P{neoFRT19A/FM6, w**) was also tested for failure to complement *nonC.*

For eye-specific mutational analysis using *EGUF-hid* the following lines were utilized: *P{w[+mC]=GMR-hid}SS1, y[1] w[*] P{ry[+t7.2]=neoFRT}19A; P{w[+m*]=GAL4-ey.H}SS5, P{w[+mC]=UAS-FLP1.D}JD2* (BL#5248), *P{neoFRT}19A; ry*^{506} (BL#1709), *inx2 neoFRT19A/FM7c* generated from an uncharacterised mutant allele, *w*^{1118} *P{w[+mGT]=GT1}inx2*^{BG02429}/FM7c (BL#12834), and *ogre neoFRT19A/Binsn* (from K. Curtin). The expression lines *w*^{1118}*,P{GAL4}repo/TM3, Sb*^{1} (BL#7415) and *GMR-GAL4* (BL#9146) were crossed with *yw,UAS-mCD8::GFP;Pin*^{YT}*/CyO* to visualize the glia and photoreceptors respectively. OR (BL#5) was used for all tissue *in situ* hybridization experiments.

5.3.2 GENERATION OF PROBES FOR *IN SITU* HYBRIDIZATION

The complete *orct1* cDNA was obtained from the *Drosophila* Genomics Resource Center (http://dgrc.cgb.indiana.edu/) as clone *GH21655*, consisting of the full length 2,564-bp *CG6331* (*orct1*) cDNA in plasmid vector *pOT2*. An *in situ* probe could not be generated using the Sp6 polymerase in the *pOT2* vector and so a 1845 bp fragment of the *orct1* cDNA was digested out of pOT2 and directionally ligated into *pBluescriptII-SK*$^{-}$. To do this both the *pBluescriptII-SK*$^{-}$ and *GH21655* were separately double-digested using EcoR1 and Xho1 restriction enzymes (MBI Fermentas, Glen Burnie, MD, USA). Digested *orct1* DNA was run at 80V on a 1% agarose gel (Sigma, St. Louis, MO, USA) using an Owl Easycast horizontal minigel system, for 2h 20min in order to carefully separate the 1845 bp and 1666 bp bands. The 1845 bp fragment from the 3' end of the *orct1* gene (bp719-2564), which corresponds to the N terminus of the protein, was isolated and purified with a GFX-PCR, DNA and gel band purification kit (Amersham Biosciences, Sweden, 27-9602-01, now GE Healthcare).

Digested *pBluescriptII-SK*$^{-}$ was dephosphorylated with CIAP (MBI Fermentas) and then the 1845 bp *orct1* DNA was ligated into *pBluescriptII-SK*$^{-}$ overnight at 22°C using T4 DNA ligase (MBI Fermentas) and a 13:1 ratio of insert to vector DNA. Vector was transfected into subcloning efficient DH5α competent cells (Invitrogen, Carlsbad, CA, USA), screened on ampicillin containing plates, amplified, miniprepped and then digested with Kpn1 (MBI Fermentas) for analysis. The transfection and miniprep protocols are described in Appendices I and F, respectively.

To generate sense and anti-sense probes *pBluescriptII-SK*$^{-}$ *orct1*$^{719\text{-}2564}$ was digested with Xho1 at the 3' or EcoR1 at the 5' end. Purified, linearized, vector DNA was then incubated at 37°C for 2.5 h in Digoxygenin (DIG)-conjugated UTP (Roche Applied Science, Mannheim, Germany, 1-227-073), polymerase-specific transcription buffer and either T7 (for Xho1 digested vector) or T3 (for EcoR1 digested vector) polymerase (MBI Fermentas) to generate DIG labelled RNA probes. The probes were precipitated in 2.5 µl of 4.0M lithium chloride in 75 µl of prechilled 100% ethanol, chilled at -80°C for 30 min, centrifuged at 13,000 g for 15 min at 4°C, and then washed in 70 % ethanol. The dehydrated pellet was then dissolved in 100 µl of double-distilled RNAse free H_20, aliquoted and stored at -80°C for later use.

This 1845 bp probe contains sequences that are found in both splice variants of the gene, coding for proteins with either 12 or 6 membrane-spanning domains (Taylor *et al.*, 1997). To generate an anti-sense probe which detects ~ 442 bp from the 3' end of the gene corresponding to the N-terminus of the long protein, *pBluescriptII-SK*$^{-}$ *orct1*$^{719\text{-}2564}$ was digested with BglII (MBI Fermentas) and incubated with T3 polymerase, buffer and DIG-UTP.

The *orct2* (*calderón*) gene was obtained from the *Drosophila* Genomics Resource Center as a full-length 2242 bp sequence, *SD08138*, in the *pOT2* vector. To generate a probe, the *SD08138*-containing vector was digested using EcoR1, which cuts at bp 139 and 2141 of the *orct2* sequence. The 2002 bp, *orct2*-containing fragment was isolated from the agarose gel and purified with a GFX-PCR, DNA and gel band purification kit (Amersham Biosciences). The insert vector *pBluescriptII-SK*$^{-}$ was similarly digested with EcoR1, dephosphorylated with CIAP and purified in a GFX column. A 5:1 ratio concentration of *orct2* fragment DNA was ligated into *pBluescriptII-SK*$^{-}$ using T4 DNA ligase. Vector DNA was screened and amplified as described above and direction of the insert analysed by digestion with BamH1 (MBI Fermentas). To generate sense and anti-

sense probes *pBluescriptII-SK- orct2*$^{13\text{-}2141}$ was digested with AgeI/BshT1 (MBI Fermentas). Purified, linearized, vector DNA was then incubated at 37°C for 2.5 h in DIG-conjugated UTP, polymerase-specific transcription buffer and either T3 (sense probe) or T7 (anti-sense probe). Isolation of the probes is as described above.

All vector ligations and restriction digests were monitored by comparison with a GeneRuler 1kb DNA Ladder (MBI Fermentas, D0428) or Invitrogen 1kb DNA ladder (Invitrogen) and after exposure to 1:500 - 1:1000 GelStar nucleic acid stain (Cambrex Bio Science Rockland Inc, Rockland, ME, USA) in 1xTBE for 30 min, followed by visualization and image capture with a Fisher Biotech Ultraviolet Transilluminator and digital camera.

5.3.3 *IN SITU* HYBRIDIZATION

Heads were removed in 0.1M PB and fixed on ice for 2-4 h in 4% formaldehyde (from paraformaldehyde, PFA) in 0.01M PBS. After an overnight wash in 0.01M PBS at 4°C, heads were embedded in 7% agarose and sectioned at 100 µm along the horizontal plane. Head slices were collected in PBS, post-fixed for 40 min in 4% PFA and washed twice in PBS for 10 min each. The following *in situ* protocol is based partially on the methods of Thimgan *et al.* (2006). After two 5 min washes in double-strength sodium chloride and sodium citrate (2x SSC; pH = 4.5), brain slices were incubated for 40 min in tris-glycine buffer and then, in order to remove melted agarose from the solution, tissue was incubated in three changes of pre-hybridization solution warmed to 65°C. Tissue was placed in pre-hybridization/blocking solution containing salmon sperm DNA for 15 min at 23°C before being incubated with sense and anti-sense probes in hybridization buffer overnight at 65°C. To remove the probes tissue slices were washed three times for 20 min in 5x SSC at 23°C. Tissue was then washed once in solution B for 40 min at 60°C, then washed again in solution B which was pre-warmed to 60°C at then allowed to cool to 23°C for 30 min, followed by a final 30 min wash in solution B at 60°C. After two 30 min washes in 2x SSC at 23°C, tissue was placed in a blocking solution of 1x BM-block (Boehringer Mannheim) in 1x Maleic Acid buffer (MAB) for 1 hr. For anti-DIG immunolabelling, tissues were incubated overnight at 4°C in 1:5000 pre-adsorbed alkaline phosphatase (AP)-conjugated sheep anti-DIG antibody (Roche Applied Science, Mannheim, Germany, 11 093 274 910). After four 10-min washes in 1xTBS, one 20-min wash in 1xTBS and a single 10-min wash in tris/ TW/ levamisole stain buffer, AP-labelled

tissues were allowed to react overnight at 4°C in 20 µl of 50xBM-NBT-BCIP solution in 1 ml of stain buffer. After two 5-min washes in Tris and EDTA (TE) buffer, sections were mounted on slides with 90% glycerol in PBS.

All solutions for *in situ* labelling were made in Diethylpyrocarbonate (DEPC) water and are listed in Appendix E.

5.3.4 IMMUNOCYTOCHEMISTRY

For standard immunocytochemistry the heads of adult flies were fixed in a solution of 4% PFA in 0.1 M phosphate buffer (PB) for 4 h or overnight at 4°C. Whole adult heads were washed in 0.1 M PB, mounted in 7% agarose, and sliced in the horizontal plane at 80-100 µm thickness by means of a Vibratome 1000. Sectioned brains were permeabilized in successive treatments of 0.2% and 2% Triton X (Tx) in 0.01 M PBS and then blocked with 5% normal goat serum (NGS) in 0.2% PBS-Tx. Tissues were incubated 48 h at 4°C in primary antibody diluted in 5% NGS-PBS-Tx. The following primary antibodies were used: 1: 50 rabbit anti-Innexin2, 1:50 rabbit anti-Innexin1 (Bauer *et al.*, 2003; Bauer *et al.*, 2004) from Michael Koch (Universität Bonn, Bonn, Germany). After six washes in 0.2% PBS-Tx, tissues were incubated overnight in 1:400 goat anti-rabbit Cy3 (Jackson ImmunoResearch Inc: West Grove, PA, USA). Tissues were washed at least six times in 0.01M PBS before being mounted in Vectashield medium (Vector Labs, Burlingame, CA, USA) and images were captured using a LSM 410 confocal microscope and associated software (Zeiss, Jena, Thüringen, Germany).

For double *in situ*-hybridization/anti-Repo immunolabelling, the *in situ* protocol was as described above until the addition of primary antibodies (Table 5.2). Brain slices were incubated overnight at 4°C in a solution of 1:5000 AP-conjugated sheep anti-DIG antibody and 1:25 mouse anti-repo (8D12, DHSB) in 1xBM block. Post-immunolabelling washes are as described above. After a 10 min incubation in stain buffer, AP-labelled tissues were allowed to react overnight at 4°C in 20 µl of 50xBM-NBT-BCIP solution in 1 ml of stain buffer. The AP reaction was stopped by washing in 0.01M PBS, followed by five 10-min washes in 0.2% Tx in 0.01M PBS. For fluorescent immunolabelling of the anti-Repo antibody AP stained tissue slices were incubated overnight at 4°C in 1:400 goat anti-mouse Cy3 (Jackson ImmunoResearch Inc: West Grove, PA, USA) in 1xBM block-PBS-Tx. Tissues were washed six times in 0.01M PBS before being mounted in

Vectashield medium (Vector Labs) and images were captured using a LSM 510 confocal microscope and associated software (Zeiss).

5.3.5 ELECTROPHYSIOLOGY

Flies were first immobilised on ice and then secured in the cut end of a 10 µl pipette tip using clear nail polish. A silver reference electrode was placed in the abdomen while a 1.2 mm glass and silver recording electrode filled with *Drosophila* Ringer was placed just under the surface of the cornea. For each fly a series of three recordings were measured and averaged using Advance P 3.61g software. Flies were exposed to a series of 30 ms light pulses, one pulse per second for 10 seconds, from a blue light emitting diode (LEDtronics type BP120CWPB2K-300) attached to a Grass SD9 stimulator set at 3.5 volts. Each 10 pulse series was separated by a 5 second dark interval.

5.3.6 HIGH PERFORMANCE LIQUID CHROMATOGRAPHY

Flies for histamine determinations were either collected from standard *Drosophila* medium and immediately frozen (for *nonC* screens), or were dehydrated for 2 h prior to being given aqueous solutions of 4% glucose with or without 0.5% carcinine to drink overnight for 16 h (for *innexin EGUF-hid* lines). Collected flies were rapidly frozen and stored at -80°C until assayed by HPLC. In all cases, histamine determinations were performed on groups of 20–50 isolated heads using HPLC with electrochemical detection as reported for *D. melanogaster* (Borycz *et al.*, 2000; Borycz *et al.*, 2002), and values are reported for the means of three to ten such samples.

TABLE 5.1 - A COMPLETE LIST OF ALL X-CHROMOSOME DEFICIENCY LINES USED FOR *nonC* COMPLEMENTATION ANALYSIS OF THE ERG PHENOTYPE.

STOCK #	GENOTYPE	LOCATION
945*	Df(1)C149/FM6	5A8-5C5
8949*	Df(1)ED6802, w^{1118} P{w[+mW.Scer\FRT.hs3]=3'.RS5+3.3'}ED6802/FM7h	5A12-5D1
7711	Df(1)Exel6237, w^{1118} P{w[+mC]=XP-U}Exel6237/FM7c	5C2-5C6
946	Df(1)N73/FM6	5C2-5D6
5281	Df(1)dx81, w*/Dp(1;Y)dx^{+}1/C(1)M5	5C3-6C3/12
8032	Df(1)ED418, w^{1118} P{w[+mW.Scer\FRT.hs3]=3'.RS5+3.3'}ED418/FM7j, B^{1}	5C7-5E4
8947*	Df(1)ED6829, w^{1118} P{w[+mW.Scer\FRT.hs3]=3'.RS5+3.3'}ED6829/FM7h	5C7-5F3
1665	Df(1)5D, y^{1}/FM6	5D1-5E
7712	Df(1)Exel6238, w^{1118} P{w[+mC]=XP-U}Exel6238/FM7c	5D3-5E4
579	Df(1)JF5, f^{1} car^{1}/FM7a	5E5-5E8
7713	Df(1)Exel6239, w^{1118} P{w[+mC]=XP-U}Exel6239/FM7c	5F2-6B1
9212*	Df(1)ED6849, w^{1118} P{3'.RS5+3.3'}ED6849/FM7h	5F3-6D3
7714	Df(1)Exel6240, w^{1118} P{w[+mC]=XP-U}Exel6240/FM7c	6B2-6C4
6605	Df(1)6C-40, w^{1118} /FM6, w^{1}	6C4-5
3196*	Df(1)Sxl-bt, y^{1}/Binsinscy	6E2-7A6
3221*	Df(1)ct4b1, y^{1}/Binsn	7B2-7C4
949*	Df(1)C128/FM6	7D1-7D5
950*	Df(1)RA2/FM7c	7D18-8A4
951*	Df(1)KA14/FM7c	7F1-8C6
6893	Df(1)Sp8A/FM7c	8A1-8A3
6001	Df(1)m13, $Gs2^{m13}$/FM7a, w^{+}	10B10-11A4/5
960	Df(1)KA6/FM7c	10E1-11A8
963	Df(1)KA10, sn^{3} m^{1}/FM7c	11A1-11A8
5371	Df(1)RC29, w*/FM7c, P{ry[+t7.2]=ftz/lacC}YH1	11A1-11A4/5

*locations of deficiencies marked by * are illustrated in Figure 5.7*

TABLE 5.2 - ANTIBODY DOCUMENTATION AND SPECIFICITY

TARGET	SEQUENCE	SPECIES	SOURCE	SPECIFICITY CHARACTERISED BY	REFERENCES
Innexin1	AAs 348–362 of Innexin1: FAKQVEPSKHDRAK conjugated to KLH via a N-terminal cysteine.	rabbit	M. Hoch	Immunoblots of ovary extracts have a weak band at the calculated molecular mass of 46 kDa, and two additional stronger bands at 43 and 41 kDa	Bauer *et al*., 2004; Bohrmann and Zimmermann 2008
Innexin2	AAs 297–310 of Innexin2: KLRHLLLRARSRLA conjugated to KLH via a N-terminal cysteine.	rabbit	M. Hoch	In western blots the antibody recognized a 43-kDa protein band from *in vitro* translated protein and from embryonic extracts. Failed to label in *inx* ^{kropf} mutant embryos	Bauer *et al*., 2004
Repo	AAs 218-612 of *Drosophila* Repo protein	mouse	DSHB (8D12:, Goodman)	Detects Repo transgene expression. Similar labelling as *repo-LacZ* reporter genes, other antibodies and *in situ* probes that target *repo* gene products	Alfonso and Jones, 2002; Lee and Jones, 2005; Xiong *et al*., 1994; Halter *et al*., 1995
DIG	DIG-tagged mRNA	Digoxygenin from *Digitalis*	sheep	Failure to label in tissue lacking DIG (Roche).	

5.4 RESULTS

5.4.1 *ORCT1* AND *ORCT2* TRANSCRIPTS ARE EXPRESSED IN CELLS THROUGHOUT THE BRAIN'S CORTEX

In order to determine the expression pattern of o*rct1* in the adult brain, DIG labelled anti-sense probes to *orct1* mRNA were generated against a sequence from the 3' end of the gene. The full length *orct1* cDNA was obtained as *GH21655* in the plasmid vector *pOT2*. However, no anti-sense probe could be generated using the SP6 polymerase in this vector. As a result, it was necessary to transfer part of the *orct1* gene into the *pBluescriptII-SK*$^{-}$ vector, which has T3 and T7 polymerase promoters.

Both the full length *orct1* gene in pOT2 vector and the *pBluescriptII-SK*$^{-}$ vector were double-digested with Xho1 and EcoR1. A 1845bp fragment containing the *orct1* gene was isolated and ligated into *pBluescriptII-SK*$^{-}$ (Figure 5.1A, B). The structure of the vector and the direction of the *orct1* insert dictate that an anti-sense probe is generated from EcoR1 digested vector transcribed by T3 polymerase (Figure 5.1C). Both sense and anti-sense probes of approximately 1845bp were detected below the linearized 4.8 kb *pBluescriptII-SK*$^{-}$ template when run in agarose gel (Figure 5.1D). A small anti-sense probe against 442 bp at the 3' end of *orct1* DNA was generated by digestion with BglII and transcription with T3 polymerase (Figure 5.1G).

The 1845bp anti-sense probe bound to transcripts throughout the cortex of the brain including the cortices of the lamina, medulla, and lobula complex in the optic lobe, as well as within the cortex of central brain regions, particularly near the antennal lobe and at posterior regions of the protocerebrum (Figure 5.1E). Strong expression of *orct1* transcripts was also detected in the retina, in areas corresponding to photoreceptor cell bodies and support cells, which appeared as a ring around the centrally located, and unstained, rhabdomeres (Figure 5.1F). No specific labelling was detected after incubating with the sense probe (Figure 5.1E inset). The 442bp anti-sense probe labelled tissues in a pattern very similar to that of the 1845bp anti-sense probe. Cells were labelled throughout the cortex; however, there was weaker labelling in the retina and specific labelling of large cells in both optic chiasmata, corresponding to the location of the outer and inner chiasm giant glia (Figure 5.1H).

Cortical regions of the brain contain the cell bodies of both neurons and a specific subtype of glia called cortex glia. To determine if *orct1* was expressed in glia, and particularly glia in the lamina, anti-Repo immunolabelling was performed on *orct1* hybridized tissues (Figure 5.2). Frontal (Figure 5.2A) and horizontal (Figure 5.2B) slices of adult *Drosophila* brains revealed the general distribution of *orct1* hybridization and anti-Repo labelling. Glial cells that co-label with nuclear anti-Repo and *orct1* were detected near the ocelli at dorsal regions of the brain (Figure 5.2C and inset), possibly surrounding the tract of the antennal nerve (Figure 5.2D-D" and insets), in the medulla (Figure 5.2E and inset) and in the lamina (Figure 5.2F and inset). The *orct1*-expressing glial cells in the lamina lie in a position corresponding to the distal satellite glia.

To analyse the *orct2* expression pattern this gene was also ligated into the *pBluescriptII-SK*$^{-}$ to generate an anti-sense probe. A 3' fragment of the *orct2* gene was digested from the *SD08138* cDNA using EcoR1 and then ligated at the EcoR1 site into the multiple cloning site (MCS) of the *pBluescriptII-SK*$^{-}$ vector (Figure 5.3A). Digestion with BamH1 produced two bands of 3219 and 1745 bp, indicating that the *orct2* gene fragment was inserted into the vector in a 3' to 5' orientation (Figure 5.3A, B). An anti-sense probe directed towards approximately 450 bp from the 3' end of the gene was produced from BshT1 digested *pBluescriptII-SK*$^{-}$ *orct2*$^{13\text{-}2141}$ vector (Figure 5.3C, D). The anti-sense probe labelled cells throughout the cortex (Figure 5.3E), in a pattern highly similar to that of *orct1 in situ* hybridization (Figure 5.1). It differed, however, by having reduced labelling in the photoreceptors. Incubation with the sense probe did not result in a detectable pattern of labelling (Figure 5.3F).

5.4.2 Innexin1 and Innexin2 Proteins are Detected in the Lamina

The production of antibodies against Innexins 1 and 2 (Bauer *et al.*, 2003; Bauer *et al.*, 2004) allowed localisation of these gap junction proteins within the lamina. The antibody for Innexin1 (encoded by the gene *ogre*) displayed inconsistent immunolabelling with our standard protocol. Innexin1 appeared to label the retina (Figure 5.4A) and even to co-localise to cells with *GMR-GAL4* driven *UAS-mCD8::GFP* in the distal regions of the retina, near the R1-R6 photoreceptor nuclei (Figure 5.4B). However, Innexin1 expression was difficult to localise more specifically. When Innexin1 was immunolabelled in flies expressing *UAS-mCD8::GFP* under the control of the glial specific *Repo-GAL4* driver, expression did not co-localise with GFP (Figure 5.4C, E) but

instead lay between the profiles of epithelial glia in both longitudinal sections (Figure 5.4C) and ensheathed by epithelial glia in cross section (Figure 5.4E). From this expression pattern, Innexin1 could be assumed to express in the R1-R6 photoreceptor terminals. Despite this, Innexin1 failed to co-localise with GFP when immunolabelled in flies expressing *UAS-mCD8::GFP* under the control of *GMR-GAL4*, which expresses in the photoreceptors (Figure 5.4D, F). In these flies, Innexin1 appeared within the 'ring' of photoreceptor terminals, suggesting that expression occurred in at least one of the monopolar neurons.

Innexin2 immunolabelling was more consistent and displayed punctate expression in distinct neuropiles or cortices throughout the brain (Figure 5.5). The overall distribution of Innexin2 immunolabelling in the adult brain, including its relatively strong expression in the lamina neuropile (Figure 5.5A, B), was visualized in slices along a frontal plane that provided lamina profiles cut in both longitudinal and cross sections. Innexin2 was detected in the serpentine layer of the medulla as well as below the medulla neuropile and throughout the deutocerebrum, in areas surrounding the olfactory centres such as the calyx of the mushroom body complex (Figure 5.5B). Within the lamina, Innexin2 partially co-localised with glial-specific, *Repo*-driven mCD8::GFP in both longitudinal (Figure 5.5D) and cross sections of the neuropile (Figure 5.5E). The antibody did not co-localise with *GMR-GAL4*-driven GFP in the photoreceptors (Figure 5.5F). Innexin2 antibody clearly labelled cells other than the epithelial glia. Based on its pattern of immunolabelling in cross section, as punctuate spots surrounding the inner edge of the cartridge glial sheath, it is possible that Innexin2 was also expressed in amacrine neurons (for the structure and organisation of amacrine cells see: Meinertzhagen and O'Neil, 1991 and Kolodziejczyk *et al.*, 2008) or the basket endings of the T1 neurons (Rister *et al.*, 2007; Hamanaka and Meinertzhagen, 2010).

Using an indirect immunofluorescent protocol is not ideal for localising epitopes in the eye because pigments in the retinas autofluoresce (Wilson and Jacobson, 1977), and neither Innexin protein was definitively localised to the adult photoreceptors in this study. Eye-specific mutations of *inx1* and *inx2*, however, both had abnormally structured retinas, suggesting that Innexins 1 and 2 are expressed in the retina at some point during development. Those with *inx1-EGUF-hid* had variegated pale retinas, while those with *inx2-EGUF-hid* had retinas that were severely reduced and lacked pigment (Appendix J). Control *neoFRT19A-EGUF-hid* flies also had small retinas. Head

histamine contents were reduced in flies with eye-specific mutations of *innexin1* (*inx1-EGUF-hid*, 0.64 ng/head ± 0.08; p>0.05) or *innexin2* (*inx2-EGUF-hid*, 0.36 ng/head ± 0.05; p<0.005), when compared with corresponding controls (*neoFRT19A-EGUF-hid*, 0.95 ng/head ± 0.17; Figure 5.5C). Only *inx2-EGUF-hid* flies had a significant reduction in head histamine contents, which may be due to their severe reduction in retina size. All flies could metabolize a solution of carcinine into histamine after consumption, but only *inx1-EGUF-hid* had histamine contents (11.17 ng/head ± 0.62; p<0.005) that were significantly greater than the control (7.99 ng/head ± 1.54). These findings indicate that retinal *inx1* somehow affects the hydrolysis of carcinine and liberation of histamine, but do not reveal by what means.

5.4.3 Deficiency Mapping of *nonC* on the X Chromosome: Narrowing the Field

A mutation in the uncharacterised gene *nonC* has a few easily characterised visual system phenotypes, including a loss of the 'on' and 'off' transients of the ERG and an increase in head histamine content when compared with the wild-type (Heisenberg, 1979; Stephenson and Pak, 1980; Meinertzhagen *et al.*, 2000). These phenotypes were used to screen for deletions on the X-chromosome (Figure 5.6A) and for genes with P-element insertions that fail to complement *nonC*.

The mutation which resulted in the *nonC* phenotype had been previously characterised as lying within cytological location 6A1-6E on the X-chromosome (A.A. Long, pers. comm.), but previous analyses from the Meinertzhagen lab had indicated lethality when $nonC^{P37}$ flies were crossed with deficiencies in the 11A4-11A7 region of the X-chromosome (M. Loubani, unpublished data), so that these offspring could not be screened to determine if their ERG or head histamine content deviated from the wild-type. Other *nonC* alleles (*Mc45π, Mc46π*, *Mc47π*) were screened to determine if they had a similar phenotype to $nonC^{P37}$. Of these, only $nonC^{Mc45\pi}$ had both an excess of head histamine (7.43 ± 0.96 ng/head, N=3), comparable to but greater than $nonC^{P37}$ (4.45 ± 0.38 ng/head, N=6) and greater than wild-type OR flies (2.59 ± 0.31 ng/head, N=10), as well as a complete loss of transients in the ERG (Figure 5.6B, C). When $nonC^{Mc45\pi}$ was crossed to flies with deficiencies in the 11A region of the X chromosome, *Df(1)KA6/FM7c* and *Df(1)KA10,* sn^3m^1*/FM7c*, the offspring not only survived but also displayed both 'on' and 'off' transients in their ERGs (data not shown). However, when screened for histamine content the heads of *Df(1)KA10,* $sn^3m^1/nonC^{Mc45\pi}$ flies had a

marked reduction in histamine content (0.88 ng/head, N=2), although these data were not compared statistically with histamine content in *nonC*$^{Mc45\pi}$ fly heads because only two samples were determined.

A number of other deficiencies between cytological locations 5A to 8A were tested against *nonC*^{P37} for a failure to complement the ERG phenotype. Deficiencies that cover large areas of the X chromosome and small areas which have not yet been tested are illustrated in Figure 5.6A. All of the deficiencies tested, including small deficiencies not shown in Figure 5.6, are described in detail in Table 5.1. Both 'on' and 'off' transients were present in the ERG of at least three trials for all combinations of *nonC*^{P37}/deficiency offspring tested. Thus, the mutation that causes the *nonC* phenotype does not lie within any of the cytological locations tested. Regions of the X chromosome between 5A and 8A that were not tested for complementation with *nonC* thus remain as candidate locations for this gene. These include regions 6D3-6E2, 7A6-7B2, 7C4-7D1 and 7D5-7D18 though most of the genes in these areas can now be eliminated from contention through the availability of new deficiency lines. The genes that lie within these non-tested regions are listed in Table 5.3.

Since no deficiency lines were available which covered the genes in cytological location 6D3-6E2, uncharacterised P-element lines that were available at the time were screened for the presence of transients[7]. These included *pod1*, a*taxin1* (*CG4547*), *CG12796*^{c02956}, *CG14435*^{f07374}*, CG4557*^{c03783}*, CG3044*^{c03148}, *CG4558*^{c03129}*, CG14434, and CG33692*^{f00206}. Female flies for each line had their ERGs analyzed and all had detectable 'on' and/or 'off' transients. Only *pod1, ataxin1*, *CG3044*^{c03148}, and *CG14434* were tested for non-complementation against *nonC*^{P37}*.* The offspring of *nonC*^{P37} and all four P-element lines had detectable transients in at least one trial and thus *ataxin1*, *CG3044* ^{c03148} and *CG14434* were rejected as candidates for *nonC* (data not shown).

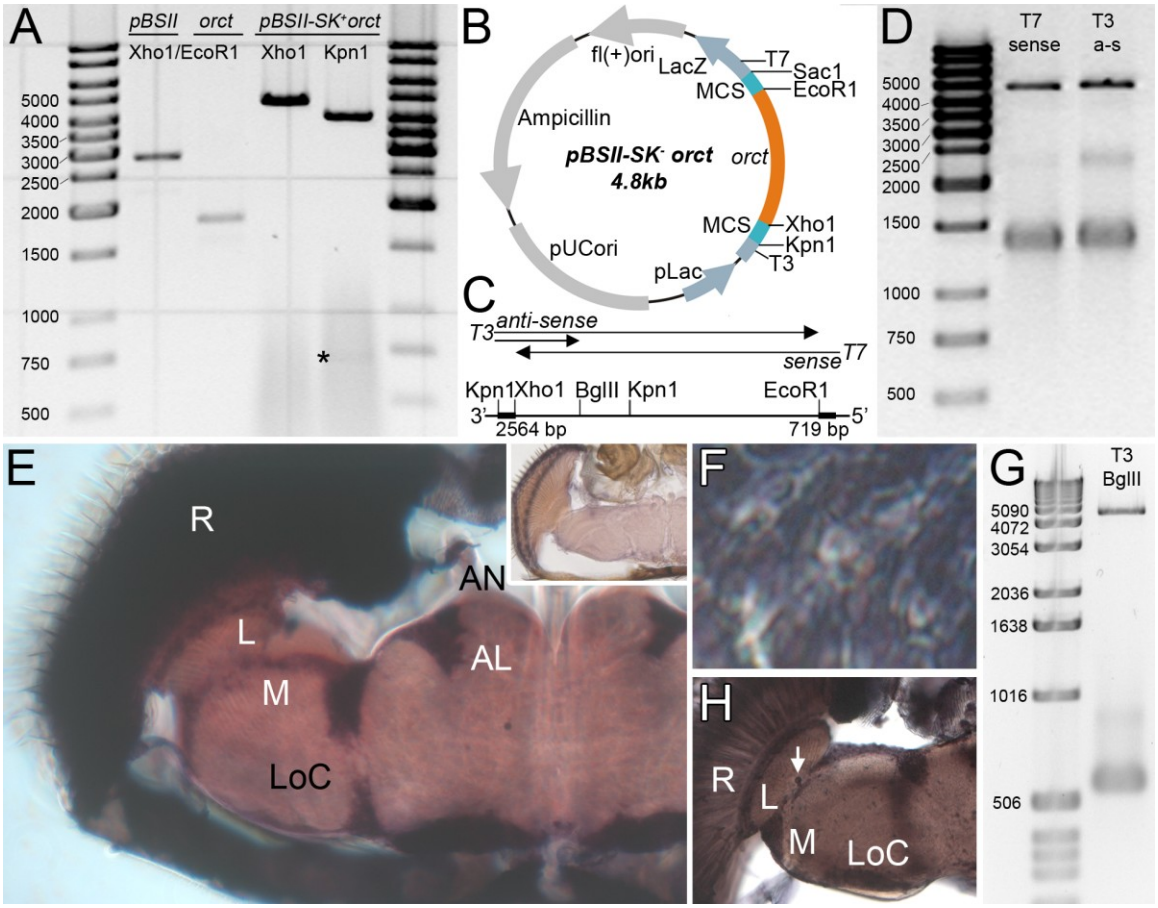

FIGURE 5.1 - MRNA TRANSCRIPTS OF *ORCT1* ARE LOCATED THROUGHOUT THE CORTEX OF THE ADULT CNS.

A-D: Production of the *orct1 in situ* probe and E-F: location of *orct1* anti-sense probe in Vibratome slices of adult *Drosophila* heads. **A**: *pBluescriptII-SK*$^{-}$ was linearized by double digestion with the restriction enzymes Xho1 and EcoR1 (lane 1). A 1845 bp fragment of the *orct1* gene was similarly digested out of clone *GH21655* using Xho1 and EcoR1 (lane 2). After the directional ligation of *orct1* into *pBluescriptII-SK*$^{-}$, the vector was digested with either Xho1 to reveal a single band of approximately 4.8kb (lane 3) or Kpn1, which produces two bands of approximately 4076bp and 696bp (asterisk) and reveals the correct directional ligation of *orct1* in *pBluescriptII-SK*$^{-}$. **B**: The structure of the *orct1* containing *pBluescriptII-SK*$^{-}$ vector from which *in situ* probes were transcribed. **C**: From the structure of the vector and the direction of the *orct1* insert, two anti-sense probes of 1845 bp and 442 bp would be generated using T3 polymerase. **D**: When run on an agarose gel alongside Fermentas GeneRuler 1kb DNA ladder (lane 1), two probes, a sense (lane 2) and an anti-sense (a-s, lane 3) of the appropriate size, approximately 1845 bp each, were detected. **E**: *orct1* anti-sense probe labels cell bodies throughout the cortex in 100 µm horizontal Vibratome slices of the adult *Drosophila* head. As a control, labelling is weaker with the sense probe (inset). **F**: Expression of *orct1* mRNA transcripts was detected in the eye, including the cell bodies of photoreceptors. **G**: A small probe of 442 bp corresponding to the 3' end of the *orct1* gene was produced by digestion with BglII and incubation with T3 polymerase (lane 2)

(FIGURE 5.1 – CONTINUED, 2 OF 2)

and its size was approximated by comparison with Invitrogen's 1kb DNA ladder (lane 1). **H**: This small antisense probe labels only mRNA which corresponds to the long form of the gene, and also labels throughout the cortex. When compared with the longer probe (E), this small probe (H) appears to have reduced labelling in the retina, but increased *in situ* hybridization in cells within the optic chiasms (arrow). Abbreviations: R – retina, L – lamina, M - medulla, LoC – lobula complex, AN – antennal nerve, AL – antennal lobe.

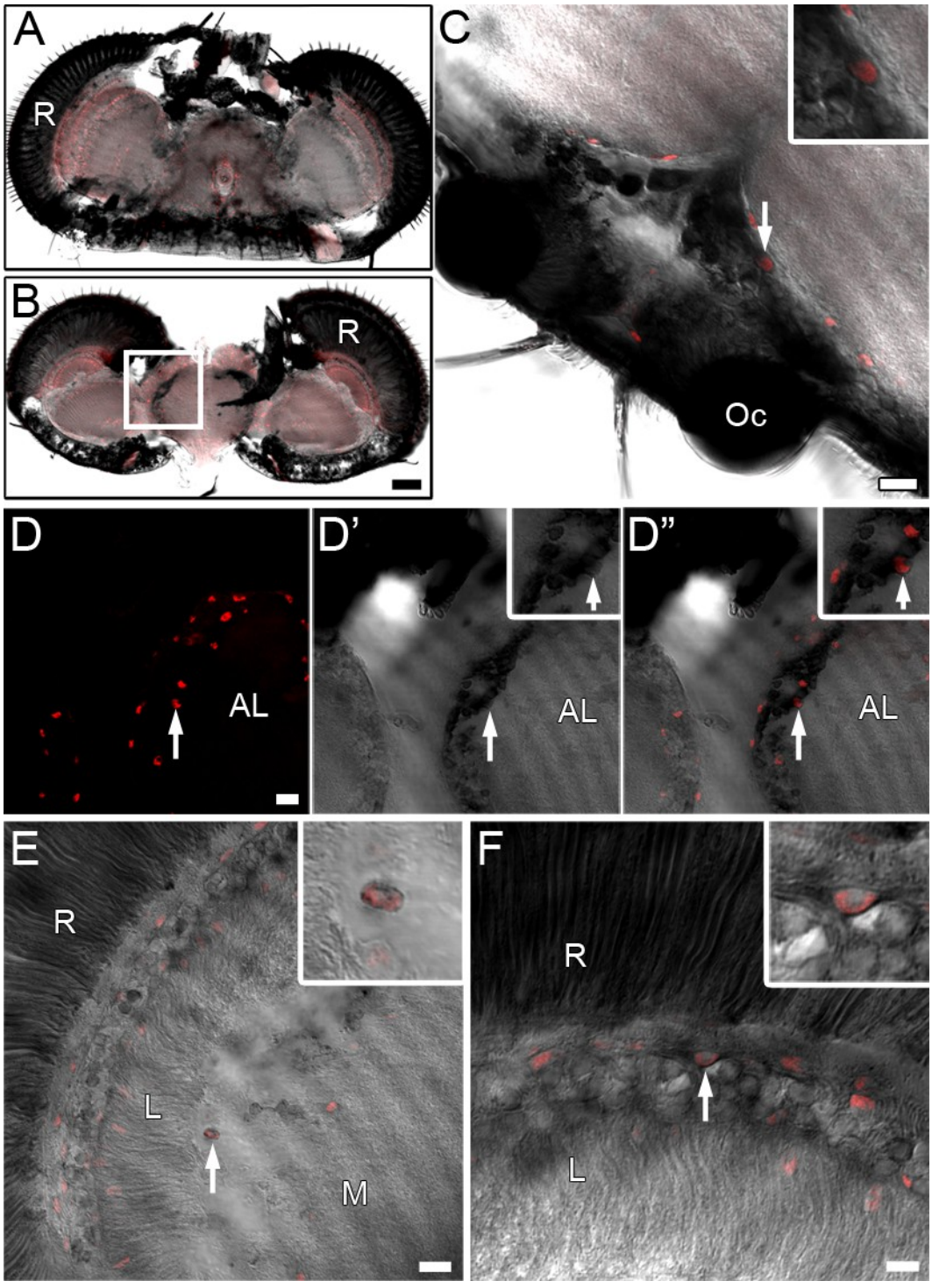

FIGURE 5.2 - *ORCT1* TRANSCRIPTS ARE EXPRESSED IN SOME CORTEX GLIA.

Vibratome slices of adult *Drosophila* heads incubated for *in situ* hybridization against the *orct1* anti-sense probe and then immunolabelled with anti-Repo, a marker for glial nuclei (red). **A**: Frontal and **B**: horizontal Vibratome slices of an adult *Drosophila* head

(FIGURE 5.2 – CONTINUED 2 OF 2)

show the relative locations of *orct1 in situ* hybridization and anti-Repo immunolabelled glia. The panel enclosed within a box in B is enlarged in D-D". **C**: A view of the dorsal region of the brain, near the ocelli (Oc), shows specific labelling of cell bodies with *orct1 in situ* probe. A single *orct1* and Repo co-expressing cell (arrow, inset C). **D-D"**: In the cortex region of the deutocerebrum, near the antennal lobes, some *orct1* expressing cells (D', D") co-label (D") with anti-Repo antibody (D, D", arrows, enlarged in inset). **E-F**: Transcripts of *orct1* are expressed in the medulla (E) and lamina (F) cortices of the optic lobe. Cells which co-label with anti-Repo (arrows), including a distal satellite glial cell of the lamina cortex (F, inset F), are indicated by arrows and enlarged in insets. Scale bars A-B, 50 μm; C-F, 10 μm. Abbreviations: R – retina, L – lamina, M – medulla, AL – antennal lobe.

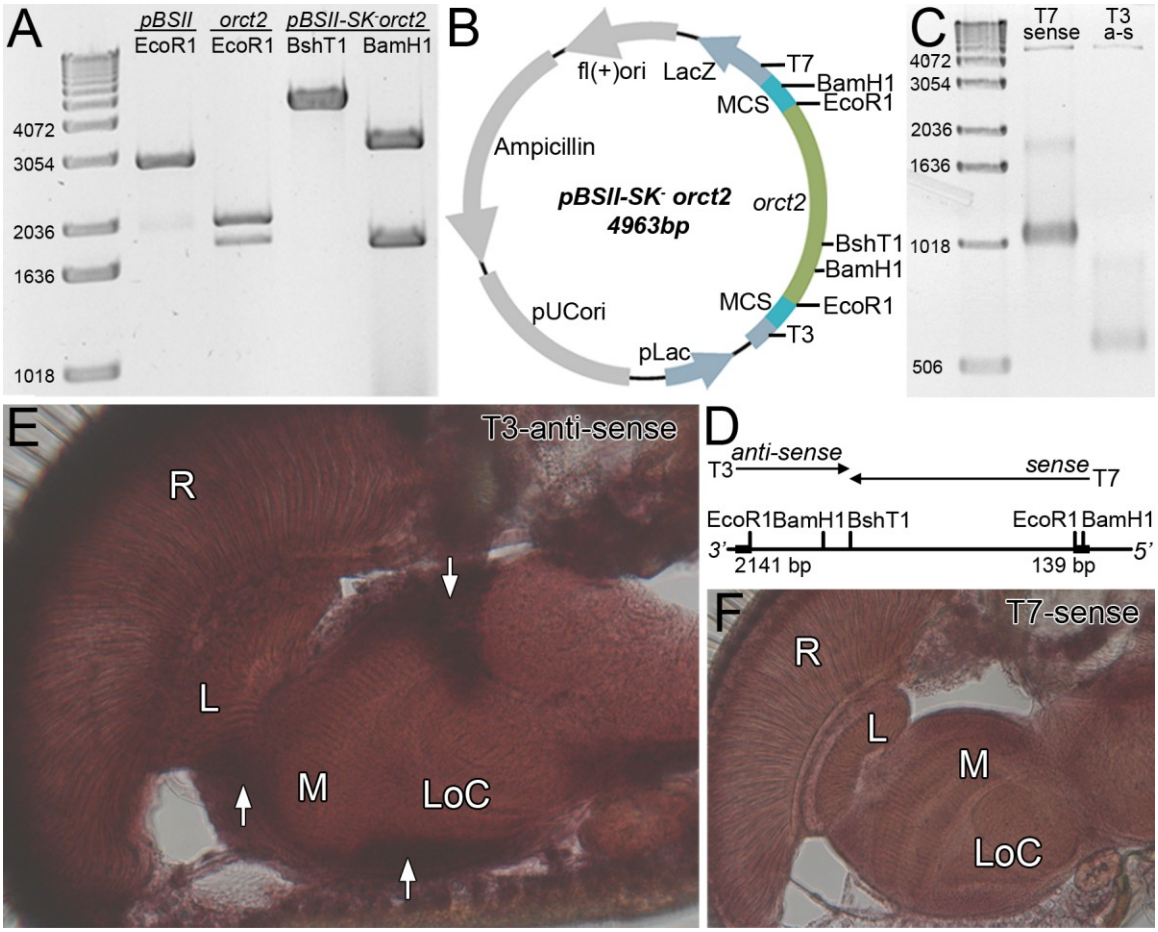

FIGURE 5.3 - MRNA TRANSCRIPTS OF *ORCT2* ARE ALSO LOCATED THROUGHOUT THE CORTICES OF THE ADULT BRAIN.

A-D: Production of *orct2 in situ* probes; and **E-F**: localisation of *orct2* probes in Vibratome slices of adult *Drosophila* heads. **A**: *pBluescriptII-SK-* was linearized by digestion with EcoR1 (lane 1). A 2002 bp fragment of *orct2* was digested out of clone *SD08138* using EcoR1 (lane 2). Ligated *pBluescriptII-SK- orct2* vector digested with BamH1 revealed two bands of approximately 3219 and 1745 bp (lane 4) indicating that the *orct2* gene was inserted in a 3' to 5' orientation. Digestion with BshT1 cuts once, approximately 1468 bp from the 5' end of the *orct2* insert (lane 3) and was used to generate sense and anti-sense probes (B-D). **B**: The structure of the *orct2* containing *pBluescriptII-SK-* vector from which *in situ* probes were transcribed. **C**: *In situ* probes for *orct2* produced from *pBluescriptII-SK- orct2* vector digested with BshT1. Two probes, a sense (T7, lane 2, ~1467 bp from *orct2*) and an anti-sense (T3, lane 3) were detected when run on an agarose gel alongside Fermentas GeneRuler 1kb DNA ladder (lane 1). The DNA ladder cannot be used as an accurate measure of RNA probe size. **D**: From the structure of the vector and the direction of the *orct2* insert, a 536 bp anti-sense probe was generated from hybridization of BshT1 digested vector with T3 polymerase. **E-F**: *orct2* anti-sense probe labels cell bodies throughout the cortex (arrows in E) in 100 µm horizontal Vibratome slices of the adult *Drosophila* head (E), in a pattern reminiscent of *orct1* mRNA *in situ* hybridization. Labelling is weaker with the sense probe (F). Abbreviations: R – retina, L – lamina, M - medulla, LoC – lobula complex.

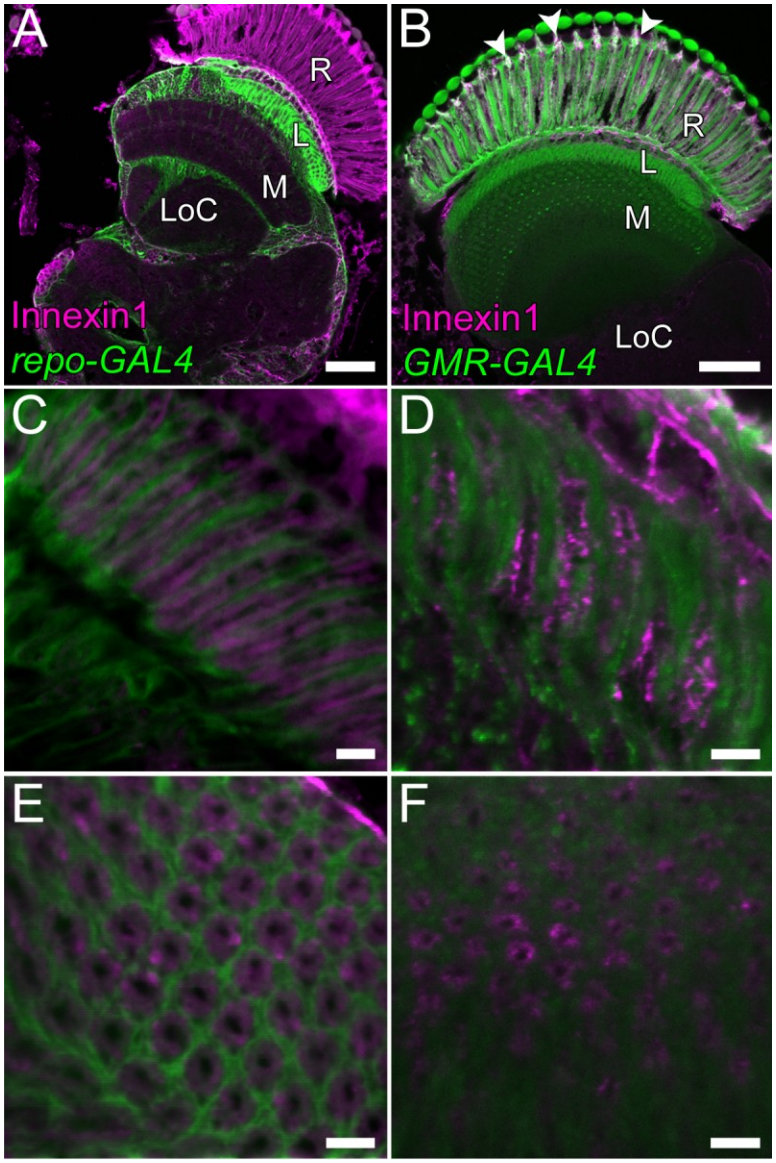

FIGURE 5.4 - INNEXIN1 IS EXPRESSED IN THE LAMINA.

Innexin1 (Ogre, magenta) immunolabelled Vibratome slices of fly brains that expressed mCD8::GFP (green) in the glia using the driver *repo-GAL4* (A,C,E) or in the photoreceptors using *GMR-GAL4* (B,D,F). **A-B**: Slices along a frontal plane imaged with a 25x/0.8 Plan Neofluar magnification show the location of Innexin1 expression relative to glial expression of mCD8::GFP (A) and photoreceptor-specific expression of mCD8::GFP (arrowheads, B). **C-D**: Innexin1 expression in the lamina as viewed in horizontal section. **E-F**: Innexin1 expression in the lamina as viewed in cross section. When visualized with glial mCD8::GFP, Innexin1 appears to be expressed in photoreceptors but paradoxically does not co-localise with mCD8::GFP in flies with the *GMR-GAL4* driver. Images in C-E were viewed with a 63x/1.4 Plan Apochromat objective. Scale bars A-B, 50 µm; C-F, 5 µm. Abbreviations: R – retina, L – lamina, M - medulla, LoC – lobula complex.

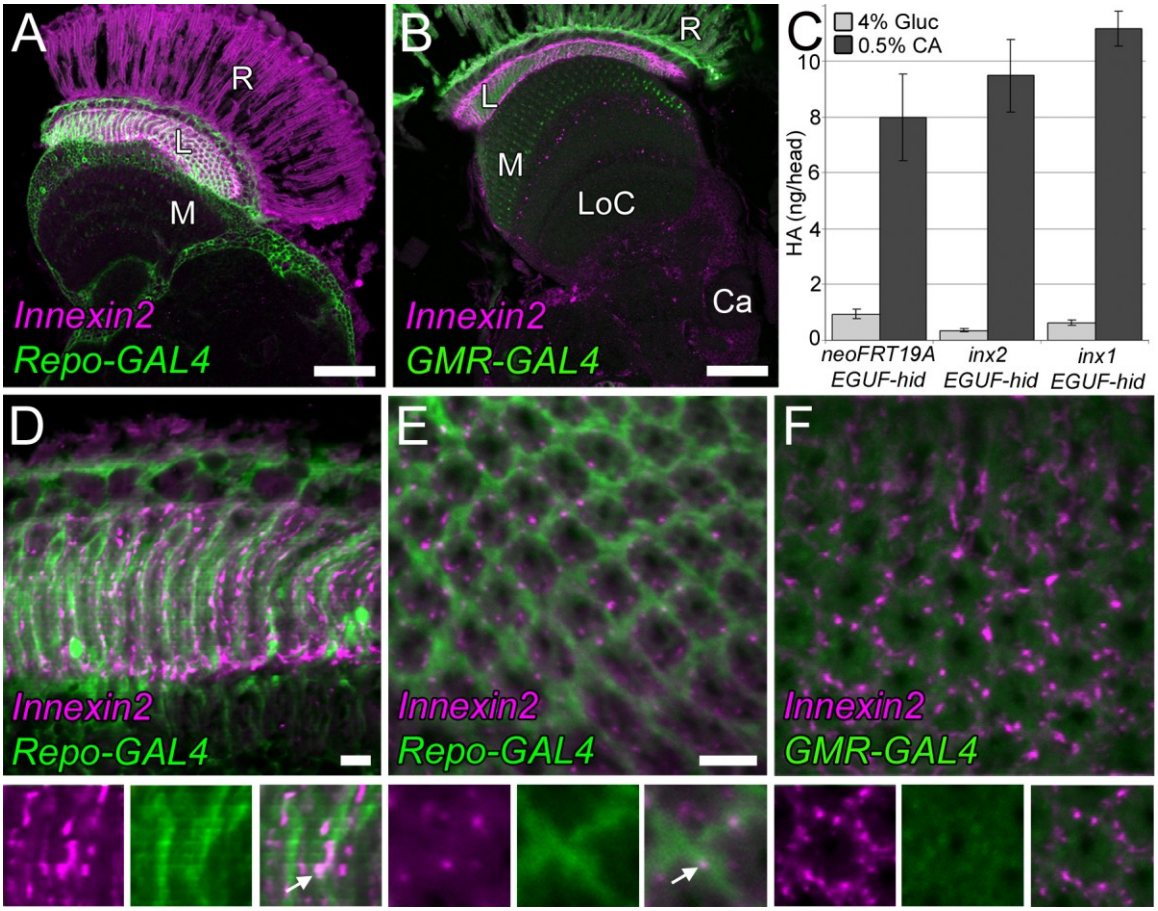

FIGURE 5.5 - INNEXIN2 IS STRONGLY EXPRESSED IN THE LAMINA.

Innexin2 (magenta) was immunolabelled in Vibratome slices of fly brains that expressed mCD8::GFP (green) in glia using the driver *repo-GAL4* (A,D,E) or in photoreceptors using *GMR-GAL4* (B,F). **A-B**: Slices in a frontal plane visualized with a Plan Neofluar 25x/0.8 Plan Neofluar objective show the location of Innexin2 expression relative to glial expression of mCD8::GFP (A) and photoreceptor-specific expression of mCD8::GFP (B). **C**: Whole-head histamine contents (measured in ng/head) of control *neoFRT19A* EGUF-hid and *innexin* EGUF-hid flies after drinking a solution of 4% glucose with or without 0.5% carcinine. **D**: Innexin2 expression in the lamina as viewed in horizontal section of flies expressing glial-specific mCD8::GFP. **E-F**: Lamina cross sections. Innexin2 antibody visualized in relation to the lamina cartridges in flies expressing mCD8::GFP under the control of *Repo-GAL4* (E) or *GMR-GAL4* (F). Co-localisation of anti-Innexin2 and mCD8::GFP is indicated below by an arrow in the representative panels enlarged from D-F. Images in D-F were viewed with a 63x/1.4 Plan Apochromat objective. Scale bars A-B, 50 µm; D, (in E), E, F, 5 µm. Abbreviations: R – retina, L – lamina, M - medulla, LoC – lobula complex, Ca – Mushroom body calyx.

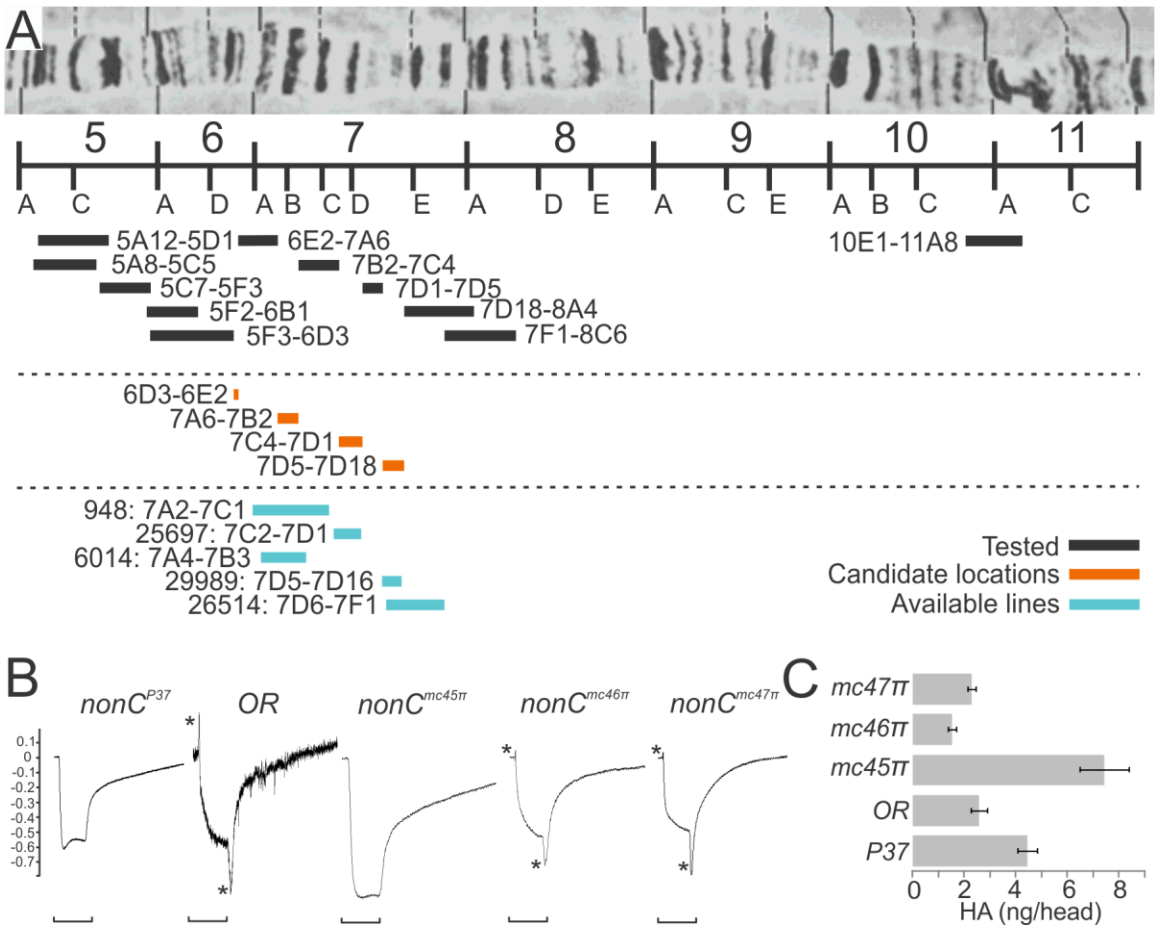

FIGURE 5.6 - DEFICIENCY MAPPING FOR *NONC* ON THE X-CHROMOSOME.

A: The general structure of the X-chromosome is illustrated from cytological map positions 5A to 11F. The *nonC* gene has been previously predicted to lie in region 6 of the X-chromosome. Deficiencies which cover large areas of the X-chromosome are indicated by black bars alongside the cytological range of these deficiencies. More information about deficiency lines used in this study is listed in Table 5.1. Orange bars indicate regions of the X-chromosome yet to be tested for complementation to the alleles $nonC^{P37}$ or $nonC^{mc45\pi}$ while blue bars indicate regions of the X-chromosome for which deficiencies exist but which have not yet been tested against *nonC*. **B**: ERG traces for $nonC^{P37}$, wild-type OR and the *nonC* alleles *mc45π*, *mc46π*, and *mc47π*. An asterisk marks the "on" and "off" transients and a scale bar below the trace indicates the duration of the 30 ms light flash. Deficiencies which fail to complement $nonC^{P37}$ will lack both 'on' and 'off' transients and will look more like the $nonC^{P37}$ phenotype than the wild-type phenotype. No such deficiencies were found. **C**: The average content of head histamine (measured in ng/head) was determined for wild-type flies and all supposed *nonC* alleles. Of these, only *P37* and *mc45π* flies contained more histamine in their heads than wild-type, and these were also the only alleles to lack transients in the ERG.

TABLE 5.3 - A COMPLETE LIST OF GENES FROM SHORT REGIONS ON THE X-CHROMOSOME FOR WHICH DEFICIENCIES WERE EITHER NON-EXISTENT, OR NOT YET TESTED AGAINST *nonC* FOR COMPLEMENTATION ANALYSIS

LOCATION	GENE	PREDICTED FUNCTION
6D3-6E2		
6D2-6D3	*pod1*	actin binding
6D3	*iav*	calcium channel activity
6D3	*Nf-Yc*	DNA binding
6D3	*CG4542*	α-1,3-glucosyltransferase activity
6D3	*Atx-1*	binding
6D3-6D4	*Smg1*	protein kinase activity
6D4	*CG12796*	G-protein coupled receptor protein signalling pathway
6D4-6D5	*CG14435*	protein binding; zinc ion binding
6D5-6D6	*CG4557*	transcription factor
6D6	*Cht11*	chitinase activity
6D6-6D7	*CG4558*	unknown
6D7	*CG14434*	adenylate cyclase activity
6E2	*CG33692*	unknown
6E2	*CG33691*	unknown
7A6-7B2		
7A7	*CG1958*	unknown
7A8-7B2	*CG1677*	zinc ion binding; nucleic acid binding
7B1	*CG2059*	unknown
7B1	*unc-119*	unknown
7B1	*brk*	transcriptional repressor activity
7B1	*Atg5*	unknown
7B1	*Dok*	insulin receptor binding
7B1	*CG18155*	long-chain-fatty-acid-CoA ligase activity
7B1	*CG42780*	unknown
7B2	*CBP*	calcium ion binding
7B2	*CG15034*	unknown
7B2	*CG1999*	unknown
7B2	*ChA7a*	unknown
7B2	*CG42781*	unknown
7B2	*CG15035*	phosphoprotein phosphatase activity
7B2	*CG32727*	heat shock protein binding
7B2	*CG42246*	unknown
7B2	*CG42704*	unknown
7B2	*CG42705*	unknown
7B2	*CG34337*	unknown
7B2	*CG9657*	sodium:iodide symporter activity/transmembrane transport
7B2	*CG15036*	unknown
7B2	*CG32726*	unknown
7B2	*CG11368*	unknown

(TABLE 5.3 - CONTINUED, 2 OF 2)

LOCATION	GENE	PREDICTED FUNCTION
7C4-7D1		
7C3-7C4	*CG10777*	RNA helicase activity
7C4	*CG10778*	alkyl or aryl transferase activity
7C6-7C7	*RpS14a*	structural constituent of ribosome
7C8	*RpS14b*	structural constituent of ribosome
7C8-7D1	*CG42593*	protein binding; ubiquitin-protein ligase; zinc ion binding
7C9	*l(1)G0193*	unknown
7D1	*CG15332*	unknown
7D1	*CG15530*	unknown
7D1	*sws*	lysophospholipase activity
7D1-7D2	*sn*	actin binding
7D5-7D18		
7D3-7D5	*fs(1)h*	protein kinase/ DNA binding
7D5	*mvs*	cell adhesion molecule binding; receptor activity
7D5	*Upf2*	protein binding
7D5	*CG1571*	ATPase activity, coupled; motor activity
7D5	*CG2254*	binding; oxidoreductase activity
7D5	*CG2256*	calcium ion binding
7D5-7D6	*Ubc-E2H*	ubiquitin-protein ligase activity
7D6	*CG2258*	protein binding
7D6	*Gclc*	glutamate-cysteine ligase activity; protein binding
7D6	*CG1575*	binding
7D6	*CG2260*	unknown
7D6	*CG15335*	unknown
7D6-7D14	*CG2116*	zinc ion binding
7D12	*CG10958*	unknown
7D12-7D13	*CG2120*	zinc ion binding; nucleic acid binding
7D13-7D14	*Smox3*	transforming growth factor β receptor
7D14-7D15	*CG17982*	unknown
7D15	*CG2263*	phenylalanine-tRNA ligase activity
7D15	*CG2129*	zinc ion binding
7D15-7D16	*CG15336*	zinc ion binding
7D16	*CG10959*	zinc ion binding; nucleic acid binding
7D16	*Gbeta5*	GTPase activity
7D16	*CG18262*	zinc ion binding
7D16	*Traf6*	protein binding
7D16	*GIIIspla2*	phospholipase A2 activity
7D17	*CG15337*	unknown
7D17	*CG10761*	zinc ion binding
7D17	*Or7a*	olfactory receptor activity
7D17	*CG2278*	unknown
7D17	*slpr*	jun kinase/ protein kinase activity

5.5 DISCUSSION

Despite, or perhaps because of, the episodic approach adopted here to finding candidate histamine, carcinine or β-alanine transporters in the visual system, none of the genes examined herein was specifically confirmed as important for transport in the histamine recycling pathway. On the other hand, the candidacy of *orct* genes has been eliminated from contention as a transporter of β-alanine in the neuropile glia.

5.5.1 *ORCT1* AND *ORCT2* ARE EXPRESSED IN THE CORTEX, THUS ELIMINATING THEM AS CANDIDATE TRANSPORTERS OF β-ALANINE IN NEUROPILE GLIA

β-alanine has long been known to play an integral part in cuticle melanization (Jacobs, 1966, 1978, 1980), so its presence throughout the body, and thus the need for a similarly widespread transporter, is predicted. In the cuticle, β-alanine is conjugated to dopamine to form N β-alanyl-dopamine (NBAD), a precursor to the primary tanning agent of most insects. This reaction is catalyzed by the action of the NBAD synthase protein, which in *Drosophila* is encoded for by the gene *ebony* (Hovemann *et al.*, 1998). Within the central nervous system, Ebony utilizes β-alanine to inactivate amine neurotransmitters such as histamine (Richardt *et al.*, 2003). NBAD is also detected in the CNS of some insects (Krueger *et al.*, 1990; Pérez *et al.*, 2004), implying that within the nervous system Ebony also inactivates dopamine via conjugation to β-alanine, a finding which has only been demonstrated *in vitro* (Richardt *et al.*, 2003). β-alanine may also act within the nervous system as an inhibitor of GABA uptake by low affinity GABA transporters. In the cockroach *Periplaneta americana*, glial accumulation of [^{3}H]-GABA was reduced after application of β-alanine (Hue *et al.*, 1982). Application of β-alanine produces a single hyperpolarization of the cockroach's fast coxal depressor motor neuron, which is similar to this neuron's response to glutamate, a known neurotransmitter (Wafford and Sattelle, 1986), and β-alanine has even been proposed to act as a small molecule neurotransmitter in mammals (Tiedje *et al.*, 2010).

Ebony is expressed in glia (Hovemann *et al.*, 1998; Richardt *et al.*, 2002; Suh and Jackson, 2007) and thus it follows that wherever Ebony is found, the presence of β-alanine and its associated transporter are to be expected. In order for Ebony to inactivate neurotransmitter it must be expressed in neuropile glia near synaptic neurotransmitter release sites. This is definitely the case for the inactivation of histamine, insofar as Ebony is expressed in the epithelial glia (Richardt *et al.*, 2002), a

type of neuropile glia associated with photoreceptor tetrad synapses in the lamina (Meinertzhagen and O'Neil, 1991). While *orct1* expression is too widespread to be expressed exclusively in glia, which constitute only about 10% of the insect brain (Ito, pers. comm.), it was unknown whether it might express in both neurons and glia, or just neurons. This problem has been resolved by immunolabelling tissue that had been previously hybridized for *orct1* with an antibody against the glial transcription factor, Repo. Transcripts for *orct1* were not found in neuropile glia, but in the cortex glia that lie amongst the cell bodies of neurons, as well as in the eye, and thus at sites removed from neurotransmitter release.

If there were differences in the expression pattern of the long and short version of the *orct1* transcript, they cannot be distinguished with the *in situ* probes utilized here because both detect the long version of the transcript. It is quite possible that the small cDNA is not as broadly expressed, and its signal would be overwhelmed by the extensive expression of the larger transcript detected by our anti-sense probes. Generating a probe to detect only the short version is impossible because the short transcript is nested within the larger one (Taylor *et al.*, 1997).

Despite this problem, the accuracy of the *orct in situ* labelling detected in this study, particularly in the retina, is supported by other studies that have localised *orct2* to the developing eye disc (Herranz *et al.*, 2006), thus suggesting that *orct* genes are indeed transcribed in the eye and function both during development and in the adult. During development, *orct2* acts downstream of an insulin receptor signalling pathway that is required for cell growth and proliferation (Herranz *et al.*, 2006). Although eliminated as a candidate β-alanine transporter, *orct* transporters may nevertheless be important for the proper functioning of the adult visual system, in a role that has yet to be elucidated. It is possible that after their expression in the eye disc *orct*-type transporters continue to play a nutritive role in the adult eye and CNS, transporting substances to and from glia and neurons to maintain cell survival.

5.5.2 Innexins in the Visual System are Unlikely to Mediate Neurotransmitter Transport

We had set three criteria for screening Innexin hemichannels as possible candidates for the transport of histamine metabolites in the visual system, that 1) they express in either the photoreceptors or neuropile glia; 2) had an effect on head histamine content when

compared with controls; and 3) possess a channel pore of sufficient size to allow the passage of histamine, carcinine or β-alanine. Despite the fact that both Innexin1 and Innexin2 immunolocalise to the lamina, neither has been definitively localised to the photoreceptors in the adult, although Innexin1 is more likely to be so than Innexin2. It is thus unlikely that either could function as a hemichannel transporter allowing carcinine to shuttle into the photoreceptor terminal or β-alanine out of it.

The third criterion is easily resolved. In the barnacle *Balanus Amphitrite* photoreceptors of the eye take up radioactive histamine (^{3}H - Molecular weight = 111 Da) when the ocelli from adults or whole larval nauplii are placed in ^{3}H-laced sea water. In the nauplii ^{3}H can thus enter the extracellular space surrounding the eye, a location from whence it is transported into the photoreceptors (Stuart *et al.*, 1996; Stuart *et al.*, 2002). *In vivo* studies in *shakB* mutants and wild-type controls show that channels composed of ShakB transport Lucifer yellow, with a molecular weight of 457 Da (Phelan *et al.*, 1996), somewhat larger than histamine or carcinine (182 Da). Channels containing Innexin2 also transport Lucifer yellow *in vivo* (Bohrmann and Zimmermann, 2008). Calmodulin, which has a molecular weight of 17-19 kDa is reported to pass into oocytes through gap junctions in species of the milkweed bug, *Oncopeltus*,and carpenter bees, *Xylocopa* (Brooks and Woodruff, 2004). Thus innexin hemichannels have a pore size amply sufficient to pass the components of the histamine recycling pathway.

The level of innexin expression seen by immunolabelling is dependent upon the age of the fly, and is highest in young flies, so that future attempts to localise expression of these proteins should make use of recently eclosed flies, for which the signal is strongest. This was especially evident for Innexin2 immunolabelling, which displayed a strong, consistent signal in some of the batches processed but not others. Innexin1 did not show consistent immunolabelling in the adult brain possibly because, even though most specimens were female, neither the age nor sex of the flies used for immunocytochemistry was controlled carefully. Immunoblots for this antibody detect three bands in extracts from *Drosophila* ovaries, the weakest of which was the band at 46 kDa, corresponding to Innexin1 (Bohrmann and Zimmermann, 2008), therefore this antibody may not be specific for Innexin1. Furthermore, the rough eye phenotype of *GMR* (Freeman, 1996), would consequently cause disruptions in the organisation of the underlying lamina, making cellular identification more difficult at the light microscope level, especially in association with inconsistent immunolabelling.

Innexin2 expression was localised to the epithelial glia in several specimens, indicating its presence in these cells. The epithelial glia have abundant gap junction plaques that interconnect them, not with photoreceptors via hemichannels, but with neighbouring glia via functional gap junctions to form an “electrical network” across the lamina (Saint Marie and Carlson, 1983a). The Innexin2 proteins in the lamina glia are most likely subunits of a “classical” gap junction and do not form a hemichannel. The findings in this thesis provide no evidence for functional hemichannels in *Drosophila.* I, thus, interpret the immunolocalisation data to indicate that Innexin2-containing channels pair with hemichannels on opposite membranes to form functional gap junctions. Innexin2 forms either homotypic junctions with itself, or oligomeric junctions when paired with Innexin3 (Stebbings *et al.*, 2000; Lehmann *et al.*, 2006). It may also partner with Innexin1 in some areas of the brain (Keane, see: www.sanpatricio.co.uk/Innexins/index.php).

Innexin2 was also expressed in cells of the lamina at a location corresponding to either the amacrine neurons or the basket endings of the T1 neurons. The neurites of T1 cells have no visible synapses in either the lamina or medulla (Meinertzhagen and O'Neil, 1991; Takemura *et al.*, 2008). Instead amacrine and T1 neurons form close appositions, known as plaque contacts, with the photoreceptor and epithelial glia. They are also associated with structures known as gnarls, bulbous projections from the epithelial glia that extend into the β neurites of T1 neurons (Campos-Ortega and Strausfeld, 1973; Meinertzhagen and O'Neil, 1991). The absence of any visible synapse in T1 cells suggests that these neurons communicate with their surroundings not by chemical means, but most likely by electrical transmission, via gap junctions. Yet, previous studies (Shaw and Stowe, 1982; Shaw, 1984b; Shimohigashi and Meinertzhagen, 1998) neither reported, nor possibly even sought, gap junctions for either of these neurons, an opportune topic for investigation.

Not surprisingly, even though Innexin2 was not conclusively demonstrated to express in photoreceptors in the adult, *inx2-EGUF-hid* constructs had a reduction in head histamine content when compared with controls. This is likely because of a severe reduction in the size of the retina, and presumably the underlying lamina, since up to 71% of the histamine in a fly’s head is contained within the retina and lamina complex (Borycz *et al*., 2005). Disruptions in the developmental expression of Innexin2 in retinal pigment cells may give rise to the abnormal retina in the eyes of *inx2-EGUF-hid* mutants. By contrast, whereas Innexin1 may be expressed in the adult photoreceptors, these flies did not have

a significant reduction in baseline concentration of head histamine. Heads of *inx1-EGUF-hid* flies, did however, have more histamine than controls after drinking a solution of carcinine, thus indicating the more efficient liberation of histamine from carcinine.

What can account for such changes in head histamine content and carcinine metabolism? Apart from external factors in the body, for which no account can be given (Chapter 4), reduction in head histamine content may reflect a developmental problem within the visual systems of these flies. The key to this possibility is that the *EGUF-hid* system causes mutations within the eye that are not restricted to the photoreceptors, and so the *innexins* tested need not be expressed in the photoreceptors to have an effect on eye development; they just have to be expressed in the pupal eye disc. Both *innexin1* and *innexin2* have been localised to secondary and tertiary pigment cells during development (Stebbings *et al.*, 2002). Within the developing *Drosophila* epithelium, Innexin2 interacts with the DE-cadherin/ β-catenin adherens junctional complex, so that mutations of *innexin2* result in disruptions in epithelial development and gut morphogenesis (Bauer *et al.*, 2004). Both DE-cadherin and β-catenin are also essential for the proper development of the optic lobes (Dumstrei *et al.*, 2002; Dumstrei *et al.*, 2003), and the eye (Grzeschik and Knust, 2005; reviewed in Tepass and Harris, 2007), which is itself a modified epithelium. Any alterations in the structure of the eye that result from improper development will also disrupt the organisation of photoreceptor terminals in the optic neuropiles (Meyerowitz and Kankel, 1978; Zheng *et al.*, 1995; reviewed in Meinertzhagen, 1975), and thus possibly disrupt their synaptic connections, their function and their histamine contents. However, mutations that affect the organisation of cartridges in the lamina do not alter the number or structure of photoreceptor synapses per terminal (Hiesinger *et al.*, 2006) and thus are unlikely to have much of an effect on synaptic physiology. Alterations in the structure of the optic lobes was not analysed here, although the brains of *inx1-EGUF-hid* flies appear relatively normal at the resolution of the light microscope (Curtin *et al.*, 2002b) .

A retinal abnormality is, however, apparent in the *ogre-EGUF-hid* line, and the retina in these flies, while apparently no smaller or rougher than those in the *EGUF-hid* control, are a variegated white colour. While both *innexin-EGUF-hid* lines could liberate histamine from carcinine after drinking a solution of 0.5% carcinine, only *inx1-EGUF-hid* had histamine contents significantly greater than those in control flies. This difference in histamine content may not result from the effects of mutant *innexin1* in the eye, but may

instead be due to inconstancies between trials for the control *1709-EGUF-hid* line. In the control, measurements of histamine content were combined from two separate carcinine-feeding experiments, with one set having a lower average histamine content than the other. Thus, when these data were combined, the measurable content of histamine in the heads of control flies appears lower, resulting in an apparent significant difference in head histamine content between controls and *inx1- EGUF-hid* flies after drinking a solution of carcinine. To resolve this uncertainty, this experiment should be confirmed by simultaneously processing more specimens. However, it is also possible that eye-specific mutations of the *innexin1* gene, which is normally expressed in surface glia (see Keane: http://www.sanpatricio.co.uk/Innexins/index.php), somehow affect the permeability of the blood-eye/ blood brain barrier, thus altering the amount of carcinine that can enter the eye from external sources, via the haemolymph. Once in the optic neuropiles, histamine is readily liberated from carcinine when exposed to Tan in the photoreceptors (Chapter 4; True *et al*., 2005; Wagner *et al*., 2007).

5.5.3 THE ELUSIVE *NONC*

Despite enthusiasm for mapping *nonC*, a lack of deficiency lines hindered early progress on this project. All of the deficiency lines available for cytological regions 5A-8A of the X-chromosome complement $nonC^{P37}$ and had either a measurable 'on' and/or 'off' transient in their ERG. Despite repeated false negatives (flies with no transients in the ERG) for some crosses, all lines did eventually produce transients under the appropriate circumstances. In the ERG, there is no such thing as a false positive, and so any deficiency that complemented *nonC* and had transients was discarded after three positive tests. The P-element lines utilized to screen for a *nonC*-like phenotype also complemented $nonC^{P37}$. However, the genes associated with the P-element lines tested cannot be completely ruled out since the P-element lines were not fully characterised. Thus, it is not known if these P-elements disrupt gene function by inserting into or near the gene of interest, nor is it known what kind of effect, if any, such an insertion would have on gene expression. Areas of the chromosome containing deficiencies that have not been screened against *nonC* are still considered candidate locations for the gene.

Simultaneous studies from the lab of K. Broadie (Vanderbilt University) have demonstrated that *nonC* plays a facilitative role in the presynaptic terminal and regulates the synaptic vesicle cycle underlying glutamate release at the neuromuscular junction.

The Broadie lab may have already identified this gene as a member of the phosphoinositide kinase family, so that further pursuit may have limited utility (see: www.mc.vanderbilt.edu/labs/broadie/Webpage/BroadieLab%20Website/Abstracts.html).

Perhaps the most interesting finding from this study is that *nonC* has a strong interaction with some gene in the 11A4-7 region of the X-chromosome, and flies that are hemizygous for $nonC^{P37}$ and a deficiency in 11A are not viable. Whichever gene or combination of genes in 11A interacts with *nonC* also causes a drastic reduction in head histamine content when *in trans* with $nonC^{mc45\pi}$. There are only five genes in 11A4-7, most of which are uncharacterised, including *CG11356* (GTP binding), *CG2750* (unknown), *CG1924* (calcium ion binding), *Tenascin accessory*, and *CG32655* (oxidoreductase activity). Of these, the calcium binding *CG1924* is the most probable candidate to affect neurotransmitter release and histamine content, especially if its action resembles that of *synaptotagmin* (Yoshihara and Littleton, 2002), and is thus a likely candidate to interact with *nonC* at the synaptic terminal.

5.5.4 CONCLUSION

Despite the lack of a candidate transporter for any of histamine, carcinine or β-alanine, all of which are required in the histamine recycling pathway, these experiments at least eliminate certain genes, such as *the orct* family of transporters, from candidacy as a neurotransmitter transporter for histamine and its conjugates, while simultaneously uncovering interesting features of all the other genes examined. More remains to be discovered regarding the role of gap junctions in the development and function of the visual system. The location and characterization of the gene coding for *nonC* will also be of great interest. If *nonC* proves to be an exocytosis mutant, then it is unclear how the mutant can survive despite affecting a number of neurotransmitter systems, including glutamate in the neuromuscular junction and histamine in the visual system. Future studies will be needed to clarify these and the many other issues raised by experiments reported in this chapter.

5.6 ACKNOWLEDGEMENTS

The Repo antibody 8D12 was developed by Corey Goodman and obtained from the Developmental Studies Hybridoma Bank, University of Iowa. The Innexin antibodies

were a generous donation from M. Koch (Universität Bonn, Bonn, Germany). The *nonC* alleles were proved by Dr. W. Pak (Purdue University, West Lafayette, Indiana, USA), and *ogre neoFRT19A/Binsn* by K. Curtin (University of Arkansas, Fayetteville, Arkansas, USA). I would like to thank Will MacDonald for guidance with *in situ* hybridization and the Lloyd lab for providing reagents and supplies for hybridization including the *pBluescriptII-SK*$^{-}$ vector. I am also indebted to S.R. Shaw and Jane Anne Horne for setting up, training and assistance with Electroretinograms, and to Nancy Butcher and Nicole Delaney for their assistance with miniprepping.

5.7 TRANSITION TO CHAPTER SIX

To form synapses, photoreceptor axons must target specific visual interneurons. The fly's compound eye visual system is ideally suited to an analysis of the complex interplay of developmental signals that instruct the photoreceptor, its axon and other organelles and other phenotypic features, to assume a particular cell fate. So, too is the interplay of developmental signals between the photoreceptor axon and its glia and interneurons. The following chapter explores these ideas, and in doing so differs from the themes of preceding chapters. In it I explore the synaptic plasticity of the nervous system by determining whether photoreceptors that are mistargeted to incorrect layers of the brain are still capable of forming synapses. This manuscript has been published in the January 2009 issue of *Journal of Neuroscience*. Over-expression of the transcription factor *runt* in the developing photoreceptors of the *Drosophila* eye causes a mistargeting phenotype whereby those R1-R6 photoreceptors that were to terminate and synapse in the lamina instead terminate within the underlying medulla. Mistargeted photoreceptors form ectopic tetrad synapse within the medulla, most likely with novel partners. There is also an increase in the diameter of invaginating glial capitate projections within the medulla. Taken together, the uniformity of synapse structure and capitate projections size suggests that the presynaptic photoreceptor terminal has cell-autonomous control over its synaptic organelles. In addition, combinatorial over-expression of *runt* in the developing photoreceptors also alters the cellular fates of these sensory neurons, resulting in a dissociation of rhabdomere size, rhodopsin expression and axon terminal targeting.

CHAPTER 6

PHOTORECEPTOR NEURONS FIND NEW SYNAPTIC TARGETS WHEN MISTARGETED BY OVER-EXPRESSING *RUNT* IN *DROSOPHILA*

Tara N. Edwards and Ian A. Meinertzhagen

Manuscript submitted March 7, 2008, revised November 28, 2008, accepted December 6, 2008 and published January 21, 2009.

Published in *The Journal of Neuroscience* 29(3): 828-841.

6.1 ABSTRACT

As a neuron differentiates, it adopts a suite of features specific to its particular type. Fly photoreceptors are of two types: R1-R6 that innervate the first optic neuropile, the lamina, and R7-R8 that innervate the second, the medulla. Photoreceptors R1-R6 normally have large light-absorbing rhabdomeres, express Rhodopsin1 and have synaptic terminals that innervate the lamina. In *Drosophila melanogaster*, we used the yeast *GAL4/UAS* system to drive exogenous expression of the transcription factor Runt in subsets of photoreceptors, resulting in aberrant axonal pathfinding and, ultimately, incorrect targeting of R1-R6 synaptic terminals to the medulla, normally occupied by terminals from R7 and R8. Even when subsets of their normal R1-R6 photoreceptor inputs penetrate the lamina, to terminate in the medulla, normal target cells within the lamina persist and maintain expression of cell-specific markers. Some R1-R6 photoreceptors form reciprocal synaptic inputs with their normal lamina targets, while supernumerary terminals targeted to the medulla also form synapses. At both sites, tetrad synapses form, with four postsynaptic elements at each release site, the usual number in the lamina. In addition, the terminals at both sites are invaginated by profiles of glia, at organelles called capitate projections, which in the lamina are photoreceptor sites of vesicle endocytosis. The size and shape of the capitate projection heads are identical at both lamina and medulla sites, even though those in the medulla are ectopic and receive invaginations from foreign glia. This uniformity indicates the cell-autonomous determination of the architecture of its synaptic organelles by the presynaptic photoreceptor terminal.

6.2 INTRODUCTION

Development of the nervous system requires that neurons not only find their correct targets in the brain but also form correct synaptic partnerships once they contact those targets. Many studies focus on either aspect of neural development, but few consider both in a single paradigm. Their strictly ordered topography (Kaas, 1997; Chklovskii and Koulakov, 2004) and development (McLaughlin and O'Leary, 2005), as well as regulated synaptic composition (Nicol and Meinertzhagen, 1982; Rao-Mirotznik *et al.*, 1995), make visual systems ideally suited to study both pathfinding and synaptogenesis. To navigate to their targets in the developing brain, axons in both vertebrate and invertebrate visual systems use related guidance molecules, such as receptor protein tyrosine kinases

(Dütting *et al.*, 1999) and phosphatases (Johnson *et al.*, 2001). Related events also occur in adult organisation. Thus, when photoreceptors degenerate in the vertebrate retina, reactive changes occur to form ectopic synapses between novel partners (Peng *et al.*, 2000; Peng *et al.*, 2003; Johnson *et al.*, 2006; Bayley and Morgans, 2007). In the visual system of *Drosophila* we can study these phenomena by genetic interventions, without invoking cell degeneration, but instead by targeting photoreceptor axons to an incorrect neuropile in the brain.

The visual system of *Drosophila* is remarkable for its numerical and spatial determinacy, especially at its identified photoreceptor synapses (Meinertzhagen and Hanson, 1993; Prokop and Meinertzhagen, 2006). The eye has two types of photoreceptors: R1-R6, which terminate in the first optic neuropile, the lamina, can be considered equivalent to vertebrate rods; while R7 and R8, with axons that terminate in different strata of the second neuropile, or medulla, are equivalent to cones. The lamina is thus formally equivalent to the outer plexiform layer of the retina, and responsible for contrast encoding (Laughlin *et al.*, 1987), while the medulla assumes many of the functions of the inner plexiform layer.

Photoreceptor axons in the fly's visual system undergo morphogenesis in three stages (Meinertzhagen and Hanson, 1993; Hiesinger *et al.*, 2006). In the initial stage, axonal pathfinding, interactions between the ingrowing photoreceptor axons and glia in the developing brain (Chotard and Salecker, 2004; Freeman, 2006) play a major role in ensuring that the axons first target their correct neuropile. This is followed by lateral targeting, during which axons find their correct synaptic partners (Meinertzhagen and Hanson, 1993). Photoreceptor synapses then assemble element by element, when dendrites from lamina cell targets converge upon presynaptic sites to form the postsynaptic tetrads of the adult (Fröhlich and Meinertzhagen, 1982). Each R1-R6 terminal forms approximately 50 evenly-dispersed tetrads (Meinertzhagen and Sorra, 2001). Correct retinotopic targeting of photoreceptors is regulated by many genes (Mast *et al.*, 2006), and is independent of neuronal activity (Hiesinger *et al.*, 2006). With these features as a basis, what then happens to R1-R6 photoreceptors that fail to terminate in the lamina and are genetically mistargeted to the medulla? Our study examines whether these photoreceptors still form synapses in the lamina, through which their axons must pass, and whether supernumerary photoreceptor terminals synapse with new partners in the medulla.

6.3 MATERIALS AND METHODS

6.3.1 FLY STRAINS

Fruit flies, *Drosophila melanogaster*, were raised on standard cornmeal molasses medium at 23°C for all crosses unless otherwise noted. The wild-type stock was Oregon R (OR). We used the *GAL4/UAS* system (Brand and Perrimon, 1993) to construct flies in which the R1-R6 photoreceptors bypass the lamina and mistarget to the medulla. For this, two *GAL4* lines were used to drive *UAS-runt* (Dormand and Brand, 1998) expression: *GMR-GAL4* (Moses and Rubin, 1991; Freeman, 1996) which drives expression in all photoreceptors, and *MT14-GAL4* (Tissot *et al.*, 1997). The *MT14-GAL4* and *UAS-runt* lines were provided by Dr. Utpal Banerjee (UCLA, CA, USA).

We distinguished subsets of R7 and R8 photoreceptors using the R7 rhodopsin (Rh)-specific expression lines *w[*]*; *cn[1]bw[1]/CyO*; P{*w[+mC]=Rh3-lacZ*.PD}3*/TM2,* and *w[*]*; P{*w[+mC]=Rh4-lacZ.PD}2*; *MKRS/TM2,* and the R8 rhodopsin expression lines: *y[1]w[*]*; *cn[1]bw[1]/CyO*; P{*w[+mC]=Rh6-lacZ.PD}3/TM2, and w[*]*; *cn[1]bw[1]/CyO*; P{*w[+mC]=Rh5-lacZ*.PD}3*/TM2*. To identify Rhodopsin1 (Rh1) expressing cells in the eye, as well as to distinguish the ectopic terminals of R1-R6 in the medulla from the terminals of R7 and R8, we utilized the P{*ry*[+t7.2]=*Rh1*(-252/+67)-*lacZ*.omSMB} line which expresses β-gal in R1-R6. We also used *y[1] w[*]*; *Pin[Yt]*/*CyO*; P{*UAS-mCD8::GFP.L}LL6* to monitor *GAL4* driver expression. The requisite stocks were all from the Bloomington Stock Center (Indiana University, Bloomington, IN, USA).

A *MARCM* technique (Lee and Luo, 1999) was used to visualize individual photoreceptors in which both *UAS-runt* and *UAS-mCD8::GFP* expression was driven by *GMR-GAL4*. To do this we crossed *hsFLP*; *NeoFRT40A actin-GAL80/CyO* to *UAS-mCD8::GFP*; *NeoFRT40A, GMR-GAL4, UAS-runt* lines and selected for *hsFLP/UAS-mCD8::GFP*; *NeoFRT40A actin-GAL80/ NeoFRT40A, GMR-GAL4, UAS-runt* adult flies. Flies were reared at 23°C and third-instar larvae were heat shocked for 5 min at 37°C.

To visualize the profiles of photoreceptor terminals by electron microscopy (EM), we used *yw*; *UAS-HRP::CD2*/CyO and *UAS-HRP::CD2* on III (Larsen *et al.*, 2003). To increase expression of the *UAS-HRP::CD2* enzymatic marker we transferred flies to 29°C during early pupal development or at least 24 h prior to dissection (when using *GMR-GAL4* to drive *UAS-runt* expression). At such elevated temperatures, the *UAS-*

runt/+; *MT14-GAL4/+* flies exhibited a genetically induced motor defect, so that most failed to eclose. As representative adults, we therefore used occasional young escaper flies that emerged naturally. Otherwise *UAS-runt/+*; *MT14-GAL4/+*, and *GMR-GAL4/UAS-runt* flies were raised at 18°C to reduce the severity of the Runt over-expression phenotype. *UAS-HRP::CD2* lines were provided by Dr. Chi-Hon Lee (NIH, Bethesda, MD, USA).

6.3.2 IMMUNOCYTOCHEMISTRY

The brains of larvae and the heads of pupal and adult flies were fixed in a solution of 4% formaldehyde (from paraformaldehyde, PFA) in 0.1M phosphate buffer (PB) for 4 h or overnight at 4°C. Pupal and adult brains were washed in 0.1M PB, mounted in 7% agarose and sliced at 80-100 µm thickness in the horizontal plane by means of a Vibratome. Brains were permeabilized in successive treatments of 0.2% Triton X (Tx) in 0.01M phosphate buffered saline (PBS) and 2% PBS-Tx, and were then blocked with 5% normal goat serum (NGS) in 0.2% PBS-Tx. Tissues were incubated overnight at 4°C in antibody diluted in 5% NGS-PBS-Tx. Primary antibodies were used at the following concentrations: 1:50 anti-prospero, MR1A (Spana and Doe, 1995), 1:50 mouse anti-Chaoptin, 24B10 (Zipursky *et al.*, 1984; Van Vactor *et al.*, 1988); 1:50 rat anti-Elav, 7E8A10 (Robinow and White, 1991; Koushika *et al.*, 1996); 1:100 mouse anti-Cysteine String Protein (CSP), 6D6 (Zinsmaier *et al.*, 1994); 1:10 anti-Fasciclin II (FasII), 1D4 (Grenningloh *et al.*, 1991); 1:20 or 1:50 nc82 (anti-Bruchpilot; Kittel *et al.*, 2006; Wagh *et al.*, 2006) and 1:50 anti-β-gal, 40-1a, all from Developmental Studies Hybridoma Bank (DSHB, Iowa City); 1:500 rabbit anti-Repo (Campbell *et al.*, 1994; Halter *et al.*, 1995); 1:400 guinea pig anti-Brain Specific Homeobox (BSH; Jones and McGinnis, 1993); 1:100 mouse anti-BOSS (Cagan *et al.*, 1992), 1:1000 rabbit anti-GFP (Invitrogen, Carlsbad, CA), and 1:100 rabbit anti-β-gal (Molecular Probes: Eugene, OR, USA). The immunogen against which each antibody was raised and information on the characterization of antibody specificity are both given in Table 6.1. After six washes in 0.2% PBS-Tx, we used one of the following single or combined secondary antibodies in 5% NGS: FITC goat anti-mouse, Cy5 goat anti-rabbit, Cy3 goat anti-rat, Cy3 goat anti-mouse, Cy3 goat anti-rabbit, Cy3 goat anti-guinea pig (all from Jackson ImmunoResearch Inc: West Grove, PA, USA); and Alexa 488 goat anti-mouse, or Alexa 488 goat anti-rabbit (Molecular Probes: Eugene, OR, USA) at a concentration of either

1:200 or 1:400, and washed at least six times in PBS before mounting in Vectashield medium (Vector Labs, Burlingame, CA, USA). Images were captured for confocal microscopy with either an LSM 410 or 510 instrument (Zeiss, Jena, Thüringen, Germany). Images were edited for publication with Adobe Photoshop CS2.

6.3.3 Electron Microscopy and Histology

The heads of adult flies were removed and bisected in a cacodylate-buffered PFA and glutaraldehyde fixative, and processed for EM, as previously described (Meinertzhagen and O'Neil, 1991). To examine retinas, tissue embedded in PolyBed 812 (Cat. No. 08792-1: PolySciences, Inc.,Warrington, PA, USA) was sectioned at 1.0 µm and stained with a 1% toluidine blue, 1% borate solution at 60°C, rinsed with H_20 then examined by light microscopy (Zeiss Axiophot) using a 40x/0.75 Plan Neofluar objective. Images were captured with a Zeiss AxioCam MRc 5 camera and Zeiss AxioVision imaging software. For EM, 60 nm sections of the optic lobe were collected, stained in uranyl acetate and lead citrate, then examined and compared with sections from similarly prepared wild-type lamina and medulla tissue.

To examine photoreceptor axons in the medulla, *MT14-GAL4* and *GMR-GAL4* with or without *UAS-runt* were crossed to the *UAS-HRP::CD2* reporter line to drive expression of Horse Radish Peroxidase (HRP) at the plasma membrane (Larsen *et al.*, 2003). Sites of HRP expression were confirmed from an electron-dense precipitate formed in the presence of 3,3'-diaminobenzidine (DAB; Graham and Karnovsky, 1966; Larsen *et al.*, 2003). Heads were fixed on ice in 4% PFA and 0.5% glutaraldehyde in 0.1M PB. For increased penetration of DAB, brains were either dissected out during fixation or after fixation heads were sliced at 100 µm using a Vibratome. After two washes in PB, brains were treated for 20 min with fresh 1% sodium borohydride in 0.01M PBS followed by four washes in 0.01M PBS. DAB solution was prepared from tablets (Cat. No. D5905: Sigma, St. Louis, MO, USA) at a concentration of 0.2 - 0.5mg/ml with 6mg/ml of nickel ammonium sulfate in 0.01M Tris Buffered Saline (pH 7.6). Brains were incubated in filtered DAB solution at least 30 min prior to adding 0.03% H_2O_2 at a final concentration of 3-6 X 10^{-6} v/v. Incubation times in reactive DAB varied up to 1 h, after which brains were washed three times in TBS and post-fixed in 0.5% osmium tetroxide (Cat. No.19150: Electron Microscopy Sciences, Hatfield, PA, USA) in veronal acetate buffer for 30 min, dehydrated, embedded in PolyBed 812 and sectioned as before. Sections

were viewed at 80kV in a Philips Tecnai 12 electron microscope.

Measurements and analysis were performed with software (NIH ImageJ). Per fly, at least 80 profiles of capitate projections were measured that contained the diameter of the capitate projection head, with the membranes of the photoreceptor and glial membranes clearly delineated and the glial core clearly visible. Measurements were made from at least two flies of each representative genotype, except for those from the R7 and R8 terminals in wild-type medulla, which were measured through the depth of three columns from a single fly.

TABLE 6.1 - ANTIBODY DOCUMENTATION AND SPECIFICITY

PROTEIN	TARGET	SEQUENCE/SOURCE	SPECIES	SOURCE	SPECIFICITY CHARACTERISED BY	REFERENCES
Chaoptin	sensory neurons	Head homogenates	mouse	DSHB (24B10: Benzer)	Western blot	Zipursky *et al*., 1984; Van Vactor *et al*., 1988
ELAV	post-mitotic neuronal nuclei	Complete ORF *D.m.* fusion protein	rat	DSHB (7E8A10: Rubin)	Immunoprecipitation, absent labelling in 28% of $elav^{e5}$ */Y* flies	Robinow and White, 1991
CSP	vesicles	*D.m.* CSP-GST fusion protein	mouse	DSHB (6D6/DCSP-2: Benzer)	Western blot	Zinsmaier *et al*., 1990; Zinsmaier *et al*., 1994
FasII	L1/L3	Complete ORF *D.m.* fusion protein	mouse	DSHB (1D4: Goodman)	Failure to label in *fasII* null mutants	Grenningloh *et al*., 1991
Bruchpilot	synaptic sites	Head homogenates	mouse	DSHB (nc82: Buchner)	Reduced label in flies w/ Brp RNAi	Wagh *et al*., 2006
Repo	glial nuclei	Whole protein	rabbit	J. Urbin	Failure to label in $repo^{2}$ and $repo^{3}$ alleles	Halter *et al*., 1995
BSH	L4/L5	Final 136 AA of BSH protein	guinea pig	L. Zipursky	Failure to label in *bsh* null mutants, 2nd generation Ab labelling identical to 1st in WT	Jones and McGinnis, 1993; Poeck et al., 2001
β-gal	β-gal	*E. coli* β-galactosidase	rabbit	Molecular Probes	Failure to label in flies lacking lacZ expression construct.	Degreave *et al*., 1996; personal observation
β-gal	β-gal	*E. coli* β-galactosidase 116kDa	mouse	DSHB (40-1A: Sanes)	Failure to label in flies lacking lacZ expression construct	personal observation
Prospero	neuroblasts, R7 and cone cells	AAs 1196 to 1320 of the Pros protein.	mouse	DSHB (MR1A: Doe)	No immunoreactivity in *pros* null alleles	Spana and Doe, 1995
BOSS	R8	N-terminal domain	mouse	L. Zipursky	Failure to label $boss^{1}$ mutant eye discs. Western blot.	Cagan *et al*., 1992
GFP	GFP	Whole *Aequorea victoria* GFP protein	rabbit	Invitrogen	Failure to label in flies lacking GFP expression construct	personal observation

6.4 RESULTS

Drosophila mutants provide many examples of aberrant photoreceptor pathfinding. Photoreceptor axons often bypass their target neuropile if: 1) they are unable to detect their target, 2) the target fails to form correctly and/or provide "stop" signals to ingrowing photoreceptors; or 3) because they are unable to defasciculate from pioneering axons when traversing the target neuropile (Mast *et al.*, 2006). Photoreceptors growing into the lamina release two signals, Hedgehog and the EGF-like ligand Spitz, that result in the final mitotic division and differentiation of lamina neurons (Selleck *et al.*, 1992; Huang and Kunes, 1996, 1998; Huang *et al.*, 1998). Given that R1-R6 normally terminate in the lamina, we first wondered whether R1-R6 axons were required to terminate there to enable their correct synaptic partners to continue to differentiate, or whether their target neurons would develop normally even when the R1-R6 photoreceptor axons bypass them to terminate in the medulla.

6.4.1 LAMINA NEURONS MAINTAIN THEIR FATES EVEN WHEN R1-R6 PHOTORECEPTORS MISTARGET TO THE MEDULLA

As previously shown (Kaminker *et al*., 2002), axons of R1-R6 photoreceptors that express the transcription factor *runt* bypass the lamina and establish terminals in the underlying medulla that persist into adulthood. We utilized the yeast *GAL4/UAS* system to drive exogenous expression of *runt* in subsets of photoreceptors, resulting in aberrant axonal pathfinding and, ultimately, incorrect synaptic targeting. Immunocytochemical analysis of nuclear Elav reveals that when R1-R6 photoreceptor axons mistarget to the medulla, lamina monopolar neurons are nevertheless induced to form, and that these then persist into adulthood (Figure 6.1A-F). To identify the structure and location of cells in the optic lobe relative to the mistargeted R1-R6 axons, we used various markers to analyze successive developmental stages, from the third-instar larva to the adult.

In wild-type larvae, the R1-R6 axons terminate in the lamina plexus, between layers of epithelial and marginal glia (Poeck *et al.*, 2001), while *runt* expressing R7-R8 axons terminate in the medulla (Figure 6.1A). When Runt is over-expressed in all photoreceptors using the *GMR-GAL4* driver, many photoreceptor axons bypass the lamina and terminate in the medulla (Kaminker *et al.*, 2002; Figure 6.1B). This transformation in R1-R6 axon trajectories enables us to examine the effects of mistargeting axons to new synaptic partners.

In the wild-type pupa (Figure 6.1C), R1-R6 growth cones form a distinct lamina plexus between layers of lamina glia and below the Elav-immunoreactive nuclei of lamina monopolar neurons, L1-L5 (Robinow and White, 1991). In developing *GMR-GAL4/UAS-runt* flies the lamina plexus is absent. Occasionally the medulla fails to rotate to its normal position, with columns lying parallel to the retinal cornea, as demonstrated in a P+40% pupa (Figure 6.1D), and in many cases the medulla completely fails to rotate by adult eclosion (data not shown). Despite the failure of the medulla to rotate, and the absence of a clear lamina plexus, neuronal nuclei, presumed to be those of L1-L5, are compressed between en-passant photoreceptor axons. In both adult OR and Runt-overexpressing flies we can distinguish layers of glia and monopolar cells in the lamina cortex (Figure 6.1E-F).

Runt over-expression also affects the structure of the retina in the second half of pupal metamorphosis. At P+40%, approximately 48 h into metamorphosis, the developing retina looks relatively normal in horizontal sections (Figure 6.1D). By P+60% it is apparent that the ommatidia have failed to elongate (not shown); some ommatidia remain in a proximal location while others appear to rise above their neighbours so that by eclosion the eyes are severely disrupted. From longitudinal sections of the adult retina (Figure 6.1F) and observation of the eye's surface, the retina is smaller than wild-type and lacks distinct facets. This reduction in eye size may be responsible for the apparent reduction in the size of the lamina, given that the number of ommatidia in the fly's eye corresponds to the number of cartridges in the lamina (Braitenberg, 1967).

Expression of lamina monopolar-cell-specific proteins, such as BSH in L5 (Poeck *et al.*, 2001) and FasII in L1 and L3, reveals that these protein markers continue to be expressed despite the mistargeting of photoreceptors (Figure 6.1G-J). Their expression suggests that cell fate is properly established and maintained in at least three subtypes of monopolar cells and possibly others, although cell number appears to be reduced for these monopolar subtypes. In mutant flies, the arrangement of proximally located BSH-labelled L5 neurons is disordered and there appear to be fewer cells overall, presumably because of a reduction in lamina size. FasII expression is also maintained in L1 and L3 at least up to P+60% pupal development (Figure 6.1I, J), after which time protein expression is down-regulated (Hiesinger *et al.*, 1999). While expression of neuron-specific markers Elav, Dachshund (Mardon *et al.*, 1994; Huang and Kunes, 1996) and BSH has been reported in the lamina cells of pathfinding mutants (Hing *et al.*, 1999;

Kaminker *et al.*, 2002; Choe *et al.*, 2006), such expression has previously been examined shortly after lamina cell differentiation, in the third-instar larva. Here, we report evidence that the fates of these neurons are maintained through development and that the cells persist in the adult lamina.

6.4.2 PHOTORECEPTORS IN THE RETINAS OF *RUNT* OVER-EXPRESSING FLIES ADOPT ALTERNATIVE FATES

Cross-sectioned ommatidia in semi-thin sections of *UAS-runt/*+; *MT14-GAL4/*+ retinas clearly reveal that after Runt over-expression ommatidia occasionally have a normal complement of eight photoreceptor neurons. As seen in the wild-type fly the large rhabdomeres of photoreceptors R1-R6 form an outer trapezoidal pattern which surrounds a smaller centrally located rhabdomere, R7 in the distal retina (Figure 6.2A) or R8 in the proximal retina (Figure 6.2B). Unlike a previous report (Kaminker *et al.*, 2002), however, our findings revealed frequent aberrations (>82% of ommatidia, N= 435) in photoreceptor structure upon *UAS-runt/*+; *MT14-GAL4/*+ over-expression. In *runt* overexpression flies (Figure 6.2C, D), any number or combination of R1-R6 photoreceptors were aberrant, from one to four per ommatidium. Their rhabdomeres were smaller in diameter and located within the circumference of neighbouring R1-R6 rhabdomeres. Rhabdomeres were clearly of one size or another, clearly discriminable and without intermediates. The aberrations are not confined to R2, and R5 the outer photoreceptors in which *MT14-GAL4* was previously reported (Kaminker *et al.*, 2002) to drive expression (Figure 6.2C) but are most frequently observed in R1, R3, R4 and R6. Our observations from *UAS-mCD8::GFP/*+;;*MT14- GAL4/*+ flies indicate that on average four photoreceptors per ommatidium in the larval eye disc have *MT14* driver expression. These include Prospero-immunolabelled R7 cells (Figure 6.3D) and BOSS-immunolabelled R8 cells (Figure 6.3I). Small diameter rhabdomeres are characteristic of R7 and R8 cells, both of which express *runt* during normal development (Kaminker *et al.*, 2002), leading us to investigate further whether these R1-R6 photoreceptors with smaller rhabdomeres had other alternate photoreceptor characteristics.

In order to determine if R1-R6 photoreceptors with transformed rhabdomeres maintained their other characteristic features we examined *Rhodopsin1* (Rh1) driver activity in *UAS-runt/Rh1-lacZ*; *MT14-GAL4/*+ eyes. Rh1, encoded by the gene *ninaE,* is the light-absorbing opsin of R1-R6 photoreceptors (O'Tousa *et al.*, 1985), and is expressed late in

development after photoreceptor cell fate is fully established. In *Rh1-lacZ* flies, the *Rh1* promoter drives expression of exogenous *lacZ,* the protein product of which -- β-gal -- is detectable by immunocytochemistry. *Rh1* can therefore be used to distinguish R1-R6 from the R7 and R8 photoreceptors, which express different opsins. In the eyes of *UAS-runt/Rh1-lacZ*; *MT14-GAL4/+* flies we identified three outcomes to this labelling: 1) R1-R6 rhabdomeres are large and all cells express *Rh1* driven β-gal (Figure 6.2E), as in wild-type; 2) a small rhabdomere forms in a cell body that has no β-gal expression (Figure 6.2F); or 3) a small rhabdomere forms but its cell body continues to express *Rh1* driven β-gal (Figure 6.2G). Of the photoreceptors with smaller rhabdomeres, most (93%, N=28) are from cell bodies that failed to express β-gal, and had thus undergone transformation to an alternative photoreceptor cell fate.

Once these findings had clearly shown that photoreceptor fate was indeed altered, it was imperative to determine if photoreceptors R1-R6 were transformed to R7 or to R8, for which reason we next sought markers for these specific photoreceptor subtypes. R7 and R8, have different peaks of spectral sensitivity (Hardie and Kirschfeld, 1983). Each photoreceptor type is divided into subclasses depending on the exact Rhodopsin expressed (Morante and Desplan, 2004). There are two subtypes of R8 cell, one that expresses Rh5 (Chou *et al.*, 1996; Papatsenko *et al.*, 1997) and absorbs light with wavelengths in the blue region of the spectrum, and the other that expresses Rh6 and absorbs in the green (Townson *et al.*, 1998; Salcedo *et al.*, 1999). R7 cells also have two subtypes with opsins Rh3 (Fryxell and Meyerowitz, 1987; Zuker *et al.*, 1987) and Rh4 (Montell *et al.*, 1987), both of which absorb light in the UV.

In *UAS-runt/+*; *MT14-GAL4/Rh3-lacZ* flies β-gal is immunolocalised to a subset of R7 (Figure 6.3A) cells as well as to a subset of small transformed outer rhabdomeres (Figure 6.3B, C). In 37 ommatidia examined, 35 transformed rhabdomeres were identified of which 66% were immunoreactive for *Rh3* driven β-gal expression, with 33% expressing an unknown opsin (Figure 6.3C). In *UAS-runt/+*; *MT14-GAL4/Rh6-lacZ* flies β-gal is immunolocalised to a small subset of central R8 photoreceptors (Figure 6.3F, G), which in a wild-type ommatidium extend their cell body between R1 and R2. Additional *Rh6-lacZ* expression was associated with small transformed outer rhabdomeres (Figure 6.3G). We crossed *Rh4-lacZ* and Rh5-lacZ into a *UAS-runt; MT14- GAL4* background but found expression of neither of these opsins in transformed outer rhabdomeres (data not shown). *LacZ* expression was virtually eliminated in *UAS-*

runt; *MT14-GAL4/Rh5-lacZ* eyes (not shown). This loss was unexpected considering that many central R8 photoreceptors in *UAS-runt/*+; *MT14-GAL4/Rh6-lacZ* do not have *Rh6-lacZ* expression (Figure 6.3H). It is unknown what opsin these R8 photoreceptors express.

Despite the presence of excess R7 and R8 photoreceptors in the adult, Prospero and BOSS immunolabelling of larval eye discs did not reveal excess R7 (Figure 6.3D, E) or R8 (Figure 6.3I, J) cells in *UAS-mCD8::GFP/*+;*UAS-runt/*+; *MT14-GAL4/*+ flies (Figure 6.3E, J) when compared with the wild-type *UAS-mCD8::GFP/*+;; *MT14-GAL4/*+ (Figure 6.3D, I) eye disc, similar to the findings of Kaminker *et al*.(2002). The lack of excess R8 photoreceptors in the eye disc is not surprising given that BOSS expression precedes *MT14-GAL4* driven *UAS-mCD8::GFP* expression in the larval eye disc (not shown), and thus would also precede *runt* over-expression using this driver line.

6.4.3 Effects of Runt Over-Expression on R7 and R8 Photoreceptor Terminals

R7 and R8, the two central photoreceptors of the ommatidium, have axons that terminate in two distinct layers of the medulla, R8 in the distal stratum M3, and R7 deeper, in stratum M6 (Fischbach and Dittrich, 1989). There, processing of the different spectral inputs from each type of terminal is presumed to occur in stratum-specific circuits (Morante and Desplan, 2004). We initially used photoreceptor-specific Chaoptin immunolabelling to visualize terminals in the medulla, making it impossible to determine the individual contributions from R7, R8, or ectopic R1-R6 photoreceptor terminals, which thus required us to utilize photoreceptor subtype-specific markers.

Before attempting EM analysis of the medulla, we examined the structure of R7 and R8 terminals in mutant flies at the light microscope level. R8 terminals were visualized using *Rh5-lacZ* and *Rh6-lacZ*, in *GMR-GAL4,UAS-runt/*+ and *UAS-runt*; *MT14-GAL4* (not shown) flies. These *lacZ* lines clearly labelled distinct subsets of wild-type R8, both of which are swollen in two locations in the medulla, distally, just above M1, and at their enlarged terminals in stratum M3, as shown here for *Rh6-lacZ* (Figure 6.4A, B). *GMR-GAL4* driven over-expression of *runt* (Figure 6.4C, D) resulted in more slender *Rh6-lacZ* expressing R8 terminals, some of which bypassed M3 to terminate deeper at M6 (Figure 6.4D). *Rh6* expressing R8 terminals have a disorganised appearance in *GMR-GAL4,UAS-runt* (Figure 6.4C) medullas when compared to wild-type (Figure 6.4A)

terminals visualized in a ~40 µm depth of tissue. In *GMR-GAL4,UAS-runt/CyO*; *Rh5-lacZ/+* flies, as was previously noted in the eye, *Rh5* driven β-gal expression is almost completely lost, with only two R8 terminals detected in the 12 brains that were analyzed (data not shown).

In order to examine R7 terminals after *runt* over-expression, the *Rh3-lacZ and Rh4-lacZ* lines were used. As seen in *Rh3-lacZ* expressing flies, wild-type R7 axons expanded in the M6 layer of the medulla where they terminated (Figure 6.4F), behaviour that was replicated in the Runt over-expression flies (Figure 6.4H), yet not all R7 axons were successful in extending and maintaining terminals down into the M6 layer of the adult medulla. Furthermore, in *runt* over-expression flies R7 terminals were more numerous (Figure 6.4G) than in the wild-type (Figure 6.4E) but do not appear to cluster into the 'blebs' characteristic of *Rh1-lacZ* expressing terminals in the medulla of mutant flies (Figure 6.5B). In *Rh4-lacZ/GMR-GAL4,UAS-runt* flies there is a reduction in *Rh4-lacZ* expressing terminals which would normally constitute 70% of wild-type R7 cells (Franceschini *et al.*, 1981). *Rh4-lacZ* expression was limited to the anterior region of the eye and thus to terminals in the posterior medulla when a strong *GAL4* driver is used, such as in *Rh4-lacZ*/*GMR- GAL4, UAS-runt*, but was more widely expressed in *Rh4/lacZ/UAS-runt*; *MT14-GAL4/+* flies (data not shown).

6.4.4 Medulla Terminals of Mistargeted R1-R6 Photoreceptors Express Synapse Associated Proteins

To recognize ectopic terminals in the adult medulla we employed the *Rh1-lacZ* expression construct in flies with both *UAS-runt* and *MT14-GAL4*, in a similar strategy as that for R7 and R8, above. In the phenotypically wild-type lamina (Figure 6.5A), R1-R6 axons converge upon a cartridge and each swells to form a cylindrical synaptic terminal running the depth of the lamina. In *UAS-runt/Rh1-lacZ*; *MT14-GAL4/+* flies some R1-R6 photoreceptors maintain the appropriate Rh1 driver expression yet terminate ectopically in the medulla. When the axons from R1-R6 extend to the medulla their terminals fail to form elongated cylindrical structures, as they do in the lamina. Instead swelling is intermittent, occurring at different levels within the medulla so as to form blebs along the length of the axons (Figure 6.5B). Axons extended into the medulla in bundles, but we were not able to discern whether these blebs represented multiple swellings along the length of a single axon or the terminal swellings of different photoreceptors in a single

axon bundle, each of which terminated at a different stratum in the medulla. Moreover, these axonal swellings were not restricted to the M3 and M6 layers, the normal terminal locations of the R8 and R7 photoreceptors.

To determine whether the blebs were sites of synaptic specialisations, we used antibodies against known synaptic or synapse-associated proteins. Photoreceptor synaptic zones have distinct specialisations that include many synaptic vesicles, capitate projections, and synaptic T-bar ribbons that comprise a pedestal, anchoring proteins and a surmounting platform (Prokop and Meinertzhagen, 2006). Synaptic vesicles were recognized by their association with CSP (Zinsmaier *et al.*, 1990), which is involved in Ca^{2+}-dependent exocytosis (Zinsmaier *et al.*, 1990; Chamberlain and Burgoyne, 2000; Evans *et al.*, 2003). CSP immunolabelling is localised to all areas of synaptic release, including the R1-R6 photoreceptor terminals in the lamina of wild-type flies (Figure 6.5C). In *runt* over-expression mutants CSP continued to be expressed in the lamina and medulla (Figure 6.5D), and overlapped *Rh1* driven β-gal around the profile perimeters of photoreceptors in the lamina (Figure 6.5G) and ectopic photoreceptor terminal blebs in the medulla (Figure 6.5H). The overlap suggests that these blebs contained synaptic vesicles, and were thus candidate sites for synapses. Presynaptic sites also contain Bruchpilot, a coiled-coil domain protein localised to the active zone of neuromuscular junctions and the optic neuropiles (Figure 6.5E) by the antibody nc82 (Kittel *et al.*, 2006). In *UAS-runt/Rh1-lacZ*; *MT14-GAL4/+* flies, nc82 co-localised with β-gal expression (Figure 6.5F) to photoreceptors in the lamina (Figure 6.5I) and to terminals of ectopic R1-R6 photoreceptors in the medulla (Figure 6.5J). This co-localisation suggests that these terminals contained the T-bar ribbons at which synaptic release occurs.

We wanted to determine if an individual Runt-overexpressing photoreceptor was capable of swelling and expressing synaptic proteins in both the lamina and medulla. To do this we utilized a *MARCM*-style approach to label individual photoreceptors which expressed both *UAS-runt* and *UAS-mCD8::GFP* under control of the *GMR-GAL4* driver. Horizontal slices of adult *hsFLP/UAS-mCD8::GFP*; *NeoFRT40A actin-GAL80/ NeoFRT40A, GMR-GAL4, UAS-runt* fly heads co-labelled with antibodies against GFP and Bruchpilot (nc82) revealed that most GFP expressing photoreceptor axons expanded and terminated either in the lamina (Figure 6.5L, N), or alternatively bypassed the lamina (Figure 6.5M) to expand and terminate in the medulla. Furthermore, the photoreceptor phenotypes

that characterise cell-fate transformation after Runt overexpression using either *GMR-GAL4* (Figure 6.1F) or *MT14-GAL4* (Figure 6.2) drivers, were not observed in GFP expressing cells in the *MARCM* eye. So, R1-R6 *MARCM* photoreceptors expressing GFP, and thus, also overexpressing Runt under control of *GMR-GAL4*, had large rhabdomeres characteristic of wild-type R1-R6 (Figure 6.5K).

Many Runt overexpressing GFP labelled cells were found in the retina. Of all ommatidia (N=302), 53% contained either an R7 or R8 cell expressing GFP. Some of these could also contain R8 or R7, but because they are tiered these could not be seen in a single section; most sections were cut at the R7 level. 24% of all R1-R6 cells (N=1830) were labelled. These relatively large numbers of cells made it difficult to discern the axons of individual cells, isolated from those of their neighbours.

Some axons (<2 per brain), appeared to expand in both the lamina and medulla (Figure 6.5O, P). Clear images of these required considerable searching. Unlike wild-type R7 or R8 axons, which do not expand in the lamina (Figure 6.5I), these axons were enlarged in both the lamina (Figure 6.5O', P') and medulla, shown terminating in the distal medulla near M3 (Figure 6.5 O", P"). These axons were wider along their entire length than those of wild-type R7 or R8 cells, and also had atypical expansions in the chiasm (Figure 6.5O). It is not known if these are single or multiple, bundled axons; the fact that the labelled profile terminated in only a single medulla stratum (M3) suggested that it was not the bundled axons of both R7 and R8. Furthermore, a lack of small transformed outer R1-R6 rhabdomeres suggested that any individual ommatidium does not project a bundled pair of R8 axons to the medulla that terminates in M3. Together, these considerations suggest that the occasional large axons may be from single photoreceptors: either an R8 cell that expands abnormally in the lamina or an R1-R6 cell that terminates ectopically in the medulla. The phenotype following *MARCM*-style Runt overexpression is considerably less severe, as it relates to photoreceptor cell fate transformation and axon termination errors, than that observed following Runt-overexpression alone.

6.4.5 R1-R6 PHOTORECEPTORS CONTINUE TO FORM SYNAPSES IN THE LAMINA

To interpret the lamina phenotype that results when Runt is expressed in R1-R6 first requires explanation of the normal axon trajectories of R1-R6 in the adult lamina. In the

wild-type lamina, axon bundles from each ommatidium innervate the lamina cortex, and the six photoreceptor axons from R1-R6 then diverge from their bundle and sort into different cartridges (Trujillo-Cenóz, 1965; Braitenberg, 1967), according to the principle of neuronal superposition (Braitenberg, 1967; Kirschfeld, 1967). Each lamina cartridge is thus a module comprising these six R1-R6 terminals and the fixed group of lamina cells they innervate (Figure 6.6A). Along the axis of the cartridge the axons of two lamina cells, L1 and L2, extend dendrites that embrace the terminals of R1-R6 and with other lamina cells form tetrad synapses (Figure 6.6C-F; Meinertzhagen and O'Neil, 1991). These are sites of release of the photoreceptor neurotransmitter, histamine (Hardie, 1987). Unlike R1-R6, the axons of R7 and R8 extend alongside the cartridge without synaptic engagement.

Flies with exogenous Runt expression in R1-R6 have disordered lamina cartridges but still display features characteristic of wild-type photoreceptor terminals. The laminas of both *GMR-GAL4* (not shown) and *MT14-GAL4* driven *UAS-runt* flies are highly disorganised (Figure 6.6B). Photoreceptor profiles bundle with the axons of lamina neurons and are surrounded by epithelial glia to form a disordered association. Such aberrant cartridges contain the expanded synaptic profiles typical of R1-R6 terminals but are formed by axons that in fact may neither sort into cartridges nor even terminate in the lamina. Other axon profiles are possibly R1-R6 axons that, like the normal profiles of R7 and R8, also bypass the lamina without forming synapses at that particular level. They may also be axons from R1-R6 cells that have transformed into supernumerary R7 and R8 cells. Expanded photoreceptor profiles in these aberrant cartridges resemble wild-type R1-R6 terminals in containing capitate projections (Trujillo-Cenóz, 1965), synaptic vesicles, mitochondria and tetrad synapses (Figure 6.6G-I). Capitate projections are photoreceptor-specific organelles, sites of endocytotic recovery of synaptic vesicle membrane and also proposed sites for localised histamine recycling (Fabian-Fine *et al.*, 2003). The presence of this suite of organelles suggests that these terminals possess the means for synaptic release, while the presence of mitochondria suggests that they are energetically equipped to do so (Górska-Andrzejak *et al.*, 2003).

Our findings from mutant lamina ultrastructure also reveal that in *UAS-runt/+*; *MT4-GAL4/+* flies, the axons of R1-R6 photoreceptors continued to form reciprocal synaptic inputs with lamina neurons, most probably with their normal targets in that neuropile. Feedback synapses onto R1-R6 in are found in the distal lamina, although we have not

identified the profiles presynaptic to these mutant photoreceptors (Figure 6.6J). In the wild-type, most synaptic feedback comes from amacrine cells, with fewer contributions from L2 and L4 in the distal lamina (Meinertzhagen and O'Neil, 1991).

6.4.6 Supernumerary Photoreceptors Form Synapses in the Medulla

When *GMR-GAL4* is crossed into the *UAS-HRP::CD2* reporter construct, the axons of all photoreceptor neurons can be identified in electron micrographs. In *UAS-HRP::CD2* expressing flies, HRP is localised to the membranes of cells and can be visualized in EM from the formation of an electron-dense precipitate after incubation with DAB and H_2O_2 (Larsen *et al.*, 2003). In the wild-type *Drosophila* lamina, the slender axons of R7 and R8 extend alongside the cartridge of their retinal R1-R6 neighbours (Figure 6.7A). They penetrate the lamina and innervate the medulla, where in the distal strata, beneath M1, their profiles were normally small and unexpanded (Figure 6.7B). Exposure to DAB/H_2O_2 revealed large terminals with electron dense membrane in the distal medulla of both *GMR-GAL4/UAS-runt*; *UAS-HRP::CD2/+* (not shown) and *UAS-HRP::CD2/UAS-runt*; *MT14-GAL4/+* flies (Figure 6.7C). These photoreceptor axons tended to cluster in groups and form terminal swellings (Figure 6.7D). Counts of photoreceptor terminal profiles from the medullas of two flies indicate variation in the number of photoreceptors terminals per column. The number of terminals per cluster ranged from 3 to 8, with an average of 4.77 terminals per column (N=13 columns), more than the normal 2 profiles (R7 and R8).

Supernumerary photoreceptor terminals in the medulla contained many of the features characteristic of wild-type R1-R6 photoreceptor terminals in the lamina. These included the mitochondria, vesicles, presynaptic T-bar ribbons and, most notably, capitate projections. The hyperinnervation of the medulla that results from supernumerary R7 photoreceptors and ectopically projecting R1-R6 photoreceptor axons appeared to be fully supported by the medulla target cells, which imposed no clear restriction to the formation of novel photoreceptor synapses. We analyzed nine columns with supernumerary photoreceptor clusters through a depth of 120-360 nm. Of these, at least eight columns had synapses in three distinct photoreceptor terminals, indicating that a column can support more photoreceptors than those two terminals (R7, R8) normally present in a wild-type medulla column. Furthermore, in four of nine columns, 100% of the supernumerary terminals contained synapses, sometimes with up to eight

photoreceptor terminals forming input synapses to a column.

While supernumerary photoreceptors in the medulla were able to form synapses complete with a T-bar ribbon, what was perhaps most striking was the number of postsynaptic partners at some release sites. Tetrads were readily detected in the medulla (Figure 6.7J-M), just as R1-R6 would normally form in the lamina. The normal synapses of wild-type R7 (Figure 6.7 E-I) and R8 terminals, by contrast, can form tetrads but are mostly triads, with three postsynaptic partners (Takemura *et al.*, 2008). For synapse counts in supernumerary terminals, a 350 nm depth of tissue was examined for seven columns each of which contained more than four photoreceptor terminals. We identified 35 synapses, 22 of which were tetrads. Of synapses that could be traced through their depth, 2/25 were triads, and 1/25 was a dyad. Of those which could not be traced entirely through their depth 9 out of 10 were at least triads and the remaining synapse was at least a dyad. These numbers probably reflect incomplete tracing rather than incomplete tetrads, and their proportions compare to those found in R1-R6 in the wild-type lamina (unpublished analyses of data reported in Meinertzhagen and Sorra, 2001). Numerical conservation of the postsynaptic ensemble suggests that this tetrad organisation is determined cell autonomously by the R1-R6 photoreceptors. In the lamina the tetrad incorporates a blend of postsynaptic elements from lamina neurons L1, L2, L3, amacrine cells, and epithelial glia (Meinertzhagen and O'Neil, 1991). While the postsynaptic partners at the ectopic R1-R6 are not known, the distal medulla does contain axon terminals from the tetrad's normal lamina constituents L1-L3 (Fischbach and Dittrich, 1989). It is therefore possible that R1-R6 may synapse in the medulla as they would do in the lamina, with any combination of these three cells, but without the usual lamina amacrine and epithelial glial cells, and only if such synapses form distal to stratum M2, where the axon of monopolar cell L2 normally terminates. Given that the second expansion of L1's terminal lies in stratum M5 of the medulla, whereas ectopic R1-R6 photoreceptors extend as deep as M6 (Figure 6.5B), any synapses formed by ectopic R1-R6 photoreceptor terminals in stratum M6 must likewise be formed with novel partners. We conclude that many synapses formed by ectopic R1-R6 terminals provide inputs to at least some novel target neurons that are of medulla origin.

Even in the absence of DAB labelling in the medulla, supernumerary photoreceptor terminals were obvious, revealed by the presence of capitate projections. These had a spherical head the shape and size (175 ± 27 nm; Figure 6.7O) of which did not differ

significantly (p = 0.49 in a two-tailed *t*-test) from their counterparts in lamina terminals of R1-R6 (192 ± 20 nm; Figure 6.7P). Those of photoreceptor terminals in the lamina or medulla of *UAS-runt/+*; *MT14-GAL4/+* flies likewise did not differ significantly in size (p = 0.34 for the medulla, p = 0.99 for the lamina) from capitate projections in the wild-type lamina (194 ± 15 nm). Wild-type R7 and R8 terminals also received invaginations that resemble capitate projections, and that arose from invaginating medulla glia (95.4 ±11.8 nm, Figure 6.7N), but their size and shape in R7 and R8 photoreceptors differed from those at both the mutant lamina and medulla sites. Thus, photoreceptors revealed a conserved synaptic architecture among their capitate projections in the medulla, even in the absence of the lamina's epithelial glia, and were invaginated instead by surrounding medulla profiles that resembled glia, even though lamina and medulla have genetically distinct subsets of glia (Tix *et al.*, 1997). The invaginating glia may have been the medulla neuropile glia that express *ebony* and are presumed to regulate the metabolism of normal medulla histamine released from R7 and R8 (Richardt *et al.*, 2002). From the size similarity of R1-R6 capitate projection heads in the two locations, and the difference between capitate projections in wild-type R7 and R8, we conclude that capitate projection head size is independent of the sub-type of glial cell that invaginates the photoreceptor terminal. Rather, the similarity strongly suggests that this feature of organelle architecture is determined by the common element in both, the photoreceptor terminal.

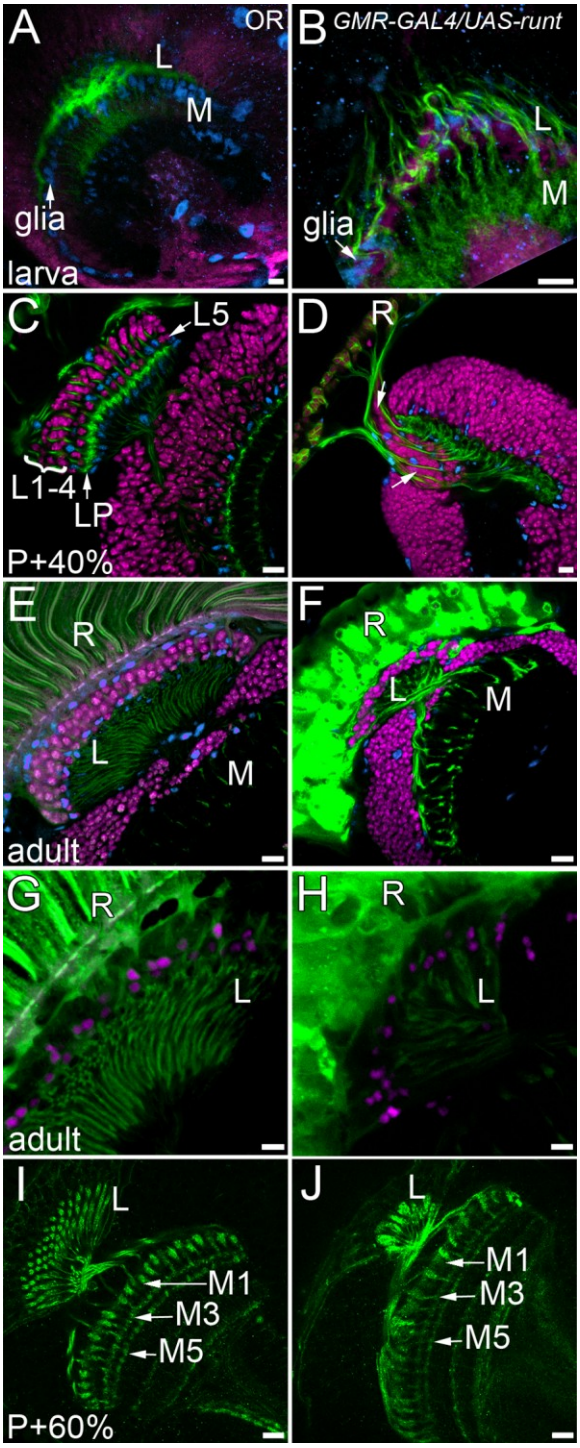

FIGURE 6.1 - LAMINA MONOPOLAR CELLS SURVIVE AND MAINTAIN EXPRESSION OF CELL-FATE MARKERS DESPITE ABERRANT PATHFINDING IN THEIR PHOTORECEPTOR INPUTS.

Oregon-R (left column, OR) and *GMR-GAL4/UAS-runt* (right column) brains, either third-instar larval wholemounts (A,B), or Vibratome slices of pupal P+40% (C,D), P+60% (I,J) or adult (E-H) brains. **A-F**: Brains are immunolabelled with antibodies against the

(FIGURE 6.1 – CONTINUED, 2 OF 2)

following markers: photoreceptor-specific Chaoptin (green); Elav (magenta), an RNA binding protein expressed in postmitotic neurons; and Repo (blue), a nuclear glial antigen. **A**: In OR larvae R1-R6 photoreceptors terminate in the lamina (L), between epithelial and marginal glia, while R7-R8 terminate in the medulla (M). **B**: When photoreceptors over-express Runt, most axons terminate in the medulla. **C**: In the wild-type pupa, R1-R6 axons terminate at the lamina plexus (LP), above which lie columns of Elav-positive nuclei of lamina neurons (L1-L5). **D**: Occasionally the medulla of *GMR-GAL4/UAS-runt* flies fails to rotate to lie parallel to the retina, as seen here at P+40%. Elav-expressing nuclei, probably those of L1-L5 (between arrows), lie compressed between *en-passant* photoreceptor axons. In adult *GMR-GMR4/UAS-runt* flies (F) the retina (R) is severely disrupted. **E**: Cell bodies of neurons are located between layers of glia in the wild-type lamina cortex. **F**: Although the lamina of *GMR-GAL4/UAS-runt* flies is highly condensed, lamina neurons survive into adulthood and are appropriately located beneath the basement membrane of the compound eye. **G-H**: BSH-immunoreactive nuclei of L5 neurons (magenta) are located just distal to photoreceptor axon terminals (Chaoptin – green) in the lamina of both OR (G) and *GMR-GAL4/UAS-runt* (H) flies. **I-J**: FasII-immunoreactive L1 and L3 monopolar neurons expand in the lamina as well as in the M1, M5 (L1) and M3 (L3) layers of the medulla, as demonstrated in the wild-type P+60% pupa (I). In *GMR-GAL4/UAS-runt* flies (J) L1 and L3 continue to express FasII and extend their axons into the medulla to terminate in the appropriate layers. Scale bars A–F, I, J, 10 μm; G, H, 5 μm.

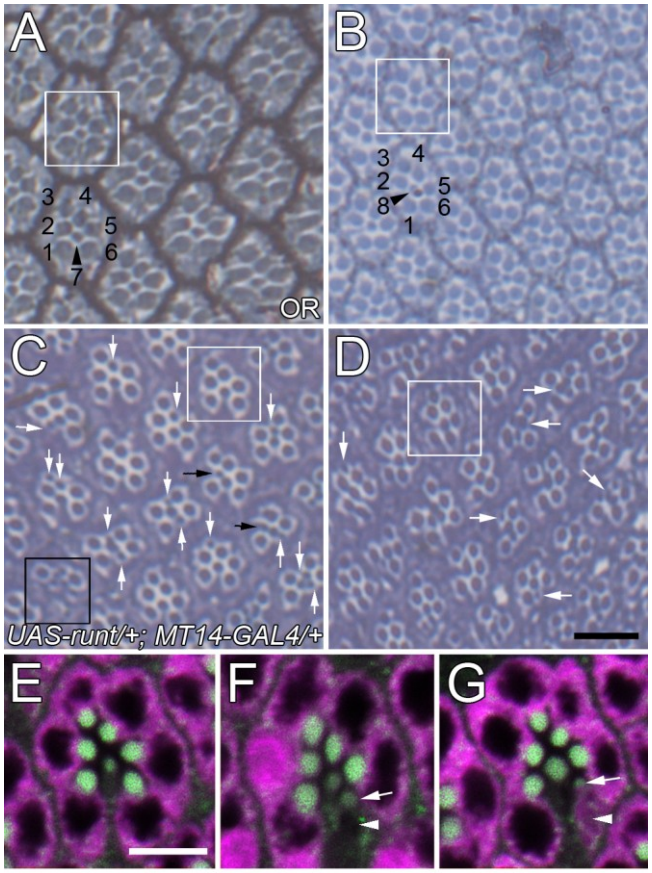

FIGURE 6.2 - PHOTORECEPTOR CELL FATES ARE ALTERED IN *UAS-RUNT/+*; *MT14-GAL4/+* FLIES.

Semi-thin sections stained with toluidine blue through the distal (A,C) and proximal (B,D) retinas of OR (A,B) and *UAS-runt/+*; *MT14-GAL4/+* (C,D) flies. **A-B**: Wild-type ommatidia have photoreceptor rhabdomes arranged in a trapezoid (white boxes in all) with larger R1-R6 rhabdomes (1-6) located external to a small centrally located rhabdomere of R7 (7-distal, A) or R8 (8-proximal, B). **C-D**: In Runt over-expressing flies some ommatidia contain the normal arrangement of rhabdomes, but most ommatidia contain at least one transformed small and centrally located rhabdomere (arrows). Even though *MT14-GAL4* is reported to drive expression in R2, R5 and R8, the transformed rhabdomeres rarely correspond to R2 or R5 (black arrows). Instead, most transformed photoreceptors are from a combination of R1, R3, R4, or R6 (white arrows), and up to 4 photoreceptors per ommatium are transformed (black box in C). **E-G**: In the eye of *UAS-runt*/*Rh1-lacZ; MT14-GAL4/+* flies, R1-R6 cells are identified with β-gal immunolabelling (magenta). **E**: In wild-type ommatidia all R1-R6 photoreceptor cell bodies express β-gal. **F-G**: When photoreceptors, visible from their rhabdomeres (green, autofluorescence), are transformed (arrows in F,G), the cell bodies of most do not express β-gal (arrowhead in F); very few transformed R1-R6 rhabdomeres neighbour a *Rh1*-driven β-gal expressing cell body (G). Scale bars A-D, 10 μm; E-G, 5 μm.

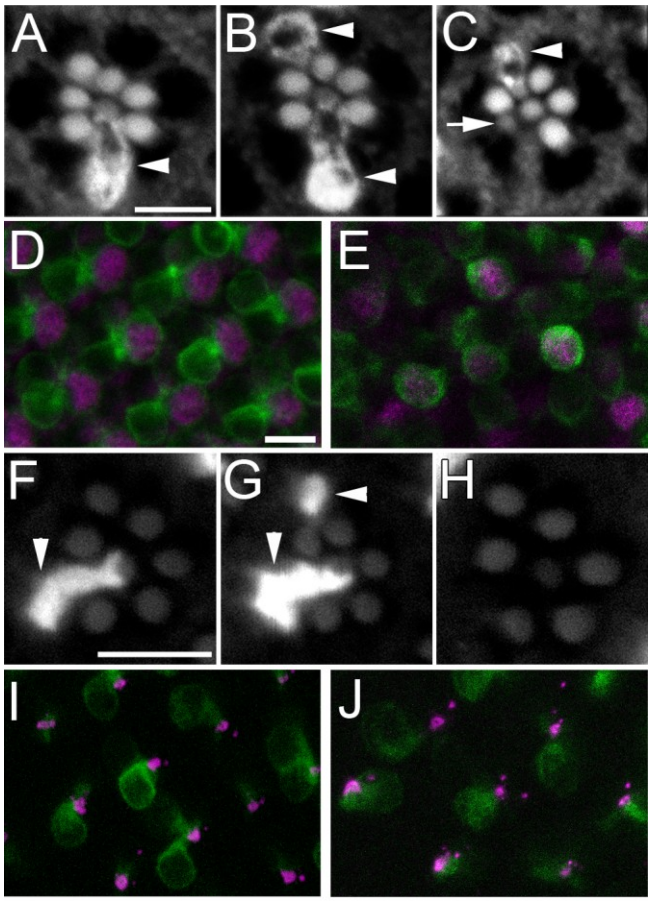

FIGURE 6.3 - TRANSFORMED R1-R6 PHOTORECEPTORS EXPRESS *RH3* AND *RH6*.

In *UAS-runt/+; MT14-GAL4/Rh3-lacZ* flies (A-C), β-gal expression is localised to R7 photoreceptors. **A**: In a wild-type ommatidium β-gal expression was limited to the cell body of the R7 photoreceptor, which has a small centrally located rhabdomere. **B-C**: In ommatidia with an excess of small rhabdomeres β-gal is immunolocalised to a subset of cells with small rhabdomeres, seen here in at the R3 position (arrowheads), independent of whether or not the central R7 also expressed β-gal. Not all transformed photoreceptors expressed *Rh3* driven β-gal expression (arrow in C). *UAS-runt/+; MT14-GAL4/ Rh6-lacZ* flies (F-H), expressed β-gal in some R8 photoreceptors. **F**: In a wild-type ommatidium the R8 rhabdomere is centrally located and the cell body protrudes between R1 and R2 (arrowhead F). **G**: However, in some mutant ommatidia outer photoreceptors, such as the one in the R3 position (arrowhead in G), are converted to *Rh6*-expressing R8 cells. **H**: Despite an almost complete lack of *Rh5* expression (not shown), many ommatidia have a central R8 photoreceptor with no *Rh6* expression. **D-E, I-J**: *MT14-GAL4* drives *UAS-mCD8::GFP* expression (green) in R7 cells (Prospero – magenta D,E), and R8 cells (BOSS – magenta I,J), however no excess of Prospero-expressing R7 nuclei (E) or BOSS-expressing R8 nuclei (J) are detected in the larval eye disc of *UAS-mCD8::GFP;UAS-runt;MT14-GAL4* flies (E) when compared with the wild-type eye discs (D,I). Scale bars (in A) A-C; (in D) D, E, I, J; (in F) F-H, 5μm.

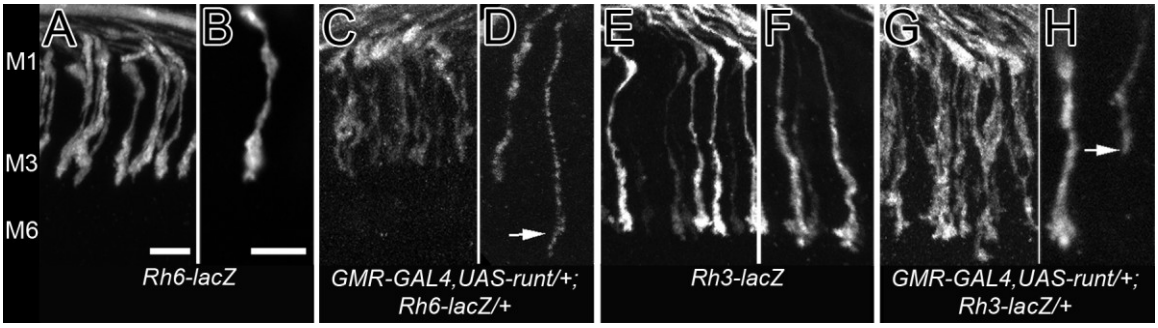

FIGURE 6.4 - RUNT OVER-EXPRESSION AFFECTS THE TERMINALS OF PHOTORECEPTORS R7 AND R8 IN THE MEDULLA.

Terminals of R7 and R8 visualized by β-gal immunolabelling from their expression of *Rh3-lacZ* (R7: E-H) or *Rh6-lacZ* (R8: A-D). For A, C, E, G, images of axon terminals were captured from a 41 μm depth of tissue. **A-B**: In the wild-type medulla all *Rh6-lacZ* expressing axons terminate in the M3 layer of the medulla (A) and have synaptic expansions at their terminal ends (B). **C-D**: Following ectopic Runt expression in *GMR-GAL4, UAS-runt/+; Rh6-lacZ/+* R8 axons in the medulla are less organised (C). There did not appear to be a change in the overall number of axons (C), however terminals appeared narrower and some extended erroneously into M6 (arrow in D). **E-F**: *Rh3-lacZ* expressing axons terminate and expand in the M6 layer of the medulla. **G-H**: Following ectopic Runt expression there are many more *Rh3-lacZ* expressing R7 terminals (G), and while the shape of correctly targeting terminals is maintained, some R7 axons terminate short of M6 (arrow in H). Scale bars (in A) A,C,E,G; (in B) B, D,F, H, 5 μm.

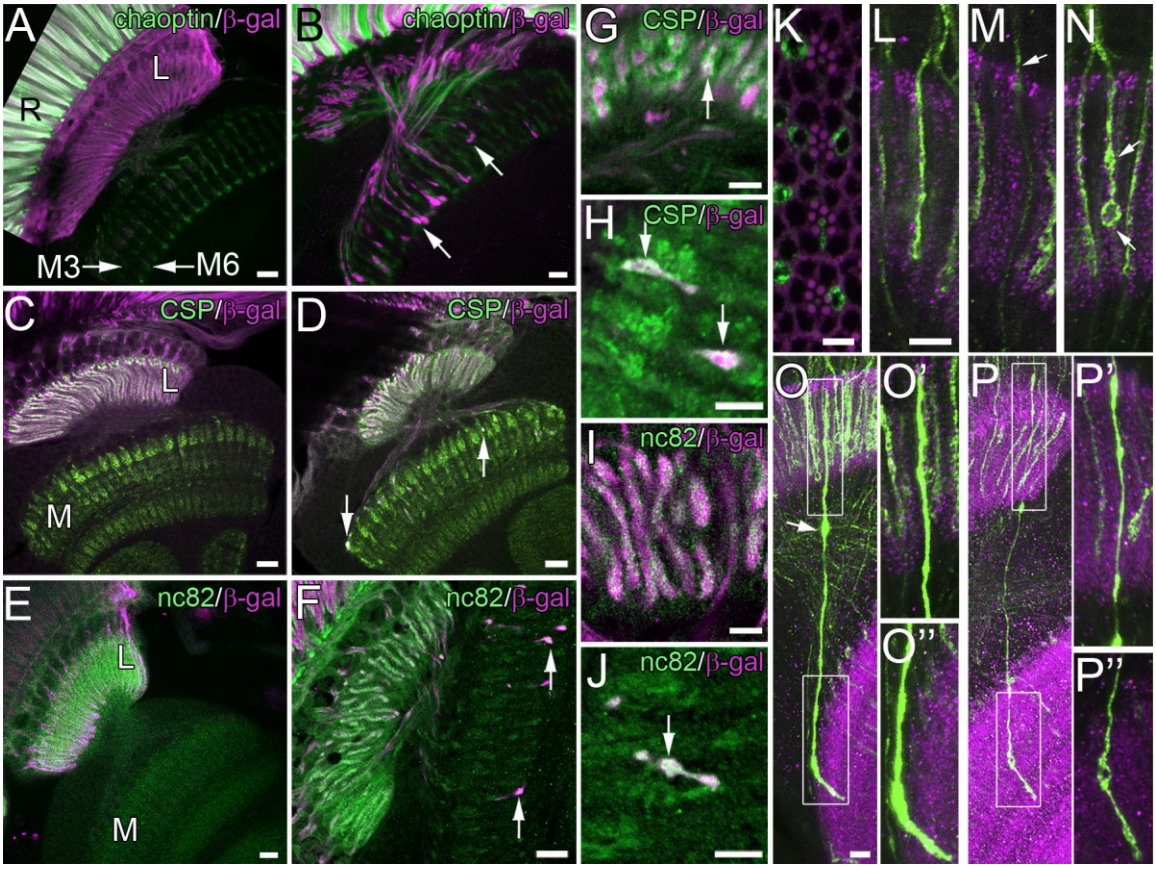

FIGURE 6.5 - ECTOPIC R1-R6 PHOTORECEPTORS IN THE MEDULLA VISUALIZED WITH *RH1-LACZ*.

A-B: Photoreceptors express *Rh1-lacZ* (R1-R6: β-gal - magenta) and anti-chaoptin immunolabelling (R1-R8: green). **A,C,E**: R1-R6 photoreceptors terminate exclusively in the lamina (L) of *Rh1-lacZ* flies. **B,D,F**: In *Rh1-lacZ/UAS-runt*; *MT14-GAL4/+* flies, ectopic R1-R6 axons innervate the medulla (M) where they extend as deep as stratum M6, forming "bleb"-like swellings along their length (arrows in B). **C-D, G-H**: Areas expressing the vesicle-associated protein, CSP, are candidate sites of synaptic release visualized in single image planes (0.8 µm) from a Vibratome slice. **C**: CSP (green) co-localised (white) to β-gal immunoreactivity (magenta) of R1-R6 photoreceptor terminals in the wild-type lamina. **D,G,H**: CSP also co-localised (arrows) to β-gal around the perimeter of R1-R6 photoreceptor terminals in the mutant lamina (D,G) and ectopic terminals in the medulla (D,H). **E-F, I-J**: The T-bar ribbon-associated protein Bruchpilot is immunolocalised to presynaptic sites with the antibody nc82 (green), and was detected in the lamina of both *Rh1-lacZ* flies (E) and mutant (F,I) flies, as well as in ectopic R1-R6 terminals (magenta, white) in the medulla (F,J, arrow). **K-P**: In the *hsFLP/UAS-mCD8::GFP*; *NeoFRT40A actin-GAL80/ NeoFRT40A, GMR-GAL4, UAS-runt* (*MARCM*) visual system subsets of Runt over-expressing photoreceptors (green cells in K) and their axons (projection images from confocal stacks in L-P) are labelled by mCD8::GFP (green) and the neuropiles are co-labelled with nc82 (magenta). In the lamina (L-N) most photoreceptor axons have a structure resembling that of wild-type R1-R6 terminals (L), are through-going like wild-type R7-R8 axons (M, arrow), or have an abnormal terminal with varicosities along its length (N, arrows). **O,P**: Occasional

(FIGURE 6.5 – CONTINUED, 2 OF 2)

photoreceptor axons appear to form synaptic swellings in both optic neuropiles. These axons expand in both the lamina (enlarged in O', P') and medulla (enlarged in O",P"), and occasionally along the axon during its passage in the chiasma (O, arrow). Scale bars A-F, 10 μm; G-K, 5 μm; (in L) L,M,N, 5 μm; (in O) O,P, 5 μm.

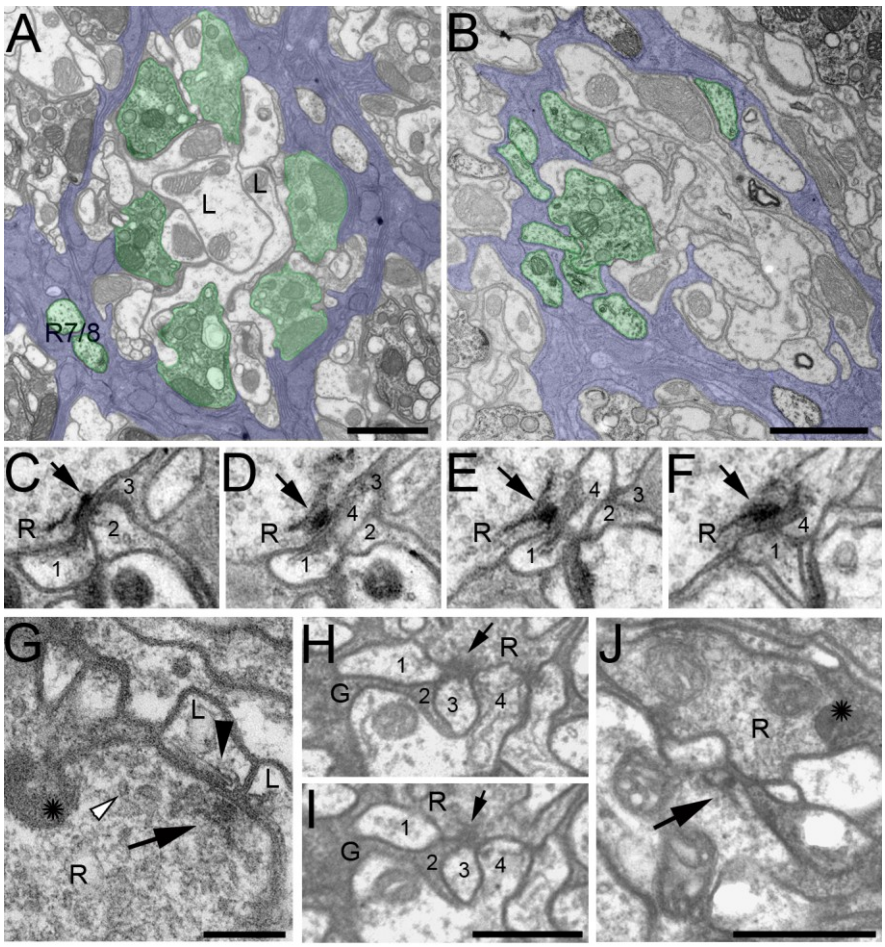

FIGURE 6.6 - FLIES WITH EXOGENOUS RUNT EXPRESSION IN R1-R6 HAVE DISORGANISED LAMINA CARTRIDGES BUT THE AXONS OF R1-R6 HAVE TERMINALS WITH FEATURES CHARACTERISTIC OF THOSE IN THE WILD-TYPE.

A: Wild-type organisation of a lamina cartridge in *UAS-HRP::CD2/+*; *MT14-GAL4/+* flies. A cartridge contains photoreceptor terminals (green) that originate from R1-R6 in neighbouring ommatidia, which innervate five lamina neurons (L1-L5) including the axons of L1 and L2 (L) that lie at the core of the cartridge. All profiles are enveloped by a sheath of three epithelial glia (blue); further details in Meinertzhagen and O'Neil (1991). Axons from R7 and R8 (R7/8: green), which terminate in the medulla, extend along the outside of the cartridge but are not synaptic in the lamina. **B**: Aberrant cartridges in *UAS-runt/UAS-CD2::HRP*; *MT14-GAL4/+* flies are sets of photoreceptors and lamina neurons ensheathed in glia. Each contains variable numbers (< 6) of expanded photoreceptor profiles populated with synaptic organelles, and also the unexpanded profiles of en-passant photoreceptor axons. **C-F**: Consecutive EM sections of a wild-type tetrad synapse, with presynaptic T-bar ribbon (arrow) in the photoreceptor (R) and four postsynaptic partners (labelled 1-4). **G-J**: Photoreceptors in *UAS-runt/+*; *MT14-GAL4/+* flies resemble wild-type terminals of R1-R6 by having capitate projections (*), and in containing synaptic vesicles (open arrowhead), and the presynaptic sites of tetrad synapses (G-I, arrows). **G**: R1-R6 synapse onto target cells with the cisternae and whiskers (arrowhead) characteristic of postsynaptic L1/L2 cells. **H-I**: Consecutive

(FIGURE 6.6 – CONTINUED, 2 OF 2)

60 nm sections through a synapse. Mutant synapses have four postsynaptic partners (labelled 1,2,3,4), and thus formally are tetrads. **J**: Forming possible feedback synapses (arrow), other neurons are presynaptic to photoreceptors. Scale bars A-B, 1 μm; G, 0.2 μm; I-J, 0.5 μm.

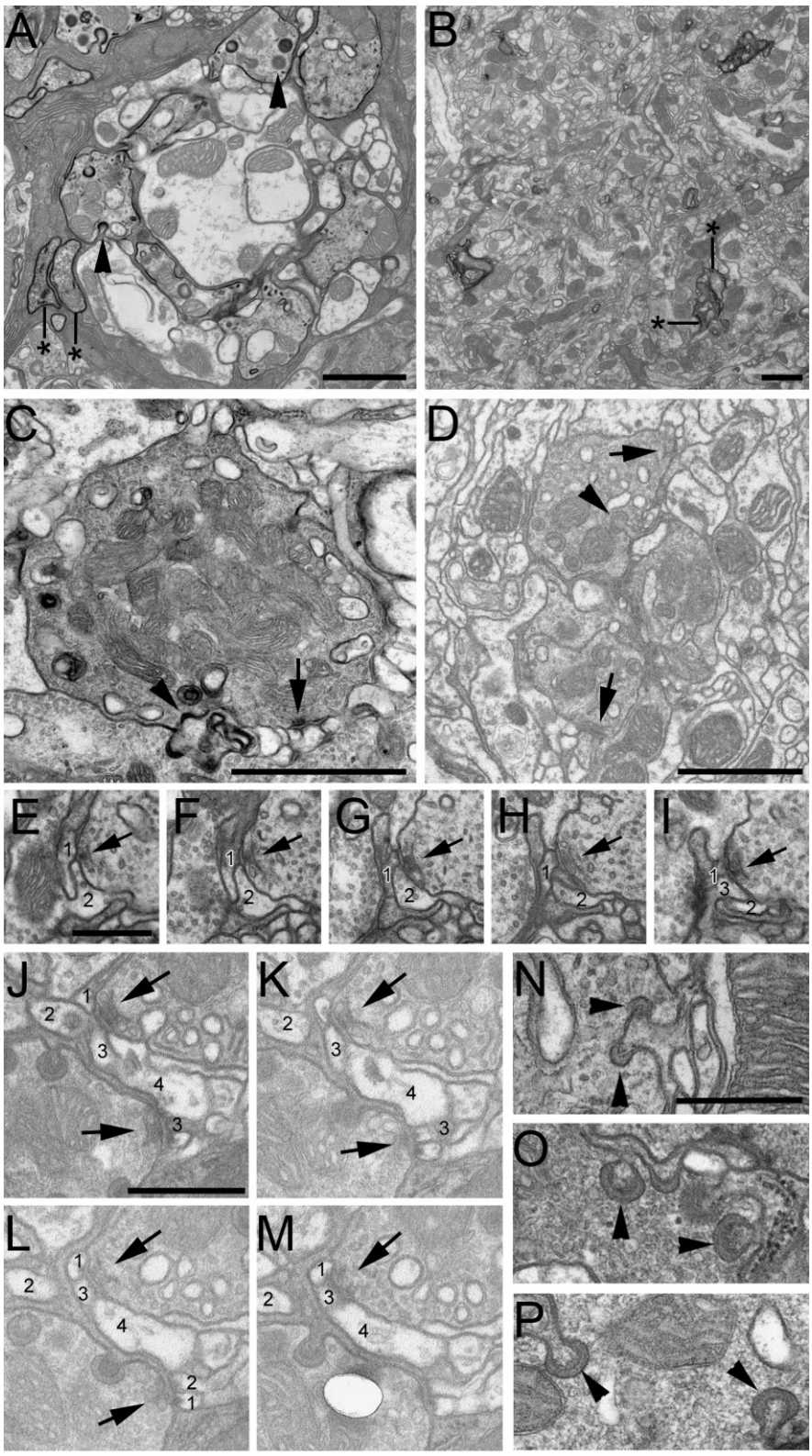

FIGURE 6.7 - PROFILES OF PHOTORECEPTORS IN THE MEDULLA CAN BE DISTINGUISHED BY THE PRESENCE OF ELECTRON-DENSE DAB ON THEIR MEMBRANES.

(FIGURE 6.7 – CONTINUED 2 OF 2)

A-B: 50 nm cross sections of DAB labelled *GMR-GAL4/UAS-HRP::CD2* brains. **A**: A wild-type lamina cartridge in which the membranes of all photoreceptors, including the penetrating axons of R7 and R8 (astrisks), were labelled with DAB. Visible in terminals of R1-R6 are heads of capitate projections (arrowheads). **B**: Unexpanded paired axons of R7/ R8 (arrows) in three columns of the wild-type distal medulla. (C-H) Sections through DAB labelled *UAS-runt/UAS-HRP::CD2; MT14-GAL4/+* flies. **C**: Ectopic photoreceptors in the distal medulla can be distinguished with DAB labelling, and because they have capitate projections (arrowhead) in their terminals (*cf* A). These terminals also contain presynaptic sites (arrow). **D**: Photoreceptors are distinguished even in the absence of DAB labelling, because they have capitate projections (arrowhead) and because transformed R1-R6 frequently form clusters of cylindrically shaped axons, such as this trio, not found in wild-type medullas. **E-I**: Series of micrographs showing the triad synapse (arrow) of a wild-type R7 photoreceptor and its three postsynaptic elements labelled 1-3. **J-M**: Series of micrographs confirming that ectopic photoreceptors form tetrad synapses (arrows). The unidentified postsynaptic partners for two neighbouring synapses (arrows) are labelled 1-4. Element 4 is postsynaptic at both synapses. **N-P**: The shape and size of capitate projections differs in R1-R6 from their counterparts in R7-R8 terminals. Cross-sectioned heads of mushroom-shaped wild-type (OR) R8 capitate projections (N) differ in shape and are smaller in diameter than heads of capitate projections from R1-R6 photoreceptors in either the lamina (P) or in ectopic photoreceptors in the medulla (O) of *UAS-runt/+; MT14-GAL4* flies. Capitate projections of mutant R1-R6 in both the lamina and medulla are similar in size to those in wild-type lamina terminals (*cf*. A). Scale bars A-C, 1 μm; D, 2 μm; E-P, 0.5 μm.

6.5 DISCUSSION

Our data support three main findings; first, that when some of the R1-R6 photoreceptors over-express *runt* either these cells or their neighbours can adopt an alternative fate; second, that when genetically mis-directed to a foreign neuropile, one which mostly comprises medulla interneurons that are novel targets, Rh1-expressing R1-R6 nevertheless form synapses; and, third, that the presynaptic terminal determines the architecture of its synaptic organelles, including capitate projections, without reference to target neurons.

6.5.1 R1-R6 PHOTORECEPTORS THAT OVEREXPRESS *RUNT* OFTEN ADOPT ALTERNATIVE FATES

Developing neurons in the brain normally undergo a sequence of interactions with their neighbours that ensures that each neuron acquires a distinct suite of phenotypic features – axon targeting, synaptic partnerships etc. These features constitute that neuron's fate in the brain. Over-expressing *runt* in R1-R6 transforms the suite of features that normally distinguishes these photoreceptors from their neighbours R7 or R8. We define the cells from the positions they adopt in the ommatidium, which are inherited from the pattern of recruitment of cells during ommatidial assembly (Tomlinson and Ready, 1987b). Three subsequent features of differentiation that are normally selected coordinately, with a fixed association in R1-R6: large rhabdomeres, Rh1 expression, and lamina synaptic terminals, become mixed independently in transformed R1-R6 neurons.

Several examples of switched photoreceptor fates are already known among photoreceptors, with the clearest cases amongst the two central cells, R7 and R8. These have long been recognized to comprise either pale or a more common yellow subtype (Franceschini *et al.*, 1981): pale ommatidia containing Rh3 in R7 and Rh5 in R8, and yellow with Rh4 in R7 in combination with Rh6 in R8 (Wernet and Desplan, 2004). This obligatory pairing arises from a signal originating in R7 (Chou *et al.*, 1996; Papatsenko *et al.*, 1997; Chou *et al.*, 1999), with *warts* and *melted* reciprocally regulating the fate in R8 (Mikeladze-Dvali *et al.*, 2005). A mutation in either *warts* (Rh6) or *melted* (Rh5) changes the opsin expressed in R8, which then fails to coordinate with the overlying R7. In either type, both cells invariably have the same rhabdomere diameter regardless of the opsin expressed. In a second example, R7 and R8 cells both express

Rh3 in the dorsal rim area of the compound eye, as specified by the gene *homothorax.* Ommatidia in the dorsal rim area also undergo a decoupling between rhabdomere size and opsin expression, with the central rhabdomeres being markedly enlarged compared to R7s outside the dorsal rim area (Tomlinson, 2003; Wernet *et al.*, 2003). Thirdly, photoreceptor classes are distinguished by their opsin expression, which is in turn dependant upon homeodomain binding sites in the opsin promoters. Orthodenticle (*otd*) binds these promoter sequences, and in its absence Rh3 and Rh5 expression are lost. Furthermore, in *otd* mutants Rh1 expression expands to R7 and R8 while Rh6 expression expands to R1-R6 (Tahayato *et al.*, 2003). We did not observe expansion of Rh1 into R7 or R8 in *runt* over-expressing flies, but Rh3 and Rh6 expression were expanded to R1-R6. In the fourth example, from frontal ommatidia of the so-called love-spot in male houseflies, *Musca domestica*, transformed R7 cells instead of projecting to the medulla terminate in the lamina, where they form a synaptic terminal like that of R1-R6 (Hardie, 1983). Our findings further exemplify that the genetic regulation of photoreceptor phenotype allows features of R1-R6 to become mixed with those of R7 and R8. An important aspect of our findings is not only that the normal coordinate expression of rhabdomere size, opsin expression and axon projection in correct combinations is perturbed, but also that the novel combinations of such features are variable. Thus some R1-R6 with small rhabdomeres still express Rh1, while some Rh1 expressing photoreceptors project to the medulla.

It remains to be seen how *runt* over-expression in the retina causes these changes in photoreceptor cell fate, either in opsin expression, rhabdomeres size, or terminal location. What is known however is that Sev expression is limited to photoreceptors R1, R3, R4, R6 and R7 during development (Banerjee *et al.*, 1987; Tomlinson *et al.*, 1987) and that in *seven-up* mutants these photoreceptors are transformed to R7 (Mlodzik *et al.*, 1990). Thus, it is not surprising that in *runt* over-expression mutants it is these outer photoreceptors which are most likely to adopt features characteristic of R7 cells, such as small rhabdomeres and Rh3 expression.

For the axons of R1-R6, the transformation after *runt* over-expression in the eye is variable. The axons resemble those of R7 and R8 in innervating the medulla but at least some may differ in continuing to innervate lamina cells, which R7 and R8 never normally do (Meinertzhagen and O'Neil, 1991). While some photoreceptor axons expand to form synaptic terminals in the lamina, others may simply form multiple synaptic zones along

their length, including along extensions into the medulla. Indeed, precedents exist in other insect visual systems for long visual fiber axons, equivalent to R7 and R8 in the fly, that project to the lamina but nonetheless form synapses *en passant* with monopolar cells in the lamina, as in the dragonfly *Sympetrum* (Meinertzhagen and Armett-Kibel, 1982; Armett-Kibel and Meinertzhagen, 1985) and in the basal brachyceran *Hermetia* (Shaw and Moore, 1989).

6.5.2 Supernumerary Photoreceptor Terminals Form Ectopic Synapses With Novel Targets in the Medulla

Terminals of *Rh1* expressing R1-R6 photoreceptors that innervate the medulla form synapses, as exhibited by their expression of the synaptic protein Bruchpilot. In addition, supernumerary photoreceptor terminals in the medulla, which must contain terminals from many transformed R1-R6, form synapses that share many features of the tetrad synapses formed by R1-R6 terminals in the lamina. This is surprising, because at least many of the target neurons must be medulla neurons, which are foreign, and this must certainly be true beyond stratum M5, the deepest termination of L1. Although some target neurons could be the terminals of lamina cells (L1,L2 etc, the normal targets of R1-R6 in the lamina), in the wild-type these terminals do not form dendrites (Fischbach and Dittrich, 1989) and are predominantly presynaptic in the medulla (Takemura *et al.*, 2008). Moreover, medulla cells are simply more numerous than lamina cells (Fischbach and Dittrich, 1989; Meinertzhagen and Sorra, 2001) and extend throughout the entire medulla depth. The participation of lamina amacrine neurons and epithelial glial cells at ectopic medulla synapses is absolutely denied, because these cells never extend to the medulla.

Ectopic synaptogenesis occurs widely in different nervous systems. Neuromuscular innervation readily forms ectopic synapses in vertebrate muscles, for example, reflecting a range of phenomena regulating the size and distribution of synaptic sites (reviewed in (Lømo, 2003). Likewise, developing *Drosophila* motoneurons denied access to their normal muscle targets form stable, ectopic synapses upon other muscles (Cash *et al.*, 1992). In the cricket, sensory afferents from transplanted cerci (abdominal sensory appendages) form functional ectopic synapses upon novel interneuron targets (Murphey *et al.*, 1983). In the vertebrate retina, genetically procured degeneration of rods results in the normal rod bipolar cell targets of these cells accepting ectopic synapses from

cones (Peng *et al.*, 2000), by a process that entails the retraction of rod terminals and neurite outgrowth from rod bipolar cell dendrites (Bayley and Morgans, 2007). Likewise, loss of cones causes cone bipolar cells to form ectopic synapses with rods, a switch that requires the presynaptic photoreceptors to be functional (Haverkamp *et al.*, 2006), unlike the fly, in which tetrad synaptogenesis is activity independent (Hiesinger *et al.*, 2006).

These examples of ectopic synaptogenesis all occur in response to some loss of input or target sites. Our findings now show that when their axons are redirected to a novel territory, sensory neurons such as R1-R6 can nevertheless form synapses with their normal targets which are still intact, as well as with novel partners in the second territory. The terminals thus act with autonomy in each neuropile. The ability of photoreceptors to form ectopic synapses in foreign neuropiles has also recently been demonstrated for ectopic eyes on the antennae and legs of *Drosophila*, which extend axons and synapse at superficial locations in the CNS (Clements *et al.*, 2008). In either case the ability of such postsynaptic sites to respond to neurotransmitter released from ectopic R1-R6 terminals is of course questionable; we would predict that only the normal partners of R7 or R8 would express histamine receptors (Witte *et al.*, 2002) and thus be able to respond to the histamine release.

6.5.3 The Presynaptic Terminal of R1-R6 Determines the Architecture of its Synaptic Organelles

Further evidence of R1-R6 terminal autonomy comes from the more detailed examination of its synaptic organelles. Several features of the latter reveal that the size, structure and composition of the organelles are highly conserved, regardless of the identity of the postsynaptic target cells. These features include at the release sites: the presynaptic T-bar ribbon and the quadripartite composition of its postsynaptic ensemble; and at the capitate projection, the diameter of the head and its invagination by a glial cell process. All of these features are determined by the presynaptic photoreceptor neuron, in an autonomy that confirms many other details of tetrad synaptogenesis in the lamina.

6.6 Acknowledgements

This work was supported by a Natural Sciences and Engineering Research Council (Ottawa) postgraduate scholarship to T.N.E. and by NIH grant EY-03592 to I.A.M.

Antibodies 24B10 and 6D6 developed by Seymour Benzer, 7E8A10 by Gerald M. Rubin, 40-1a by Joshua Sanes, nc82 by Erich Buchner, 1D4 by Corey Goodman, MR1A by Chris Doe, and 4C5 by Heinz Gert de Couet and Teiichi Tanimura were obtained from the Developmental Studies Hybridoma Bank, University of Iowa. Anti-Repo was provided by Dr. J. Urbin (Gutenberg Universität, Mainz, Germany), anti-BOSS and anti-BSH by Dr. Larry Zipursky (UCLA). *MT14-GAL4* and *UAS-runt* stocks were generously provided by Dr. Utpal Banerjee (UCLA); and *UAS-HRP::CD2* and *neoFRT* lines for *MARCM* crosses by Dr. Chi-Hon Lee (NIH, Bethesda). All other stocks were provided by the Bloomington Stock Center. We thank Zhiyuan Lu and Rita Kostyleva for assistance with EM techniques and sectioning, Dr. Claudia Groh for comments on the manuscript, and Dr. Chi-Hon Lee for advice.

6.7 SUMMARY TO CHAPTER SIX AND TRANSITION TO ADDENDUM

In order to determine the means by which over-expression of *runt* controls the transformation of R1-R6 photoreceptors into R7 and R8 subtypes, I attempted to offset this phenomenon, as described in the following addendum. Flies which are mutant for *sevenless* lack R7 photoreceptors, and when *runt* is over-expressed in a *sevenless* background there is a marked reduction in the transformation of R1-R6 photoreceptors into cells of an R7-like fate, but no effect on transformation into an R8-like fate. This suggests that *runt* functions downstream of *sevenless* in controlling the R7 phenotype.

6.8 INTRODUCTION

During the late stages of larval life and early pupal metamorphosis, the eye disc transforms from an undifferentiatedmulti-cellular epithelium to a highly structured retina consisting of 750-800 ommatidia (Ready *et al.*, 1976). The cells of the eye disc epithelium are initially derived from about 20 cells in the embryonic blastoderm (Garcia-Bellido and Merriam, 1969). In the early third-instar larva a wave of mitotic division progresses from posterior to anterior across the eye disc. This wave is followed closely by the progression of the morphogenetic furrow, a condensation of post-mitotic cells and a physical landmark for cellular differentiation that also migrates in a posterior to anterior direction as successive rows of photoreceptors begin to differentiate behind it (Ready *et al.*, 1976). The first mitotic wave gives rise to ommatidial pre-clusters containing the R8, R2/5 and R3/4 photoreceptors (Ready *et al.*, 1976; Tomlinson and Ready, 1987a; Tomlinson and Ready, 1987b). Approximately 10 hours later, a second wave of mitotic activity located about five ommatidial rows behind the first, gives rise to cells destined to become R1, R6, R7 and the support cells of the ommatidium (Ready *et al.*, 1976; Tomlinson, 1985; Tomlinson and Ready, 1987a; Tomlinson and Ready, 1987b; Cagan and Ready, 1989b; Wolff and Ready, 1991). Mitotic activity and photoreceptor cell morphogenesis then progress across the eye disc in an anterior direction until approximately 10% of pupal development (Cagan and Ready 1989b).

The position a cell occupies within the eye field will ultimately determine its fate, since cells receive fate-determining signals from their immediate neighbours (Cagan and Ready, 1989b). Approximately every two hours (at 22^{o}C) a new row of ommatidia emerges from the anteriorly progressing morphogenetic furrow (Campos-Ortega and Hofbauer, 1977). The first neuron to be determined is R8, followed in succession by pairs of R2/R5, R3/R4, R1/R6 photoreceptor cells and lastly R7. Accessory cone and pigment cells are determined after the photoreceptor cells (Ready *et al.*, 1976; Wolff and Ready, 1991). The terminal differentiation of photoreceptors is finalized during pupal metamorphosis and involves axon targeting between 20-40% of pupal development (Clandinin and Zipursky, 2000; Clandinin *et al.*, 2001; Lee *et al.*, 2001; Lee *et al.*, 2003; Nern *et al.*, 2005; Prakash *et al.*, 2005; Ting *et al.*, 2005), the formation of rhabdomeres at about 50-55% of pupal development (Van Vactor *et al.*, 1988; Cagan and Ready, 1989a; Pollock *et al.*, 1990; Kumar and Ready, 1995), and *rhodopsin* expression which

begins after 75% of pupal development (Kumar and Ready, 1995; Mollereau *et al.*, 2001; Tahayato *et al.*, 2003; Wernet *et al.*, 2003; Mikeladze-Dvali *et al.*, 2005).

In the *Drosophila sevenless* (*sev*) mutant, all photoreceptors form normally except for R7, which fails to develop. The cell that was positionally set to become R7 is instead transformed into a lens-secreting cone cell (Tomlinson and Ready, 1986). The protein coded for by *sev* is a cell surface receptor with tyrosine kinase activity that is transiently expressed on the apical surface of presumptive photoreceptor and cone cells at different times during the development of the ommatidial cell cluster (Banerjee *et al.*, 1987; Hafen *et al.*, 1987; Tomlinson *et al.*, 1987). Sev protein interacts with the membrane bound ligand Bride of sevenless (BOSS) on the R8 cell. While many photoreceptors are competent and express *sev*, the only *sev*-expressing cell which is able to bind and internalize the BOSS ligand, is that which contacts the BOSS expressing R8 cell (Krämer *et al.*, 1991). Activation of Sev initiates the Rasl/MAP kinase pathway of signal transduction factors which, in turn, phosphorylates downstream targets (Brunner *et al.*, 1994; Kauffmann *et al.*, 1996). The activity of Seven in absentia (SINA) in the R7 nucleus is regulated by the BOSS/Sev pathway (Dickson *et al.*, 1992), and the transcription factor encoded by *sina* is necessary for R7 to receive and interpret other developmental signals (Carthew and Rubin, 1990; Carthew *et al.*, 1994). After activation by both Notch/Epidermal Growth Factor Receptor (EGFR) and BOSS/Sev, high-levels of *prospero* expression become restricted to the R7 cell (Kauffmann *et al.*, 1996), either via a *pointed/yan* or via a *sina*-dependant pathway. Prospero is a transcription factor which controls R7 versus R8 cell fate determination. Prospero expression in R7 photoreceptors represses both the transcription of the R8-specific rhodopsins (Rh5, Rh6) and the establishment of an R8-like morphology. Mutations in *prospero* also alter axon terminal location in the medulla (Cook *et al.*, 2003).

Misexpression of the pair-rule transcription factor *runt* in all photoreceptors during early development by means of *GMR-GAL4*, or a subset of photoreceptors using *MT14-GAL4*, not only causes mistargeting of photoreceptor axons (Kaminker *et al.*, 2002) but also results in transformation of R1-R6 photoreceptors to an R7 or R8-like fate in the adult (Edwards and Meinertzhagen, 2009). Our analysis of photoreceptor subtype specific markers in the larval eye discs of *UAS-runt/+;MT14-GAL4/ +* flies reveals that there is no excess of BOSS-expressing R8 cells or Prospero-expressing R7 cells in the eye disc even though 82% of adult ommatidia contain supernumerary Rh3 expressing R7 cells

and/or Rh6 expressing R8 cells (Edwards and Meinertzhagen, 2009). There is an increase in the number of Rh3-expressing R7 cells, which normally represent only about 30% of the R7 cell population (Montell *et al.*, 1987), but account for 66% of all transformed photoreceptors in *runt*-overexpressing eyes. Thus, the initial stages of photoreceptor determination proceed in their natural order, but since photoreceptors are not fully differentiated their fate can change at later stages of pupal development. Using a temperature-sensitive allele of *sev* I set out to determine if *runt*-induced cell fate transformation could be limited by removing the earliest signals for R7 determination.

6.9 METHODS

Immunocytochemistry and EM preparation were performed as described in Chapter 6. In order to generate *runt* overexpressing flies in a *sev* mutant background, all of *GMR-GAL4*, *MT14-GAL4* and *UAS-runt* were individually crossed into sev^{AE2} (from C-H. Lee, NIH Bethesda) to produce stable sev^{AE2}*;;MT14-GAL4*, sev^{AE2}*; GMR-GAL4* and sev^{AE2}*;UAS-runt* isoparental stocks. When *GAL4* lines were crossed with sev^{AE2}*;UAS-runt* the offspring had a homozygous sev^{AE2} background (Appendix K).

6.10 RESULTS

6.10.1 *SEV* PARTIALLY RESCUES THE EYE PHENOTYPE OF *RUNT*-OVEREXPRESSING EYES AND REDUCES THE NUMBER OF R7 TERMINALS IN THE MEDULLA

Over-expressing *runt* by means of the strong *GMR-GAL4* driver results in a loss of facets and the disruption of retinal structure (Figure 6.8B; see also Figure 6.1F in Edwards and Meinertzhagen, 2009). The disruption was so severe that *GMR-GAL4/UAS-runt* flies could not be used for analysis of ommatidial subtypes. Instead, *UAS-runt/+; MT14-GAL4/+* flies (Figure 6.8D), which from the external surface of the cornea had what appeared to be a wild-type eye (Figure 6.8A), were used for all analyses of ommatidial subtypes. When *UAS-runt* was over-expressed in the whole eye using *GMR-GAL4* in a *sev* background, facets were restored on the surface of the retinal cornea (Figure 6.8C); however, underlying the lens, the structure of the eye was still grossly abnormal and lacked distinct ommatidial clusters, and could therefore not be used for EM analysis of photoreceptor cell type.

Anti-Chaoptin immunolabelling marked all photoreceptor axons in the lamina and medulla, but did not allow us to distinguish between different photoreceptor terminal types in the medulla. Flies with either *GMR-GAL4* driven (Figure 6.8E) or *MT14-GAL4* driven (Figure 6.8G) *runt* overexpression had abnormal column arrangements in the medulla, but photoreceptor terminal expansions in the M3 and M6 layers were still detected in most columns. Isoparental controls with a *sev* background, such as *sev^{AE2}; UAS-runt* (Figure 6.8H) lacked photoreceptor axons extending into M6, where R7 normally terminates. Immunolabelling along the M6 layer in *sev* isoparental controls is likely due to Chaoptin expression in at least one of the medulla tangential interneurons that expands in this layer, the anatomy of which can be seen in Fischbach and Dittrich (1989). In the brains of both *sev^{AE2}; GMR-GAL4/UAS-runt* (Figure 6.8F) and *sev^{AE2}; UAS-runt/+; MT14-GAL4/+* (Figure 6.8I) flies, there is a reduction in the number of photoreceptor terminals in the M6 layer, suggesting that there are fewer R7 terminals (compare with *Rh3-lacZ* labelled R7 axons in Figure 6.4G). In the brains of *sev^{AE2}; GMR-GAL4/UAS-runt* flies some columns contain only R8-like axons which terminate in M3, though columns containing photoreceptors that terminate in M6 are still present. In *sev^{AE2}; UAS-runt/+; MT14-GAL4/+* brains the number of columns with photoreceptor axons that terminate in M6 (Figure 6.8I) appears to be even fewer than in their *GMR-GAL4* driven counterparts (Figure 6.8F).

6.10.2 The Frequency of Transformation From Large R1-R6 Rhabdomeres Into Small, Distally Located R7-Type Rhabdomeres is Reduced in a *sev^{AE2}* Mutant Background

The normal ommatidial unit contains the large rhabdomeres of six outer photoreceptors, which, in cross section, are arranged in a skewed trapezoidal pattern around a small central R7 (distal) or R8 (proximal) rhabdomere (Figure 6.9A). Isoparental *sev^{AE2}* mutants (Figure 6.9B, C) had the six, large outer rhabdomeres but lacked the small centrally located R7 rhabdomere in the distal retina. As previously described for the eyes of *UAS-runt/+; MT14-GAL4/+* examined at the level of light microscopy (Edwards and Meinertzhagen, 2009), ommatidia have less than six R1-R6 rhabdomeres and more of the small rhabdomeres typical of the R7 and R8 central cells, the structure of which was visualized more clearly with EM (Figure 6.9D). Ommatidia contained no more than eight rhabdomeres, the normal content in a wild-type eye, implying that only photoreceptors and not the surrounding cone or pigment cells were transformed into

supernumerary R7 or R8 cells. After expressing *UAS-runt/+; MT14-GAL4/+ in a sev^{AE2}* background the number of ommatidia containing supernumerary R7/R8 photoreceptors was reduced, from 82% (see Edwards and Meinertzhagen, 2009) to 25% (N= 176), although other abnormalities in ommatidial structure were detected in about 43% of all ommatidia (Figure 6.9E-I). These abnormalities included a reduction in the number of rhabdomeres, so that some ommatidia contained five or fewer rhabdomeres (Figure 6.9H,I).

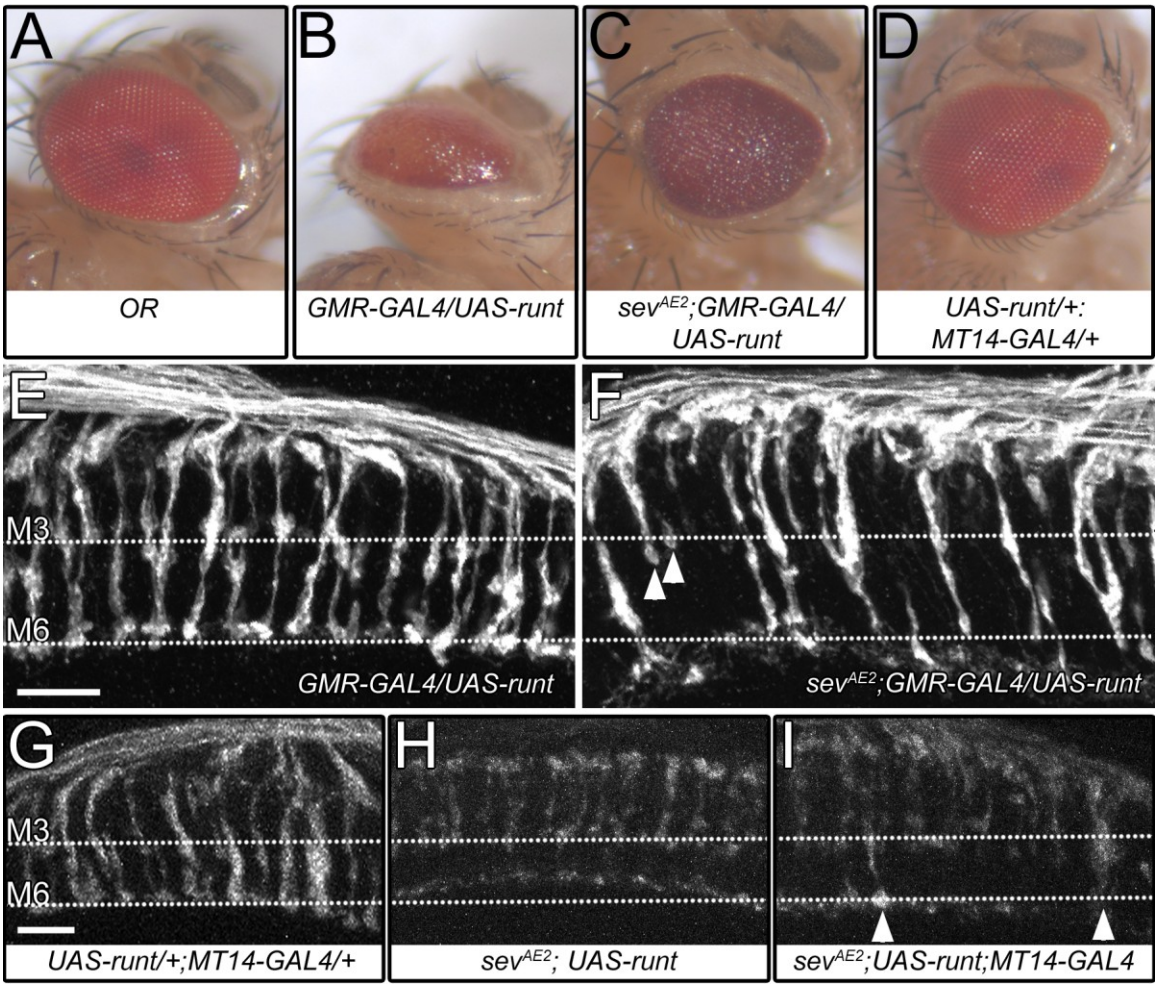

FIGURE 6.8 - *SEV* PREVENTS THE FORMATION OF SUPERNUMERARY R7 PHOTORECEPTORS IN *RUNT* OVER- EXPRESSING EYES.

A-D: The external structure of wild-type and *runt*-overexpressing retinas. **A,D**: *UAS-runt*/+; *MT14-GAL4*/+ (D) flies have eyes similar to those of wild-type OR (A). **B**: The external structure of the eye is severely disrupted in *GMR-GAL4*/*UAS-runt* flies and lacks distinct facets. **C**: Some semblance of facet structure is restored when *runt* is over-expressed in a *sev* background in sev^{E2};*GMR-GAL4*/*UAS-runt* flies. **E-F**: A 13 µm projection image stack of Chaoptin immunolabelled photoreceptors from horizontal slices of Vibratome sectioned brains in *GMR-GAL4*/*UAS-runt* (E) reveals many photoreceptor axons projecting into the M6 layer of the medulla. sev^{E2};*GMR-GAL4*/*UAS-runt* brains (F) have axons which terminate in M3 (arrowheads) and fewer columns containing photoreceptor axons that project to M6. **G-H**: A 10 µm projected image of Chaoptin immunolabelled photoreceptors from horizontal slices of Vibratome sectioned brains in *UAS-runt*/+; *MT14-GAL4*/+ flies (G), illustrates many columns containing photoreceptors that terminate in M6, unlike sev^{E2};*UAS-runt* flies (H), in which all photoreceptors terminate at M3. **I**: The brains of sev^{E2}; *UAS-runt*/+; *MT14-GAL4*/+ flies have occasional photoreceptor terminal projections as deep as M6 (arrowheads) but most terminate in M3. Scale bars (in E) E,F, 10µm; (in G) G,H,I, 10µm.

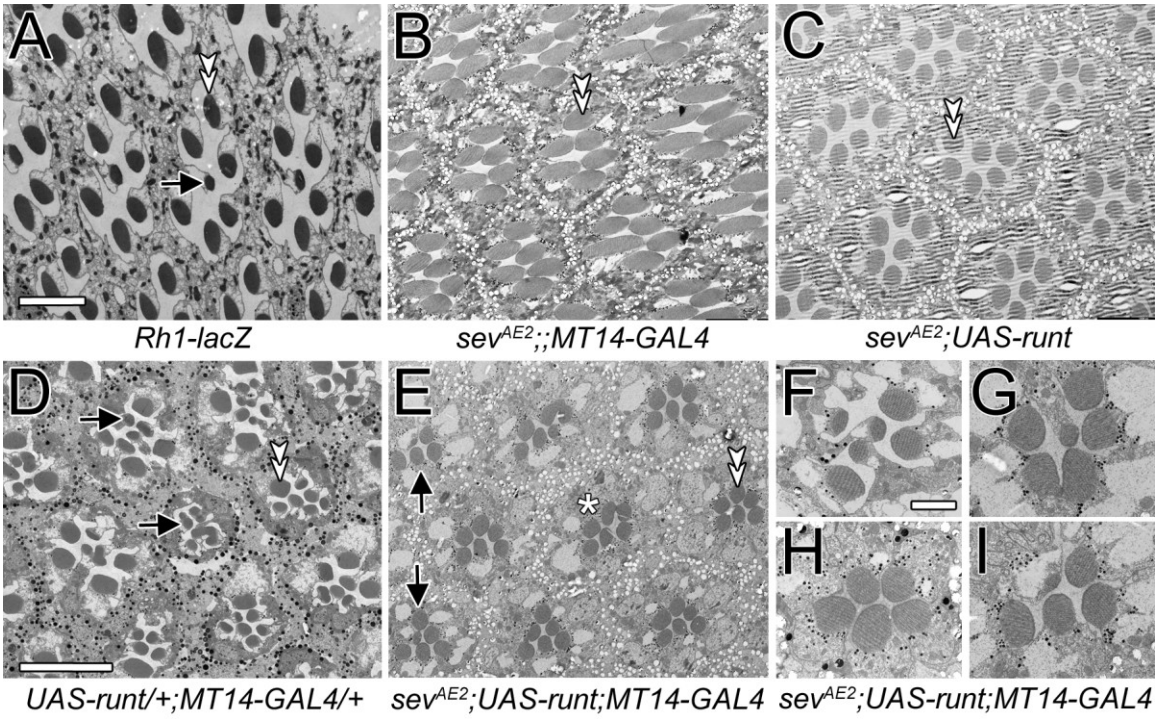

FIGURE 6.9 - *SEV* DOES NOT PREVENT THE FORMATION OF SUPERNUMERARY R8 PHOTORECEPTORS IN *RUNT* OVER-EXPRESSING EYES.

Images of 50 nm cross sections of eyes visualized by TEM. **A**: the wild-type structure at the distal margins of the ommatidia in *Rh1-lacZ* flies. Large R1-R6 rhabdomeres (open arrowheads for R3) are arranged in a skewed trapezoid surrounding a smaller, centrally located R7 rhabdomere (arrow). **B-C**: Parental controls sev^{E2};;*MT14-GAL4* (B) and sev^{E2}; *UAS-runt* (C) flies have large rhabdomeres in their facets (arrowheads) but lack the small, centrally located R7 rhabdomere. **D**: The ommatidia of *UAS-runt*/+; *MT14-GAL4*/+ flies contain normal size R1-R6 rhabdomeres (open arrowheads) but also many small R7- and R8-like rhabdomeres (arrows). **E**: Small axial rhabdomeres are still observed in some ommatidia (arrows) when *runt* is over-expressed in a *sev* background, as visualized here in a sev^{E2};*UAS-runt*/+; *MT14-GAL4*/+ expressing fly. Most ommatidia, however have a normal complement of rhabdomeres, either *sev*-like (35%, asterisk in E) or wild-type (22%). **F-I**: Abnormal ommatidia in sev^{E2};*UAS-runt*/+; *MT14-GAL4*/+ expressing flies sometimes have only six rhabdomeres, of which one (G) or more (F) is R7/R8-like. Others have a reduced number of rhabdomeres which either contain transformed rhabdomeres (I) or have only large R1-R6-type rhabdomeres (H). Scale bars: A, 10μm; (in D) B,C,D,E; 10μm; (in F) F, G, H, I, 2μm.

6.11 DISCUSSION

Ectopic overexpression of *runt* causes the formation of supernumerary R7 and R8 photoreceptors, and this phenotype, in part, is subverted by mutations in *sev* which disrupt the *BOSS*/*sev* R7 fate specification signalling pathway. When *runt* is overexpressed in a *sev* mutant background there are fewer disrupted ommatidia and fewer R7-like terminals in the M6 layer of the medulla.

Analysis of these findings is not without its complications, however. The allele sev^{AE2} used in this study is temperature-sensitive, with 98% of ommatidia containing an R7 cell at 18°C and only 5% containing an R7 cell at 28°C (Mullins and Rubin, 1991). In sev^{AE2}*; UAS-runt/+; MT14-GAL4/+* flies, approximately 22% of ommatidia were wild-type at 18°C, possessing six large R1-R6 outer rhabdomeres and a small centrally located R7 rhabdomere. The temperature-sensitive nature of this mutation complicates analysis in this instance because in order to have the most efficient mutation of *sev* there would need to be a shift in temperature towards 28°C. However, because the *GAL4/UAS* system is also temperature-sensitive (Duffy, 2002), any increase in temperature will increase the strength of *runt* over-expression, enhancing the mutant phenotype. Thus results we have obtained need to be interpreted with the knowledge that some 'original' R7 cells have been maintained despite a mutation in the *sev* allele. While it is not known if photoreceptor terminals in M6 represent R7 cells that have persisted, R1-R6 cells that have mistargeted axons, or R8 cells that have mistargeted axons, the reduction in M6 terminals does suggest an overall reduction in the number of R7 photoreceptors, especially in sev^{AE2}*; UAS-runt/+; MT14-GAL4/+.* This reduction may represent not only a loss of the normal single R7 terminal per column, but also the loss of supernumerary R7 photoreceptors.

In sev^{E2};*UAS-runt*/+; *MT14-GAL4*/+ flies, most ommatidia have a normal complement of rhabdomeres, either *sev*-like (35%) or wild-type (22%). Abnormal ommatidia sometimes have only six rhabdomeres, of which one or more is R7/R8-like. This suggests that the *sev* mutant background not only eliminates the central R7 cell, but that at least one other rhabdomere has been transformed. Still other ommatidia contain only five large R1-R6-type rhabdomeres, again suggesting that not only is a central R7 lost, but other cells that would have become R7 have also been lost. Either that, or a sixth photoreceptor persists but lies more proximal in the retina, as twinned R8 rhabdomeres. Our previous analysis of ommatidial subtype found R8-like cells expressing R8-like opsins in the distal

retina of *UAS-runt*/+; *MT14-GAL4*/+ flies (Edwards and Meinertzhagen, 2009), and R8 cells have been shown to migrate apically in the absence of R7 cells (Tomlinson and Ready, 1987a). Therefore, even though R7 and R8 rhabdomeres would normally lie at different depths within the retina, there is no way to distinguish by ommatidial anatomy alone whether the transformed rhabdomeres that persist in the distal retina of sev^{E2};*UAS-runt*/+; *MT14-GAL4*/+ flies are R7- or R8-like.

The fact that a *sev* mutation reduces the number of transformed cells implies that *runt* over-expression and the transformation of R1-R6 cells to an R7 like-fate occurs through a *sev* dependent pathway. It also suggests that genes downstream of *sev* activation are necessary for *runt* to affect R7 cell determination. As previously noted, expression of *sev* is limited to photoreceptor sets R1/R6, R3/R4 and R7 (Banerjee *et al.*, 1987; Tomlinson *et al.*, 1987), and these are the same photoreceptors that are most likely to adopt features characteristic of R7 cells after *runt* over-expression (Edwards and Meinertzhagen, 2009).

6.10.1 How to Produce Ectopic R7 or R8 Photoreceptors

The gene *runt* is exclusively expressed in R7 and R8 photoreceptors during normal development, and so it is not surprising that ectopic expression *of runt* in R1-R6 alters the features of these photoreceptors so that they take on the adult characteristics of R7 or R8. Despite implications that *runt* functions through the Sev receptor pathway to alter photoreceptor cell fate, particularly for R7 photoreceptors, we still do not know exactly how *runt* functions to cause the transformation of R1-R6 into R7 or R8-like cells. Many of the cell fate decisions in eye development depend upon an intricate series of transcription factor-based gene activation and/or deactivation. R7 and R8 share expression of one key set of transcription factors necessary for their respective cell-fate dependant decisions, the *spalt* complex. Spalt is required for early establishment of R7 fate via the Notch pathway, mutations of which eliminate the expression of genes expressed in R7 including, but not limited to, *prospero* and *runt.* Furthermore, *GMR*-induced mis-expression of the *spalt* complex genes, *sal major and sal related,* induce ectopic *senseless* expression and, ultimately, ectopic *Rh3-lacZ* expression in the outer R1-R6 photoreceptors. Strangely, *spalt* complex mis-expression in R1-R6 did not alter axonal pathfinding, and so photoreceptors terminated in the lamina despite exhibiting R7-specific *Rh3-lacZ* expression. Spalt also promotes the terminal differentiation of R8

and mis-expression of either *spalt* or *senseless* in the late pupa using *Rh1-GAL4* induced ectopic expression of Rh6 and suppression of Rh1 in R1-R6 photoreceptors (Domingos *et al.*, 2004b). Runt is therefore expressed relatively early in the development of R7 and R8, and so it likely acts in the early or mid stages of the developmental pathway that establishes the cell-specific characteristics of R7 and R8.

One possibility is that *runt* functions like *lozenge* (*lz*), a *runt*-family homologue. *lz* is required for pre-patterning in the undifferentiated precursors of R1/R6 and R7 and regulates other transcription factors required for cellular specification, including the positive regulation of *prospero*, and the negative regulation of *seven-up* in R7 (Daga *et al.*, 1996; Flores *et al.*, 1998; Xu *et al.*, 2000). Thus, when the lz^{Sprite} allele is mis-expressed in R3/R4, *seven-up* expression is repressed, and these *sev*-expressing cells then differentiate as R7s (Flores *et al.*, 1998). Is it possible that *runt* acts like *lz*, and interferes with pre-patterning in R3/4 and R1/R6 cells, making them susceptible to an R7 fate? The two genes share a similar binding partner in Big-Brother, and a heterodimeric complex between Big-Brother and Lozenge functions to determine cell-fate specification in the eye (Kaminker *et al.*, 2001). It may be necessary to test whether *runt* and its associated binding partners, which are normally expressed in R7 and R8 (Kaminker *et al.*, 2001; Kaminker *et al.*, 2002), alter the expression of transcription factors other than *prospero,* and or monitor changes in transcription factor expression at stages other than in the third-instar larva.

A number of different mutations can result in an excess of R7 photoreceptors. Mutations of *gap1* lead to *sev*-independent transformation of cone cells into R7 cells by mimicking the constitutive activation of Sev (Gaul *et al.*, 1992). Mutations of the steroid-like receptor molecule *seven-up* cause the transformation of R3/R4/R1/R6 into R7 while over-expression of *seven-up* in R7 cells causes transformation of the R7 cell into an R1-R6 cell fate by repressing the expression of BOSS on R8 cells and subverting the signal which initiates R7 cell fate specification (Mlodzik *et al.*, 1990; Hiromi *et al.*, 1993). Loss of function of both the *yan* and *tramtrack* genes results in supernumerary R7 formation (Lai and Rubin, 1992; Lai *et al.*, 1996; Siddall *et al.*, 2009). Yan normally acts antagonistically to Sev and Ras to prevent formation of R7 cells early in the third-instar (Lai and Rubin, 1992; Lai *et al.*, 1996), whereas *tramtrack* functions during both larval development (Siddall *et al.*, 2009) and during the late pupal stages (Lai *et al.*, 1996). Interestingly, Runt immunolabelling is localised to early-onset supernumerary R7 cells in

tramtrack mutants (Siddall *et al.*, 2009), implicating Runt in the early establishment of R7 fate specification.

It is also not known how additional R8 cells arise following *runt* over-expression in photoreceptors. There are very few cases in which mutations give rise to supernumerary R8 cells. Overexpressing *atonal* early in the establishment of the R8 equivalency group will cause twinning of R8s (White and Jarman, 2000), and mutations of the cell adhesion molecule Echinoid promote the twinning of R8 as well as enhance the twinning phenotype caused by over-expression of *atonal*. In both of these examples R8 is duplicated because EGFR signalling within the R8 equivalence group is de-repressed, and this causes inappropriate inductive interactions between cells of the equivalence group (Rawlins *et al.*, 2003). Even so, R8 is not twinned in the larval eye disc of *runt* over-expression mutants, so the excess of R8 cells we observe in the adult probably does not result from alterations in *atonal* or *echinoid*. The change likely lies instead with the mis-expression of transcription factors during early to middle stages of cell-fate determination, some time after the *spalt* complex transcription factors which are activated by the Notch/EGFR signalling cascade.

R8 determines the fate of its neighbouring cell by interacting with the Sev receptor on its surface and initiating a pathway for R7 cell fate specification (Cagan *et al.*, 1992). Thus, if there are excess R8 cells early in development, then more R7 cells should be induced. However, BOSS and Prospero expression in *runt* over-expressing flies reveal no excess of R8 or R7 cells in the larval eye disc (Edwards and Meinertzhagen, 2009). Furthermore, R7 is established after R8, and thus mutations in *sev* should have no direct effect on R8 cell specification, with excess transformed R8 cells likely represented here by the supernumerary small rhabdomeres in 25% of the ommatidia in sev^{AE2}*;UAS-runt/+; MT14-GAL4/+* flies. So how do these excess Rh6-expressing R8 cells arise? The answer may lie, in part, in how the Rhodopsin-specific patterning interactions of R7 and R8 are established in the retina at the latest stages of pupal development.

A completely different set of transcription factors from those involved in early photoreceptor fate specification is responsible for the specific control of Rhodopsin expression. Orthodenticle positively regulates the expression of Rh3 and Rh5 by a directly binding to their respective promoters (Tahayato *et al.*, 2003) while *spineless* controls the expression of Rh4 in R7 (Wernet *et al.*, 2006). Similarly, the transcription factors *warts* and *lats* ensure that the opsins of R7 and R8 photoreceptors within a single

ommatidium are co-ordinately expressed, such that Rh3 in R7 is matched with Rh5 in R8, while Rh4 in R7 is matched with Rh6 in R8 (Chou *et al.*, 1996; Papatsenko *et al.*, 1997; Mikeladze-Dvali *et al.*, 2005). Only about 30% of all ommatidia contain the Rh3/Rh5 pairing and establishment of opsin expression pairs within the eye is stochastic (Franceschini *et al.*, 1981; Wernet *et al.*, 2006; Bell *et al.*, 2007). Rh4, and thus Rh6, are the default rhodopsins for R7 and R8 respectively, while Rh5 expression is induced by Rh3 in its coordinate R7 partner (Chou *et al.*, 1999; Mikeladze-Dvali *et al.*, 2005). Yet, while an excess of Rh3 expressing R7 cells is present in *runt* over-expressing flies there is a complete absence of Rh5 expressing R8 cells, so it is unlikely that the opsin expression pattern of *runt* over-expression flies results from simultaneous over-expression of Orthodenticle. Errors downstream of the *spalt*/*senseless* induced pathway that control normal expression of *runt* in R7 and R8 are a good place to start looking. However, the fact that there is there is a loss of the coordinate expression of opsins in photoreceptors within the same ommatidium in *runt* over-expressing flies suggests a signalling problem between R7 and R8 cells in the same ommatidium, and so it remains possible that *runt* flies have a defect in *melted*, which triggers Rh5 expression on R8 cells (Mikeladze-Dvali *et al.*, 2005).

One problem in cell-fate decision making may lie in the fact that within any one ommatidium R7 photoreceptors express either Rh3 or Rh4 (Edwards and Meinertzhagen, 2009), thus providing contradictory signals to the R8 neighbours. In this situation, it may be that the default state, Rh6-expression, comes to rule. I did not analyse Rhodopsin expression patterns following *runt* overexpression in a *sev* background, a situation in which there are fewer R7 photoreceptors and thus less 'noise' being signalled to the neighbouring R8 cell. A loss of late onset *prospero* expression causes R7 cells to lose their adult characteristics, and take on R8-like characteristics, as if R8 were a "ground state" for inner photoreceptors (Cook *et al.*, 2003), compatible with the suggestion from the *sev* phenotype that R7 was a later evolutionary recruit to the ommatidium (Tomlinson and Ready, 1987a). R1-R6 is a default cell fate for photoreceptors (Tahayato *et al.*, 2003), yet the possibility exists that in *runt* over-expressing flies some cells begin to transform into R7-like cells via a *sev*-dependent pathway. Once they pass a certain point in differentiation their fate cannot be reversed, and so interfering signals that alter late-onset *prospero* expression may cause partially transformed cells instead to adopt an R8-like fate and express Rh6. Confirmation of this hypothesis requires further investigation.

6.12 TRANSITION TO CHAPTER SEVEN

Chapter seven is a summary of the research presented in this thesis that highlights the structure of glia in the lamina and speculates upon their possible roles in neurotransmitter recovery and recycling. A model is outlined for the transport of histamine and carcinine not only within the lamina, but also into the lamina from locations outside the CNS. The capitate projection phenotype of mistargeting photoreceptor terminals in the medulla may represent a compensatory response to modulate the interaction between photoreceptors and glia in the face of functional adversity.

CHAPTER 7

CONCLUSION

7.1 IDENTIFYING GLIA SUBTYPES IS INTEGRAL TO UNDERSTANDING GLIAL FUNCTION

Often billed as the Cinderellas of the nervous system, glia remain a vastly underappreciated cell type. Often thought of only as "other cells" in the brain, until recently they have not been subject to the detailed study afforded their neighbouring neurons. Considering the eye alone, with its eight photoreceptors, no worker who studies the visual system would claim that these cells are the same and could readily advance reasons why they should be considered not identical: opsin expression, rhabdomere size, axon terminal location, synaptic partners, gene expression, and development. Yet, glia which constitute about 10% of the *Drosophila* brain (Ito, Pers. Comm.), roughly 10,000 of the 100,000 or-so cells in the CNS (Truman *et al.*, 1993), are considered a relatively homogenous group. While the brain undoubtedly contains many unique neuronal cell types, as defined by their development, location, neurotransmitter expression and projection patterns, the glia of the adult are divided into only three main groups, surface, cortex and neuropile, with little distinction based on their origin or associated neuropile.

The glia that are intimately associated with any set of neurons must be programmed to deal with the needs of those particular neurons. Some glia are even derived from the same progenitors as their associated neurons (Udolph *et al.*, 1993; Ito *et al.*, 1997; Akiyama-Oda *et al.*, 1999). Cells in clonal units presumably express a set of genes that will allow them to co-ordinate action with their neuronal partners in the adult (Chotard *et al.*, 2005), and cells from associated sets of clonal units come together to form distinct and highly stereotyped neural circuits (Hofbauer and Campos-Ortega, 1990; Huang and Kunes, 1998; Ng *et al.*, 2002; Wilson *et al.*, 2004), often with little contribution from members of other clonal units (Ito and Awasaki, 2008). The neurons within any given neuropile express a specific combination of neurotransmitters and neuropeptides, and the glia within and surrounding that neuropile are equipped, accordingly, to deal with these secreted molecules.

Within any given neuropile, some neurochemicals will be more abundant than others. Histamine is the principal neurotransmitter of the photoreceptors in the visual system (Hardie, 1987). In the antennal lobe, olfactory receptor neurons contain acetylcholine (Blake *et al.*, 1993; Yasuyama and Salvaterra, 1999), while the majority of interneurons express GABA (Jackson *et al.*, 1990; Wilson and Laurent, 2005; Okada *et al.*, 2009). The mushroom bodies contain projection neurons that are widely presumed invariably to

express acetylcholine (Buchner *et al.*, 1986; Yasuyama and Salvaterra, 1999; Yasuyama *et al.*, 2003), extrinsic neurons that express GABA (Yasuyama *et al.*, 2002), and dopamine positive neurons that innervate broad areas of the mushroom body lobes (Nässel and Elekes, 1992). Octopaminergic neurons extend many neurites that ramify profusely throughout the brain, including in the antennal lobes, in distinct regions of the mushroom bodies and in the deeper optic neuropiles (Busch *et al.*, 2009; Busch and Tanimoto, 2010). In addition, each neuropile will contains a number of neurochemicals and neuropeptides (Nässel and Winther, 2010) released from local interneurons, each of which specifically modulates incoming signal or transmits it downstream. Thus, each neuropile should have a unique neurochemical identity which will change as the neuropile develops, and the associated glia should be correspondingly programmed uniquely to deal with this. In the lamina, for example, not only is histamine abundant but PDF is released by clock neurons (Meinertzhagen and Pyza, 1999), GABA is the likely neurotransmitter of centrifugal neurons (Datum *et al.*, 1986; Meyer *et al.*, 1986; Kolodziejczyk *et al.*, 2008), and acetylcholine is expressed in L4 and a subset of wide-field tangential neurons (Kolodziejczyk *et al.*, 2008). The large monopolar neurons L1 and L2 are immunoreactive to glutamate (Meinertzhagen and Sun, 1996) as well as a vesicular glutamate transporter (Kolodziejczyk *et al.*, 2008), although these monopolar cells also express immunoreactivity to Choline acetyltransferase, suggesting they have the means to produce acetylcholine (Buchner *et al.*, 1986; Yasuyama and Salvaterra, 1999). Amacrine cells may also express glutamate (Kolodziejczyk *et al.*, 2008). Finally, wide-field tangential neurons, LBO5HT, which spread across the distal surface of the lamina are thought to express serotonin (Nässel and Elekes, 1984). Moreover, these neurotransmitters are present in widely differing quantities, with histamine content, which is housed mostly in the visual system (Borycz *et al.*, 2002), being more than two orders of magnitude greater than other biogenic amines (Borycz *et al.*, 2008).

In the adult lamina of *Drosophila* there are at least six subtypes of glia (Eule *et al.*, 1995), two types of surface glia - the perineurial and subperineurial, two types of cortex glia – the distal and proximal satellite glia, and two types of neuropile glia – the epithelial and marginal glia. I have been involved in a project, in association with Aljoscha Nern (Janelia Farm), to identify and characterise transgenic lines of *Drosophila* which allow us to visualize these unique glial cell lines (Chapter 3). These lines will also allow careful cell-specific manipulation of genes to help better understand the function of specific glial subtypes in the adult. A seventh type of glia not characterised here (Edwards,

unpublished) was traced through pupal development with the larval surface glia specific driver line *c527-GAL4* and, in the adult, lines the lateral margins of the lamina. In addition I have identified two unique glial cell types in the medulla, chandelier glia and serpentine glia, and shown that the glia lying at the distal medulla are of two unique types, presumably ensheathing and astrocyte-like neuropile glia, by demonstrating that the driver lines *dEAAT-GAL4* or *Mz97-GAL4* label only one of at least two repo-expressing cell types that lie here.

The drivers that express in the different subtypes of glia provide some indication as to the gene expression patterns of these glia and, hence, their neuropile-specific function. An early approach that explored this idea came from raising antibodies against glia in the cricket brain (Meyer *et al.*, 1987). In *Drosophila*, genetic reporters reveal the far greater subtlety of the expression profiles of brain glia. For example, the distal satellite glia express drivers for *pointed*, *dimm*, *nrv2*, *spinster*, and *gliotactin* while their neighbouring proximal satellite glia share expression of some drivers but do not express those for *dimm, spinster* or *nrv2* and instead express drivers for *swiss cheese* and *ebony*. Their shared expression of drivers for septate junction-associated *gliotactin* (Auld *et al.*, 1995; Genova and Fehon, 2003; Schulte *et al.*, 2003) implicates both types of cortex glia in barrier formation. Furthermore, proximal satellite glia appear to engage in histamine/dopamine and serotonin inactivation because they express Ebony (Richardt *et al.*, 2003), while distal satellite glia are implicated in the storage of peptides (*dimm*; Hamanaka *et al.*, 2010), the homeostatic maintenance of neighbouring neurons and the regulation of neural apoptosis (*spinster*; Nakano *et al.*, 2001; Sweeney and Davis, 2002). Thus, although these two glial cell types reside in neighbouring regions of the lamina cortex they assume two very different functions. Despite their similar location in the adult, the divergent roles of cortex glia may not be so surprising given their independent larval origins, with distal satellite arising from wrapping glia of the eye disc (Chapter 3) and proximal satellite glia arising from precursors in the brain (Perez and Steller, 1996). Glial subtypes with a similar origin, such as the distal satellite glia and the pseudocartridge glia, both of which arise from the larval eye disc wrapping glia, have some shared and some distinct patterns of gene expression in the adult. While both express septate junction markers, such as *gliotactin*, the pseudocartridge glia express distinct proteins such as Moody (Bainton *et al.*, 2005) which implicates them in controlling permeability of the blood brain barrier. The pseudocartridge glia do not express *dimm* or *spinster*, suggesting that, unlike the distal satellite glia with which they

share a common precursor, they have no role in peptide storage, cellular maintenance or apoptosis.

7.2 Many Different Subtypes of Lamina Glia Play a Role in Histamine Metabolism

Of the six subtypes of glia described in the visual system, four have so far been implicated in histamine metabolism or storage. The distal-most fenestrated glia use the membrane associated vesicular transporter protein dVMAT-B in the uptake and storage of histamine (Borycz *et al.*, 2002; Romero-Calderón *et al.*, 2008). Surface glia, in general, appear to be involved in the regulated uptake of substances from the haemolymph, which is isolated from the nervous system by septate junction-rich subperineurial glia (Shaw, 1978; Shaw and Henken, 1984; Carlson *et al.*, 2000; Bainton *et al.*, 2005; Stork *et al.*, 2008; Kasuya *et al.*, 2009). In *hdc* mutants with limited production of histamine, histamine immunolabelling is either not detected or is restricted to the photoreceptors. In the wild-type, histamine is detected in the fenestrated glia, photoreceptors, mechanosensory neurons and large interneurons of the central brain, yet none of the *hdc* mutants has histamine immunolabelling in the fenestrated glia (Melzig *et al.*, 1996), suggesting that fenestrated glia contain histamine only when this neurotransmitter is abundant outside of the eye. This is also the case in flies that have consumed a solution of carcinine, which is converted to histamine in the body. Such flies show extensive distribution of histamine in the surface glia surrounding the entire brain, including the fenestrated glia that lie below the retina (Chapter 4).

Epithelial glia, which express the ABC transporter unit White (Borycz *et al.*, 2008) and the β-alanyl-histamine synthase Ebony (Richardt *et al.*, 2002; Richardt *et al.*, 2003), are involved in the uptake and β-alanyl conjugation of histamine. Results from Chapter 4 also implicate both the proximal satellite glia and the marginal glia in histamine recycling or storage. The proximal satellite glia express Ebony, enabling them to inactivate histamine by conjugation to β-alanine, and possibly also serotonin from neighbouring LBO5HT neuronal processes (Nässel and Elekes, 1984; Meinertzhagen and Pyza, 1999). The marginal glia are immunoreactive to histamine even though they lack *hdc* and cannot synthesize this neurotransmitter. The marginal glia also lack Ebony, so they cannot inactivate histamine by converting it to carcinine. It appears, then, that the marginal glia must store histamine which has been released synaptically by the

photoreceptors, and that this histamine must then, in some way, find its way back into the visual system for reuse.

7.2.1 The Surface Glia are a Barrier That Allows Selective Uptake of Ectopic Sources of Histamine

The NBAD/carcinine hydrolase enzyme Tan is essential for recycling histamine and flies with mutations in the *tan*/*CG12120* locus have reduced contents of whole-head histamine relative to the wild-type (Borycz *et al.*, 2002; True *et al.*, 2005) and a reduction in the transients of their ERG (Heisenberg, 1971; True *et al.*, 2005). Within the head, Tan is localised exclusively to the photoreceptors of the compound eyes and is not associated with mechanoreceptors or histamine expressing interneurons (Wagner *et al.*, 2007), although I observed some immunolabelling in cells at the posterior cuticle, possibly associated with mechanoreceptors or ocelli. Tan is also expressed throughout the body in cells that underlie the cuticle where it liberates dopamine and thereby modulates pigmentation (True *et al.*, 2005). In addition, I have localised Tan to non-cuticular tissue in the abdomen, specifically in areas surrounding eggs in females. Cuticular and abdominal expression of Tan helps explain why even *tan-EGUF-hid* flies, which lack all photoreceptor-specific expression of Tan, can still hydrolyse carcinine to histamine after consuming a solution of carcinine in glucose.

Flies with R1-R6 photoreceptor-specific rescue of *tan* also hydrolyse exogenous sources of carcinine despite the fact that the photoreceptors are within the nervous system and thus physically isolated from the source of carcinine by the blood brain barrier. Carcinine must therefore be selectively taken up by perineurial and subperineurial glia and transported into the visual system, and eventually the cytoplasm of photoreceptors, where it is acted upon by Tan. Similar, and possibly related, uptake of exogenous histamine has already been demonstrated (Melzig *et al.*, 1998).

7.2.2 The Photoreceptors Efficiently Utilize Tan

While Tan protein in both the body and the photoreceptors is capable of liberating histamine from carcinine, it is the photoreceptors that naturally express Tan and, under normal circumstances, are in the correct location to make efficient use of this protein for carcinine hydrolysis. Hence, when *tan* expression is rescued in the eye using a strong

Rh1-GAL4 driver, the average whole-head histamine content (2.7 ± 0.22 ng/head) of these flies surpasses even the average wild-type adult, measured by Borycz (2000) as 1.9890 ± 15 ng /head and measured here as 2.53 ± 0.11 ng. This is found even despite the fact that *Rh1-GAL4* drives *tan* expression in only three quarters of all photoreceptors.

Neither the body, nor the photoreceptors alone are as capable of hydrolysing exogenous sources of carcinine as efficiently as a fly with wild-type *tan* expression. Measurements of whole-head histamine that follow carcinine feeding experiment are, in fact a, reflection of histamine liberation in the CNS and in the body. Histamine that is liberated in the body then has access to the head via the haemolymph, and once in the head it is present in the haemolymph, the surface glia and the brain.

7.2.3 A Model for Histamine Movement in the Visual System

Histamine is produced in the photoreceptors (Burg *et al.*, 1993; Melzig *et al.*, 1996) and released from synapses within the photoreceptor axon terminals at the level of the lamina and medulla (Meinertzhagen and O'Neil, 1991; Takemura *et al.*, 2008). Released neurotransmitter is then taken up into the neighbouring epithelial glia from the synaptic cleft by some means that is dependent upon the action of the ABC transporter subunit White (Borycz *et al.*, 2008). Once in the epithelial glia, the product of the *ebony* gene inactivates histamine by conjugation to β-alanine to produce carcinine (Hovemann *et al.*, 1998; Borycz *et al.*, 2002; Richardt *et al.*, 2002; Richardt *et al.*, 2003), which is not known to have a function in the nervous system. Carcinine is difficult to detect by HPLC (Borycz *et al.*, 2000) and this, in part, leads us to believe that carcinine turnover within the visual system is rapid. Carcinine must be transported out of the epithelial glia and back into the photoreceptor where Tan dissociates histamine from β-alanine in the cytoplasm, allowing liberated histamine to be packaged into vesicles for re-release (True *et al.*, 2005; Wagner *et al.*, 2007). How carcinine is transported from glia into photoreceptors is not known, and while the evidence is not entirely solid, the $Na^{+}Cl^{-}$ dependant SLC6 family transporter, Inebriated, has been proposed to play such a role (Gavin *et al.*, 2007).

Mutations of both *tan* and *ebony* have an increase in the number of their capitate projections (Meinertzhagen and Wang, 1997), whose stalks are sites of Clathrin-mediated endocytosis (Fabian-Fine *et al.*, 2003). Little else is known about the function

of capitate projections, but they are a site of close apposition between epithelial glial and photoreceptor membranes in the lamina (Stark and Carlson, 1986) and respond dynamically to conditions in which histamine content or release is altered (Meinertzhagen and Wang, 1997; Rybak and Meinertzhagen, 1997; Meinertzhagen *et al.*, 2000), implying that these organelles are involved in carcinine transport from the epithelial glia into photoreceptors. They have previously been proposed as sites of combined membrane and histamine recycling (Fabian-Fine *et al*., 2003), but evidence for the latter has been based mostly on the idea that these two essential functions may be economically integrated into a single organelle.

At least three other glial cell types are involved in the metabolism, movement or storage of histamine. The surface glia, which include the perineurial glia and the fenestrated glia of the lamina, are the first layer of the blood brain and eye-brain barrier, respectively, and while perineurial glia do not restrict extracellular passage (Shaw, 1978), they do take up and store excess histamine (Romero-Calderón *et al.*, 2008). The source of the histamine is likely to be from the haemolymph and, at least in *Musca*, perineurial fenestrated glia contain coated vesicles implicating them in active pinocytosis (Saint Marie and Carlson, 1983b). Histamine accumulates in the haemolymph either because of dietary increases in histamine (Melzig *et al.*, 1998), L-histidine (Morgan *et al.*, 1999), carcinine (Borycz *et al.*, 2002; True *et al.*, 2005) or because of release at other histaminergic neurons (Nässel *et al.*, 1990). When normal amounts of histamine are involved, uptake appears to be via the fenestrated glia which underlie the photoreceptors (Borycz *et al.*, 2002; Romero-Calderón *et al.*, 2008), but when excess histamine is present in the haemolymph, the perineurial glia, which surround the entire brain, have a more active role in histamine uptake. Some of this excess histamine, or, in my experiments - carcinine, is selectively transported into the CNS. This means that histamine/carcinine must be transported through the pseudocartridge and/or subperineurial glia, the septate junction rich “barrier” layer of the eye-brain barrier (Saint Marie and Carlson, 1983a; Stork *et al.*, 2008). It is not known what becomes of the excess histamine that it housed in the surface glia, and it is not necessarily shuttled into histaminergic neurons. It is possible that a feedback system exists within the photoreceptors and other histaminergic neurons to modulate *de-novo* synthesis of histamine when neurotransmitter content in the brain reaches a concentration above or below the norm.

In the cortex, the proximal satellite glia, which lie closest to the lamina neuropile, express Ebony, thus implicating them in histamine inactivation. While these glia express septate junction associated genes such as *gliotactin* (Auld *et al.*, 1995), and while septate junctions are detected between proximal satellite glia in the closely related species *Musca domestica* (Saint Marie and Carlson, 1983a), they have not been confirmed to exist between the glia of the proximal cortex in *Drosophila*. It is possible that these glial cells prevent the extracellular diffusion of histamine, which is released within the neuropile, into distal layers of the cortex. Their expression of *ebony* also implicates the proximal satellite glia in the uptake of histamine and its subsequent conversion to carcinine. This carcinine can then be transported back into the neuropile for recycling. Any role that the proximal satellite glia play in histamine inactivation does not prohibit them from also being involved in the uptake and inactivation of serotonin released by the neighbouring neurites of LBO5HT.

At the base of the neuropile, marginal glia extend branches between the proximal ends of photoreceptor terminals and their surrounding epithelial glia, forming a little cork at the base of the cartridge through which only unexpanded axons pass. The marginal glia do not express Ebony but they do contain clathrin coated vesicles and are immunoreactive to histamine, suggesting that they retrieve excess histamine from the extracellular space by pinocytosis. What becomes of this histamine, and how it gets back into the photoreceptor is unknown. One possibility is that a system exists for the inter-glial transport of substances, in this case between the marginal glia and the epithelial glia. A system of gap junctions has been proposed to connect successive layers of glia in the lamina of *Musca* (Saint Marie and Carlson, 1983a), but this has not been supported in *Drosophila* and immunoreactivity to neither of the gap junction innexins, Ogre/Innexin1 or Innexin2 localise to an area specifically corresponding to the marginal glial/epithelial glia boundary (Chapter 5). While it would appear as if a system for inter-glial communication and transport may exist between fenestrated glia themselves (Chi and Carlson, 1981), as well as between the two layers of surface glia (Shaw, 1978), evidence to support inter-glial transport awaits resolution. This conclusion underscores a general need to identify sites of gap junction coupling in the *Drosophila* nervous system, for which existing antibodies are too few or give too poor a signal.

The potential pathways for histamine and carcinine movement within the lamina are illustrated in Figure 7.1.

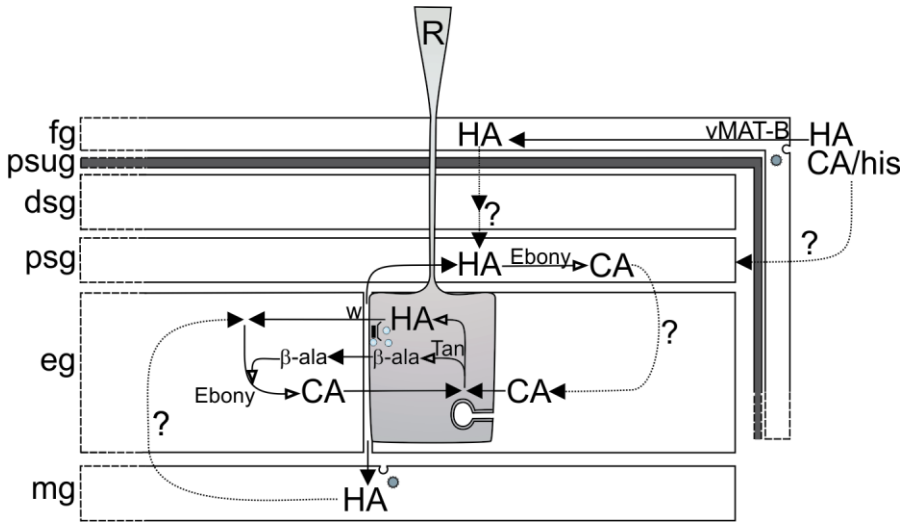

FIGURE 7.1 - POTENTIAL PATHWAYS FOR HISTAMINE AND CARCININE TRANSPORT WITHIN THE LAMINA OF *DROSOPHILA*.

Inferred sites of transport are indicated by large, solid arrowheads. Enzymatic reactions are indicated by small, open arrowheads. Histamine released from the synapses of photoreceptors (R), is taken into neighbouring epithelial glia (eg) by a *white* (w^-) dependent mechanism, and is there conjugated to β-alanine by Ebony to form carcinine. Carcinine is transported back into photoreceptors where free histamine and β-alanine are liberated by the action of Tan. Histamine transport into the fenestrated glia (fg) is dependent upon VMAT-B (Romero-Calderón *et al.*, 2008), but the equivalent uptake into perineurial glia must be by an independent mechanism because these glia do not express vMAT-B. The fate of histamine stored in the fenestrated glia is not known, but all of histamine, carcinine and L-histidine pass through the eye-brain barrier, which begins at the pseudocartridge glia (psug), to gain eventual access to the photoreceptors. Exogenous histamine may re-enter the visual system via the proximal satellite glia (psg), which express Ebony and therefore inactivate histamine, converting it to carcinine before allowing this to pass into the neuropile. Alternatively, Ebony-expressing proximal satellite glia may act as a dorsal barrier that prevents histamine efflux into the cortex by taking up and inactivating free histamine and then shuttling carcinine back into the neuropile for recycling. At the base of the lamina, marginal glia (mg) which lie close to the proximal terminals of photoreceptors, but which do not express Ebony, also accumulate histamine, possibly by pinocytosis, and may transport this neurotransmitter into the epithelial glia for inactivation before recycling. It is so far not known what, if any role the distal satellite glia (dsg) may play in histamine recycling or recovery.

7. 3 RUNT AND LESSONS LEARNED: THE PROBLEM WITH MIS-EXPRESSION STUDIES

Photoreceptors are defined by the size and position of their rhabdomere in the ommatidial array, by their expression of one of six types of the light absorbing Rhodopsin, and by the terminal location of their axon, and consequently, their synaptic partners. Mis-expression of Runt was shown to cause defects in photoreceptor axonal targeting, causing the R1-R6 axons to overshoot their interim targets, the marginal glia, at the base of the lamina and terminate instead within the medulla. It was proposed that when Runt, which is normally only expressed in the nucleus of R7 and R8, is expressed in R2 and R5, axons from these cells overshoot their lamina targets and cause axons projectioning from their neighbouring R1,R3, R4 and R6 photoreceptors to do the same. All photoreceptors were reported to maintain their fate and appeared to have normal rhabdomere size and organization in the retina (Kaminker *et al.*, 2002). These previous conclusions seemed to support an ideal system in which to observe ectoptic synaptogeneis of R1-R6 terminals with novel targets in the medulla. Unfortunately, upon closer examination, ectopic *runt* expression in photoreceptors caused severe disruptions in the organisation of the ommatidium and many R1-R6 photoreceptors were, in fact, transformed into R7- and R8-like cells, thus complicating the identification and synaptic characterisation of mistargeted R1-R6 terminals in the medulla. In retrospect, analysis of ectopic photoreceptor synapses would have been better if performed on a mutant such as *breakless*, which has independent R1-R6 targeting errors and only occasional transformation of R7 cells to an R1-R6-like fate (Rao *et al.*, 2000; Senti *et al.*, 2000; Kaminker *et al.*, 2002).

Despite its complications the "*runt*" study is not without its own interesting findings. First and foremost is that every photoreceptor axon that was identified and examined in the medulla contained tetrad synapses. A proportion of these photoreceptor terminals were likely those of mis-projected R1-R6 axons, allowing us to conclude that mis-projected photoreceptor terminals form ectopic synapses in the medulla. These ectopic tetrad synapses would thus form with novel partners since neither amacrine cells nor epithelial glia, both typical partners at the tetrad in the lamina (Meinertzhagen and O'Neil, 1991), are present in the medulla. Second, the terminals of all photoreceptors in the medulla contained many large capitate projections, measuring approximately 190 nm in diameter. This is unusual in that photoreceptors within the medulla normally contain small (95 nm diameter), sparse, capitate projection-like structures presumably formed by

the penetration of medulla neuropile glia. In *runt*-overexpressing flies most photoreceptor terminals in the medulla are from either ectopic R1-R6 axons or the axons of transformed R1-R6 cells, and so it appears that the size of the capitate projection is not determined by the penetrating glia, but by the photoreceptor itself. Either that, or abnormalities in the structure of the medulla result in altered and ineffective histamine release and recycling near the photoreceptor synapse in the medulla, which then elicits a compensatory response that alters the size and number of capitate projections. Lastly, the transcription factor Runt is involved in the establishment of an R7 or R8 cell-like fate. In the case of R7, Runt mediates cell fate specification via a *sevenless* dependent pathway, but it does not appear to modify cell fate in a cell-autonomous manner. When individual photoreceptors over-express *runt,* using a *MARCM*-like *FLP*-out technique, they continue to display abnormalities in axon targeting and terminal formation, but do not undergo changes in cell fate. Runt dependent R7 and R8 cell-fate transformation appears to rely on combinatorial expression of this transcription factor in a number of photoreceptors, and the more cells that express *runt* in combination, the more degraded the retinal phenotype.

Ultimately, we must address the question of what phenotypic characteristics define a cell. Rhabdomere size, cell position, Rhodopsin expression and axon projection, which all coordinately express in predictable combinations in each of the three R cell types become scrambled after *runt* mis-expression. This vitiates somewhat the concept of cell fate, but endorses the idea of the separate selection of phenotypic features.

REFERENCES

Akiyama-Oda, Y., Hosoya, T. and Hotta, Y. 1999. Asymmetric cell division of thoracic neuroblast 6-4 to bifurcate glial and neuronal lineage in *Drosophila*. Development 126, 1967-1974.

Alfonso, T.B. and Jones, B.W. 2002. *gcm2* promotes glial cell differentiation and is required with *glial cells missing* for macrophage development in *Drosophila*. Dev. Biol. 248, 369-383.

Amphoux, A., Vialou, V., Drescher, E., Brüss, M., Mannoury La Cour, C., Rochat, C., Millan, M.J., Giros, B., Bönisch, H. and Gautron, S. 2006. Differential pharmacological in vitro properties of organic cation transporters and regional distribution in rat brain. Neuropharmacology 50, 941-952.

Andretic, R. and Hirsh, J. 2000. Circadian modulation of dopamine receptor responsiveness in *Drosophila melanogaster*. Proc. Natl. Acad. Sci. U.S.A. 97, 1873-1878.

Armett-Kibel, C. and Meinertzhagen, I.A. 1985. The long visual fibers of the dragonfly optic lobe: their cells of origin and lamina connections. J. Comp. Neurol. 242, 459-474.

Artalejo, C.R., Henley, J.R., McNiven, M.A. and Palfrey, H.C. 1995. Rapid endocytosis coupled to exocytosis in adrenal chromaffin cells involves Ca^{2+}, GTP, and dynamin but not clathrin. Proc. Natl. Acad. Sci. U.S.A. 92, 8328-8332.

Augustin, H., Grosjean, Y., Chen, K., Sheng, Q. and Featherstone, D.E. 2007. Nonvesicular release of glutamate by glial xCT transporters suppresses glutamate receptor clustering *in vivo*. J. Neurosci. 27, 111-123.

Auld, V.J., Fetter, R.D., Broadie, K. and Goodman, C.S. 1995. Gliotactin, a novel transmembrane protein on peripheral glia, is required to form the blood-nerve barrier in Drosophila. Cell 81, 757-767.

Aust, S., Brüsselbach, F., Pütz, S. and Hovemann, B.T. 2010. Alternative tasks of *Drosophila* Tan in neurotransmitter recycling vs cuticle sclerotization disclosed by kinetic properties. J. Biol. Chem. 285 20740-20747.

Awasaki, T., Saito, M., Sone, M., Suzuki, E., Sakai, R., Ito, K. and Hama, C. 2000. The *Drosophila* trio plays an essential role in patterning of axons by regulating their directional extension. Neuron 26, 119-131.

Awasaki, T., Tatsumi, R., Takahashi, K., Arai, K., Nakanishi, Y., Ueda, R. and Ito, K. 2006. Essential role of the apoptotic cell engulfment genes *draper* and *ced-6* in programmed axon pruning during *Drosophila* metamorphosis. Neuron 50, 855-867.

Awasaki, T., Lai, S.-L., Ito, K. and Lee, T. 2008. Organization and postembryonic development of glial cells in the adult central brain of *Drosophila*. J. Neurosci. 28, 13742-13753.

Bainton, R.J., Tsai, L.T.-Y., Schwabe, T., DeSalvo, M., Gaul, U. and Heberlein, U. 2005. *moody* encodes two GPCRs that regulate cocaine behaviors and blood-brain barrier permeability in *Drosophila*. Cell 123, 145-156.

Banerjee, S., Bainton, R.J., Mayer, N., Beckstead, R. and Bhat, M.A. 2008. Septate junctions are required for ommatidial integrity and blood-eye barrier function in *Drosophila*. Dev. Biol. 317, 585-599.

Banerjee, U., Renfranz, P.J., Hinton, D.R., Rabin, B.A. and Benzer, S. 1987. The *sevenless*$^{+}$ protein is expressed apically in cell membranes of developing Drosophila retina; it is not restricted to cell R7. Cell 51, 151-158.

Barth, M., Hirsch, H.V., Meinertzhagen, I.A. and Heisenberg, M. 1997. Experience-dependent developmental plasticity in the optic lobe of *Drosophila melanogaster*. J. Neurosci. 17, 1493-1504.

Bashaw, G.J. and Goodman, C.S. 1999. Chimeric axon guidance receptors: The cytoplasmic domains of slit and netrin receptors specify attraction versus repulsion. Cell 97, 917-926.

Battye, R., Stevens, A. and Jacobs, J.R. 1999. Axon repulsion from the midline of the *Drosophila* CNS requires *slit* function. Development 126, 2475-2481.

Bauer, R., Martini, J., Lehmann, C. and Hoch, M. 2003. Cellular distribution of Innexin 1 and 2 gap junctional channel proteins in epithelia of the *Drosophila* embryo. Cell Commun. Adhes. 10, 221-225.

Bauer, R., Lehmann, C., Martini, J., Eckardt, F. and Hoch, M. 2004. Gap junction channel protein Innexin 2 is essential for epithelial morphogenesis in the *Drosophila* embryo. Mol. Biol. Cell 15, 2992-3004.

Baumgartner, S., Littleton, J.T., Broadie, K., Bhat, M.A., Harbecke, R., Lengyel, J.A., Chiquet-Ehrismann, R., Prokop, A. and Bellen, H.J. 1996. A *Drosophila* neurexin is required for septate junction and blood-nerve barrier formation and function. Cell 87, 1059-1068.

Bausenwein, B., Dittrich, A.P.M. and Fischbach, K.-F. 1992. The optic lobe of *Drosophila melanogaster.* II. Sorting of retinotopic pathways in the medulla. Cell Tissue Res. 267, 17-28.

Bayley, P.R. and Morgans, C.W. 2007. Rod bipolar cells and horizontal cells form displaced synaptic contacts with rods in the outer nuclear layer of the *nob2* retina. J. Comp. Neurol. 500, 286-298.

Bazigou, E., Apitz, H., Johansson, J., Lorén, C.E., Hirst, E.M.A., Chen, P.-L., Palmer, R.H. and Salecker, I. 2007. Anterograde Jelly belly and Alk receptor tyrosine kinase signaling mediates retinal axon targeting in *Drosophila*. Cell 128, 961-975.

Beall, C.J. and Hirsh, J. 1987. Regulation of the *Drosophila* dopa decarboxylase gene in neuronal and glial cells. Genes Dev. 1, 510-520.

Beckervordersandforth, R. (2007) Differenzierung, Spezifizierung und Migration der lateralen Gliazellen im spätembryonalen Bauchmark von *Drosophila melanogaster*. *PhD thesis, Biologie*. p. 134. Johannes Gutenberg Universität Mainz: Mainz.

Beckervordersandforth, R.M., Rickert, C., Altenhein, B. and Technau, G.M. 2008. Subtypes of glial cells in the *Drosophila* embryonic ventral nerve cord as related to lineage and gene expression. Mech. Dev. 125, 542-557.

Behr, M., Riedel, D. and Schuh, R. 2003. The Claudin-like Megatrachea is essential in septate junctions for the epithelial barrier function in *Drosophila*. Dev. Cell 5, 611-620.

Bell, M.L., Earl, J.B. and Britt, S.G. 2007. Two types of *Drosophila* R7 photoreceptor cells are arranged randomly: A model for stochastic cell-fate determination. J. Comp. Neurol. 502, 75-85.

Benton, R., Vannice, K.S., Gomez-Diaz, C. and Vosshall, L.B. 2009. Variant ionotropic glutamate receptors as chemosensory receptors in *Drosophila*. Cell 136, 149-162.

Besson, M.-T., Soustelle, L. and Birman, S. 2000. Selective high-affinity transport of aspartate by a *Drosophila* homologue of the excitatory amino-acid transporters. Curr. Biol. 10, 207-210.

Bettencourt da Cruz, A., Wentzell, J. and Kretzschmar, D. 2008. Swiss Cheese, a protein involved in progressive neurodegeneration, acts as a noncanonical regulatory subunit for PKA-C3. J. Neurosci. 28, 10885-10892.

Bhat, M.A., Rios, J.C., Lu, Y., Garcia-Fresco, G.P., Ching, W., St. Martin, M., Li, J., Einheber, S., Chesler, M., Rosenbluth, J., Salzer, J.L. and Bellen, H.J. 2001. Axon-glia interactions and the domain organization of myelinated axons requires Neurexin IV/Caspr/Paranodin. Neuron 30, 369-383.

Bilder, D. and Perrimon, N. 2000. Localization of apical epithelial determinants by the basolateral PDZ protein Scribble. Nature 403, 676-680.

Blake, A.D., Anthony, N.M., Chen, H.H., Harrison, J.B., Nathanson, N.M. and Sattelle, D.B. 1993. *Drosophila* nervous system muscarinic acetylcholine receptor: transient functional expression and localization by immunocytochemistry. Mol. Pharmacol. 44, 716-724.

Blakely, R.D., DeFelice, L.J. and Galli, A. 2005. Biogenic amine neurotransmitter transporters: Just when you thought you knew them. Physiology 20, 225-231.

Blinkov, S.M. and Glezer, I.I. (1968) *The human brain in figures and tables. A quantitative handbook*. Basic Books: Plenum: New York.

Blumenthal, E.M. 2008. Cloning of the neurodegeneration gene *drop-dead* and characterization of additional phenotypes of its mutation. Fly 2, 180-188.

Boekhoff-Falk, G. 2005. Hearing in *Drosophila*: development of Johnston's organ and emerging parallels to vertebrate ear development. Dev. Dyn. 232, 550-558.

Bohrmann, J. and Zimmermann, J. 2008. Gap junctions in the ovary of *Drosophila melanogaster*: localization of innexins 1, 2, 3 and 4 and evidence for intercellular communication via innexin-2 containing channels. BMC Dev. Biol. 8, 111.

Booth, G.E., Kinrade, E.F. and Hidalgo, A. 2000. Glia maintain follower neuron survival during *Drosophila* CNS development. Development 127, 237-244.

Boothroyd, C.E. and Young, M.W. 2008. The in(put)s and out(put)s of the *Drosophila* circadian clock. Ann. N.Y. Acad. Sci. 1129, 350-357.

Borst, A. 2000. Models of motion detection. Nat. Neurosci. 3, 1168.

Borycz, J., Vohra, M., Tokarczyk, G. and Meinertzhagen, I.A. 2000. The determination of histamine in the *Drosophila* head. J. Neurosci. Methods 101, 141-148.

Borycz, J., Borycz, J.A., Loubani, M. and Meinertzhagen, I.A. 2002. *tan* and *ebony* genes regulate a novel pathway for transmitter metabolism at fly photoreceptor terminals. J. Neurosci. 22, 10549-10557.

Borycz, J., Borycz, J.A., Kubów, A., Lloyd, V. and Meinertzhagen, I.A. 2008. *Drosophila* ABC transporter mutants *white*, *brown* and *scarlet* have altered contents and distribution of biogenic amines in the brain. J. Exp. Biol. 211, 3454-3466.

Borycz, J.A., Borycz, J., Kubów, A., Kostyleva, R. and Meinertzhagen, I.A. 2005. Histamine compartments of the *Drosophila* brain with an estimate of the quantum content at the photoreceptor synapse. J. Neurophysiol. 93, 1611-1619.

Boschek, C.B. 1971. On the fine structure of the peripheral retina and lamina ganglionaris of the fly, *Musca domestica*. Z. Zellforsch. Mikrosk. Anat. 118, 369-409.

Braitenberg, V. 1967. Patterns of projection in the visual system of the fly. I. Retina-lamina projections. Exp. Brain Res. 3, 271-298.

Brand, A.H. and Perrimon, N. 1993. Targeted gene expression as a means of altering cell fates and generating dominant phenotypes. Development 118, 401-415.

Brandstätter, J.H., Shaw, S.R. and Meinertzhagen, I.A. 1991. Terminal degeneration and synaptic disassembly following receptor photoablation in the retina of the fly's compound eye. J. Neurosci. 11, 1930-1941.

Brandstätter, J.H., Seyan, H.S. and Meinertzhagen, I.A. 1992. The effects of the loss of target cells upon photoreceptor inputs in the fly's optic lobe. J. Neurocytol. 21, 693-705.

Brandstätter, J.H. and Meinertzhagen, I.A. 1995. The rapid assembly of synaptic sites in photoreceptor terminals of the fly's optic lobe recovering from cold shock. Proc. Natl. Acad. Sci. U.S.A. 92, 2677-2681.

Brazitikos, P.D. and Tsacopoulos, M. 1991. Metabolic signaling between photoreceptors and glial cells in the retina of the drone (*Apis mellifera*). Brain Res. 567, 33-41.

Bremer, J. 1983. Carnitine-metabolism and functions. Physiol. Rev. 63, 1420-1480.

Brooks, R.A. and Woodruff, R.I. 2004. Calmodulin transmitted through gap junctions stimulates endocytic incorporation of yolk precursors in insect oocytes. Dev. Biol. 271, 339-349.

Brown, K.E. and Freeman, M. 2003. Egfr signalling defines a protective function for ommatidial orientation in the *Drosophila* eye. Development 130, 5401-5412.

Brunner, D., Oellers, N., Szabad, J., Biggs, W.H., 3rd, Zipursky, S.L. and Hafen, E. 1994. A gain-of-function mutation in Drosophila MAP kinase activates multiple receptor tyrosine kinase signaling pathways. Cell 76, 875-888.

Buchanan, R.L. and Benzer, S. 1993. Defective glia in the *Drosophila* brain degeneration mutant *drop-dead*. Neuron 10, 839-850.

Buchner, E., Buchner, S., Crawford, G., Mason, W.T., Salvaterra, P.M. and Sattelle, D.B. 1986. Choline acetyltransferase-like immunoreactivity in the brain of *Drosophila melanogaster*. Cell Tissue Res. 246, 57-62.

Buchner, E., Buchner, S., Burg, M.G., Hofbauer, A., Pak, W.L. and Pollack, I. 1993. Histamine is a major mechanosensory neurotransmitter candidate in *Drosophila melanogaster*. Cell Tissue Res. 273, 119-125.

Bullock, T.H. and Horridge, G.A. (1965) *Structure and function in the nervous systems of invertebrates.* Volume II. W.H. Freeman and Company: San Francisco.

Bülthoff, H. 1982. *Drosophila* mutants disturbed in visual orientation I. Mutants affected in early visual processing. Biol. Cybern. 45, 63-70.

Burg, M.G., Sarthy, P.V., Koliantz, G. and Pak, W.L. 1993. Genetic and molecular identification of a *Drosophila* histidine decarboxylase gene required in photoreceptor transmitter synthesis. EMBO J. 12, 911-919.

Burg, M.G., Geng, C., Guan, Y., Koliantz, G. and Pak, W.L. 1996. *Drosophila rosA* gene, which when mutant causes aberrant photoreceptor oscillation, encodes a novel neurotransmitter transporter homologue. J. Neurogenet. 11, 59-79.

Burkhardt, W. and Braitenberg, V. 1976. Some peculiar synaptic complexes in the first visual ganglion of the fly, *Musca domestica*. Cell Tissue Res. 173, 287-308.

Burns, T.A., Huston, J.P. and Spieler, R.E. 2003. Circadian variation of brain histamine in goldfish. Brain Res. Bull. 59, 299-301.

Busch, S., Selcho, M., Ito, K. and Tanimoto, H. 2009. A map of octopaminergic neurons in the *Drosophila* brain. J. Comp. Neurol. 513, 643-667.

Busch, S. and Tanimoto, H. 2010. Cellular configuration of single octopamine neurons in *Drosophila*. J. Comp. Neurol. 518, 2355-2364.

Cagan, R.L. and Ready, D.F. 1989a. The emergence of order in the *Drosophila* pupal retina. Dev. Biol. 136, 346-362.

Cagan, R.L. and Ready, D.F. 1989b. *Notch* is required for successive cell decisions in the developing *Drosophila* retina. Genes Dev. 3, 1099-1112.

Cagan, R.L., Krämer, H., Hart, A.C. and Zipursky, S.L. 1992. The bride of sevenless and sevenless interaction: internalization of a transmembrane ligand. Cell 69, 393-399.

Cammack, J.N. and Schwartz, E.A. 1993. Ions required for the electrogenic transport of GABA by horizontal cells of the catfish retina. J. Physiol. 472, 81-102.

Campbell, G., Göring, H., Lin, T., Spana, E., Andersson, S., Doe, C.Q. and Tomlinson, A. 1994. RK2, a glial-specific homeodomain protein required for embryonic nerve cord condensation and viability in *Drosophila*. Development 120, 2957-2966.

Campos-Ortega, J.A. and Strausfeld, N.J. 1972. The columnar organization of the second synaptic region of the visual system of *Musca domestica* L. I. Receptor terminals in the medulla. Z. Zellforsch. Mikrosk. Anat. 124, 561-585.

Campos-Ortega, J.A. and Strausfeld, N.J. 1973. Synaptic connections of intrinsic cells and basket arborizations in the external plexiform layer of the fly's eye. Brain Res. 59, 119-136.

Campos-Ortega, J.A. 1974. Autoradiographic localization of ^{3}H-γ-aminobutyric acid uptake in the lamina ganglionaris of *Musca* and *Drosophila*. Z. Zellforsch. Mikrosk. Anat. 147, 415-431.

Campos-Ortega, J.A. and Hofbauer, A. 1977. Cell clones and pattern formation: On the lineage of photoreceptor cells in the compound eye of *Drosophila*. Roux's Arch. Dev. Biol. 181, 227-245.

Campos, A.R., Fischbach, K.F. and Steller, H. 1992. Survival of photoreceptor neurons in the compound eye of *Drosophila* depends on connections with the optic ganglia. Development 114, 355-366.

Cantera, R. 1993. Glial cells in adult and developing prothoracic ganglion of the hawk moth *Manduca sexta*. Cell Tissue Res. 272, 93-108.

Cantera, R. and Trujillo-Cenóz, O. 1996. Glial cells in insect ganglia. Microsc. Res. Tech. 35, 285-293.

Carlson, S.D. and Saint Marie, R.L. 1990. Structure and function of insect glia. Annu. Rev. Entomol. 35, 597-621.

Carlson, S.D., Hilgers, S.L. and Garment, M.B. 1998. Blood-eye barrier of the developing *Drosophila melanogaster* (Diptera : *Drosophilidae*). Int. J. Insect Morphol. Embryol. 27, 241-247.

Carlson, S.D., Juang, J.-L., Hilgers, S.L. and Garment, M.B. 2000. Blood barriers of the insect. Annu. Rev. Entomol. 45, 151-174.

Carthew, R.W. and Rubin, G.M. 1990. *seven in absentia*, a gene required for specification of R7 cell fate in the Drosophila eye. Cell 63, 561-577.

Carthew, R.W., Neufeld, T.P. and Rubin, G.M. 1994. Identification of genes that interact with the *sina* gene in *Drosophila* eye development. Proc. Natl. Acad. Sci. U.S.A. 91, 11689-11693.

Cash, S., Chiba, A. and Keshishian, H. 1992. Alternate neuromuscular target selection following the loss of single muscle fibers in *Drosophila*. J. Neurosci. 12, 2051-2064.

Cayre, M., Strambi, C., Charpin, P., Augier, R., Meyer, M.R., Edwards, J.S. and Strambi, A. 1996. Neurogenesis in adult insect mushroom bodies. J. Comp. Neurol. 371, 300-310.

Ceriani, M.F., Hogenesch, J.B., Yanovsky, M., Panda, S., Straume, M. and Kay, S.A. 2002. Genome-wide expression analysis in *Drosophila* reveals genes controlling circadian behavior. J. Neurosci. 22, 9305-9319.

Chamberlain, L.H. and Burgoyne, R.D. 2000. Cysteine-String Protein: The chaperone at the synapse. J. Neurochem. 74, 1781-1789.

Chang, H.Y., Grygoruk, A., Brooks, E.S., Ackerson, L.C., Maidment, N.T., Bainton, R.J. and Krantz, D.E. 2005. Overexpression of the *Drosophila* vesicular monoamine transporter increases motor activity and courtship but decreases the behavioral response to cocaine. Mol. Psychiatry 11, 99-113.

Chen, N.-H., Reith, M.E.A. and Quick, M.W. 2004. Synaptic uptake and beyond: the sodium- and chloride-dependent neurotransmitter transporter family SLC6. Pflugers Arch. - Eur. J. Physiol. 447, 519-531.

Chi, C. and Carlson, S.D. 1980. Membrane specializations in the first optic neuropil of the housefly, *Musca domestica* L. I. Junctions between neurons. J. Neurocytol. 9, 429-449.

Chi, C. and Carlson, S.D. 1981. The perineurium of the adult housefly: Ultrastructure and permeability to lanthanum. Cell Tissue Res. 217, 373-386.

Chiang, A., Priya, R., Ramaswami, M., VijayRaghavan, K. and Rodrigues, V. 2009. Neuronal activity and Wnt signaling act through Gsk3-β to regulate axonal integrity in mature *Drosophila* olfactory sensory neurons. Development 136, 1273-1282.

Chiu, C.-S., Ross, L.S., Cohen, B.N., Lester, H.A. and Gill, S.S. 2000. The transporter-like protein Inebriated mediates hyperosmotic stimuli through intracellular signaling. J. Exp. Biol. 203, 3531-3546.

Chklovskii, D.B. and Koulakov, A.A. 2004. Maps in the brain: What can we learn from them? Annu. Rev. Neurosci. 27, 369-392.

Choe, K.-M., Prakash, S., Bright, A. and Clandinin, T.R. 2006. Liprin-α is required for photoreceptor target selection in *Drosophila*. Proc. Natl. Acad. Sci. U.S.A. 103, 11601-11606.

Choi, K.-W. and Benzer, S. 1994. Migration of glia along photoreceptor axons in the developing *Drosophila* eye. Neuron 12, 423-431.

Chotard, C. and Salecker, I. 2004. Neurons and glia: team players in axon guidance. Trends Neurosci. 27, 655-661.

Chotard, C., Leung, W. and Salecker, I. 2005. *glial cells missing* and *gcm2* cell autonomously regulate both glial and neuronal development in the visual system of *Drosophila*. Neuron 48, 237-251.

Chotard, C. and Salecker, I. 2007. Glial cell development and function in the *Drosophila* visual system. Neuron Glia Biol. 3, 17-25.

Chou, W.-H., Hall, K.J., Wilson, D.B., Wideman, C.L., Townson, S.M., Chadwell, L.V. and Britt, S.G. 1996. Identification of a novel Drosophila opsin reveals specific patterning of the R7 and R8 photoreceptor cells. Neuron 17, 1101-1115.

Chou, W.-H., Huber, A., Bentrop, J., Schulz, S., Schwab, K., Chadwell, L.V., Paulsen, R. and Britt, S.G. 1999. Patterning of the R7 and R8 photoreceptor cells of *Drosophila*: evidence for induced and default cell-fate specification. Development 126, 607-616.

Chou, Y.-H. and Chien, C.-T. 2002. Scabrous controls ommatidial rotation in the *Drosophila* compound eye. Dev. Cell 3, 839-850.

Clandinin, T.R. and Zipursky, S.L. 2000. Afferent growth cone interactions control synaptic specificity in the *Drosophila* visual system. Neuron 28, 427-436.

Clandinin, T.R., Lee, C.-H., Herman, T., Lee, R.C., Yang, A.Y., Ovasapyan, S. and Zipursky, S.L. 2001. *Drosophila* LAR regulates R1-R6 and R7 target specificity in the visual system. Neuron 32, 237-248.

Claridge-Chang, A., Wijnen, H., Naef, F., Boothroyd, C., Rajewsky, N. and Young, M.W. 2001. Circadian regulation of gene expression systems in the *Drosophila* head. Neuron 32, 657-671.

Clements, J., Lu, Z., Gehring, W.J., Meinertzhagen, I.A. and Callaerts, P. 2008. Central projections of photoreceptor axons originating from ectopic eyes in *Drosophila*. Proc. Natl. Acad. Sci. U.S.A. 105, 8968-8973.

Clyne, P.J., Warr, C.G., Freeman, M.R., Lessing, D., Kim, J. and Carlson, J.R. 1999. A novel family of divergent seven-transmembrane proteins: candidate odorant receptors in *Drosophila*. Neuron 22, 327-338.

Cook, T., Pichaud, F., Sonneville, R., Papatsenko, D. and Desplan, C. 2003. Distinction between color photoreceptor cell fates is controlled by Prospero in *Drosophila*. Dev. Cell 4, 853-864.

Coombe, P.E. 1986. The large monopolar cells L1 and L2 are responsible for ERG transients in *Drosophila*. J. Comp. Physiol. A. 159, 655-665.

Coombe, P.E. and Heisenberg, M. 1986. The structural brain mutant *vacuolar medulla* of *Drosophila melanogaster* with specific behavioral defects and cell degeneration in the adult. J. Neurogenet. 3, 135-158.

Corey, J.L., Quick, M.W., Davidson, N., Lester, H.A. and Guastella, J. 1994. A cocaine-sensitive *Drosophila* serotonin transporter: Cloning, expression, and electrophysiological characterization. Proc. Natl. Acad. Sci. U.S.A. 91, 1188-1192.

Couto, A., Alenius, M. and Dickson, B.J. 2005. Molecular, anatomical, and functional organization of the *Drosophila* olfactory system. Curr. Biol. 15, 1535-1547.

Cowman, A.F., Zuker, C.S. and Rubin, G.M. 1986. An opsin gene expressed in only one photoreceptor cell type of the *Drosophila* eye. Cell 44, 705-710.

Curtin, K.D., Zhang, Z. and Wyman, R.J. 2002a. Gap junction proteins are not interchangeable in development of neural function in the *Drosophila* visual system. J. Cell Sci. 115, 3379-3388.

Curtin, K.D., Zhang, Z. and Wyman, R.J. 2002b. Gap junction proteins expressed during development are required for adult neural function in the *Drosophila* optic lamina. J. Neurosci. 22, 7088-7096.

Curtin, K.D., Meinertzhagen, I.A. and Wyman, R.J. 2005. Basigin (EMMPRIN/CD147) interacts with integrin to affect cellular architecture. J. Cell Sci. 118, 2649-2660.

Curtin, K.D., Wyman, R.J. and Meinertzhagen, I.A. 2007. Basigin/EMMPRIN/CD147 mediates neuron-glia interactions in the optic lamina of Drosophila. Glia 55, 1542-1553.

Daga, A., Karlovich, C.A., Dumstrei, K. and Banerjee, U. 1996. Patterning of cells in the *Drosophila* eye by Lozenge, which shares homologous domains with AML1. Genes Dev. 10, 1194-1205.

Daniels, R.W., Collins, C.A., Gelfand, M.V., Dant, J., Brooks, E.S., Krantz, D.E. and DiAntonio, A. 2004. Increased expression of the *Drosophila* vesicular glutamate transporter leads to excess glutamate release and a compensatory decrease in quantal content. J. Neurosci. 24, 10466-10474.

Daniels, R.W., Collins, C.A., Chen, K., Gelfand, M.V., Featherstone, D.E. and DiAntonio, A. 2006. A single vesicular glutamate transporter is sufficient to fill a synaptic vesicle. Neuron 49, 11-16.

Datum, K.-H., Weiler, R. and Zettler, F. 1986. Immunocytochemical demonstration of γ-amino butyric acid and glutamic acid decarboxylase in R7 photoreceptors and C2 centrifugal fibres in the blowfly visual system. J. Comp. Physiol. A. 159, 241-249.

de Belle, J.S. and Heisenberg, M. 1994. Associative odor learning in *Drosophila* abolished by chemical ablation of mushroom bodies. Science 263, 692-695.

Dearborn, R., Jr. and Kunes, S. 2004. An axon scaffold induced by retinal axons directs glia to destinations in the *Drosophila* optic lobe. Development 131, 2291-2303.

Degraeve, P., Delorme, P. and Lemay, P. 1996. Pressure-induced inactivation of *E. coli* β-galactosidase: influence of pH and temperature. Biochim. Biophys. Acta 1292, 61-68.

Demchyshyn, L.L., Pristupa, Z.B., Sugamori, K.S., Barker, E.L., Blakely, R.D., Wolfgang, W.J., Forte, M.A. and Niznik, H.B. 1994. Cloning, expression, and localization of a chloride-facilitated, cocaine-sensitive serotonin transporter from *Drosophila melanogaster*. Proc. Natl. Acad. Sci. U.S.A. 91, 5158-5162.

Dickson, B., Sprenger, F., Morrison, D. and Hafen, E. 1992. Raf functions downstream of Ras1 in the Sevenless signal transduction pathway. Nature 360, 600-603.

Dietrich, W. 1909. Die Facettenaugen der Dipteren. Z. Wissen. Zool. 92, 465-539.

Ditzel, M., Wilson, R., Tenev, T., Zachariou, A., Paul, A., Deas, E. and Meier, P. 2003. Degradation of DIAP1 by the N-end rule pathway is essential for regulating apoptosis. Nature Cell Biol. 5, 467-473.

Doherty, J., Logan, M.A., Taşdemir, Ö.E. and Freeman, M.R. 2009. Ensheathing glia function as phagocytes in the adult *Drosophila* brain. J. Neurosci. 29, 4768-4781.

Domingos, P.M., Mlodzik, M., Mendes, C.S., Brown, S., Steller, H. and Mollereau, B. 2004a. Spalt transcription factors are required for R3/R4 specification and establishment of planar cell polarity in the *Drosophila* eye. Development 131, 5695-5702.

Domingos, P.M., Brown, S., Barrio, R., Ratnakumar, K., Frankfort, B.J., Mardon, G., Steller, H. and Mollereau, B. 2004b. Regulation of R7 and R8 differentiation by the *spalt* genes. Dev. Biol. 273, 121-133.

Donly, B.C., Richman, A., Hawkins, E., McLean, H. and Caveney, S. 1997. Molecular cloning and functional expression of an insect high-affinity Na^+-dependent glutamate transporter. Eur. J. Biochem. 248, 535-542.

Dormand, E.-L. and Brand, A.H. 1998. Runt determines cell fates in the *Drosophila* embryonic CNS. Development 125, 1659-1667.

Duffy, J.B. 2002. GAL4 system in *Drosophila*: a fly geneticist's Swiss army knife. Genesis 34, 1-15.

Dumstrei, K., Wang, F., Shy, D., Tepass, U. and Hartenstein, V. 2002. Interaction between EGFR signaling and DE-cadherin during nervous system morphogenesis. Development 129, 3983-3994.

Dumstrei, K., Wang, F., Nassif, C. and Hartenstein, V. 2003. Early development of the *Drosophila* brain: V. Pattern of postembryonic neuronal lineages expressing DE-cadherin. J. Comp. Neurol. 455, 451-462.

Dütting, D., Handwerker, C. and Drescher, U. 1999. Topographic targeting and pathfinding errors of retinal axons following overexpression of ephrinA ligands on retinal ganglion cell axons. Dev. Biol. 216, 297-311.

Edwards, J.S., Swales, L.S. and Bate, M. 1993. The differentiation between neuroglia and connective tissue sheath in insect ganglia revisited: The neural lamella and perineurial sheath cells are absent in a mesodermless mutant of *Drosophila*. . J. Comp. Neurol. 333, 301-308.

Edwards, J.S. and Tolbert, L.P. (1998) Insect Neuroglia. In: *Microscopic Anatomy of the Invertebrates*. pp. 449-466. Ed. M. Locke. Wiley-Liss Inc.

Edwards, T.N. and Meinertzhagen, I.A. 2009. Photoreceptor neurons find new synaptic targets when misdirected by overexpressing *runt* in *Drosophila*. J. Neurosci. 29, 828-841.

Edwards, T.N. and Meinertzhagen, I.A. 2010. The functional organisation of glia in the adult brain of *Drosophila* and other insects. Prog. Neurobiol. 90, 471-497.

Enomoto, A., Wempe, M.F., Tsuchida, H., Shin, H.J., Cha, S.H., Anzai, N., Goto, A., Sakamoto, A., Niwa, T., Kanai, Y., Anders, M.W. and Endou, H. 2002. Molecular identification of a novel carnitine transporter specific to human testis. Insights into the mechanism of carnitine recognition. J. Biol. Chem. 277, 36262-36271.

Eule, E., Tix, S. and Fischbach, K.F. (1995) Glial cells in the optic lobe of *Drosophila melanogaster*. www.flybrain.org, poster accession no. PP00004.

Eulenburg, V. and Gomeza, J. 2010. Neurotransmitter transporters expressed in glial cells as regulators of synapse function. Brain Res. Rev. 63, 103-112.

Eulenburg, V., Retiounskaia, M., Papadopoulos, T., Gomeza, J. and Betz, H. 2010. Glial glycine transporter 1 function is essential for early postnatal survival but dispensable in adult mice. Glia 58, 1066-1073.

Evans, G.J.O., Morgan, A. and Burgoyne, R.D. 2003. Tying everything together: the multiple roles of Cysteine String Protein (CSP) in regulated exocytosis. Traffic 4, 653-659.

Evêquoz-Mercier, V. and Tsacopoulos, M. 1991. The light-induced increase of carbohydrate metabolism in glial cells of the honeybee retina is not mediated by K^+ movement nor by cAMP. J. Gen. Physiol. 98, 497-515.

Ewer, J., Frisch, B., Hamblen-Coyle, M.J., Rosbash, M. and Hall, J.C. 1992. Expression of the *period* clock gene within different cell types in the brain of *Drosophila* adults and mosaic analysis of these cells' influence on circadian behavioral rhythms. J. Neurosci. 12, 3321-3349.

Fabian-Fine, R., Verstreken, P., Hiesinger, P.R., Horne, J.A., Kostyleva, R., Zhou, Y., Bellen, H.J. and Meinertzhagen, I.A. 2003. Endophilin promotes a late step in endocytosis at glial invaginations in *Drosophila* photoreceptor terminals. J. Neurosci. 23, 10732-10744.

Faeder, I.R. and Salpeter, M.M. 1970. Glutamate uptake by a stimulated insect nerve muscle preparation. J. Cell Biol. 46, 300-307.

Fahrbach, S.E. 2006. Structure of the mushroom bodies of the insect brain. Annu. Rev. Entomol. 51, 209-232.

Faivre-Sarrailh, C., Banerjee, S., Li, J., Hortsch, M., Laval, M. and Bhat, M.A. 2004. *Drosophila* contactin, a homolog of vertebrate contactin, is required for septate junction organization and paracellular barrier function. Development 131, 4931-4942.

Fehon, R.G., Dawson, I.A. and Artavanis-Tsakonas, S. 1994. A *Drosophila* homologue of membrane-skeleton protein 4.1 is associated with septate junctions and is encoded by the *coracle* gene. Development 120, 545-557.

Fei, H., Karnezis, T., Reimer, R.J. and Krantz, D.E. 2007. Membrane topology of the *Drosophila* vesicular glutamate transporter. J. Neurochem. 101, 1662-1671.

Fei, H., Chow, D.M., Chen, A., Romero-Calderón, R., Ong, W.S., Ackerson, L.C., Maidment, N.T., Simpson, J.H., Frye, M.A. and Krantz, D.E. 2010. Mutation of the *Drosophila* vesicular GABA transporter disrupts visual figure detection. J. Exp. Biol. 213, 1717-1730.

Fischbach, K.-F. and Dittrich, A.P.M. 1989. The optic lobe of *Drosophila melanogaster*. Part I. A Golgi analysis of wild-type structure. . Cell Tissue Res. 258, 441-475.

Fishilevich, E. and Vosshall, L.B. 2005. Genetic and functional subdivision of the *Drosophila* antennal lobe. Curr. Biol. 15, 1548-1553.

Flores, G.V., Daga, A., Kalhor, H.R. and Banerjee, U. 1998. Lozenge is expressed in pluripotent precursor cells and patterns multiple cell types in the *Drosophila* eye through the control of cell-specific transcription factors. Development 125, 3681-3687.

Franceschini, N., Kirschfeld, K. and Minke, B. 1981. Fluorescence of photoreceptor cells observed *in vivo*. Science 213, 1264-1267.

Franzdóttir, S.R., Engelen, D., Yuva-Aydemir, Y., Schmidt, I., Aho, A. and Klämbt, C. 2009. Switch in FGF signalling initiates glial differentiation in the *Drosophila* eye. Nature 460, 758-761.

Freeman, M. 1996. Reiterative use of the EGF receptor triggers differentiation of all cell types in the Drosophila eye. Cell 87, 651-660.

Freeman, M. 1997. Cell determination strategies in the *Drosophila* eye. Development 124, 261-270.

Freeman, M.R., Delrow, J., Kim, J., Johnson, E. and Doe, C.Q. 2003. Unwrapping glial biology: Gcm target genes regulating glial development, diversification, and function. Neuron 38, 567-580.

Freeman, M.R. 2006. Sculpting the nervous system: glial control of neuronal development. Curr. Opin. Neurobiol. 16, 119-125.

Freeman, M.R. and Doherty, J. 2006. Glial cell biology in *Drosophila* and vertebrates. Trends Neurosci. 29, 82-90.

Fröhlich, A. and Meinertzhagen, I.A. 1982. Synaptogenesis in the first optic neuropile of the fly's visual system. J. Neurocytol. 11, 159-180.

Fröhlich, A. and Meinertzhagen, I.A. 1983. Quantitative features of synapse formation in the fly's visual system. I. The presynaptic photoreceptor terminal. J. Neurosci. 3, 2336-2349.

Fryxell, K.J. and Meyerowitz, E.M. 1987. An opsin gene that is expressed only in the R7 photoreceptor cell of *Drosophila*. EMBO J. 6, 443-451.

Gainetdinov, R.R., Sotnikova, T.D. and Caron, M.G. 2002. Monoamine transporter pharmacology and mutant mice. Trends Pharmacol. Sci. 23, 367-373.

Gainetdinov, R.R. and Caron, M.G. 2003. Monoamine transporters: from genes to behavior. Annu. Rev. Pharmacol. Toxicol. 43, 261-284.

Galizia, C.G. and Rössler, W. 2010. Parallel olfactory systems in insects: anatomy and function. Annu. Rev. Entomol. 55, 399-420.

Gao, Q. and Chess, A. 1999. Identification of candidate *Drosophila* olfactory receptors from genomic DNA sequence. Genomics 60, 31-39.

Gao, Q., Yuan, B. and Chess, A. 2000. Convergent projections of *Drosophila* olfactory neurons to specific glomeruli in the antennal lobe. Nat. Neurosci. 3, 780-785.

Gao, S., Takemura, S.-y., Ting, C.-Y., Huang, S., Lu, Z., Luan, H., Rister, J., Thum, A.S., Yang, M., Hong, S.-T., Wang, J.W., Odenwald, W.F., White, B.H., Meinertzhagen, I.A. and Lee, C.-H. 2008. The neural substrate of spectral preference in *Drosophila*. Neuron 60, 328-342.

Garcia-Bellido, A. and Merriam, J.R. 1969. Cell lineage of the imaginal discs in *Drosophila* gynandromorphs. J. Exp. Zool. 170, 61-75.

Gaul, U., Mardon, G. and Rubin, G.M. 1992. A putative Ras GTPase activating protein acts as a negative regulator of signaling by the Sevenless receptor tyrosine kinase. Cell 68, 1007-1019.

Gavin, B.A., Arruda, S.E. and Dolph, P.J. 2007. The role of carcinine in signaling at the *Drosophila* photoreceptor synapse. PLoS Genet. 3, e206.

Gengs, C., Leung, H.-T., Skingsley, D.R., Iovchev, M.I., Yin, Z., Semenov, E.P., Burg, M.G., Hardie, R.C. and Pak, W.L. 2002. The target of *Drosophila* photoreceptor synaptic transmission is a histamine-gated chloride channel encoded by *ort* (*hclA*). J. Biol. Chem. 277, 42113-42120.

Genova, J.L. and Fehon, R.G. 2003. Neuroglian, Gliotactin, and the Na^+/K^+ ATPase are essential for septate junction function in *Drosophila*. J. Cell Biol. 161, 979-989.

Gisselmann, G., Pusch, H., Hovemann, B.T. and Hatt, H. 2002. Two cDNAs coding for histamine-gated ion channels in *D. melanogaster*. Nat. Neurosci. 5, 11-12.

Goldman, A.L., Van der Goes van Naters, W., Lessing, D., Warr, C.G. and Carlson, J.R. 2005. Coexpression of two functional odor receptors in one neuron. Neuron 45, 661-666.

Gong, Q., Rangarajan, R., Seeger, M. and Gaul, U. 1999. The Netrin receptor Frazzled is required in the target for establishment of retinal projections in the *Drosophila* visual system. Development 126, 1451-1456.

Gonzalez-Bellido, P.T., Wardill, T.J., Kostyleva, R., Meinertzhagen, I.A. and Juusola, M. 2009. Overexpressing temperature-sensitive Dynamin decelerates phototransduction and bundles microtubules in *Drosophila* photoreceptors. J. Neurosci. 29, 14199-14210.

Goodman, C.S. 1996. Mechanisms and molecules that control growth cone guidance. Annu. Rev. Neurosci. 19, 341-377.

Górska-Andrzejak, J., Stowers, R.S., Borycz, J., Kostyleva, R., Schwarz, T.L. and Meinertzhagen, I.A. 2003. Mitochondria are redistributed in *Drosophila* photoreceptors lacking Milton, a kinesin-associated protein. J. Comp. Neurol. 463, 372-388.

Górska-Andrzejak, J., Salvaterra, P.M., Meinertzhagen, I.A., Krzeptowski, W., Görlich, A. and Pyza, E. 2009. Cyclical expression of Na^+/K^+-ATPase in the visual system of *Drosophila melanogaster*. J. Insect Physiol. 55, 459-468.

Graham, R.C., Jr. and Karnovsky, M.J. 1966. The early stages of absorption of injected horseradish peroxidase in the proximal tubules of mouse kidney: Ultrastructural cytochemistry by a new technique. J. Histochem. Cytochem. 14, 291-302.

Granderath, S., Bunse, I. and Klämbt, C. 2000. gcm and pointed synergistically control glial transcription of the *Drosophila* gene *loco*. Mech. Dev. 91, 197-208.

Green, P., Hartenstein, A.Y. and Hartenstein, V. 1993. The embryonic development of the *Drosophila* visual system. Cell Tissue Res. 273, 583-598.

Greer, C.L., Grygoruk, A., Patton, D.E., Ley, B., Romero-Calderón, R., Chang, H.-Y., Houshyar, R., Bainton, R.J., DiAntonio, A. and Krantz, D.E. 2005. A splice variant of the *Drosophila* vesicular monoamine transporter contains a conserved trafficking domain and functions in the storage of dopamine, serotonin, and octopamine. J. Neurobiol. 64, 239-258.

Grenningloh, G., Rehm, E.J. and Goodman, C.S. 1991. Genetic analysis of growth cone guidance in Drosophila: fasciclin II functions as a neuronal recognition molecule. Cell 67, 45-57.

Griffin, J.W., George, E.B., Hsieh, S.T. and Glass, J.D. (1995) Axonal degeneration and disorders of the axonal cytoskeleton. In: *The Axon: Structure, Function and Pathophysiology,*. pp. 375-390. Eds. S. G. Waxman, J. D. Kocsis, P. S. Stys. Oxford University Press: New York.

Griffiths, G.W. and Boschek, C.B. 1976. Rapid degeneration of visual fibers following retinal lesions in the dipteran compound eye. Neurosci. Lett. 3, 253-258.

Griffiths, G.W. 1979. Transport of glial cell acid phosphatase by endoplasmic reticulum into damaged axons. J. Cell Sci. 36, 361-389.

Grosjean, Y., Grillet, M., Augustin, H., Ferveur, J.-F. and Featherstone, D.E. 2008. A glial amino-acid transporter controls synapse strength and courtship in *Drosophila*. Nat. Neurosci. 11, 54-61.

Grygoruk, A., Fei, H., Daniels, R.W., Miller, B.R., DiAntonio, A. and Krantz, D.E. 2010. A tyrosine-based motif localizes a *Drosophila* vesicular transporter to synaptic vesicles *in vivo*. J. Biol. Chem. 285, 6867-6878.

Grzeschik, N.A. and Knust, E. 2005. IrreC/rst-mediated cell sorting during *Drosophila* pupal eye development depends on proper localisation of DE-cadherin. Development 132, 2035-2045.

Hafen, E., Basler, K., Edstroem, J.E. and Rubin, G.M. 1987. Sevenless, a cell-specific homeotic gene of *Drosophila*, encodes a putative transmembrane receptor with a tyrosine kinase domain. Science 236, 55-63.

Hähnlein, I. and Bicker, G. 1996. Morphology of neuroglia in the antennal lobes and mushroom bodies of the brain of the honeybee. J. Comp. Neurol. 367, 235-245.

Hähnlein, I., Härtig, W. and Bicker, G. 1996. *Datura stramonium* lectin staining of glial associated extracellular material in insect brains. J. Comp. Neurol. 376, 175-187.

Halter, D.A., Urban, J., Rickert, C., Ner, S.S., Ito, K., Travers, A.A. and Technau, G.M. 1995. The homeobox gene *repo* is required for the differentiation and maintenance of glia function in the embryonic nervous system of *Drosophila melanogaster*. Development 121, 317-332.

Hamanaka, Y. and Meinertzhagen, I.A. 2010. Immunocytochemical localization of synaptic proteins to photoreceptor synapses of *Drosophila melanogaster*. J. Comp. Neurol. 518, 1133-1155.

Hamanaka, Y., Park, D., Yin, P., Annangudi, S.P., Edwards, T.N., Sweedler, J., Meinertzhagen, I.A. and Taghert, P.H. 2010. Transcriptional orchestration of the regulated secretory pathway in neurons by the bHLH protein DIMM. Curr. Biol. 20, 9-18.

Hamilton, C.M. (2004) The affects of visual stimulation and the phototransduction pathway on histamine accumulation over development of the adult visual system in *Drosophila melanogaster*. *Honours thesis, Biology*. p. 55. Dalhousie University: Halifax.

Hardie, R.C. 1983. Projection and connectivity of sex-specific photoreceptors in the compound eye of the male housefly (*Musca domestica*). Cell Tissue Res. 233, 1-21.

Hardie, R.C. and Kirschfeld, K. 1983. Ultraviolet sensitivity of fly photoreceptors R7 and R8: evidence for a sensitizing function. Biophys. Struct. Mech. 9, 171-180.

Hardie, R.C. (1985) Functional organization of the fly retina. In: *Progress in Sensory Physiology*. pp. 1–79. Ed. D. Ottoson. Springer New York.

Hardie, R.C. 1987. Is histamine a neurotransmitter in insect photoreceptors? J. Comp. Physiol. A. 161, 201-213.

Hardie, R.C. 1989. A histamine-activated chloride channel involved in neurotransmission at a photoreceptor synapse. Nature 339, 704-706.

Hartenstein, V., Nassif, C. and Lekven, A. 1998. Embryonic development of the *Drosophila* brain. II. Pattern of glial cells. J. Comp. Neurol. 402, 32-47.

Hasegawa, J., Obara, T., Tanaka, K. and Tachibana, M. 2006. High-density presynaptic transporters are required for glutamate removal from the first visual synapse. Neuron 50, 63-74.

Haverkamp, S., Michalakis, S., Claes, E., Seeliger, M.W., Humphries, P., Biel, M. and Feigenspan, A. 2006. Synaptic plasticity in *CNGA3*$^{-/-}$ mice: Cone bipolar cells react on the missing cone input and form ectopic synapses with rods. J. Neurosci. 26, 5248-5255.

Heisenberg, M. 1971. Separation of receptor and lamina potentials in the electroretinogram of normal and mutant *Drosophila*. J. Exp. Biol. 55, 85-100.

Heisenberg, M. 1972. Comparative behavioral studies on two visual mutants of *Drosophila*. J. Comp. Physiol. A. 80, 119-136.

Heisenberg, M. and Götz, K.G. 1975. The use of mutations for the partial degradation of vision in *Drosophila melanogaster*. J. Comp. Physiol. A. 98, 217-241.

Heisenberg, M. and Buchner, E. 1977. The rôle of retinula cell types in visual behavior of *Drosophila melanogaster*. J. Comp. Physiol. A. 117, 127-162.

Heisenberg, M. (1979) Genetic approach to a visual system. In: *Handbook of sensory physiology*. pp. 665-680. Ed. H. Autrum. Springer Berlin, Heidelberg, New York.

Heisenberg, M. and Wolf, R. (1984) *Vision in Drosophila*. Springer-Verlag: Berlin.

Helfrich-Förster, C. and Homberg, U. 1993. Pigment-dispersing hormone-immunoreactive neurons in the nervous system of wild-type *Drosophila melanogaster* and of several mutants with altered circadian rhythmicity. J. Comp. Neurol. 337, 177-190.

Helfrich-Förster, C. 1995. The period clock gene is expressed in central nervous system neurons which also produce a neuropeptide that reveals the projections of circadian pacemaker cells within the brain of *Drosophila melanogaster*. Proc. Natl. Acad. Sci. U.S.A. 92, 612-616.

Helfrich-Förster, C. 2009. Does the morning and evening oscillator model fit better for flies or mice? J. Biol. Rhythms 24, 259-270.

Herranz, H., Morata, G. and Milán, M. 2006. *calderón* encodes an organic cation transporter of the major facilitator superfamily required for cell growth and proliferation of *Drosophila* tissues. Development 133, 2617-2625.

Hidalgo, A., Kinrade, E.F.V. and Georgiou, M. 2001. The *Drosophila* neuregulin Vein maintains glial survival during axon guidance in the CNS. Dev. Cell 1, 1-20.

Hidalgo, A. 2002. Interactive nervous system development: control of cell survival in *Drosophila*. Trends Neurosci. 25, 365-370.

Hiesinger, P.R., Reiter, C., Schau, H. and Fischbach, K.-F. 1999. Neuropil pattern formation and regulation of cell adhesion molecules in *Drosophila* optic lobe development depend on synaptobrevin. J. Neurosci. 19, 7548-7556.

Hiesinger, P.R., Zhai, R.G., Zhou, Y., Koh, T.-W., Mehta, S.Q., Schulze, K.L., Cao, Y., Verstreken, P., Clandinin, T.R., Fischbach, K.-F., Meinertzhagen, I.A. and Bellen, H.J. 2006. Activity-independent prespecification of synaptic partners in the visual map of *Drosophila*. Curr. Biol. 16, 1835-1843.

Hing, H., Xiao, J., Harden, N., Lim, L. and Zipursky, S.L. 1999. Pak functions downstream of Dock to regulate photoreceptor axon guidance in *Drosophila*. Cell 97, 853-863.

Hiromi, Y., Mlodzik, M., West, S.R., Rubin, G.M. and Goodman, C.S. 1993. Ectopic expression of *seven-up* causes cell fate changes during ommatidial assembly. Development 118, 1123-1135.

Hofbauer, A. and Campos-Ortega, J.A. 1990. Proliferation pattern and early differentiation of the optic lobes in *Drosophila melanogaster*. Roux's Arch. Dev. Biol. 198, 264-274.

Hofmeyer, K., Maurel-Zaffran, C., Sink, H. and Treisman, J.E. 2006. Liprin-α has LAR-independent functions in R7 photoreceptor axon targeting. Proc. Nat. Acad. Sci. U.S.A. 103, 11595-11600.

Homyk, T., Jr., Szidonya, J. and Suzuki, D.T. 1980. Behavioral mutants of *Drosophila melanogaster*. III. Isolation and mapping of mutations by direct visual observations of behavioral phenotypes. Mol. Gen. Genet. 177, 553-565.

Hoopfer, E.D., McLaughlin, T., Watts, R.J., Schuldiner, O., O'Leary, D.D.M. and Luo, L. 2006. Wld^{s} protection distinguishes axon degeneration following injury from naturally occurring developmental pruning. Neuron 50, 883-895.

Hortsch, M. and Goodman, C.S. 1991. Cell and substrate adhesion molecules in *Drosophila*. Annu. Rev. Cell Biol. 7, 505-557.

Hotta, Y. and Benzer, S. 1969. Abnormal electroretinograms in visual mutants of *Drosophila*. Nature 222, 354-356.

Hough, C.D., Woods, D.F., Park, S. and Bryant, P.J. 1997. Organizing a functional junctional complex requires specific domains of the *Drosophila* MAGUK Discs large. Genes Dev. 11, 3242-3253.

Hovemann, B.T., Ryseck, R.-P., Walldorf, U., Störtkuhl, K.F., Dietzel, I.D. and Dessen, E. 1998. The *Drosophila ebony* gene is closely related to microbial peptide synthetases and shows specific cuticle and nervous system expression. Gene 221, 1-9.

Hoyle, G. 1986. Glial cells of an insect ganglion. J. Comp. Neurol. 246, 85-103.

Huang, X., Huang, Y., Chinnappan, R., Bocchini, C., Gustin, M.C. and Stern, M. 2002. The *Drosophila inebriated*-encoded neurotransmitter/osmolyte transporter: Dual roles in the control of neuronal excitability and the osmotic stress response. Genetics 160, 561-569.

Huang, Y. and Stern, M. 2002. *In vivo* properties of the *Drosophila inebriated*-encoded neurotransmitter transporter. J. Neurosci. 22, 1698-1708.

Huang, Z. and Kunes, S. 1996. Hedgehog, transmitted along retinal axons, triggers neurogenesis in the developing visual centers of the Drosophila brain. Cell 86, 411-422.

Huang, Z. and Kunes, S. 1998. Signals transmitted along retinal axons in *Drosophila*: Hedgehog signal reception and the cell circuitry of lamina cartridge assembly. Development 125, 3753-3764.

Huang, Z., Shilo, B.-Z. and Kunes, S. 1998. A retinal axon fascicle uses Spitz, an EGF receptor ligand, to construct a synaptic cartridge in the brain of *Drosophila*. Cell 95, 693-703.

Huber, A., Schulz, S., Bentrop, J., Groell, C., Wolfrum, U. and Paulsen, R. 1997. Molecular cloning of *Drosophila* Rh6 rhodopsin: the visual pigment of a subset of R8 photoreceptor cells. FEBS Lett 406, 6-10.

Hue, B., Gabriel, A. and Le Patezour, A. 1982. Autoradiographic localization of [^{3}H]-GABA accumulation in the sixth abdominal ganglion of the cockroach, *Periplaneta americana* L. J. Insect Physiol. 28, 753-757, 759.

Hummel, T., Krukkert, K., Roos, J., Davis, G. and Klämbt, C. 2000. *Drosophila* Futsch/22C10 is a MAP1B-like protein required for dendritic and axonal development. Neuron 26, 357-370.

Hummel, T., Attix, S., Gunning, D. and Zipursky, S.L. 2002. Temporal control of glial cell migration in the *Drosophila* eye requires *gilgamesh*, *hedgehog*, and eye specification genes. Neuron 33, 193-203.

Iglesias, R., Dahl, G., Qiu, F., Spray, D.C. and Scemes, E. 2009. Pannexin 1: the molecular substrate of astrocyte "hemichannels". J. Neurosci. 29, 7092-7097.

Ito, K., Urban, J. and Technau, G. 1995. Distribution, classification, and development of *Drosophila* glial cells in the late embryonic and early larval ventral nerve cord. Roux's Arch. Dev. Biol. 204, 284-307.

Ito, K., Awano, W., Suzuki, K., Hiromi, Y. and Yamamoto, D. 1997. The *Drosophila* mushroom body is a quadruple structure of clonal units each of which contains a virtually identical set of neurones and glial cells. Development 124, 761-771.

Ito, K. and Awasaki, T. (2008) Clonal unit architecture of the adult fly brain. In: *Brain Development in Drosophila melanogaster*. pp. 137-158. Ed. G. M. Technau. Springer: New York.

Jackson, F.R., Newby, L.M. and Kulkarni, S.J. 1990. *Drosophila* GABAergic systems: Sequence and expression of Glutamic acid decarboxylase. J. Neurochem. 54, 1068-1078.

Jacobs, M.E. 1966. Deposition of labeled β-alanine in ebony and non-ebony *Drosophila melanogaster* with notes on other amino acids. Genetics 53, 777-784.

Jacobs, M.E. 1978. β-alanine tanning of *Drosophila* cuticles and chitin. Insect Biochem. 8, 37-41.

Jacobs, M.E. 1980. Influence of β-alanine on ultrastructure, tanning, and melanization of *Drosophila melanogaster* cuticles. Biochem. Genet. 18, 65-76.

Jhaveri, D., Sen, A. and Rodrigues, V. 2000. Mechanisms underlying olfactory neuronal connectivity in *Drosophila* - the atonal lineage organizes the periphery while sensory neurons and glia pattern the olfactory lobe. Dev. Biol. 226, 73-87.

Johnson, D.A., Donovan, S.L. and Dyer, M.A. 2006. Mosaic deletion of *Rb* arrests rod differentiation and stimulates ectopic synaptogenesis in the mouse retina. J. Comp. Neurol. 498, 112-128.

Johnson, K., Knust, E. and Skaer, H. 1999. *bloated tubules (blot)* encodes a *Drosophila* member of the neurotransmitter transporter family required for organisation of the apical cytocortex. Dev. Biol. 212, 440-454.

Johnson, K.G., McKinnell, I.W., Stoker, A.W. and Holt, C.E. 2001. Receptor protein tyrosine phosphatases regulate retinal ganglion cell axon outgrowth in the developing *Xenopus* visual system. J. Neurobiol. 49, 99-117.

Jones, B. and McGinnis, W. 1993. A new *Drosophila* homeobox gene, *bsh*, is expressed in a subset of brain cells during embryogenesis. Development 117, 793-806.

Jones, B.W., Fetter, R.D., Tear, G. and Goodman, C.S. 1995. *glial cells missing*: a genetic switch that controls glial versus neuronal fate. Cell 82, 1013-1023.

Juang, J.-L. and Carlson, S.D. 1992. A blood-brain barrier without tight junctions in the fly central nervous system in the early postembryonic stage. Cell Tissue Res. 270, 95-103.

Kaas, J.H. 1997. Topographic maps are fundamental to sensory processing. Brain Res. Bull. 44, 107-112.

Kamermans, M., Fahrenfort, I., Schultz, K., Janssen-Bienhold, U., Sjoerdsma, T. and Weiler, R. 2001. Hemichannel-mediated inhibition in the outer retina. Science 292, 1178-1180.

Kaminker, J.S., Singh, R., Lebestky, T., Yan, H. and Banerjee, U. 2001. Redundant function of Runt Domain binding partners, Big brother and Brother, during *Drosophila* development. Development 128, 2639-2648.

Kaminker, J.S., Canon, J., Salecker, I. and Banerjee, U. 2002. Control of photoreceptor axon target choice by transcriptional repression of Runt. Nat. Neurosci. 5, 746-750.

Kasuya, J., Kaas, G.A. and Kitamoto, T. 2009. A putative amino acid transporter of the solute carrier 6 family is upregulated by lithium and is required for resistance to lithium toxicity in *Drosophila*. Neuroscience 163, 825-837.

Kato, K., Awasaki, T. and Ito, K. 2009. Neuronal programmed cell death induces glial cell division in the adult *Drosophila* brain. Development 136, 51-59.

Kauffmann, R.C., Li, S., Gallagher, P.A., Zhang, J. and Carthew, R.W. 1996. Ras1 signaling and transcriptional competence in the R7 cell of *Drosophila*. Genes Dev. 10, 2167-2178.

Kearney, J.B., Wheeler, S.R., Estes, P., Parente, B. and Crews, S.T. 2004. Gene expression profiling of the developing *Drosophila* CNS midline cells. Dev. Biol. 275, 473-492.

Kim, J., Jones, B.W., Zock, C., Chen, Z., Wang, H., Goodman, C.S. and Anderson, D.J. 1998. Isolation and characterization of mammalian homologs of the *Drosophila* gene *glial cells missing*. Proc. Natl. Acad. Sci. U.S.A. 95, 12364-12369.

Kim, S.H. and Crews, S.T. 1993. Influence of *Drosophila* ventral epidermal development by the CNS midline cells and *spitz* class genes. Development 118, 893-901.

Kinchen, J.M., Cabello, J., Klingele, D., Wong, K., Feichtinger, R., Schnabel, H., Schnabel, R. and Hengartner, M.O. 2005. Two pathways converge at CED-10 to mediate actin rearrangement and corpse removal in *C. elegans*. Nature 434, 93-99.

Kirschfeld, K. 1967. Die Projektion der optischen Umwelt auf das Raster der Rhabdomere im Komplexauge von MUSCA. Exp. Brain Res. 3, 248-270.

Kittel, R.J., Wichmann, C., Rasse, T.M., Fouquet, W., Schmidt, M., Schmid, A., Wagh, D.A., Pawlu, C., Kellner, R.R., Willig, K.I., Hell, S.W., Buchner, E., Heckmann, M. and Sigrist, S.J. 2006. Bruchpilot promotes active zone assembly, Ca^{2+} channel clustering, and vesicle release. Science 312, 1051-1054.

Klaes, A., Menne, T., Stollewerk, A., Scholz, H. and Klämbt, C. 1994. The Ets transcription factors encoded by the Drosophila gene *pointed* direct glial cell differentiation in the embryonic CNS. Cell 78, 149-160.

Klämbt, C. 1993. The *Drosophila* gene *pointed* encodes two ETS-like proteins which are involved in the development of the midline glial cells. Development 117, 163-176.

Klein, J. 2000. Membrane breakdown in acute and chronic neurodegeneration: focus on choline-containing phospholipids. J. Neural Transm. 107, 1027-1063.

Kolodziejczyk, A., Sun, X., Meinertzhagen, I.A. and Nässel, D.R. 2008. Glutamate, GABA and acetylcholine signaling components in the lamina of the *Drosophila* visual system. PLoS ONE 3, e2110.

Korey, C.A. and Van Vactor, D. 2000. From the growth cone surface to the cytoskeleton: one journey, many paths. J. Neurobiol. 44, 184-193.

Koushika, S.P., Lisbin, M.J. and White, K. 1996. ELAV, a *Drosophila* neuron-specific protein, mediates the generation of an alternatively spliced neural protein isoform. Curr. Biol. 6, 1634-1641.

Krämer, H., Cagan, R.L. and Zipursky, S.L. 1991. Interaction of *bride of sevenless* membrane-bound ligand and the *sevenless* tyrosine-kinase receptor. Nature 352, 207-212.

Kretzschmar, D., Hasan, G., Sharma, S., Heisenberg, M. and Benzer, S. 1997. The *swiss cheese* mutant causes glial hyperwrapping and brain degeneration in *Drosophila*. J. Neurosci. 17, 7425-7432.

Kretzschmar, D., Poeck, B., Roth, H., Ernst, R., Keller, A., Porsch, M., Strauss, R. and Pflugfelder, G.O. 2000. Defective pigment granule biogenesis and aberrant behavior caused by mutations in the Drosophila AP-3β adaptin gene *ruby*. Genetics 155, 213-223.

Kretzschmar, D., Tschäpe, J., Bettencourt Da Cruz, A., Asan, E., Poeck, B., Strauss, R. and Pflugfelder, G.O. 2005. Glial and neuronal expression of polyglutamine proteins induce behavioral changes and aggregate formation in *Drosophila*. Glia 49, 59-72.

Krueger, R.R., Kramer, K.J., Hopkins, T.L. and Speirs, R.D. 1990. N-β-alanyldopamine and N-acetyldopamine occurrence and synthesis in the central nervous system of *Manduca sexta* (L.). Insect Biochemistry 20, 605-610.

Kumar, J. and Moses, K. 1997. Transcription factors in eye development: a gorgeous mosaic? Genes Dev. 11, 2023-2028.

Kumar, J.P. and Ready, D.F. 1995. Rhodopsin plays an essential structural role in *Drosophila* photoreceptor development. Development 121, 4359-4370.

Kumar, J.P. and Moses, K. 2001. The EGF receptor and notch signaling pathways control the initiation of the morphogenetic furrow during *Drosophila* eye development. Development 128, 2689-2697.

Kunes, S. and Steller, H. 1993. Topography in the *Drosophila* visual system. Curr. Opin. Neurobiol. 3, 53-59.

Kurant, E., Axelrod, S., Leaman, D. and Gaul, U. 2008. Six-microns-under acts upstream of Draper in the glial phagocytosis of apoptotic neurons. Cell 133, 498-509.

Lai, Z.-C. and Rubin, G.M. 1992. Negative control of photoreceptor development in Drosophila by the product of the *yan* gene, an ETS domain protein. Cell 70, 609-620.

Lai, Z.-C., Harrison, S.D., Karim, F., Li, Y. and Rubin, G.M. 1996. Loss of tramtrack gene activity results in ectopic R7 cell formation, even in a *sina* mutant background. Proc. Natl. Acad. Sci. U.S.A. 93, 5025-5030.

Laissue, P.P., Reiter, C., Hiesinger, P.R., Halter, S., Fischbach, K.F. and Stocker, R.F. 1999. Three-dimensional reconstruction of the antennal lobe in *Drosophila melanogaster*. J. Comp. Neurol. 405, 543-552.

Lane, N.J., Martinucci, G., Dallai, R. and Burighel, P. Eds (1994) *Electron microscopic structure and evolution of epithelial junctions. Molecular Mechanisms of Epithelial Cell Junctions*. R.G. Landes Company: Austin, TX.

Larsen, C.W., Hirst, E., Alexandre, C. and Vincent, J.-P. 2003. Segment boundary formation in *Drosophila* embryos. Development 130, 5625-5635.

Laughlin, S.B. 1973. Neural integration in the first optic neuropile of dragonflies. I. Signal amplification in dark-adapted second order neurons. J. Comp. Physiol. A. 84, 335-355.

Laughlin, S.B. and Hardie, R.C. 1978. Common strategies for light adaptation in the peripheral visual systems of fly and dragonfly. J. Comp. Physiol. A. 128, 319-340.

Laughlin, S.B. (1981) Neural principles in the visual system. In: *Comparative Physiology and Evolution of Vision in Invertebrates (Handbook of Sensory Physiology)*. pp. 133-280. Ed. H. Autrum. Springer-Verlag: Berlin.

Laughlin, S.B., Howard, J. and Blakeslee, B. 1987. Synaptic limitations to contrast coding in the retina of the blowfly *Calliphora*. Proc. R. Soc. Lond. B. Biol. Sci. 231, 437-467.

Laughlin, S.B. and Weckström, M. 1993. Fast and slow photoreceptors — a comparative study of the functional diversity of coding and conductances in the Diptera. J. Comp. Physiol. A. 172, 593-609.

Lear, B.C., Merrill, C.E., Lin, J.-M., Schroeder, A., Zhang, L. and Allada, R. 2005. A G protein-coupled receptor, *groom-of-PDF*, is required for PDF neuron action in circadian behavior. Neuron 48, 221-227.

Learte, A.R., Forero, M.G. and Hidalgo, A. 2008. Gliatrophic and gliatropic roles of PVF/PVR signaling during axon guidance. Glia 56, 164-176.

Lee, B.P. and Jones, B.W. 2005. Transcriptional regulation of the *Drosophila* glial gene *repo*. Mech. Dev. 122, 849-862.

Lee, C.-H., Herman, T., Clandinin, T.R., Lee, R. and Zipursky, S.L. 2001. N-cadherin regulates target specificity in the *Drosophila* visual system. Neuron 30, 437-450.

Lee, R.C., Clandinin, T.R., Lee, C.-H., Chen, P.-L., Meinertzhagen, I.A. and Zipursky, S.L. 2003. The protocadherin Flamingo is required for axon target selection in the *Drosophila* visual system. Nat. Neurosci. 6, 557-563.

Lee, T. and Luo, L. 1999. Mosaic analysis with a repressible cell marker for studies of gene function in neuronal morphogenesis. Neuron 22, 451-461.

Lehmann, C., Lechner, H., Löer, B., Knieps, M., Herrmann, S., Famulok, M., Bauer, R. and Hoch, M. 2006. Heteromerization of innexin gap junction proteins regulates epithelial tissue organization in *Drosophila*. Mol. Biol. Cell 17, 1676-1685.

Leiss, F., Groh, C., Butcher, N.J., Meinertzhagen, I.A. and Tavosanis, G. 2009. Synaptic organization in the adult *Drosophila* mushroom body calyx. J. Comp. Neurol. 517, 808-824.

Liévens, J.-C., Rival, T., Iché, M., Chneiweiss, H. and Birman, S. 2005. Expanded polyglutamine peptides disrupt EGF receptor signaling and glutamate transporter expression in *Drosophila*. Hum. Mol. Genet. 14, 713-724.

Liu, Q.A. and Hengartner, M.O. 1998. Candidate adaptor protein CED-6 promotes the engulfment of apoptotic cells in *C. elegans*. Cell 93, 961-972.

Liu, Y., Peter, D., Roghani, A., Schuldiner, S., Privé, G.G., Eisenberg, D., Brecha, N. and Edwards, R.H. 1992. A cDNA that suppresses MPP^+ toxicity encodes a vesicular amine transporter. Cell 70, 539-551.

Llimargas, M., Strigini, M., Katidou, M., Karagogeos, D. and Casanova, J. 2004. Lachesin is a component of a septate junction-based mechanism that controls tube size and epithelial integrity in the *Drosophila* tracheal system. Development 131, 181-190.

Lømo, T. 2003. What controls the position, number, size, and distribution of neuromuscular junctions on rat muscle fibers? J. Neurocytol. 32, 835-848.

Lowery, L.A. and Van Vactor, D. 2009. The trip of the tip: understanding the growth cone machinery. Nat. Rev. Mol. Cell. Biol. 10, 332-343.

MacDonald, J.M., Beach, M.G., Porpiglia, E., Sheehan, A.E., Watts, R.J. and Freeman, M.R. 2006. The *Drosophila* cell corpse engulfment receptor Draper mediates glial clearance of severed axons. Neuron 50, 869-881.

Mahr, A. and Aberle, H. 2006. The expression pattern of the *Drosophila* vesicular glutamate transporter: A marker protein for motoneurons and glutamatergic centers in the brain. Gene Expr. Patterns 6, 299-309.

Marcaggi, P., Thwaites, D.T., Deitmer, J.W. and Coles, J.A. 1999. Chloride-dependent transport of NH_4^+ into bee retinal glial cells. Eur. J. Neurosci. 11, 167-177.

Marcaggi, P. and Coles, J.A. 2000. A Cl^- cotransporter selective for NH_4^+ over K^+ in glial cells of bee retina. J. Gen. Physiol. 116, 125-141.

Mardon, G., Solomon, N.M. and Rubin, G.M. 1994. *dachshund* encodes a nuclear protein required for normal eye and leg development in *Drosophila*. Development 120, 3473-3486.

Masson, J., Sagné, C., Hamon, M. and El Mestikawy, S. 1999. Neurotransmitter transporters in the central nervous system. Pharmacol. Rev. 51, 439-464.

Mast, J.D., Prakash, S., Chen, P.-L. and Clandinin, T.R. 2006. The mechanisms and molecules that connect photoreceptor axons to their targets in *Drosophila*. Semin. Cell Dev. Biol. 17, 42-49.

Mastick, G.S. and Scholnick, S.B. 1992. Repression and activation of the *Drosophila* dopa decarboxylase gene in glia. Mol. Cell. Biol 12, 5659-5666.

Mayer, F., Mayer, N., Chinn, L., Pinsonneault, R.L., Kroetz, D. and Bainton, R.J. 2009. Evolutionary conservation of vertebrate blood-brain barrier chemoprotective mechanisms in *Drosophila*. J. Neurosci. 29, 3538-3550.

Mayr, E. (1997) *This Is Biology: The Science of the Living World*. Harvard University Press: Cambridge, MA.

Mbungu, D., Ross, L.S. and Gill, S.S. 1995. Cloning, functional expression, and pharmacology of a GABA transporter from *Manduca sexta*. Arch. Biochem. Biophys. 318, 489-497.

McLaughlin, T. and O'Leary, D.D.M. 2005. Molecular gradients and development of retinotopic maps. Annu. Rev. Neurosci. 28, 327-355.

Meinertzhagen, I.A. (1973) Development of the compound eye and optic lobe of insects. In: *Developmental Neurobiology of Arthropods*. pp. 51-104. Ed. D. Young. Cambridge Univ. Press: Cambridge.

Meinertzhagen, I.A. (1975) The development of neuronal connection patterns in the visual systems of insects. In: *Cell Patterning. Ciba Foundation Symposium* pp. 265-288. Associated Scientific Publishers: Amsterdam.

Meinertzhagen, I.A. (1977) Development of neuronal circuitry in the insect optic lobe. In: *Approaches to the Cell Biology of Neurons, Society for Neuroscience Symposia*. pp. 92-119. Eds. W. M. Cowan, J. A. Ferrendelli. Society for Neuroscience: Bethesda, MD.

Meinertzhagen, I.A. and Armett-Kibel, C. 1982. The lamina monopolar cells in the optic lobe of the dragonfly *Sympetrum*. Phil. Trans. R. Soc. Lond. B. 297, 27-49.

Meinertzhagen, I.A. and O'Neil, S.D. 1991. Synaptic organization of columnar elements in the lamina of the wild type in *Drosophila melanogaster*. J. Comp. Neurol. 305, 232-263.

Meinertzhagen, I.A. and Hanson, T.E. (1993) The development of the optic lobe. In: *The Development of Drosophila melanogaster*. pp. 1363–1491. Eds. M. Bate, A. Martinez-Arias. Cold Spring Harbor Press: Cold Spring Harbor, NY.

Meinertzhagen, I.A. and Sun, X.J. (1996) Monopolar cell axons in the lamina cartridge of the flies *Drosophila Musca* and *Calliphora* exhibit glutamate-like immunoreactivity. In: *Soc. Neurosci.* p. Abstr 22:655.

Meinertzhagen, I.A. and Wang, Y. (1997) *Drosophila* mutants *tan* and *ebony* have altered numbers of capitate projections, glial invaginations into photoreceptor terminals. In: *Neurobiology from membrane to mind. Proceedings of the 25th Göttingen Neurobiology Conference*. p. 457. Eds. N. Elsner, H. Wässle. Georg Thieme Verlag: Göttingen.

Meinertzhagen, I.A. and Pyza, E. 1999. Neurotransmitter regulation of circadian structural changes in the fly's visual system. Microsc. Res. Tech. 45, 96-105.

Meinertzhagen, I.A. 2000. Wiring the fly's eye. Neuron 28, 310-313.

Meinertzhagen, I.A., Borycz, J., Horne, J.A. and Shimohigashi, M. (2000) Photoreceptor phenotypes for *Drosophila* mutants *nonC* and *hdc*^{Ik910}. In: *Canadian Society of Zoology. Bull. Can. Soc. Zool.*

Meinertzhagen, I.A. and Sorra, K.E. 2001. Synaptic organization in the fly's optic lamina: few cells, many synapses and divergent microcircuits. Prog. Brain Res. 131, 53-69.

Meinertzhagen, I.A., Takemura, S.-y., Lu, Z., Huang, S., Gao, S., Ting, C.-Y. and Lee, C.-H. 2009. From form to function: the ways to know a neuron. J. Neurogenet. 23, 68-77.

Melamed, J., and Trujillo-Cenóz, O. 1968. The fine structure of the central cells in the ommatidia of dipterans. J. Ultrastruct. Res. 21, 313-334.

Melzig, J., Buchner, S., Wiebel, F., Wolf, R., Burg, M., Pak, W.L. and Buchner, E. 1996. Genetic depletion of histamine from the nervous system of *Drosophila* eliminates specific visual and mechanosensory behavior. J. Comp. Physiol. A. 179, 763-773.

Melzig, J., Burg, M., Gruhn, M., Pak, W.L. and Buchner, E. 1998. Selective histamine uptake rescues photo- and mechanoreceptor function of Histidine decarboxylase-deficient *Drosophila* mutant. J. Neurosci. 18, 7160-7166.

Mertens, I., Vandingenen, A., Johnson, E.C., Shafer, O.T., Li, W., Trigg, J.S., De Loof, A., Schoofs, L. and Taghert, P.H. 2005. PDF receptor signaling in *Drosophila* contributes to both circadian and geotactic behaviors. Neuron 48, 213-219.

Meyer, E.P., Matute, C., Streit, P. and Nässel, D.R. 1986. Insect optic lobe neurons identifiable with monoclonal antibodies to GABA. Histochem. Cell Biol. 84, 207-216.

Meyer, M.R., Reddy, G.R. and Edwards, J.S. 1987. Immunological probes reveal spatial and developmental diversity in insect neuroglia. J. Neurosci. 7, 512-521.

Meyerowitz, E.M. and Kankel, D.R. 1978. A genetic analysis of visual system development in *Drosophilia melanogaster*. Dev. Biol. 62, 112-142.

Mikeladze-Dvali, T., Wernet, M.F., Pistillo, D., Mazzoni, E.O., Teleman, A.A., Chen, Y.-W., Cohen, S. and Desplan, C. 2005. The growth regulators *warts/lats* and *melted* interact in a bistable loop to specify opposite fates in *Drosophila* R8 photoreceptors. Cell 122, 775-787.

Miller, M.M., Popova, L.B., Meleshkevitch, E.A., Tran, P.V. and Boudko, D.Y. 2008. The invertebrate B^0 system transporter, *D. melanogaster* NAT1, has unique D-amino acid affinity and mediates gut and brain functions. Insect Biochem. Mol. Biol. 38, 923-931.

Mismer, D. and Rubin, G.M. 1987. Analysis of the promoter of the *ninaE* opsin gene in *Drosophila melanogaster*. Genetics 116, 565-578.

Mitchell, K.J., Doyle, J.L., Serafini, T., Kennedy, T.E., Tessier-Lavigne, M., Goodman, C.S. and Dickson, B.J. 1996. Genetic analysis of *netrin* genes in Drosophila: Netrins guide CNS commissural axons and peripheral motor axons. Neuron 17, 203-215.

Mlodzik, M., Hiromi, Y., Weber, U., Goodman, C.S. and Rubin, G.M. 1990. The *Drosophila seven-up* gene, a member of the steroid receptor gene superfamily, controls photoreceptor cell fates. Cell 60, 211-224.

Mobbs, P.G. (1985) Brain structure. In: *Comprehensive Insect Physiology, Pharmacology and Biochemistry of Nervous Systems: Structure and Motor Function*. pp. 299-370. Eds. G. Kerkut, L. I. Gilbert. Pergamon Press: Oxford, New York. Toronto, Sydney, Paris and Frankfurt.

Mollereau, B., Dominguez, M., Webel, R., Colley, N.J., Keung, B., de Celis, J.F. and Desplan, C. 2001. Two-step process for photoreceptor formation in *Drosophila*. Nature 412, 911-913.

Montell, C., Jones, K., Zuker, C. and Rubin, G. 1987. A second opsin gene expressed in the ultraviolet-sensitive R7 photoreceptor cells of *Drosophila melanogaster*. J. Neurosci. 7, 1558-1566.

Morante, J. and Desplan, C. 2004. Building a projection map for photoreceptor neurons in the *Drosophila* optic lobes. Semin. Cell Dev. Biol. 15, 137-143.

Morante, J., Desplan, C. and Celik, A. 2007. Generating patterned arrays of photoreceptors. Curr. Opin. Genet. Dev. 17, 314-319.

Morante, J. and Desplan, C. 2008. The color-vision circuit in the medulla of *Drosophila*. Curr. Biol. 18, 553-565.

Morgan, J.R., Gebhardt, K.A. and Stuart, A.E. 1999. Uptake of precursor and synthesis of transmitter in a histaminergic photoreceptor. J. Neurosci. 19, 1217-1225.

Moses, K. and Rubin, G.M. 1991. *glass* encodes a site-specific DNA-binding protein that is regulated in response to positional signals in the developing *Drosophila* eye. Genes Dev. 5, 583-593.

Moyer, K.E. and Jacobs, J.R. 2008. Varicose: a MAGUK required for the maturation and function of *Drosophila* septate junctions. BMC Dev. Biol. 8, 99.

Mühlig-Versen, M., Bettencourt da Cruz, A., Tschäpe, J.-A., Moser, M., Büttner, R., Athenstaedt, K., Glynn, P. and Kretzschmar, D. 2005. Loss of Swiss cheese/neuropathy target esterase activity causes disruption of phosphatidylcholine homeostasis and neuronal and glial death in adult *Drosophila*. J. Neurosci. 25, 2865-2873.

Mullins, M.C. and Rubin, G.M. 1991. Isolation of temperature-sensitive mutations of the tyrosine kinase receptor sevenless (*sev*) in *Drosophila* and their use in determining its time of action. Proc. Natl. Acad. Sci. U.S.A. 88, 9387-9391.

Murakami, S., Umetsu, D., Maeyama, Y., Sato, M., Yoshida, S. and Tabata, T. 2007. Focal adhesion kinase controls morphogenesis of the *Drosophila* optic stalk. Development 134, 1539-1548.

Murphey, R.K., Bacon, J.P., Sakaguchi, D.S. and Johnson, S.E. 1983. Transplantation of cricket sensory neurons to ectopic locations: arborizations and synaptic connections. J. Neurosci. 3, 659-672.

Nadrowski, B., Effertz, T., Senthilan, P.R. and Gopfert, M.C. 2010. Antennal hearing in insects - New findings, new questions. Hear. Res. DOI:10.1016

Nakano, Y., Fujitani, K., Kurihara, J., Ragan, J., Usui-Aoki, K., Shimoda, L., Lukacsovich, T., Suzuki, K., Sezaki, M., Sano, Y., Ueda, R., Awano, W., Kaneda, M., Umeda, M. and Yamamoto, D. 2001. Mutations in the novel membrane protein Spinster interfere with programmed cell death and cause neural degeneration in *Drosophila melanogaster*. Mol. Cell Biol. 21, 3775-3788.

Narasimha, M., Uv, A., Krejci, A., Brown, N.H. and Bray, S.J. 2008. Grainy head promotes expression of septate junction proteins and influences epithelial morphogenesis. J. Cell Sci. 121, 747-752.

Nässel, D.R. and Elekes, K. 1984. Ultrastructural demonstration of serotonin-immunoreactivity in the nervous system of an insect (*Calliphora erythrocephala*). Neurosci. Lett. 48, 203-210.

Nässel, D.R., Holmqvist, M.H., Hardie, R.C., Håkanson, R. and Sundler, F. 1988. Histamine-like immunoreactivity in photoreceptors of the compound eyes and ocelli of the flies *Calliphora erythrocephala* and *Musca domestica*. Cell Tissue Res. 253, 639-646.

Nässel, D.R., Pirvola, U. and Panula, P. 1990. Histaminelike immunoreactive neurons innervating putative neurohaemal areas and central neuropil in the thoraco-abdominal ganglia of the flies *Drosophila* and *Calliphora*. J. Comp. Neurol. 297, 525-536.

Nässel, D.R. and Elekes, K. 1992. Aminergic neurons in the brain of blowflies and *Drosophila*: dopamine- and tyrosine hydroxylase-immunoreactive neurons and their relationship with putative histaminergic neurons. Cell Tissue Res. 267, 147-167.

Nässel, D.R. 1999. Histamine in the brain of insects: a review. Microsc. Res. Tech. 44, 121-136.

Nässel, D.R. and Winther, Å.M.E. 2010. *Drosophila* neuropeptides in regulation of physiology and behavior. Prog. Neurobiol. 92, 42-104.

Neckameyer, W.S. 1998. Dopamine and mushroom bodies in *Drosophila*: experience-dependent and -independent aspects of sexual behavior. Learn. Mem. 5, 157-165.

Neckameyer, W.S. and Cooper, R.L. 1998. GABA transporters in *Drosophila melanogaster*: molecular cloning, behavior, and physiology. Invertebr. Neurosci. 3, 279-294.

Nern, A., Nguyen, L.-V.T., Herman, T., Prakash, S., Clandinin, T.R. and Zipursky, S.L. 2005. An isoform-specific allele of *Drosophila N-cadherin* disrupts a late step of R7 targeting. Proc. Natl. Acad. Sci. U.S.A. 102, 12944-12949.

Nern, A., Zhu, Y. and Zipursky, S.L. 2008. Local N-cadherin interactions mediate distinct steps in the targeting of lamina neurons. Neuron 58, 34-41.

Newby, L.M. and Jackson, F.R. 1991. *Drosophila ebony* mutants have altered circadian activity rhythms but normal eclosion rhythms. J. Neurogenet. 7, 85-101.

Newsome, T.P., Åsling, B. and Dickson, B.J. 2000. Analysis of *Drosophila* photoreceptor axon guidance in eye-specific mosaics. Development 127, 851-860.

Ng, M., Roorda, R.D., Lima, S.Q., Zemelman, B.V., Morcillo, P. and Miesenböck, G. 2002. Transmission of olfactory information between three populations of neurons in the antennal lobe of the fly. Neuron 36, 463-474.

Nicol, D. and Meinertzhagen, I.A. 1982. An analysis of the number and composition of the synaptic populations formed by photoreceptors of the fly. J. Comp. Neurol. 207, 29-44.

Nikolaev, A., Zheng, L., Wardill, T.J., O'Kane, C.J., de Polavieja, G.G. and Juusola, M. 2009. Network adaptation improves temporal representation of naturalistic stimuli in *Drosophila* eye: II Mechanisms. PLoS ONE 4, e4306.

O'Tousa, J.E., Baehr, W., Martin, R.L., Hirsh, J., Pak, W.L. and Applebury, M.L. 1985. The *Drosophila ninaE* gene encodes an opsin. Cell 40, 839-850.

Ogasawara, M., Yamauchi, K., Satoh, Y., Yamaji, R., Inui, K., Jonker, J.W., Schinkel, A.H. and Maeyama, K. 2006. Recent advances in molecular pharmacology of the histamine systems: organic cation transporters as a histamine transporter and histamine metabolism. J. Pharmacol. Sci. 101, 24-30.

Okada, R., Awasaki, T. and Ito, K. 2009. Gamma-aminobutyric acid (GABA)-mediated neural connections in the *Drosophila* antennal lobe. J. Comp. Neurol. 514, 74-91.

Oland, L.A., Marrero, H.G. and Burger, I. 1999. Glial cells in the developing and adult olfactory lobe of the moth *Manduca sexta*. Cell Tissue Res. 297, 527-545.

Oland, L.A., Biebelhausen, J.P. and Tolbert, L.P. 2008. Glial investment of the adult and developing antennal lobe of *Drosophila*. J. Comp. Neurol. 509, 526-550.

Oland, L.A., Gibson, N.J. and Tolbert, L.P. 2010. Localization of a GABA transporter to glial cells in the developing and adult olfactory pathway of the moth *Manduca sexta*. J. Comp. Neurol. 518, 815-838.

Ostroy, S.E., Wilson, M. and Pak, W.L. 1974. *Drosophila* rhodopsin: Photochemistry, extraction and differences in the *norp* A^{P12} phototransduction mutant. Biochem. Biophys. Res. Commun. 59, 960-966.

Pak, W.L. (1975) Mutations affecting the vision of *Drosophila melanogaster*. In: *Handbook of genetics*. pp. 703-733. Ed. R. C. King. Plenum Press: New York.

Palgi, M., Lindström, R., Peränen, J., Piepponen, T.P., Saarma, M. and Heino, T.I. 2009. Evidence that DmMANF is an invertebrate neurotrophic factor supporting dopaminergic neurons. Proc. Natl. Acad. Sci. U.S.A. 106, 2429-2434.

Pantazis, A., Segaran, A., Liu, C.-H., Nikolaev, A., Rister, J., Thum, A.S., Roeder, T., Semenov, E., Juusola, M. and Hardie, R.C. 2008. Distinct roles for two histamine receptors (*hclA* and *hclB*) at the *Drosophila* photoreceptor synapse. J. Neurosci. 28, 7250-7259.

Panula, P., Häppölä, O., Airaksinen, M.S., Auvinen, S. and Virkamäki, A. 1988. Carbodiimide as a tissue fixative in histamine immunohistochemistry and its application in developmental neurobiology. J. Histochem. Cytochem. 36, 259-269.

Panula, P., Flügge, G., Fuchs, E., Pirvola, U., Auvinen, S. and Airaksinen, M.S. 1989. Histamine-immunoreactive nerve fibers in the mammalian spinal cord. Brain Res. 484, 234-239.

Papatsenko, D., Sheng, G. and Desplan, C. 1997. A new rhodopsin in R8 photoreceptors of *Drosophila*: evidence for coordinate expression with Rh3 in R7 cells. Development 124, 1665-1673.

Parker, R.J. and Auld, V.J. 2004. Signaling in glial development: differentiation migration and axon guidance. Biochem. Cell Biol. 82, 694-707.

Parpura, V., Scemes, E. and Spray, D.C. 2004. Mechanisms of glutamate release from astrocytes: gap junction "hemichannels", purinergic receptors and exocytotic release. Neurochem. Int. 45, 259-264.

Peng, Y.-W., Hao, Y., Petters, R.M. and Wong, F. 2000. Ectopic synaptogenesis in the mammalian retina caused by rod photoreceptor-specific mutations. Nat. Neurosci. 3, 1121-1127.

Peng, Y.-W., Senda, T., Hao, Y., Matsuno, K. and Wong, F. 2003. Ectopic synaptogenesis during retinal degeneration in the Royal College of Surgeons Rat. Neuroscience 119, 813-820.

Pereanu, W., Shy, D. and Hartenstein, V. 2005. Morphogenesis and proliferation of the larval brain glia in *Drosophila*. Dev. Biol. 283, 191-203.

Pereanu, W., Spindler, S., Cruz, L. and Hartenstein, V. 2007. Tracheal development in the *Drosophila* brain is constrained by glial cells. Dev. Biol. 302, 169-180.

Pérez, M., Schachter, J. and Quesada-Allué, L.A. 2004. Constitutive activity of N-β-alanyl-catecholamine ligase in insect brain. Neurosci. Lett. 368, 186-191.

Perez, S.E. and Steller, H. 1996. Migration of glial cells into retinal axon target field in *Drosophila melanogaster*. J. Neurobiol. 30, 359-373.

Pfeiffer, B.D., Jenett, A., Hammonds, A.S., Ngo, T.-T.B., Misra, S., Murphy, C., Scully, A., Carlson, J.W., Wan, K.H., Laverty, T.R., Mungall, C., Svirskas, R., Kadonaga, J.T., Doe, C.Q., Eisen, M.B., Celniker, S.E. and Rubin, G.M. 2008. Tools for neuroanatomy and neurogenetics in *Drosophila*. Proc. Natl. Acad. Sci. U.S.A. 105, 9715-9720.

Pfrieger, F.W. and Barres, B.A. 1995. What the fly's glia tell the fly's brain. Cell 83, 671-674.

Phelan, P., Nakagawa, M., Wilkin, M.B., Moffat, K.G., O'Kane, C.J., Davies, J.A. and Bacon, J.P. 1996. Mutations in *shaking-B* prevent electrical synapse formation in the *Drosophila* giant fiber system. J. Neurosci. 16, 1101-1113.

Phelan, P. and Starich, T.A. 2001. Innexins get into the gap. BioEssays 23, 388-396.

Phelan, P. 2005. Innexins: members of an evolutionarily conserved family of gap-junction proteins. Biochim. Biophys. Acta. 1711, 225-245.

Phillips, A.M., Salkoff, L.B. and Kelly, L.E. 1993. A neural gene from *Drosophila melanogaster* with homology to vertebrate and invertebrate glutamate decarboxylases. J. Neurochem. 61, 1291-1301.

Pichaud, F., Briscoe, A. and Desplan, C. 1999. Evolution of color vision. Curr. Opin. Neurobiol. 9, 622-627.

Piyankarage, S.C., Augustin, H., Grosjean, Y., Featherstone, D.E. and Shippy, S.A. 2008. Hemolymph amino acid analysis of individual *Drosophila* larvae. Anal. Chem. 80, 1201-1207.

Poeck, B., Fischer, S., Gunning, D., Zipursky, S.L. and Salecker, I. 2001. Glial cells mediate target layer selection of retinal axons in the developing visual system of *Drosophila*. Neuron 29, 99-113.

Pollack, I. and Hofbauer, A. 1991. Histamine-like immunoreactivity in the visual system and brain of *Drosophila melanogaster*. Cell Tissue Res. 266, 391-398.

Pollock, J.A., Ellisman, M.H. and Benzer, S. 1990. Subcellular localization of transcripts in *Drosophila* photoreceptor neurons: *chaoptic* mutants have an aberrant distribution. Genes Dev. 4, 806-821.

Pörzgen, P., Park, S.K., Hirsh, J., Sonders, M.S. and Amara, S.G. 2001. The antidepressant-sensitive dopamine transporter in *Drosophila melanogaster*: A primordial carrier for catecholamines. Mol. Pharmacol. 59, 83-95.

Pottek, M., Hoppenstedt, W., Janssen-Bienhold, U., Schultz, K., Perlman, I. and Weiler, R. 2003. Contribution of connexin26 to electrical feedback inhibition in the turtle retina. J. Comp. Neurol. 466, 468-477.

Prakash, S., Caldwell, J.C., Eberl, D.F. and Clandinin, T.R. 2005. Drosophila N-cadherin mediates an attractive interaction between photoreceptor axons and their targets. Nat. Neurosci. 8, 443-450.

Prakash, S., McLendon, H.M., Dubreuil, C.I., Ghose, A., Hwa, J., Dennehy, K.A., Tomalty, K.M.H., Clark, K.L., Van Vactor, D. and Clandinin, T.R. 2009. Complex interactions amongst N-cadherin, DLAR, and Liprin-α regulate *Drosophila* photoreceptor axon targeting. Dev. Biol. 336, 10-19.

Prokop, A. and Meinertzhagen, I.A. 2006. Development and structure of synaptic contacts in *Drosophila*. Semin. Cell Dev. Biol. 17, 20-30.

Pyza, E. and Meinertzhagen, I.A. 1996. Neurotransmitters regulate rhythmic size changes amongst cells in the fly's optic lobe. J. Comp. Physiol. A. 178, 33-45.

Pyza, E. and Meinertzhagen, I.A. 1999. Daily rhythmic changes of cell size and shape in the first optic neuropil in *Drosophila melanogaster*. J. Neurobiol. 40, 77-88.

Pyza, E. and Górska-Andrzejak, J. 2004. Involvement of glial cells in rhythmic size changes in neurons of the housefly's visual system. J. Neurobiol. 59, 205-215.

Rajaram, S. and Nash, H.A. 2004. A specific alteration in the electroretinogram of *Drosophila melanogaster* is induced by halothane and other volatile general anesthetics. Anesth. Analg. 98, 1705-1711.

Rangarajan, R., Gong, Q. and Gaul, U. 1999. Migration and function of glia in the developing *Drosophila* eye. Development 126, 3285-3292.

Rangarajan, R., Courvoisier, H. and Gaul, U. 2001. Dpp and Hedgehog mediate neuron-glia interactions in *Drosophila* eye development by promoting the proliferation and motility of subretinal glia. Mech. Dev. 108, 93-103.

Rao-Mirotznik, R., Harkins, A.B., Buchsbaum, G. and Sterling, P. 1995. Mammalian rod terminal: architecture of a binary synapse. Neuron 14, 561-569.

Rao, Y., Pang, P., Ruan, W., Gunning, D. and Zipursky, S.L. 2000. *brakeless* is required for photoreceptor growth-cone targeting in *Drosophila*. Proc. Natl. Acad. Sci. U.S.A. 97, 5966-5971.

Rawlins, E.L., White, N.M. and Jarman, A.P. 2003. Echinoid limits R8 photoreceptor specification by inhibiting inappropriate EGF receptor signalling within R8 equivalence groups. Development 130, 3715-3724.

Rawls, J.M., Jr. 2006. Analysis of pyrimidine catabolism in *Drosophila melanogaster* using epistatic interactions with mutations of pyrimidine biosynthesis and β-alanine metabolism. Genetics 172, 1665-1674.

Ready, D.F., Hanson, T.E. and Benzer, S. 1976. Development of the *Drosophila* retina, a neurocrystalline lattice. Dev. Biol. 53, 217-240.

Reiff, D.F., Plett, J., Mank, M., Griesbeck, O. and Borst, A. 2010. Visualizing retinotopic half-wave rectified input to the motion detection circuitry of *Drosophila*. Nat. Neurosci. 13, 973-978.

Richardt, A., Rybak, J., Störtkuhl, K.F., Meinertzhagen, I.A. and Hovemann, B.T. 2002. Ebony protein in the *Drosophila* nervous system: Optic neuropile expression in glial cells. J. Comp. Neurol. 452, 93-102.

Richardt, A., Kemme, T., Wagner, S., Schwarzer, D., Marahiel, M.A. and Hovemann, B.T. 2003. Ebony, a novel nonribosomal peptide synthetase for β-alanine conjugation with biogenic amines in *Drosophila*. J. Biol. Chem. 278, 41160-41166.

Rister, J., Pauls, D., Schnell, B., Ting, C.-Y., Lee, C.-H., Sinakevitch, I., Morante, J., Strausfeld, N.J., Ito, K. and Heisenberg, M. 2007. Dissection of the peripheral motion channel in the visual system of *Drosophila melanogaster*. Neuron 56, 155-170.

Rival, T., Soustelle, L., Strambi, C., Besson, M.-T., Iché, M. and Birman, S. 2004. Decreasing glutamate buffering capacity triggers oxidative stress and neuropil degeneration in the *Drosophila* brain. Curr. Biol. 14, 599-605.

Rival, T., Soustelle, L., Cattaert, D., Strambi, C., Iché, M. and Birman, S. 2006. Physiological requirement for the glutamate transporter dEAAT1 at the adult *Drosophila* neuromuscular junction. J. Neurobiol. 66, 1061-1074.

Robinow, S. and White, K. 1991. Characterization and spatial distribution of the ELAV protein during *Drosophila melanogaster* development. J. Neurobiol. 22, 443-461.

Rogina, B., Benzer, S. and Helfand, S.L. 1997. *Drosophila drop-dead* mutations accelerate the time course of age-related markers. Proc. Natl. Acad. Sci. U.S.A. 94, 6303-6306.

Romero-Calderón, R., M. Shome, R., Simon, A.F., Daniels, R.W., DiAntonio, A. and Krantz, D.E. 2007. A screen for neurotransmitter transporters expressed in the visual system of *Drosophila melanogaster* identifies three novel genes. Dev. Neurobiol. 67, 550-569.

Romero-Calderón, R., Uhlenbrock, G., Borycz, J., Simon, A.F., Grygoruk, A., Yee, S.K., Shyer, A., Ackerson, L.C., Maidment, N.T., Meinertzhagen, I.A., Hovemann, B.T. and Krantz, D.E. 2008. A glial variant of the vesicular monoamine transporter is required to store histamine in the *Drosophila* visual system. PLoS Genet. 4, e1000245.

Rössler, W., Oland, L.A., Higgins, M.R., Hildebrand, J.G. and Tolbert, L.P. 1999. Development of a glia-rich axon-sorting zone in the olfactory pathway of the moth *Manduca sexta*. J. Neurosci. 19, 9865-9877.

Rybak, J. and Meinertzhagen, I.A. 1997. The effects of light reversals on photoreceptor synaptogenesis in the fly *Musca domestica*. Eur. J. Neurosci. 9, 319-333.

Saint Marie, R.L. and Carlson, S.D. 1983a. Glial membrane specializations and the compartmentalization of the lamina ganglionaris of the housefly compound eye. J. Neurocytol. 12, 243-275.

Saint Marie, R.L. and Carlson, S.D. 1983b. The fine structure of neuroglia in the lamina ganglionaris of the housefly, *Musca domestica* L. J. Neurocytol. 12, 213-241.

Saint Marie, R.L. and Carlson, S.D. 1985. Interneuronal and glial-neuronal gap junctions in the lamina ganglionaris of the compound eye of the housefly, *Musca domestica*. Cell Tissue Res. 241, 43-52.

Salcedo, E., Huber, A., Henrich, S., Chadwell, L.V., Chou, W.-H., Paulsen, R. and Britt, S.G. 1999. Blue- and green-absorbing visual pigments of *Drosophila:* ectopic expression and physiological characterization of the R8 photoreceptor cell-specific Rh5 and Rh6 rhodopsins. J. Neurosci. 19, 10716-10726.

Salecker, I., Clandinin, T.R. and Zipursky, S.L. 1998. Hedgehog and Spitz: making a match between photoreceptor axons and their targets. Cell 95, 587-590.

Sánchez y Sánchez, D. 1935. Contribucion à l'étude de l'origine et de l'évolution de certains types de neuroglie chez les insectes. Trab. Lab Invest. Biol. (Madrid) 30, 299-353.

Sarthy, P.V. 1991. Histamine: a neurotransmitter candidate for *Drosophila* photoreceptors. J. Neurochem. 57, 1757-1768.

Sasaki, Y., Araki, T. and Milbrandt, J. 2006. Stimulation of nicotinamide adenine dinucleotide biosynthetic pathways delays axonal degeneration after axotomy. J. Neurosci. 26, 8484-8491.

Savarit, F. and Ferveur, J.-F. 2002. Genetic study of the production of sexually dimorphic cuticular hydrocarbons in relation with the sex-determination gene *transformer* in *Drosophila melanogaster*. Genet. Res. 79, 23-40.

Scemes, E., Spray, D.C. and Meda, P. 2009. Connexins, pannexins, innexins: novel roles of "hemi-channels". Pflugers Arch. - Eur. J. Physiol 457, 1207-1226.

Schmucker, D., Taubert, H. and Jäckle, H. 1992. Formation of the *Drosophila* larval photoreceptor organ and its neuronal differentiation require continuous Krüppel gene activity. Neuron 9, 1025-1039.

Schmucker, D., Jäckle, H. and Gaul, U. 1997. Genetic analysis of the larval optic nerve projection in *Drosophila*. Development 124, 937-948.

Schneider, E., Rolli-Derkinderen, M., Arock, M. and Dy, M. 2002. Trends in histamine research: new functions during immune responses and hematopoiesis. Trends Immunol. 23, 255-263.

Schulte, J., Tepass, U. and Auld, V.J. 2003. Gliotactin, a novel marker of tricellular junctions, is necessary for septate junction development in *Drosophila*. J. Cell Biol. 161, 991-1000.

Schwabe, T., Bainton, R.J., Fetter, R.D., Heberlein, U. and Gaul, U. 2005. GPCR signaling is required for blood-brain barrier formation in *Drosophila*. Cell 123, 133-144.

Schwartz, J.-C., Pollard, H. and Quach, T.T. 1980. Histamine as a neurotransmitter in mammalian brain: Neurochemical evidence. J. Neurochem. 35, 26-33.

Seal, R.P., Daniels, G.M., Wolfgang, W.J., Forte, M.A. and Amara, S.G. 1998. Identification and characterization of a cDNA encoding a neuronal glutamate transporter from *Drosophila melanogaster*. Receptors Channels 6, 51-64.

Seal, R.P. and Amara, S.G. 1999. Excitatory amino acid transporters: A family in flux. Annu. Rev. Pharmacol. Toxicol. 39, 431-456.

Seid, M.A. and Wehner, R. 2009. Delayed axonal pruning in the ant brain: A study of developmental trajectories. Dev. Neurobiol. 69, 350-364.

Selleck, S.B. and Steller, H. 1991. The influence of retinal innervation on neurogenesis in the first optic ganglion of Drosophila. Neuron 6, 83-99.

Selleck, S.B., Gonzalez, C., Glover, D.M. and White, K. 1992. Regulation of the G1-S transition in postembryonic neuronal precursors by axon ingrowth. Nature 355, 253-255.

Sen, A., Shetty, C., Jhaveri, D. and Rodrigues, V. 2005. Distinct types of glial cells populate the *Drosophila* antenna. BMC Dev. Biol. 5, 25.

Senti, K.-A., Keleman, K., Eisenhaber, F. and Dickson, B.J. 2000. *brakeless* is required for lamina targeting of R1-R6 axons in the *Drosophila* visual system. Development 127, 2291-2301.

Senti, K.-A., Usui, T., Boucke, K., Greber, U., Uemura, T. and Dickson, B.J. 2003. Flamingo regulates R8 axon-axon and axon-target interactions in the *Drosophila* visual system. Curr. Biol. 13, 828-832.

Sepp, K.J., Schulte, J. and Auld, V.J. 2000. Developmental dynamics of peripheral glia in *Drosophila melanogaster*. Glia 30, 122-133.

Sepp, K.J., Schulte, J. and Auld, V.J. 2001. Peripheral glia direct axon guidance across the CNS/PNS transition zone. Dev. Biol. 238, 47-63.

Shaw, S.R. 1975. Retinal resistance barriers and electrical lateral inhibition. Nature 255, 480-483.

Shaw, S.R. 1977. Restricted diffusion and extracellular space in the insect retina. J. Comp. Physiol. A. 113, 257-282.

Shaw, S.R. 1978. The extracellular space and blood-eye barrier in an insect retina: An ultrastructural study. Cell Tissue Res. 188, 35-61.

Shaw, S.R. and Stowe, S. 1982. Freeze-fracture evidence for gap junctions connecting the axon terminals of dipteran photoreceptors. J. Cell Sci. 53, 115-141.

Shaw, S.R. 1984a. Early visual processing in insects. J. Exp. Biol. 112, 225-251.

Shaw, S.R. 1984b. Asymmetric distribution of gap junctions amongst identified photoreceptor axons of *Lucilia cuprina* (Diptera). J. Cell Sci. 66, 65-80.

Shaw, S.R. and Henken, D.B. (1984) The formation of the insect blood-brain: evidence from the cockroach nerve cord against the tight junction hypothesis. In *Insect Neurochemistry and Neurophysiology*. pp. 471-473. Eds. A. B. Borkovec & T. J. Kelly. Plenum Press: New York.

Shaw, S.R. and Moore, D. 1989. Evolutionary remodeling in a visual system through extensive changes in the synaptic connectivity of homologous neurons. Vis. Neurosci. 3, 405-410.

Shaw, S.R. and Varney, L.P. 1999. Primitive, crustacean-like state of blood-brain barrier in the eye of the apterygote insect *Petrobius* (Archaeognatha) determined from uptake of fluorescent tracers. J. Neurobiol. 41, 452-470.

Shimohigashi, M. and Meinertzhagen, I.A. 1998. The *shaking B* gene in *Drosophila* regulates the number of gap junctions between photoreceptor terminals in the lamina. J. Neurobiol. 35, 105-117.

Shinza-Kameda, M., Takasu, E., Sakurai, K., Hayashi, S. and Nose, A. 2006. Regulation of layer-specific targeting by reciprocal expression of a cell adhesion molecule, Capricious. Neuron 49, 205-213.

Shpetner, H.S. and Vallee, R.B. 1989. Identification of dynamin, a novel mechanochemical enzyme that mediates interactions between microtubules. Cell 59, 421-432.

Siddall, N.A., Hime, G.R., Pollock, J.A. and Batterham, P. 2009. Ttk69-dependent repression of *lozenge* prevents the ectopic development of R7 cells in the *Drosophila* larval eye disc. BMC Dev. Biol. 9, 64.

Silies, M., Yuva, Y., Engelen, D., Aho, A., Stork, T. and Klämbt, C. 2007. Glial cell migration in the eye disc. J. Neurosci. 27, 13130-13139.

Silies, M., Yuva-Aydemir, Y., Franzdóttir, S.R. and Klämbt, C. 2010. The eye imaginal disc as a model to study the coordination of neuronal and glial development. Fly 4, 71-79.

Sinakevitch, I. and Strausfeld, N.J. 2004. Chemical neuroanatomy of the fly's movement detection pathway. J. Comp. Neurol. 468, 6-23.

Siraganian, R.P. 1983. Histamine secretion from mast cells and basophils. Trends Pharmacol. Sci. 4, 432-437.

Smith, L.A., Peixoto, A.A., Kramer, E.M., Villella, A. and Hall, J.C. 1998. Courtship and visual defects of *cacophony* mutants reveal functional complexity of a Calcium-channel α1 subunit in Drosophila. Genetics 149, 1407-1426.

Smith, P.J.S., Howes, E.A. and Treherne, J.E. 1990. Cell proliferation in the repairing adult insect central nervous system: incorporation of the thymidine analogue 5-bromo-2-deoxyuridine *in vivo*. J. Cell Sci. 95, 599-604.

Soehnge, H., Huang, X., Becker, M., Whitley, P., Conover, D. and Stern, M. 1996. A neurotransmitter transporter encoded by the *Drosophila* inebriated gene. Proc. Natl. Acad. Sci. U.S.A. 93, 13262-13267.

Spana, E.P. and Doe, C.Q. 1995. The prospero transcription factor is asymmetrically localized to the cell cortex during neuroblast mitosis in *Drosophila*. Development 121, 3187-3195.

Srinivasan, M.V., Poteser, M. and Kral, K. 1999. Motion detection in insect orientation and navigation. Vision Res. 39, 2749-2766.

Stark, W.S. and Carlson, S.D. 1982. Ultrastructural pathology of the compound eye and optic neuropiles of the retinal degeneration mutant (*w rdgB*^{KS222}) *Drosophila melanogaster*. Cell Tissue Res. 225, 11-22.

Stark, W.S. and Carlson, S.D. 1984. Blue and ultraviolet light induced damage to the *Drosophila* retina: ultrastructure. Curr. Eye Res. 3, 1441-1454.

Stark, W.S. and Carlson, S.D. 1985. Retinal degeneration in *rdgA* mutants of *Drosophila melanogaster* meigen (Diptera : Drosophilidae). Int. J. Insect Morphol. Embryol. 14, 243-254.

Stark, W.S. and Carlson, S.D. 1986. Ultrastructure of capitate projections in the optic neuropil of Diptera. Cell Tissue Res. 246, 481-486.

Stark, W.S., Sapp, R. and Carlson, S.D. 1989. Ultrastructure of the ocellar visual system in normal and mutant *Drosophila melanogaster*. J. Neurogenet. 5, 127-153.

Stebbings, L.A., Todman, M.G., Phelan, P., Bacon, J.P. and Davies, J.A. 2000. Two *Drosophila* innexins are expressed in overlapping domains and cooperate to form gap-junction channels. Mol. Biol. Cell 11, 2459-2470.

Stebbings, L.A., Todman, M.G., Phillips, R., Greer, C.E., Tam, J., Phelan, P., Jacobs, K., Bacon, J.P. and Davies, J.A. 2002. Gap junctions in *Drosophila*: developmental expression of the entire innexin gene family. Mech. Dev. 113, 197-205.

Stephenson, R.S. and Pak, W.L. 1980. Heterogenic components of a fast electrical potential in *Drosophila* compound eye and their relation to visual pigment photoconversion. J. Gen. Physiol. 75, 353-379.

Stern, M. and Ganetzky, B. 1992. Identification and characterization of *inebriated*, a gene affecting neuronal excitability in *Drosophila*. J. Neurogenet. 8, 157-172.

Stork, T., Engelen, D., Krudewig, A., Silies, M., Bainton, R.J. and Klämbt, C. 2008. Organization and function of the blood-brain barrier in *Drosophila*. J. Neurosci. 28, 587-597.

Strausfeld, N.J. 1970. Golgi studies on insects. Part II. The optic lobes of Diptera. . Phil. Trans. R. Soc. Lond. B. 258, 135-223.

Strausfeld, N.J. (1976) *Atlas of an insect brain*. Springer: Berlin-Heidelberg-New York.

Strigini, M., Cantera, R., Morin, X., Bastiani, M.J., Bate, M. and Karagogeos, D. 2006. The IgLON protein Lachesin is required for the blood-brain barrier in *Drosophila*. Mol. Cell. Neurosci. 32, 91-101.

Stuart, A.E., Morgan, J.R., Mekeel, H.E., Kempter, E. and Callaway, J.C. 1996. Selective, activity-dependent uptake of histamine into an arthropod photoreceptor. J. Neurosci. 16, 3178-3188.

Stuart, A.E., Mekeel, H.E. and Kempter, E. 2002. Uptake of the neurotransmitter histamine into the eyes of larvae of the barnacle (*Balanus amphitrite*). Biol. Bull. 202, 53-60.

Stuart, A.E., Borycz, J. and Meinertzhagen, I.A. 2007. The dynamics of signaling at the histaminergic photoreceptor synapse of arthropods. Prog. Neurobiol. 82, 202-227.

Suh, G.S., Poeck, B., Chouard, T., Oron, E., Segal, D., Chamovitz, D.A. and Zipursky, S.L. 2002. *Drosophila* JAB1/CSN5 acts in photoreceptor cells to induce glial cells. Neuron 33, 35-46.

Suh, J. and Jackson, F.R. 2007. *Drosophila* Ebony activity is required in glia for the circadian regulation of locomotor activity. Neuron 55, 435-447.

Sweeney, S.T. and Davis, G.W. 2002. Unrestricted synaptic growth in *spinster* - a late endosomal protein implicated in TGF-β-mediated synaptic growth regulation. Neuron 36, 403-416.

Tachibana, M. and Kaneko, A. 1988. L-Glutamate-induced depolarization in solitary photoreceptors: A process that may contribute to the interaction between photoreceptors *in situ*. Proc. Natl. Acad. Sci. U.S.A. 85, 5315-5319.

Tahayato, A., Sonneville, R., Pichaud, F., Wernet, M.F., Papatsenko, D., Beaufils, P., Cook, T. and Desplan, C. 2003. Otd/Crx, a dual regulator for the specification of ommatidia subtypes in the *Drosophila* retina. Dev. Cell 5, 391-402.

Takemura, S.-y., Lu, Z. and Meinertzhagen, I.A. 2008. Synaptic circuits of the *Drosophila* optic lobe: the input terminals to the medulla. J. Comp. Neurol. 509, 493-513.

Tatler, B., O'Carroll, D.C. and Laughlin, S.B. 2000. Temperature and the temporal resolving power of fly photoreceptors. J. Comp. Physiol. A. 186, 399-407.

Tayler, T.D. and Garrity, P.A. 2003. Axon targeting in the *Drosophila* visual system. Curr. Opin. Neurobiol. 13, 90-95.

Taylor, C.A., Stanley, K.N. and Shirras, A.D. 1997. The *Orct* gene of *Drosophila melanogaster* codes for a putative organic cation transporter with six or 12 transmembrane domains. Gene 201, 69-74.

Tepass, U. and Hartenstein, V. 1994. The development of cellular junctions in the *Drosophila* embryo. Dev. Biol. 161, 563-596.

Tepass, U. and Harris, K.P. 2007. Adherens junctions in *Drosophila* retinal morphogenesis. Trends Cell Biol. 17, 26-35.

Tessier-Lavigne, M. and Goodman, C.S. 1996. The molecular biology of axon guidance. Science 274, 1123-1133.

Thimgan, M.S., Berg, J.S. and Stuart, A.E. 2006. Comparative sequence analysis and tissue localization of members of the SLC6 family of transporters in adult *Drosophila melanogaster*. J. Exp. Biol. 209, 3383-3404.

Tiedje, K.E., Stevens, K., Barnes, S. and Weaver, D.F. 2010. β-alanine as a small molecule neurotransmitter. Neurochem. Int. 57, 177-188.

Ting, C.-Y., Yonekura, S., Chung, P., Hsu, S.-n., Robertson, H.M., Chiba, A. and Lee, C.-H. 2005. *Drosophila* N-cadherin functions in the first stage of the two-stage layer-selection process of R7 photoreceptor afferents. Development 132, 953-963.

Ting, C.-Y. and Lee, C.-H. 2007. Visual circuit development in *Drosophila*. Curr. Opin. Neurobiol. 17, 65-72.

Tissot, M., Gendre, N., Hawken, A., Störtkuhl, K.F. and Stocker, R.F. 1997. Larval chemosensory projections and invasion of adult afferents in the antennal lobe of *Drosophila*. J. Neurobiol. 32, 281-297.

Tix, S., Eule, E., Fischbach, K.-F. and Benzer, S. 1997. Glia in the chiasms and medulla of the *Drosophila melanogaster* optic lobes. Cell Tissue Res. 289, 397-409.

Tolbert, L.P. and Hildebrand, J.G. 1981. Organization and synaptic ultrastructure of glomeruli in the antennal lobes of the moth *Manduca sexta*: A study using thin sections and freeze-fracture. Proc. R. Soc. Lond. B. Biol. Sci. 213, 279-301.

Tomlinson, A. 1985. The cellular dynamics of pattern formation in the eye of *Drosophila*. J. Embryol. Exp. Morph. 89, 313-331.

Tomlinson, A. and Ready, D.F. 1986. Sevenless: A cell-specific homeotic mutation of the *Drosophila* eye. Science 231, 400-402.

Tomlinson, A., Bowtell, D.D.L., Hafen, E. and Rubin, G.M. 1987. Localization of the *sevenless* protein, a putative receptor for positional information, in the eye imaginal disc of Drosophila. Cell 51, 143-150.

Tomlinson, A. and Ready, D.F. 1987a. Cell fate in the *Drosophila* ommatidium. Dev. Biol. 123, 264-275.

Tomlinson, A. and Ready, D.F. 1987b. Neuronal differentiation in the *Drosophila* ommatidium. Dev. Biol. 120, 366-376.

Tomlinson, A. 1988. Cellular interactions in the developing *Drosophila* eye. Development 104, 183-193.

Tomlinson, A. 2003. Patterning the peripheral retina of the fly: decoding a gradient. Dev. Cell 5, 799-809.

Torres, G.E., Gainetdinov, R.R. and Caron, M.G. 2003. Plasma membrane monoamine transporters: structure, regulation and function. Nat. Rev. Neurosci. 4, 13-25.

Townson, S.M., Chang, B.S.W., Salcedo, E., Chadwell, L.V., Pierce, N.E. and Britt, S.G. 1998. Honeybee blue- and ultraviolet-sensitive opsins: cloning, heterologous expression in *Drosophila*, and physiological characterization. J. Neurosci. 18, 2412-2422.

Treherne, J.E. (1985) Blood-brain barrier. In: *Comprehensive Insect Physiology, Biochemistry and Pharmacology*. pp. 115-137. Eds. G.A. Kerkut., L.I. Gilbert. Pergamon: Oxford.

True, J.R., Yeh, S.-D., Hovemann, B.T., Kemme, T., Meinertzhagen, I.A., Edwards, T.N., Liou, S.-R., Han, Q. and Li, J. 2005. *Drosophila tan* encodes a novel hydrolase required in pigmentation and vision. PLoS Genet. 1, e63.

Trujillo-Cenóz, O. 1965. Some aspects of the structural organization of the intermediate retina of dipterans. J. Ultrastruct. Res. 13, 1-33.

Trujillo-Cenóz, O. and Melamed, J. 1973. The development of the retina-lamina complex in muscoid flies. J. Ultrastruct. Res. 42, 554-581.

Truman, J.W., Taylor, B.J. and Award, T.A. (1993) Formation of the adult nervous system. In: *The Development of Drosophila melanogaster.* . pp. 1245–1275. Eds. M. Bate, A. M. Arias. Cold Spring Harbor Laboratory Press: Cold Spring Harbor, NY.

Tsacopoulos, M. and Poitry, S. 1982. Kinetics of oxygen consumption after a single flash of light in photoreceptors of the drone (*Apis mellifera*). J. Gen. Physiol. 80, 19-55.

Tsacopoulos, M., Coles, J.A. and Van de Werve, G. 1987. The supply of metabolic substrate from glia to photoreceptors in the retina of the honeybee drone. J. Physiol. Paris 82, 279-287.

Tsacopoulos, M., Evêquoz-Mercier, V., Perrottet, P. and Buchner, E. 1988. Honeybee retinal glial cells transform glucose and supply the neurons with metabolic substrate. Proc. Natl. Acad. Sci. U.S.A. 85, 8727-8731.

Tsacopoulos, M., Veuthey, A.-L., Saravelos, S.G., Perrottet, P. and Tsoupras, G. 1994. Glial cells transform glucose to alanine, which fuels the neurons in the honeybee retina. J. Neurosci. 14, 1339-1351.

Tsacopoulos, M. and Magistretti, P.J. 1996. Metabolic coupling between glia and neurons. J. Neurosci. 16, 877-885.

Udolph, G., Prokop, A., Bossing, T. and Technau, G.M. 1993. A common precursor for glia and neurons in the embryonic CNS of *Drosophila* gives rise to segment-specific lineage variants. Development 118, 765-775.

Ueda, H.R., Matsumoto, A., Kawamura, M., Iino, M., Tanimura, T. and Hashimoto, S. 2002. Genome-wide transcriptional orchestration of circadian rhythms in *Drosophila*. J. Biol. Chem. 277, 14048-14052.

Usui, T., Shima, Y., Shimada, Y., Hirano, S., Burgess, R.W., Schwarz, T.L., Takeichi, M. and Uemura, T. 1999. Flamingo, a seven-pass transmembrane cadherin, regulates planar cell polarity under the control of Frizzled. Cell 98, 585-595.

Uusitalo, R.O., Juusola, M., Kouvalainen, E. and Weckström, M. 1995a. Tonic transmitter release in a graded potential synapse. J. Neurophysiol. 74, 470-473.

Uusitalo, R.O., Juusola, M. and Weckström, M. 1995b. Graded responses and spiking properties of identified first-order visual interneurons of the fly compound eye. J. Neurophysiol. 73, 1782-1792.

van Marle, J., Piek, T., Lammertse, T., Lind, A. and van Weeren-Kramer, J. 1985. Selectivity of the uptake of glutamate and GABA in two morphologically distinct insect neuromuscular synapses. Brain Res. 348, 107-111.

Van Vactor, D., Jr., Krantz, D.E., Reinke, R. and Zipursky, S.L. 1988. Analysis of mutants in chaoptin, a photoreceptor cell-specific glycoprotein in Drosophila, reveals its role in cellular morphogenesis. Cell 52, 281-290.

Vaney, D.I., Nelson, J.C. and Pow, D.V. 1998. Neurotransmitter coupling through gap junctions in the retina. J. Neurosci. 18, 10594-10602.

Venkatesh, S. and Naresh Singh, R. 1984. Sensilla on the third antennal segment of *Drosophila melanogaster* meigen (Diptera : Drosophilidae). Int. J. Insect Morphol. Embryol. 13, 51-63.

von Hilchen, C.M., Beckervordersandforth, R.M., Rickert, C., Technau, G.M. and Altenhein, B. 2008. Identity, origin, and migration of peripheral glial cells in the *Drosophila* embryo. Mech. Dev. 125, 337-352.

von Trotha, J.W., Egger, B. and Brand, A.H. 2009. Cell proliferation in the *Drosophila* adult brain revealed by clonal analysis and bromodeoxyuridine labelling. Neural Dev. 4, 9.

Vosshall, L.B., Amrein, H., Morozov, P.S., Rzhetsky, A. and Axel, R. 1999. A spatial map of olfactory receptor expression in the *Drosophila* antenna. Cell 96, 725-736.

Vosshall, L.B., Wong, A.M. and Axel, R. 2000. An olfactory sensory map in the fly brain. Cell 102, 147-159.

Vosshall, L.B. and Stocker, R.F. 2007. Molecular architecture of smell and taste in *Drosophila*. Annu. Rev. Neurosci. 30, 505-533.

Wafford, K.A. and Sattelle, D.B. 1986. Effects of amino acid neurotransmitter candidates on an identified insect motoneurone. Neurosci. Lett. 63, 135-140.

Wagh, D.A., Rasse, T.M., Asan, E., Hofbauer, A., Schwenkert, I., Dürrbeck, H., Buchner, S., Dabauvalle, M.-C., Schmidt, M., Qin, G., Wichmann, C., Kittel, R., Sigrist, S.J. and Buchner, E. 2006. Bruchpilot, a protein with homology to ELKS/CAST, is required for structural integrity and function of synaptic active zones in *Drosophila*. Neuron 49, 833-844.

Wagner, S., Heseding, C., Szlachta, K., True, J.R., Prinz, H. and Hovemann, B.T. 2007. *Drosophila* photoreceptors express cysteine peptidase Tan. J. Comp. Neurol. 500, 601-611.

Watanabe, T. and Kankel, D.R. 1990. Molecular cloning and analysis of *l(1)ogre*, a locus of *Drosophila melanogaster* with prominent effects on the postembryonic development of the central nervous system. Genetics 126, 1033-1044.

Watts, R.J., Hoopfer, E.D. and Luo, L. 2003. Axon pruning during *Drosophila* metamorphosis: Evidence for local degeneration and requirement of the ubiquitin-proteasome system. Neuron 38, 871-885.

Weinshilboum, R.M., Thoa, N.B., Johnson, D.G., Kopin, I.J. and Axelrod, J. 1971. Proportional release of norepinephrine and dopamine-β-hydroxylase from sympathetic nerves. Science 174, 1349-1351.

Wernet, M.F., Labhart, T., Baumann, F., Mazzoni, E.O., Pichaud, F. and Desplan, C. 2003. Homothorax switches function of *Drosophila* photoreceptors from color to polarized light sensors. Cell 115, 267-279.

Wernet, M.F. and Desplan, C. 2004. Building a retinal mosaic: cell-fate decision in the fly eye. Trends Cell Biol. 14, 576-584.

Wernet, M.F., Mazzoni, E.O., Çelik, A., Duncan, D.M., Duncan, I. and Desplan, C. 2006. Stochastic *spineless* expression creates the retinal mosaic for colour vision. Nature 440, 174-180.

White, N.M. and Jarman, A.P. 2000. *Drosophila* Atonal controls photoreceptor R8-specific properties and modulates both Receptor Tyrosine Kinase and Hedgehog signalling. Development 127, 1681-1689.

Wigglesworth, V.B. 1959. The histology of the nervous system of an insect, *Rhodnius prolixus* (Hemiptera): II. The central ganglia. J. Cell Science 100, 299-313.

Wilson, R.I., Turner, G.C. and Laurent, G. 2004. Transformation of olfactory representations in the *Drosophila* antennal lobe. Science 303, 366-370.

Wilson, R.I. and Laurent, G. 2005. Role of GABAergic inhibition in shaping odor-evoked spatiotemporal patterns in the *Drosophila* antennal lobe. J. Neurosci. 25, 9069-9079.

Wilson, T.G. and Jacobson, K.B. 1977. Isolation and characterization of pteridines from heads of *Drosophila melanogaster* by a modified thin-layer chromatography procedure. Biochem. Genet. 15, 307-319.

Winberg, M.L., Perez, S.E. and Steller, H. 1992. Generation and early differentiation of glial cells in the first optic ganglion of *Drosophila melanogaster*. Development 115, 903-911.

Witte, I., Kreienkamp, H.-J., Gewecke, M. and Roeder, T. 2002. Putative histamine-gated chloride channel subunits of the insect visual system and thoracic ganglion. J. Neurochem. 83, 504-514.

Wolff, T. and Ready, D.F. 1991. The beginning of pattern formation in the *Drosophila* compound eye: the morphogenetic furrow and the second mitotic wave. Development 113, 841-850.

Wolff, T. and Ready, D.F. (1993) Pattern formation in the *Drosophila* retina. In: *The Development of Drosophila melanogaster*. pp. 1277–1325. Eds. M. Bate, A. M. Arias. Cold Spring Harbor Laboratory Press: Cold Spring Harbor, N.Y.

Woods, D.F. and Bryant, P.J. 1991. The discs-large tumor suppressor gene of Drosophila encodes a guanylate kinase homolog localized at septate junctions. Cell 66, 451-464.

Wu, V.M., Schulte, J., Hirschi, A., Tepass, U. and Beitel, G.J. 2004. Sinuous is a *Drosophila* claudin required for septate junction organization and epithelial tube size control. J. Cell Biol. 164, 313-323.

Wu, V.M., Yu, M.H., Paik, R., Banerjee, S., Liang, Z., Paul, S.M., Bhat, M.A. and Beitel, G.J. 2007. *Drosophila* Varicose, a member of a new subgroup of basolateral MAGUKs, is required for septate junctions and tracheal morphogenesis. Development 134, 999-1009.

Xiong, W.-C., Okano, H., Patel, N.H., Blendy, J.A. and Montell, C. 1994. *repo* encodes a glial-specific homeo domain protein required in the *Drosophila* nervous system. Genes Dev. 8, 981-994.

Xiong, W.-C. and Montell, C. 1995. Defective glia induce neuronal apoptosis in the *repo* visual system of Drosophila. Neuron 14, 581-590.

Xu, C., Kauffmann, R.C., Zhang, J., Kladny, S. and Carthew, R.W. 2000. Overlapping activators and repressors delimit transcriptional response to receptor tyrosine kinase signals in the *Drosophila* eye. Cell 103, 87-97.

Yager, J., Richards, S., Hekmat-Scafe, D.S., Hurd, D.D., Sundaresan, V., Caprette, D.R., Saxton, W.M., Carlson, J.R. and Stern, M. 2001. Control of *Drosophila* perineurial glial growth by interacting neurotransmitter-mediated signaling pathways. Proc. Natl. Acad. Sci. U.S.A. 98, 10445-10450.

Yamaguchi, S., Desplan, C. and Heisenberg, M. 2010. Contribution of photoreceptor subtypes to spectral wavelength preference in *Drosophila*. Proc. Natl. Acad. Sci. U.S.A. 107, 5634-5639.

Yang, C.-h., Axelrod, J.D. and Simon, M.A. 2002. Regulation of Frizzled by fat-like cadherins during planar polarity signaling in the *Drosophila* compound eye. Cell 108, 675-688.

Yao, Y., Wu, Y., Yin, C., Ozawa, R., Aigaki, T., Wouda, R.R., Noordermeer, J.N., Fradkin, L.G. and Hing, H. 2007. Antagonistic roles of Wnt5 and the Drl receptor in patterning the *Drosophila* antennal lobe. Nat. Neurosci. 10, 1423-1432.

Yasuyama, K. and Salvaterra, P.M. 1999. Localization of choline acetyltransferase-expressing neurons in *Drosophila* nervous system. Microsc. Res. Tech. 45, 65-79.

Yasuyama, K., Meinertzhagen, I.A. and Schürmann, F.-W. 2002. Synaptic organization of the mushroom body calyx in *Drosophila melanogaster*. J. Comp. Neurol. 445, 211-226.

Yasuyama, K., Meinertzhagen, I.A. and Schürmann, F.-W. 2003. Synaptic connections of cholinergic antennal lobe relay neurons innervating the lateral horn neuropile in the brain of *Drosophila melanogaster*. J. Comp. Neurol. 466, 299-315.

Ye, Z.-C., Wyeth, M.S., Baltan-Tekkok, S. and Ransom, B.R. 2003. Functional hemichannels in astrocytes: a novel mechanism of glutamate release. J. Neurosci. 23, 3588-3596.

Yonekura, S., Xu, L., Ting, C.-Y. and Lee, C.-H. 2007. Adhesive but not signaling activity of *Drosophila* N-cadherin is essential for target selection of photoreceptor afferents. Dev. Biol. 304, 759-770.

Yoshihara, M. and Littleton, J.T. 2002. Synaptotagmin I functions as a calcium sensor to synchronize neurotransmitter release. Neuron 36, 897-908.

Younossi-Hartenstein, A., Tepass, U. and Hartenstein, V. 1993. Embryonic origin of the imaginal discs of the head of Drosophila melanogaster. Roux's Arch. Dev. Biol. 203, 60-73.

Yu, T.W. and Bargmann, C.I. 2001. Dynamic regulation of axon guidance. Nat. Neurosci. 4, 1169-1176.

Zaccheo, O., Dinsdale, D., Meacock, P.A. and Glynn, P. 2004. Neuropathy target esterase and its yeast nomologue degrade phosphatidylcholine to glycerophosphocholine in living cells. J. Biol. Chem. 279, 24024-24033.

Zhai, Q., Wang, J., Kim, A., Liu, Q., Watts, R., Hoopfer, E., Mitchison, T., Luo, L. and He, Z. 2003. Involvement of the ubiquitin-proteasome system in the early stages of wallerian degeneration. Neuron 39, 217-225.

Zhang, Z., Curtin, K.D., Sun, Y.-A. and Wyman, R.J. 1999. Nested transcripts of gap junction gene have distinct expression patterns. J. Neurobiol. 40, 288-301.

Zheng, L., Zhang, J. and Carthew, R.W. 1995. *frizzled* regulates mirror-symmetric pattern formation in the *Drosophila* eye. Development 121, 3045-3055.

Zheng, L., de Polavieja, G.G., Wolfram, V., Asyali, M.H., Hardie, R.C. and Juusola, M. 2006. Feedback network controls photoreceptor output at the layer of first visual synapses in *Drosophila*. J. Gen. Physiol. 127, 495-510.

Zheng, Y., Hirschberg, B., Yuan, J., Wang, A.P., Hunt, D.C., Ludmerer, S.W., Schmatz, D.M. and Cully, D.F. 2002. Identification of two novel *Drosophila melanogaster* histamine-gated chloride channel subunits expressed in the eye. J. Biol. Chem. 277, 2000-2005.

Zhu, B., Pennack, J.A., McQuilton, P., Forero, M.G., Mizuguchi, K., Sutcliffe, B., Gu, C.-J., Fenton, J.C. and Hidalgo, A. 2008. *Drosophila* neurotrophins reveal a common mechanism for nervous system formation. PLoS Biol. 6, e284.

Zhu, Y., Nern, A., Zipursky, S.L. and Frye, M.A. 2009. Peripheral visual circuits functionally segregate motion and phototaxis behaviors in the fly. Curr. Biol. 19, 613-619.

Ziegenfuss, J.S., Biswas, R., Avery, M.A., Hong, K., Sheehan, A.E., Yeung, Y.-G., Stanley, E.R. and Freeman, M.R. 2008. Draper-dependent glial phagocytic activity is mediated by Src and Syk family kinase signalling. Nature 453, 935-939.

Ziegler, A.B. and Hovemann, B.T. (2010) Aspartate decarboxylase Black as a part of visual signal transduction (P113). In: *Neurofly*: Manchester, UK.

Zinsmaier, K.E., Hofbauer, A., Heimbeck, G., Pflugfelder, G.O., Buchner, S. and Buchner, E. 1990. A cysteine-string protein is expressed in retina and brain of *Drosophila*. J. Neurogenet. 7, 15-29.

Zinsmaier, K.E., Eberle, K.K., Buchner, E., Walter, N. and Benzer, S. 1994. Paralysis and early death in cysteine string protein mutants of *Drosophila*. Science 263, 977-980.

Zipursky, S.L., Venkatesh, T.R., Teplow, D.B. and Benzer, S. 1984. Neuronal development in the *Drosophila* retina: monoclonal antibodies as molecular probes. Cell 36, 15-26.

Zoidl, G., Bruzzone, R., Weickert, S., Kremer, M., Zoidl, C., Mitropoulou, G., Srinivas, M., Spray, D.C. and Dermietzel, R. 2004. Molecular cloning and functional expression of zfCx52.6: a novel connexin with hemichannel-forming properties expressed in horizontal cells of the zebrafish retina. J. Biol. Chem. 279, 2913-2921.

Zuker, C.S., Montell, C., Jones, K., Laverty, T. and Rubin, G.M. 1987. A rhodopsin gene expressed in photoreceptor cell R7 of the *Drosophila* eye: homologies with other signal-transducing molecules. J. Neurosci. 7, 1550-1557.

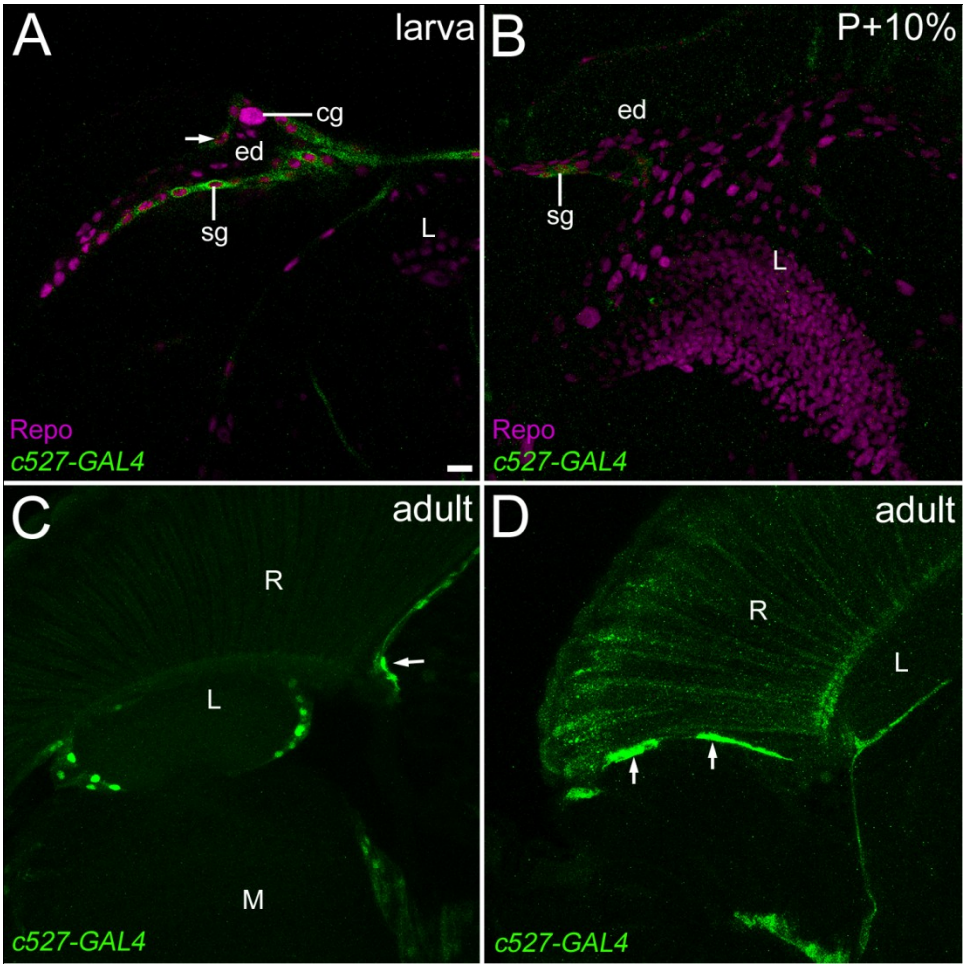

The larval surface slia driver *C527-GAL4* expresses in cells around the periphery of the adult retina and lamina. **A**: *c527-GAL4* drives mCD8::GFP (green) expression in the surface glia (sg) of the larval eye disc (ed). All glial nuclei are labelled with an antibody directed against Repo (magenta), including the large carpet glia (cg) in the eye disc. **B**: GFP is expressed in the pupal eye disc (49.5 µm projection) at P+10% but is reduced in intensity compared to in the third-instar larva. **C-D**: In Vibratome slices of adult brains (C, 23 µm projection; D, 16 µm projection), GFP is expressed in cells around the periphery of the retina (R, arrows) and the lamina (L). M indicates the location of the medulla. Scale in A, as in all, 10 µm.

tan[1]neoFRT19A/ tan[1]neoFRT19A [1];;Rh1-GAL4

Part 1:

P df6C4-6C5 ; + ; + x + ;; MKRS
FM6w[-] + + Y TM6b-Tb

F1 FM6w[-] ;; MKRS x df6C4-6C5 ; +
\+ + Y TM6b-Tb

F2 tan[1]neoFRT19A ;; + x FM6w[-] ;; MKRS
tan[1]neoFRT19A + Y TM6b-Tb

F3 tan[1]neoFRT19A ;; MKRS x tan[1]neoFRT19A ;; +
FM6w[-] + Y TM6b-Tb

F4 tan[1]neoFRT19A ;; MKRS
tan[1]neoFRT19A TM6b-Tb MAINTAIN STOCK

Part 2:

P tan[1]neoFRT19A ;; MKRS x + ;; Rh1-GAL4
tan[1]neoFRT19A TM6b-Tb Y Rh1-GAL4

F1 tan[1]neoFRT19A ;; MKRS x tan[1]neoFRT19A ;; Rh1-GAL4
tan[1]neoFRT19A TM6b-Tb Y MKRS

F2 tan[1]neoFRT19A ;; Rh1-GAL4 and tan[1]neoFRT19A ; Rh1-GAL4
tan[1]neoFRT19A- MKRS Y MKRS

Cross to self and select against MKRS

tan[1]/tan[1]; UAS-CG12120

Part 1:

P df6C4-6C5 / FM6w[-] ; + / + ; + / + x yw[a]z / Y ; Tft / CyO ; + / +

F1 FM6w[-] / yw[a]z ; Tft / + x df6C4-6C5 / Y ; + / CyO

F2 tan[1]neoFRT19A / tan[1]neoFRT19A ; + / + x FM6w[-] / Y ; Tft / CyO

F3 tan[1]neoFRT19A / FM6w[-] ; Tft / + x tan[1]neoFRT19A / Y ; + / CyO

F4 tan[1]neoFRT19A / tan[1]neoFRT19A ; Tft / CyO MAINTAIN STOCK

Part 2:

P tan[1]neoFRT19A / tan[1]neoFRT19A ; Tft / CyO x + / Y ; UAS-CG12120 / UAS-CG12120

F1 tan[1]neoFRT19A / tan[1]neoFRT19A ; Tft / CyO x tan[1]neoFRT19A / Y ; UAS-CG12120 / CyO

F2 tan[1]neoFRT19A / tan[1]neoFRT19A- ; UAS-CG12120 / CyO and tan[1]neoFRT19A / Y ; UAS-CG12120 / CyO

Cross to self and select against CyO

APPENDIX C CROSSES FOR THE GENERATION OF *TAN EGUF-HID* LINES

Parental $\frac{tan^1}{tan^1}$ x $\frac{p\{ry^+=neoFRT19A\};\ ry^{508}}{Y;\ ry^{508}}$

F1 $\frac{tan^1}{p\{ry^+=neoFRT19A\}}$ x $\frac{tan^1}{Y}$

Recombination at gametogenesis

F2 $\frac{HA92}{FM7c}$ x $\frac{tan^1 \pm p\{ry^+=neoFRT19A\}}{Y}$

SELECT TAN MALES: do at least 10 matings to HA92/FM7c.

F3 $\frac{tan^1 \pm p\{ry^+=neoFRT19A\}}{FM7c}$ x $\frac{FM7c}{Y}$

F4

Females: $\frac{tan^1 \pm p\{ry^+=neoFRT19A\}}{FM7c}$

Males: $\frac{tan^1 \pm p\{ry^+=neoFRT19A\}}{Y}$ and $\frac{FM7c}{Y}$

Cross males and females and select *tan* offspring.

APPENDIX D DESCRIPTION OF *P{D07784}* EXCISION LINES USED IN CHAPTER 4

	pigmentation phenotype		
line	body	antennae	description
EXP20A	weak *tan*-like	clear	-951 to +2 deleted, replaced by 26 bp insert[a]
EXP27A	weak *tan*-like	light	38 bp insert[b] remains at P insertion site (+11)
EXP37C	strong *tan*-like	light	-773 to +868 deleted, replaced by ACATAAA
EXP42A	strong *tan*-like	clear	77 bp insert[c] remains at P insertion site (+11)
EXP017B	wild-type[d]	wild-type	12 bp insert (dupl. of +3 to +14) remains at pos. +3
EXP019A	wild-type[d]	light	843 bp P-element frag. remains P insertion site (+11)
EXP038B	wild-type[d]	wild-type	403 bp P-element frag. remains P insertion site (+11)
EXP051C	wild-type[d]	light	1.2 kb P-element frag. remains at P insertion site (+11)

notes:

[a] CTTTCATTTGATGTTATTTCATCATG

[b] GTTTGAATCATGATGAAATAACATGTTATTTCATCATG

[c] CATGATGAAATAACATGATATGTGATAAATATATAATACATACATATAATATTATGTTATTTCATCATG

[d] Abdominal pigmentation weaker in females compared to wild-type females; males similar to wild-type.

This data was generously provided by John True and performed by John True, Shu-Dan Yeh and Shian-Ren Liou in the True lab (Stony Brook University, Long Island, NY)

10XPBS (Phosphate buffered Saline)
80g NaCl
2.0g KCl
14.4g Na2HPO4
2.4g KH2PO4
Add 800ml MilliQ H2O
pH to 7.4 and top off to 1.0L
aliquot and autoclave

20XSSC (saline-sodium citrate):
175.3g NaCl
88.2g Sodium Citrate
Add 800ml H_2O
pH to 7.0
raise volume to 1L

5XTris glycine buffer
15.1g Tris base
94g glycine
50ml of 10% SDS
Top to 1L with H_2O

Pre-hybridization Buffer:
50% formamide
50% 5xSSC
40ug/ml Salmon Sperm DNA

Solution B
20% formamide
0.5x SSC

1xTBS (Tris buffered Saline)
8g NaCl
0.2g KCl
3g Tris base
pH to 7.4 with HCl
H2O to 1L
autoclave

Blocking solution
1x BM Blocking reagent in 1x MAB

1x MAB (Maleic acid buffer)
Maleic acid: 116.1g
NaCl: 87.66g
Water to about 800ml

APPENDIX E CONTINUED

Stain Buffer:
2.0 ml 5M NaCl
10 ml 0.5M $MgCl_2$
10 ml 1M Tris (pH = 9.5)
1 ml 0.1M levamisome (autoclaved; 0.204g in 10 ml H_2O
1.0 ml 10% Tween 20
76 ml MilliQ-H2O

1xTEB = Tris-EDTA Buffer
10mM Tris (pH = 8.0)
1mM EDTA

Acetylation solution:
295 ml H_20
4ml triethanolamine (Fluka 90279)
0.525 ml 12M glacial HCl
Mix well
Add 0.75 ml acetic anhydride immediately before adding to sections

50x Denhardt's Solution (store at -20°C)
0.5g Ficoll 400
0.5g Polyvinylpyrolidone
0.5g Bovine Serum Albumin
H_20 to 500ml

100 ml Hybridization buffer
50ml Formamide
20 ml 20x SSC
10mg heparin
2ml 50x Denhardt's
0.1% Tween 20 (100 µl)
2ml EDTA
H_20 to 100ml
+2 ul RNA probe (at a concentration of 50mg/ml)

APPENDIX F MINIPREP PROTOCOL

Solutions:
200 µl TE (pH = 8)
200 µl Lysis solution = 800µl H2O
100µl 10% SDS
100µl 2M NaOH
200µl 5.0M KAc (pH = 4.8)
200µl phenol:chloroform (pipette from the bottom phase, below the interface)
1.0ml 95% ethanol (chilled)
200µl 70% ethanol (chilled)

Method:
1) pipette cultured e-coli into 1.5ml eppendorph tubes and centrifuge for 20 minutes at 5000 RPM. Pour off the supernatant
2) wash cells in TE, respin and pour off the supernatant
3) resuspend cells in 200 µl TE
4) add 200µl of freshly made lysis solution
5) mix gently by inverting 3x
6) leave tube for 5 min while cells lyse
7) add 200µl of 5.0M KAc
8) mix gently by inverting 3x then place on ice for 5 min
9) centrifuge 10 minutes at 4°C then pipette off and save the supernatant into a new labelled tube
10) in a fume hood add 200 µl of 1:1 phenol chloroform mix and cap the tubes securely
11) shake vigorously for 30 seconds
12) centrifuge for 10 minutes and save the top layer to a new tube
13) add 1.0 ml of 95% ethanol, mix by inversion and chill at -20°C for 20 minutes.
14) centrifuge 10 minutes and pour off the supernatant
15) add 200 µl of 70% ethanol. Shake briefly to wash the tube then centrifuge for 5 minutes
16) remove the ethanol completely and leave the eppendorph tube open at RT to dry the pellet
17) resuspend in 50 µl TE

APPENDIX G HEAD HISTAMINE CONTENTS IN MEDIUM FED VS GLUCOSE FED *TAN* LINES

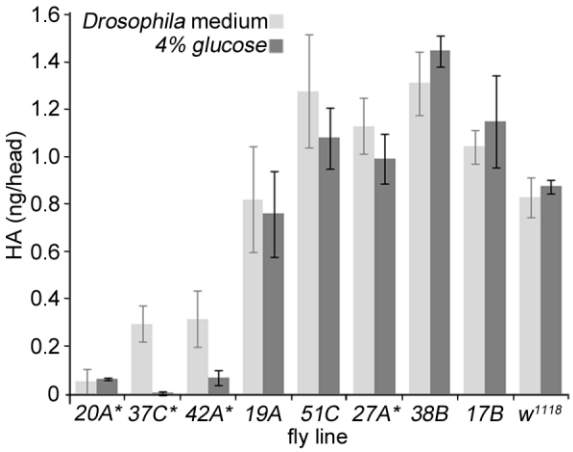

Excision lines are marked with an *

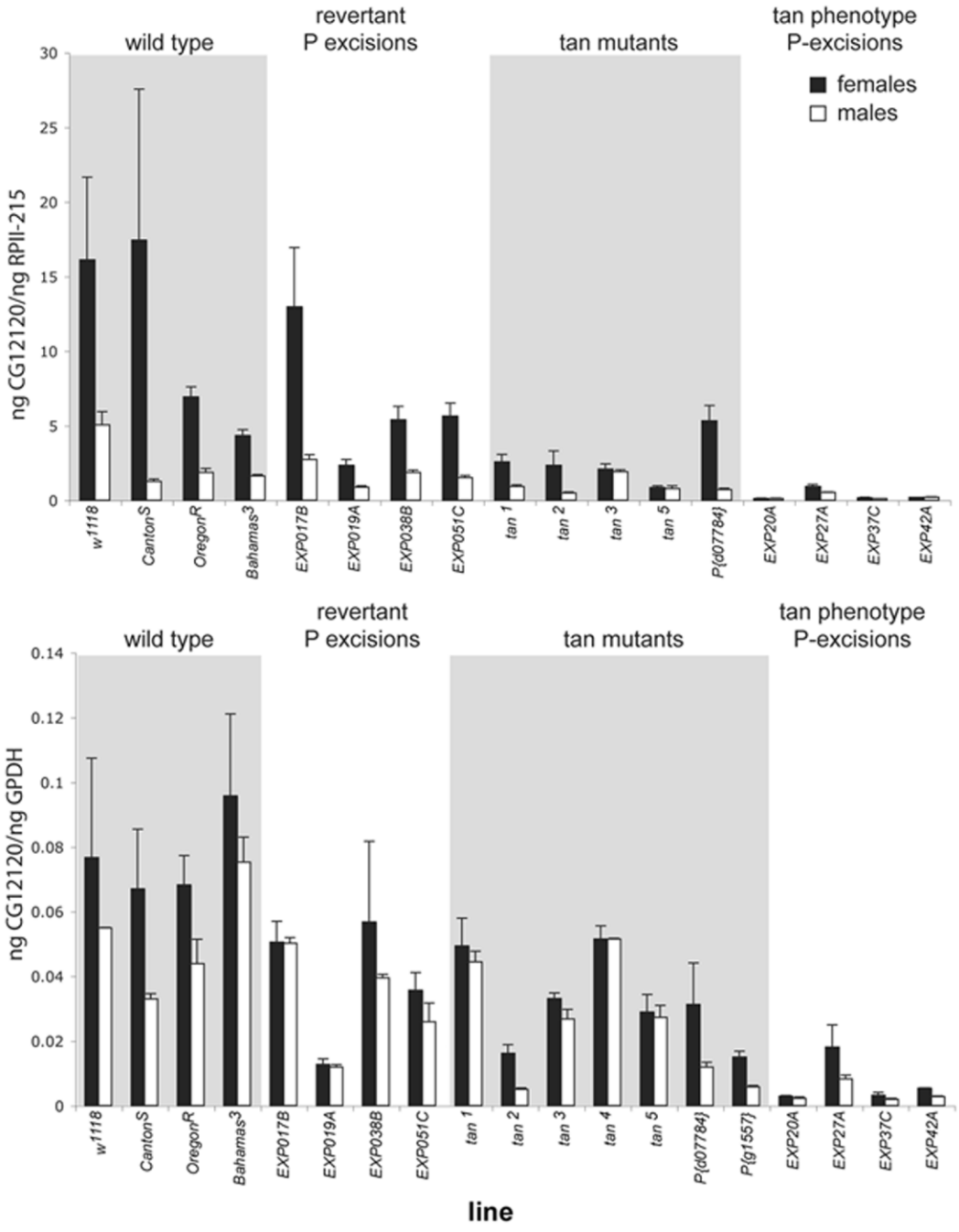

A: 60-75h pupae; n=4-6 replicate estimates for each strain. **B:** 0-8h adults; n=2-5 replicate estimates for each strain. Bars represent one standard error. The above is data provided by John True and performed by John True, Shu-Dan Yeh and Shian-Ren Liou in the True lab (Stony Brook University, Long Island, NY)

Plates for vector amplification

LB
20.0g Luria Broth (LB - Sigma)
Add H2O to 1L to make a liquid

To make a solid: add 15.0g of Agar. Autoclave 20 minutes on the liquid cycle. 100 ml makes ~3 plates

When solution reaches 55°C, add ~ 0.0025g of antibody for every 100ml solution (0.125/500ml). Swirl and pour into plates (25ug/ml) wrap plates in parafilm and store upside down at 4°C.

Antibody Stock solution:
10 mg/ml (0.01g antibiotic /ml ethanol)
Stock solution diluted 1:10 in H_2O (1.0ml antibody solution: 9.0ml H_2O)
Store at 4°C and use within 30 days

***E. coli* transformation**
1) turn on water bath to 37°C
2) obtain 50 µl of competent cells (stored at -80°C) and place on ice
3) add 0.5 µl of DNA in vector (or 10 µl of ligation mix) and mix gently with light vortexing or pipetting
4) leave on ice for 30 min
5) 90 sec heat shock in 37°C water bath
6) place back in ice for 2 minutes
7) add 500 µl liquid Luria Broth
8) put tube in 37°C incubator for 30 minutes to 3 hours
9) pipet contents onto antibiotic containing bacterial plates
10) incubate overnight with Petrie dish placed upside down at 37°C

To prepare more vector:
Make additional LB with antibiotic. Use E. coli from starter culture at a concentration of 1:500. Put in 37°C overnight on shaker.

APPENDIX J THE RETINAL PHENOTYPE OF *INX-EGUF-HID* FLIES

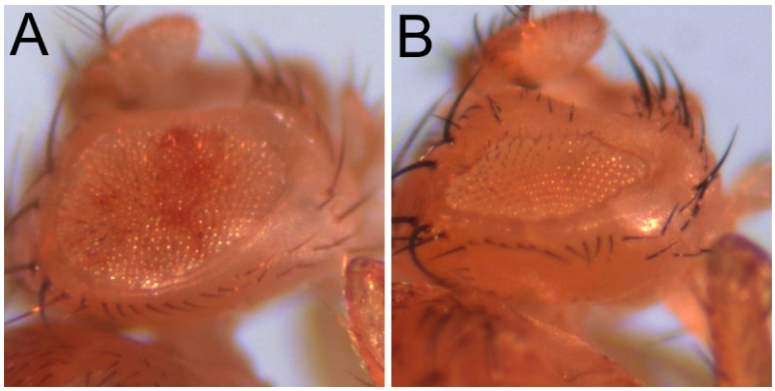

A: The retina of an adult female *inx1-EGUF-hid* fly. B: The retina of an adult female *inx2-EGUF-hid* fly.

APPENDIX K CROSSES FOR THE GENERATION OF FLIES WITH *RUNT* OVER-EXPRESSION IN A *SEV* MUTANT BACKGROUND

sev^{AE2} ; GMR-GAL4 + UAS-runt

P $\frac{+}{Y}$; $\frac{\text{GMR-GAL4 + UAS-runt}}{\text{CyO}}$ x $\frac{\text{Df(1)6C-40, w}^{1118}}{\text{FM6,w}^{1}}$; $\frac{+}{+}$

F1 $\frac{\text{FM6,w}^{1}}{+}$; $\frac{+}{\text{CyO}}$ x $\frac{\text{FM6,w}^{1}}{Y}$; $\frac{\text{GMR-GAL4 + UAS-runt}}{+}$

F2 $\frac{\text{FM6,w}^{1}}{Y}$; $\frac{\text{GMR-GAL4 + UAS-runt}}{\text{CyO}}$ x $\frac{\text{sev}^{AE2}}{\text{sev}^{AE2}}$; $\frac{+}{+}$

F3 $\frac{\text{sev}^{AE2}}{Y}$; $\frac{\text{GMR-GAL4 + UAS-runt}}{+}$ x $\frac{\text{sev}^{AE2}}{\text{FM6,w}^{1}}$; $\frac{+}{\text{CyO}}$

F4 $\frac{\text{sev}^{AE2}}{\text{sev}^{AE2}}$; $\frac{\text{GMR-GAL4 + UAS-runt}}{\text{CyO}}$ x $\frac{\text{sev}^{AE2}}{Y}$; $\frac{\text{GMR-GAL4 + UAS-runt}}{\text{CyO}}$

MAINTAIN STOCK

sev^{AE2} ;; MT14-GAL4 (annotated as MT14)

P-1 $\frac{\text{sev}^{AE2}}{\text{sev}^{AE2}}$; $\frac{+}{+}$ x $\frac{\text{FM6}}{Y}$;; $\frac{\text{MKRS}}{\text{TM6BTb}}$

F1-1 $\frac{\text{sev}^{AE2}}{\text{FM6}}$; $\frac{\text{MKRS}}{+}$ x $\frac{\text{sev}^{AE2}}{Y}$;; $\frac{+}{\text{TM6BTb}}$

F2-1 $\frac{\text{sev}^{AE2}}{\text{FM6}}$;; $\frac{\text{MKRS}}{\text{TM6BTb}}$

P -2 $\frac{\text{Kr}^{\text{Ifi}}}{\text{CyO}}$; $\frac{\text{MT14}}{\text{Ser}}$ x $\frac{\text{FM6}}{Y}$; $\frac{\text{MKRS}}{\text{TM6BTb}}$

F1-2 $\frac{\text{FM6}}{+}$; $\frac{\text{Kr}^{\text{Ifi}}}{+}$; $\frac{\text{MT14}}{\text{MKRS}}$ x $\frac{+}{Y}$; $\frac{+}{\text{CyO}}$; $\frac{\text{MT14}}{\text{MKRS}}$

F2-2 $\frac{\text{FM6}}{Y}$; $\frac{\text{Kr}^{\text{Ifi}}}{\text{CyO}}$; $\frac{\text{MT14}}{\text{MKRS}}$

F3 -A $\frac{\text{sev}^{AE2}}{\text{FM6}}$;; $\frac{\text{MKRS}}{\text{TM6BTb}}$ x $\frac{\text{FM6}}{Y}$; $\frac{\text{Kr}^{\text{Ifi}}}{\text{CyO}}$; $\frac{\text{MT14}}{\text{MKRS}}$

F4-A $\frac{\text{sev}^{AE2}}{}$; $\frac{+}{}$; $\frac{\text{MT14}}{}$ x $\frac{\text{sev}^{AE2}}{}$; $\frac{\text{Kr}^{\text{Ifi}}}{}$; $\frac{\text{MT14}}{}$

FM6 CyO MKRS Y + MKRS

F5 -A $\frac{sev^{AE2}}{sev^{AE2}}$; $\frac{Kr^{lfi}}{CyO}$; $\frac{MT14}{MKRS}$

sev^{AE2} ; UAS-runt

P-1 $\frac{sev^{AE2}}{sev^{AE2}}$; $\frac{+}{+}$ x $\frac{FM6}{Y}$; $\frac{Tft}{CyO}$

F1-1 $\frac{sev^{AE2}}{FM6}$; $\frac{Tft}{+}$ x $\frac{sev^{AE2}}{Y}$; $\frac{+}{CyO}$

F2-1 $\frac{sev^{AE2}}{FM6}$; $\frac{Tft}{CyO}$

P -2 $\frac{UAS\text{-}runt}{CyO}$; $\frac{D}{Ser}$ x $\frac{FM6}{Y}$; $\frac{Tft}{CyO}$

F1-2 $\frac{FM6}{+}$; $\frac{UAS\text{-}runt}{CyO}$; $\frac{D}{+}$ x $\frac{+}{Y}$; $\frac{UAS\text{-}runt}{CyO}$; $\frac{+}{Ser}$

F2-2 $\frac{FM6}{Y}$; $\frac{UAS\text{-}runt}{CyO}$; $\frac{D}{Ser}$

F3 -B $\frac{sev^{AE2}}{FM6}$; $\frac{Tft}{CyO}$ x $\frac{FM6}{Y}$; $\frac{UAS\text{-}runt}{CyO}$; $\frac{D}{Ser}$

F4-B $\frac{sev^{AE2}}{FM6}$; $\frac{UAS\text{-}runt}{CyO}$; $\frac{D}{+}$ $\frac{sev^{AE2}}{Y}$; $\frac{UAS\text{-}runt}{CyO}$; $\frac{+}{Ser}$

F5 -B $\frac{sev^{AE2}}{sev^{AE2}}$; $\frac{UAS\text{-}runt}{CyO}$; $\frac{D}{Ser}$

F5 -A $\frac{sev^{AE2}}{sev^{AE2}}$; $\frac{Kr^{lfi}}{CyO}$; $\frac{MT14}{MKRS}$ x **5F-B** $\frac{sev^{AE2}}{sev^{AE2}}$; $\frac{UAS\text{-}runt}{CyO}$; $\frac{D}{Ser}$

F6 $\frac{sev^{AE2}}{sev^{AE2}}$; $\frac{UAS\text{-}runt}{CyO}$; $\frac{MT14}{Ser}$

Cross F6 back into *sev^{AE2}* to eliminate balancers

APPENDIX L COPYRIGHT RELEASE REQUESTS